FINAL REPORT

WAVE LOADING ON BRIDGE DECKS

FDOT NUMBER: BD545-58

UF NUMBER: 00056675

SUBMITTED TO:

FLORIDA DEPARTMENT OF TRANSPORTATION

RESEARCH OFFICE

605 SUWANNEE STREET

TALLAHASSEE, FLORIDA 32399-0450

SUBMITTED BY:

D. MAX SHEPPARD

JUSTIN MARIN

CIVIL AND COASTAL ENGINEERING DEPARTMENT

UNIVERSITY OF FLORIDA

GAINESVILLE, FL 32611

DECEMBER 2009

Disclaimer

The opinions, findings, and conclusions expressed in this publication are those of the authors and not necessarily those of the State of Florida Department of Transportation.

SI (MODERN METRIC) CONVERSION FACTORS (from FHWA)

APPROXIMATE CONVERSIONS TO SI UNITS

SYMBOL	WHEN YOU KNOW	MULTIPLY BY	TO FIND	SYMBOL
		LENGTH		
in	inches	25.4	millimeters	mm
ft	feet	0.305	meters	m
yd	yards	0.914	meters	m
mi	miles	1.61	kilometers	km
		AREA		
in^2	square inches	645.2	square millimeters	mm^2
ft^2	square feet	0.093	square meters	m^2
yd^2	square yard	0.836	square meters	m^2
ac	acres	0.405	hectares	ha
mi^2	square miles	2.59	square kilometers	km^2
		VOLUME		
fl oz	fluid ounces	29.57	milliliters	mL
gal	gallons	3.785	liters	L
ft^3	cubic feet	0.028	cubic meters	m^3
yd^3	cubic yards	0.765	cubic meters	m^3
NOTE: volumes greater than 1000 L shall be shown in m^3				
		MASS		
oz	ounces	28.35	grams	g
lb	pounds	0.454	kilograms	kg
T	short tons (2000 lb)	0.907	megagrams (or "metric ton")	Mg (or "t")
		TEMPERATURE (exact degrees)		
^oF	Fahrenheit	5 (F-32)/9 or (F-32)/1.8	Celsius	^oC
		ILLUMINATION		
fc	foot-candles	10.76	lux	lx
fl	foot-Lamberts	3.426	candela/m^2	cd/m^2
		FORCE and PRESSURE or STRESS		
lbf	poundforce	4.45	newtons	N
lbf/in^2	poundforce per square inch	6.89	kilopascals	kPa
		LENGTH		
mm	millimeters	0.039	inches	in
m	meters	3.28	feet	ft

SYMBOL	WHEN YOU KNOW	MULTIPLY BY	TO FIND	SYMBOL
LENGTH				
m	meters	1.09	yards	yd
km	kilometers	0.621	miles	mi
AREA				
mm^2	square millimeters	0.0016	square inches	in^2
m^2	square meters	10.764	square feet	ft^2
m^2	square meters	1.195	square yards	yd^2
ha	hectares	2.47	acres	ac
km^2	square kilometers	0.386	square miles	mi^2
VOLUME				
mL	milliliters	0.034	fluid ounces	fl oz
L	liters	0.264	gallons	gal
m^3	cubic meters	35.314	cubic feet	ft^3
m^3	cubic meters	1.307	cubic yards	yd^3
MASS				
g	grams	0.035	ounces	oz
kg	kilograms	2.202	pounds	lb
Mg (or "t")	megagrams (or "metric ton")	1.103	short tons (2000 lb)	T
TEMPERATURE (exact degrees)				
^oC	Celsius	1.8C+32	Fahrenheit	^oF
ILLUMINATION				
lx	lux	0.0929	foot-candles	fc
cd/m^2	candela/m^2	0.2919	foot-Lamberts	fl
FORCE and PRESSURE or STRESS				
N	newtons	0.225	poundforce	lbf
kPa	kilopascals	0.145	poundforce per square inch	lbf/in^2

*SI is the symbol for the International System of Units. Appropriate rounding should be made to comply with Section 4 of ASTM E380.

(Revised March 2003)

Technical Report Documentation Page

1. Report No.	2. Government Accession No.	3. Recipient's Catalog No.	
4. Title and Subtitle Wave Loading on Bridge Decks		5. Report Date December 2009	
		6. Performing Organization Code 00056675	
7. Author(s) D. Max Sheppard Justin Marin		8. Performing Organization Report No.	
9. Performing Organization Name and Address Department of Civil and Coastal Engineering 365 Weil Hall University of Florida Gainesville, Florida 32611		10. Work Unit No. (TRAIS)	
		11. Contract or Grant No. BD545-58	
12. Sponsoring Agency Name and Address Florida Department of Transportation 605 Suwannee Street, MS 30 Tallahassee, FL 32399		13. Type of Report and Period Covered: Final Report August 19, 2005 - December 31, 2009	
		14. Sponsoring Agency Code	
15. Supplementary Notes			

16. Abstract

This report covers the results of experimental and theoretical analyses of wave loading on bridge superstructures. A number of wave tank tests were performed on both slab and girder type spans with different water depths, span positions relative to the still water level and wave heights and periods. The model structures were instrumented with three component load cells and pressure transducers. The wave forces which are, in general, composed of a wave frequency (quasi-static) component and a high frequency slamming force component were both measured and analyzed.

A theoretical model for the wave forces was developed and the wave tank test results used to determine the drag and inertia coefficients in the equations. The resulting equations were tested using field data from the damage to and destruction of the I10-Escambia Bay Bridge located near Pensacola, Florida caused by Hurricane Ivan in 2004.

17. Key Word	18. Distribution Statement		
Wave forces, bridge superstructures, wave loading, horizontal structures	No restrictions.		
19. Security Classif. (of this report) Unclassified.	20. Security Classif. (of this page) Unclassified.	21. No. of Pages 177	22. Price

ACKNOWLEDGMENTS

The authors would like to thank the Florida Department of Transportation project manager, Rick Renna, for his technical and financial support of this and other related research projects. His insight into the research needs in hydraulics, sediment transport, coastal and environmental engineering and the benefits that can be derived from such research are remarkable. Through his efforts he has saved the taxpayers millions of dollars while at the same time providing the designers of Florida's roadways and bridges better design parameters. He is truly an asset to the State and Nation.

Thanks also to the laboratory staff in the Coastal Engineering Laboratory at the University of Florida, Sidney Schofield, Jim Joiner and Vick Adams. Their assistance with the instrumentation and the construction of the models and model support system was essential to the success of this project.

EXECUTIVE SUMMARY

During the past few years, several major bridges in the Gulf Coast States in the US were destroyed by hurricane generated storm surge and wave loading. The I10-Escambia Bay Bridge located near Pensacola, Florida suffered severe damage due to Hurricane Ivan and had to be replaced. These failures pointed to the need for a better understanding of wave forces on horizontal structures and for improved methods for predicting their magnitudes.

The approach taken was both theoretical and experimental. Wave tank tests with model bridge spans and theoretical model development were initiated at the same time. The work of Kaplan (1992) and Kaplan et al. (1995) was modified and extended to include bridge superstructures and the meteorological and oceanographic (met/ocean) conditions experienced by bridges located in coastal waters. Wave tank tests with slab and girder bridge spans were performed in a 6 ft wide by 6 ft deep by 130 ft long wave tank in the Coastal Engineering Laboratory at the University of Florida. A wide range of water depths, span low chord position relative to the still water level, and wave heights and periods were tested. In general, wave forces have both a low (wave) frequency component and a much higher slamming frequency component. Both components were investigated in this study. The wave tank test results were used to compute the drag and inertia coefficients needed for the theoretical model. Girder type spans can trap air between the beams, significantly increasing the buoyancy force. The amount of air entrapped is an input to the theoretical model and this quantity is difficult to predict. However, the range of forces can be obtained by evaluating the model for both zero and the maximum air entrapment.

The Florida Department of Transportation (FDOT) obtained detailed damage information for the I10-Escambia Bay Bridge after Hurricane Ivan. Ocean Engineering Associates, Inc. conducted a thorough hindcast of Hurricane Ivan as part of the bridge hydraulics report for the replacement bridge yielding the time history of water elevations and wave heights and periods at the bridge throughout the storm. This information was used to test the theoretical wave forces model developed by this research under prototype structure and wave conditions, with the drag and inertia coefficients obtained from the laboratory tests. The model did a good job of predicting failure for the spans that failed and survival of those spans that did not fail. The model was also tested on other bridges that were subjected to hurricane storm surge and waves.

For these cases the predicted forces did not exceed the resistive forces (dead weight plus tie-downs) and the bridges were not damaged, indicating that the model is not overly conservative in its predictions.

The model was adopted by AASHTO and used to perform numerical experiments that covered a wide range of span types and met/ocean conditions to generate a data set for the development of parametric equations for the AASHTO specs, “Guide Specifications for Bridges Vulnerable to Coastal Storms”.

In summary, an extensive wave force on bridge superstructures data set was obtained through wave tank tests during this study. Both wave frequency (quasi-static) and high frequency (slamming) forces were measured and analyzed. Information from these tests was used to compute drag and inertia coefficients for the theoretical wave force model, which was also developed as part of this study. The theoretical model has been tested with prototype structure and met/ocean data and it performed well.

Table of Contents

LIST OF FIGURES

LIST OF TABLES

FINAL REPORT
WAVE LOADING ON BRIDGE DECKS
THEORETICAL AND LABORATORY STUDY
CHAPTER 1 - INTRODUCTION

Over the course of 2004 and 2005, several bridges sustained critical damage during major storm events. The cause of these failures was attributed to the effects of storm surge and water wave loading, a forcing mechanism previously unaccounted for in coastal bridge design.

The purpose of this study is to provide an investigation of wave loading on bridge superstructures and a methodology for predicting these loads. To do this, a theoretical, physics based, model was developed and a corresponding numerical model was created to evaluate it. Extensive physical model testing was carried out for the purposes of empirical coefficient determination, and theoretical model laboratory scale verification. The model was used to develop parametric wave force equations for an American Association of State Highway and Transportation Officials **(**AASHTO) code.

Bridge Failures Attributed to Wave Loading

In this study, bridge failure is defined as any damage that renders the bridge unsafe for continued use. The variety of damage can include the failure of span tie-downs, the displacement of spans from their initial position on their pile caps, the complete removal of spans from their pile caps, the shifting or collapse of bents and piles from the above movements of the spans, the removal or wash out of railings, and the excessive cracking or spalling of concrete. The severity of these incidents can range from a single visible material stress and fatigue to the complete destruction and collapse of an entire bridge.

The recent bridge failures of 2004 and 2005 drew national attention to the impact of wave forces on bridges. Similar incidents during hurricanes were recorded as early as 1969 with the failures displaying similar structural damage. A brief review of the damage caused by previous storms helps to demonstrate the extent of damage involved.

Hurricane Camille

In 1969 Hurricane Camille severely damaged the US 90 bridges over St. Louis Bay, Mississippi and Biloxi Bay, Mississippi (USACE 1970). At landfall, Camille was a Category 5 storm on the Saffir-Simpson scale with unknown maximum wind speeds (Army Corp estimated as high as 200 mph at the time) and a storm surge over 24 feet. About one-third of the spans of the St. Louis Bay Bridge and one-half of the spans of the Biloxi Bay Bridge were either completely removed or displaced significantly. These same two bridges were destroyed again by Hurricane Katrina in 2005.

Hurricane Frederic

In 1979 Hurricane Frederic caused similar damage to the Dauphin Island Causeway Bridge, Alabama, and an I-10 onramp near Mobile, Alabama (USACE 1981). A Category 3 storm on the Saffir-Simpson scale at landfall, wind gusts of 145 mph and a storm surge in the range of 8ft to 13 ft were recorded at the bridge site. From the causeway, 135 spans were completely removed from their pile caps (Figure 1- 1 and Figure 1- 2). From the I-10 onramp, several spans were displaced varying distances from their pile caps. This same I-10 onramp was also damaged in Hurricane Katrina.

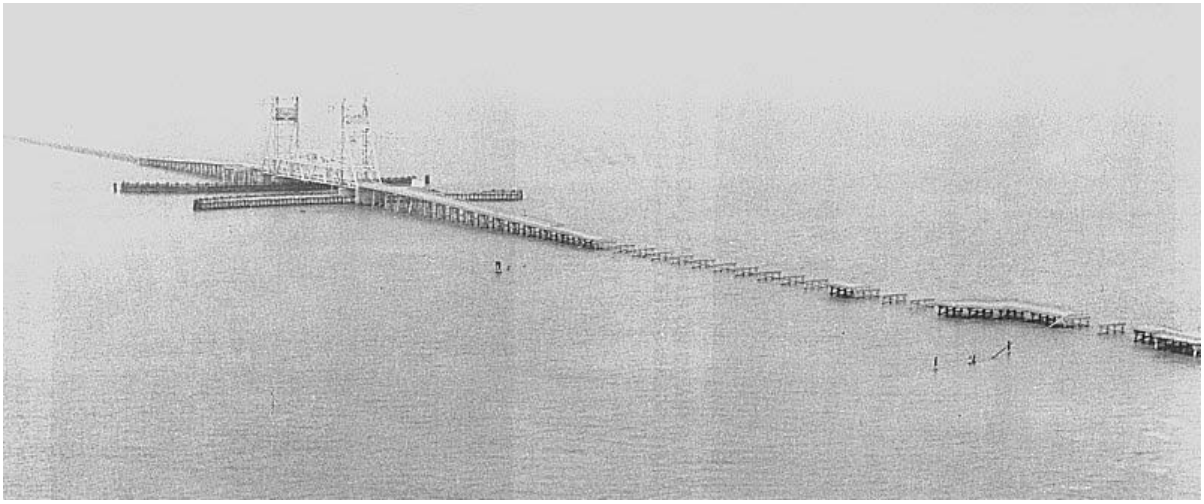

Figure 1- 1 Damage to Dauphin Island Causeway (Alabama) caused by Hurricane Frederic.

Figure 1- 2 Dauphin Island Causeway channel crossing.

Hurricane Ivan

In 2004 Hurricane Ivan made landfall in the Florida panhandle, causing massive damage (Figure 1- 3) to the I-10 Bridge over Escambia Bay (Sheppard 2006). This Category 3 storm on the Saffir-Simpson scale made landfall with sustained winds of 130 mph and an estimated surge of 10.7 ft at the bridge site. Fifty-one spans from the eastbound bridge and 12 spans from the westbound bridge were completely removed (Figure 1- 4) from their support structures. Thirty-three spans from the eastbound bridge and 19 spans from the westbound bridge were displaced varying distances (Figure 1- 5) from their initial positions. Support structures were also damaged as 25 bents from the eastbound bridge and 7 bents from the westbound bridge were affected (Figure 1- 6) by the displacement and collapse of the above superstructures. Failed tie downs between bents and the decks showed both shear and tension failure in the bolts. In some, the tie down systems had been completely removed from the pile cap as seen by the cracking and spalling in the concrete where the bolts and bearing pads had previously been (Figure 1- 7).

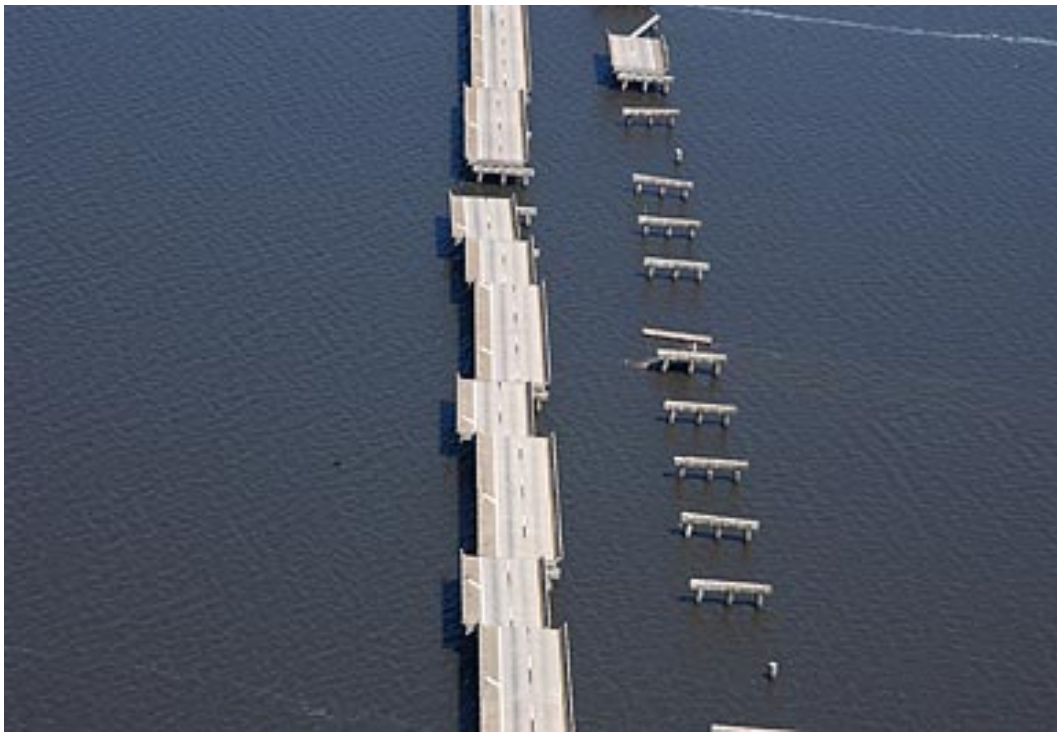

Figure 1- 3 I-10 - Escambia Bay Bridge damage from Hurricane Ivan.

Figure 1- 4 I-10 - Escambia Bay Bridge spans removed by Hurricane Ivan.

Figure 1- 5 I-10 - Escambia Bay Bridge spans displaced by Hurricane Ivan.

Figure 1- 6 I-10 - Escambia Bay Bridge pile bents damaged by Hurricane Ivan.

Figure 1- 7 I-10 Escambia Bay Bridge tie-downs damaged by Hurricane Ivan.

Hurricane Katrina

In 2005, Hurricane Katrina severely damaged the gulf coasts of Louisiana and Mississippi. Three major bridges (I-10 Bridge over Lake Pontchartrain, Louisiana; US 90 Bridge over St. Louis Bay, Mississippi; US 90 Bridge over Biloxi Bay, Mississippi) were brought down by the resulting storm surge and waves. An I-10 onramp near Mobile Bay, Alabama, also suffered the displacement of several spans (Figure 1- 8) by wave action. At landfall, Katrina was a Category 3 storm on the Saffir-Simpson scale with sustained maximum winds of 125 mph and a storm surge that varied along the coast with ranges of 10 ft to 19 ft in Louisiana, 17 ft to 28 ft in Mississippi, and 10 ft to15 ft in Alabama.

Damage to the I-10 Bridge over Lake Pontchartrain (Figure 1- 9) was extensive (Chen et al. 2005). Thirty-eight spans from the eastbound bridge and 20 spans from the westbound bridge were completely removed (Figure 1- 10) from their support structures. Supporting pile structures were also damaged from the collapsed spans (Figure 1- 11) while 379 more spans were laterally displaced varying distances (Figure 1- 12).

The US-90 Bridge over Biloxi Bay was severely damaged (Schumacher et al 2008). Nearly all of its 124 spans were removed by the storm (Figure 1- 13) with the exception of the approach spans and the higher drawbridge spans. The US-90 Bridge over St. Louis Bay experienced similar destruction (Figure 1- 14).

Some of these failures were used to test the model that was developed using coefficients based on wave tank data.

Figure 1- 8 I-10 Mobile Bay Bridge onramp spans displaced by Hurricane Katrina.

Figure 1- 9 I-10 - Lake Pontchartrain Bridge damage from Hurricane Katrina.

Figure 1- 10 I-10 Lake Pontchartrain Bridge spans removed by Hurricane Katrina.

Figure 1- 11 I-10 Lake Pontchartrain Bridge support structures damaged by Hurricane Katrina.

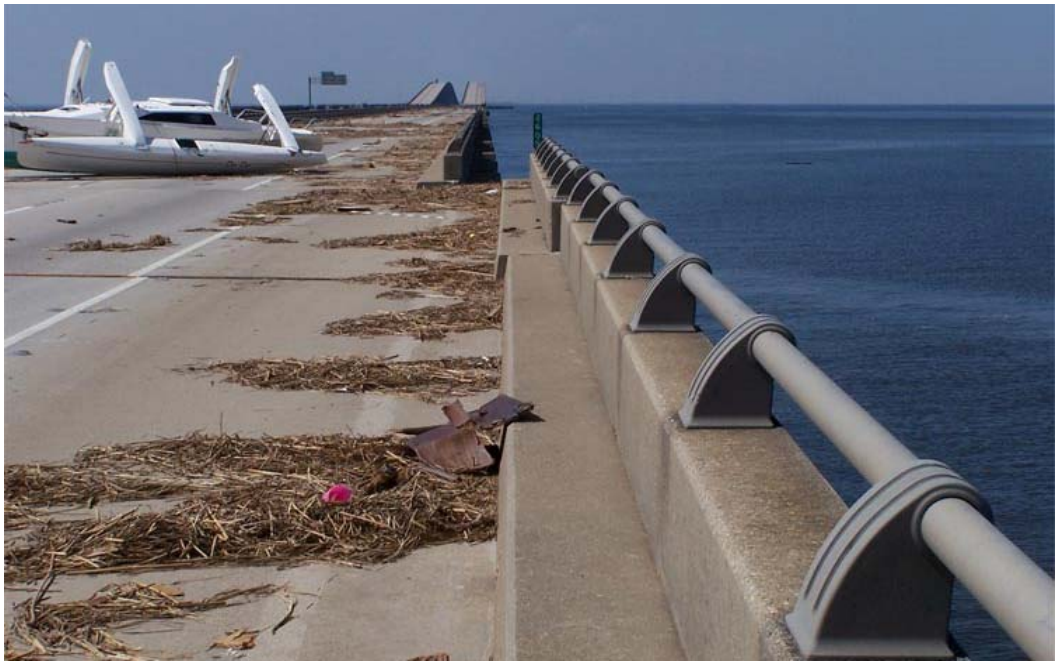

Figure 1- 12 I-10 Lake Pontchartrain Bridge spans displaced by Hurricane Katrina.

Figure 1- 13 US 90 - Biloxi Bay Bridge damaged by Hurricane Katrina.

Figure 1- 14 US 90 - St. Louis Bay Bridge damaged by Hurricane Katrina.

Motivation

The bridges discussed and shown above were all major bridges and the destruction of these routes was both costly to replace and a serious impact to the communities served by these facilities. The loss of commerce from the destruction of the traffic routes, the cost of replacement

bridges, impacts to users (including emergency services), the risk of repeat failures, and the lack of standardized predictive and design methods were the driving motivations behind this work.

Existing methods for design

Only two studies (Denson 1978, 1980) directly addressed wave forces on bridges. However, if one expands the search beyond bridges to work done on similar structures, numerous studies regarding wave loading on offshore platforms, decks, jetties, and docks can be found and even more regarding horizontally suspended cylinders and cylindrical elements. Unfortunately, the cross-application of these methods to the case of a bridge is problematic at best due to the inherent differences between the offshore/nearshore environments and structural characteristics. Major differences include structure to wave size ratios, finite thickness of the structures, air trapping concerns, and the variability between shallow water, intermediate, and deep water waves.

Because of these differences, the bridge/wave problem is unique, and requires separate study. Some principles, though, from previous work, especially in the offshore industry, provide an excellent foundation from which to begin. A complete literature review of relevant previous work is presented in Chapter 2.

Wave Loading Problem

The first element in the problem is the structure. Its shape can be as simple as a flat plate or as complex as a beam and deck bridge with overhangs and rails. Its location can be either subaerial or submerged relative to still water level (SWL) with its orientation relative to an approaching wave variable in three dimensions.

The second element in the problem is the wave. Waves have varying heights, lengths, and periods and for a given wave the portion in contact with the structure is dependent on the location of the structure relative to the still water level and the wave shape.

Bridges vary in complexity from a simple slab spanning a small stream to a combination of beams, diaphragms, decks, rails, overhangs, pile caps, pilings, bents, tie downs, box girders and in some cases, suspensions or arches. The individual components vary in size and shape from

bridge to bridge. To categorically define a bridge by a single setup would exclude any number of bridge types that also exist in coastal waters. However, it would be neither practical nor cost effective to investigate every conceivable setup and conduct physical model tests covering the full variety of these parameters. As such, the most common bridge superstructure elements used on bridges in coastal environments in Florida are described below.

Bridge Superstructure Types

For comparison, cross sectional diagrams of slab, girder and slab, and segmental box girder spans are shown in Figure 1- 15. Each of these structures will interact differently with a wave propagating past it; however, there are common features that can be utilized in their analyses.

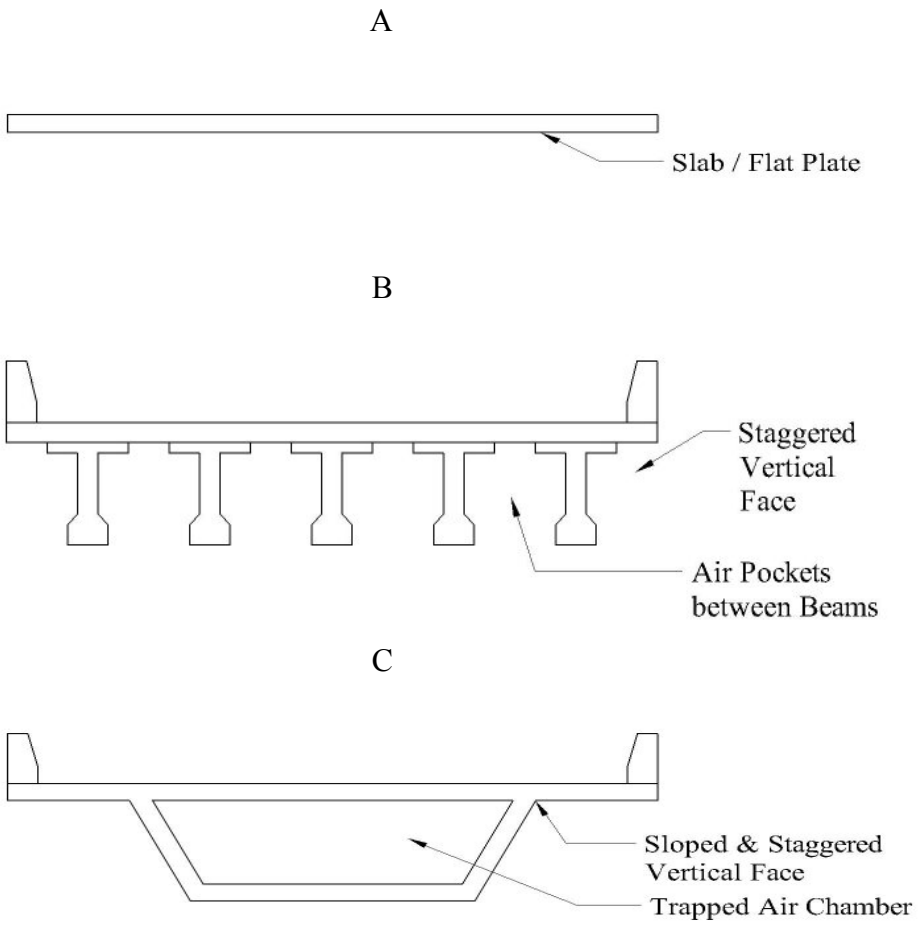

Figure 1- 15 Common bridge superstructure types in Florida. A) slab, B) slab and girder, C) segmental box girder.

Bridge Support Structure Types

The system used for the linking and supporting of adjacent spans also plays a role in the analysis of the forces. A span may be simply supported and rest on a pile cap or bent with no additional supports (Figure 1- 16A). Longer spans may extend over several bents or pile caps, creating an indeterminate system of forcing with variable structural characteristics (especially in terms of natural frequency). These are often referred to as a continuous span (Figure 1- 16B). In rare cases, some spans are unsupported supported only by connections to the two adjacent spans (Figure 1- 16C).

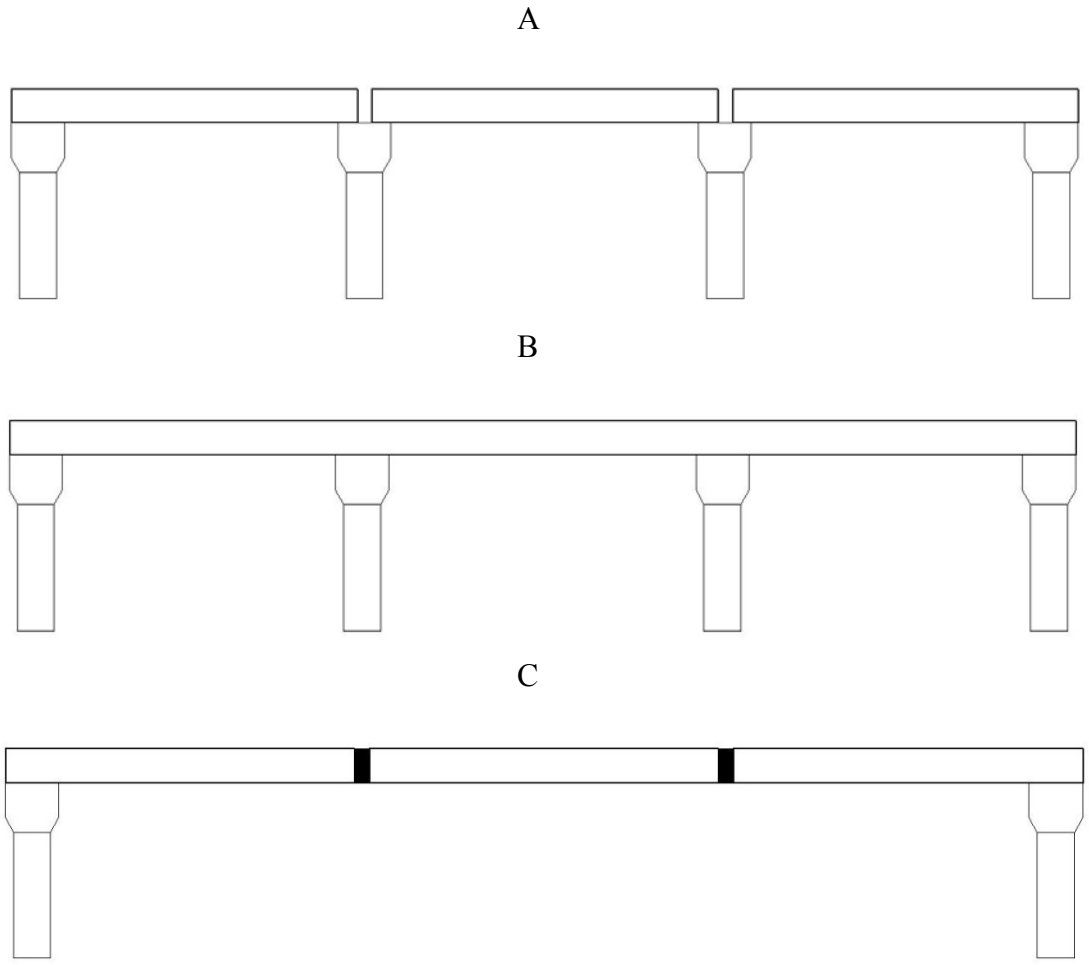

Figure 1- 16 Common pile-support setups for bridge superstructures. A) simple, B) continuous, C) linked.

Water Waves

One of the key differences between the problems of offshore structures and bridges is the characteristics of the wave field. Offshore structures are generally located in ‘deep’ water while bridges are located in areas of ‘shallow’ or ‘intermediate’ water.

The limits of these depth designations are based on the ratio of water depth (Z_D) and wave length (λ). These boundaries as applied to waves affect certain properties of the wave field. In deep water, wave particles travel in circular motions while these motions flatten into ellipses as the wave propagates into shallow water. Wave lengths also shorten during the change from deep to shallow water and the wave shoals, altering the wave height and steepness which leads to

breaking. Lastly, wave celerity while variable in deep water, is only a function of water depth in shallow water.

As will be seen later, the effects of individual particle kinematics, wave length, and wave celerity play important roles in the loading experienced by a structure during wave inundation. So the differences inherent to the variation between offshore and nearshore wave climates also become important. For the majority of bridge locations, a structure susceptible to wave attack will be in intermediate water depths.

Another wave concept that is important in the study of wave loading is that of dispersion. In reality, a wave group consists of many waves of varying heights and frequencies propagating at assorted velocities in multiple directions. The distribution of wave heights and therefore wave energy can be quantified with directional wave energy density spectra diagrams. This energy content of a wave spectrum is critically different from offshore to nearshore. In the deepwater realm, ocean swell (very large period waves) can make up a significant portion of the energy content. In the nearshore, the swell is negligible, and in the case of protected water bodies completely absent. For the case of bridges then, the wave spectrum is composed entirely of shorter locally wind generated waves.

Wave/Structure Interaction

It is important to understand some of the key basic ideas that play a significant role in the wave loading. A significant amount of variation in the forcing magnitude and distribution occurs according to the ranges within these concepts. Each are looked at in more detail in subsequent sections.

Vertical wave force

A wave propagates into a suspended structure, inundates it, and propagates away from it. In the majority of the literature, a generalized forcing time series over this interaction was consistently found by the researchers. An example of this forcing is presented in Figure 1- 17. Two separate forcing mechanisms working at significantly different frequencies can be seen. As the wave first strikes the structure a large magnitude short duration force occurs, followed by a slowly building positive force as the wave enters the structure. As the wave propagates away from the structure,

the force becomes negative, though not as large in magnitude as the positive value (due to the absence of buoyancy and the dissipation of wave energy).

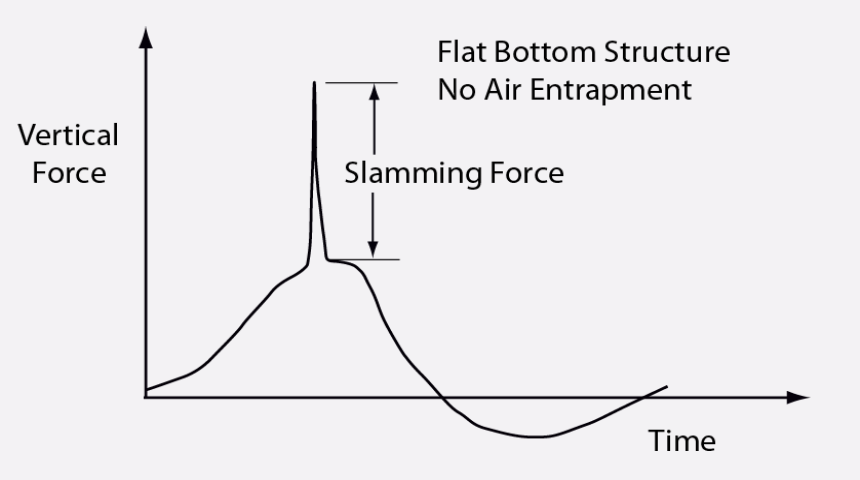

Figure 1- 17 Typical vertical wave force versus time plot for a subaerial, flat-bottomed structure.

The large short-duration, high frequency spike is often referred to as the slamming force or the impact force. It occurs during the initial contact between the structure and the air/water interface where a large exchange of momentum takes place very quickly.

The slowly varying force is sometimes referred to as the quasi-static force. It occurs over the full inundation cycle of the structure by the wave and has a forcing frequency nominally equivalent to the wave frequency. It is not a single forcing source, but rather is composed of several independent forcing contributions.

For the quasi-static force naming convention to hold true, the frequency that these forces act at must be significantly lower than the natural frequency of the structure. If the two frequencies are satisfactorily different, the loads can in essence be treated as static loads because no dynamic effects will be induced. While these forces will always act at the frequency of the wave, the natural frequency of the structure must be analyzed to determine if the ratio of frequencies between the two is suitably small.

For the remainder of this work, the mechanisms of forcing will be referred to by separate terms. The short-duration (high frequency forcing) is referred to as the s*lamming* force, a force that is

highly variable and susceptible to the natural response characteristics of the structure, wave shape, and structure shape. The slowly-varying force is referred to as the *quasi-static* force, but is subdivided into three separate components. They are the *buoyancy* force, consisting of the purely hydrostatic variation throughout the water column, the *drag* force, consisting of the pressure drag and skin friction, and the *inertia* force, consisting of the momentum driven forces.

The slamming and quasi-static forces are different forcing mechanisms and will be discussed separately in Chapter 3.

The clearance height (Z_c) of the structure is the distance between the still water level (SWL) and the lowest chord of the structure (when SWL is referred to, it includes all contributions from storm surge, wind setup, and tides). For a girder and slab bridge, the base of the girder would constitute the lowest chord.

Unique to this work is the inclusion of negative clearance heights. In all reviewed work, the level of water in the vicinity of the structures was always below or right at the lowest chord of the structure. However, the recent storms and failures have produced situations of submerged and partially submerged structures.

These instances of negative clearance are important because they produce a different typical force curve (Figure 1- 18). The slamming force decreases as the vertical clearance the wave and the underside of the structure is reduced and the negative forces become generally larger in magnitude. An understanding of the transition in forcing between the submerged and subaerial cases is vital, since a structure may actually be less vulnerable to failure if the storm surge is high enough to partially submerge the structure due to the elimination of the slamming force.

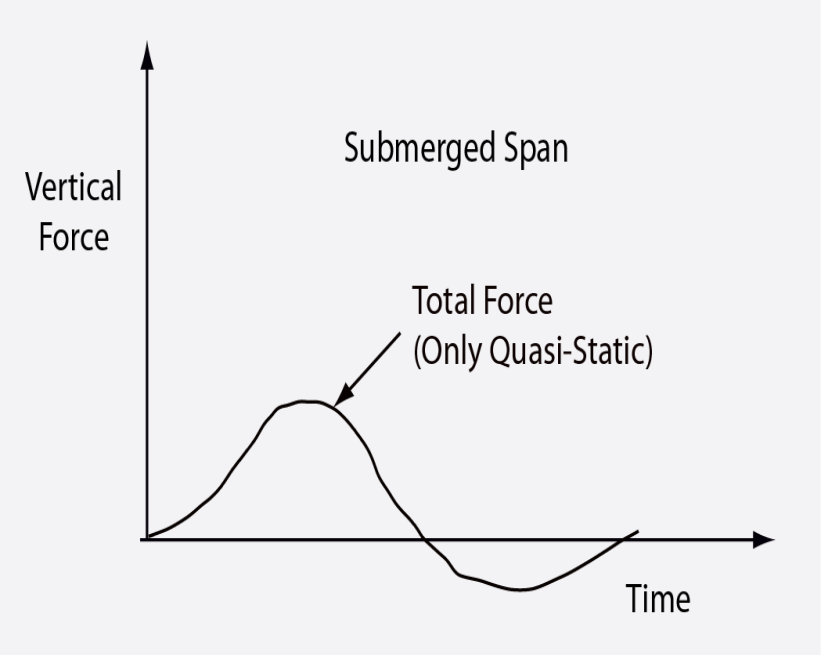

Figure 1- 18 Typical vertical wave force curve versus time plot for a submerged horizontal, flat bottom structure.

Air entrapment

The natural cavities created by the girders and diaphragms trap air as a wave propagates past the structure. The net effect of the entrapped air is an increase in the buoyancy force. Entrapped air also has a significant effect on the slamming force. The air entrapped between the girders acts somewhat like a spring in a spring-mass system when the superstructure encounters a wave. The magnitude of the slamming force is reduced and the duration is increased thus reducing its frequency. The actual frequency depends on the spacing of the girders and the celerity of the wave. The number of slamming oscillations in the total vertical force is the number of air cavities (number of girders minus one) as shown in the sketch in Figure 1- 19.

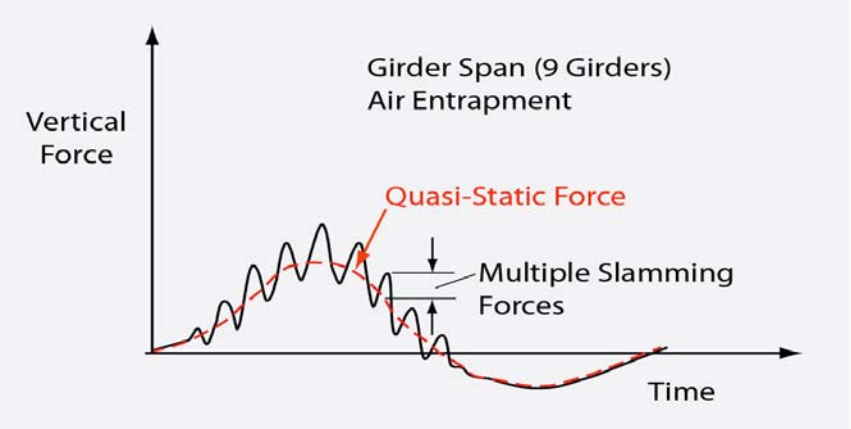

Figure 1- 19 Typical vertical wave force versus time plot for a subaerial structure with girders.

In the nearshore environment, both wave periods and wave lengths are generally smaller than their offshore counterparts. Unlike the offshore environment, this creates a forcing system where the structure and wave are of comparable size.

For a structure that is much smaller than the wave impacting it, there is very little variation in the kinematics of the wave over the length of the structure. This allows for the use of averaged velocities and accelerations and semi-uniform flow directions in offshore work. Because in the nearshore case the structure and the wave are of comparable size, the structure would experience a radically divergent kinematic field, creating coupled internal moments and other forcing dilemma. Figure 1- 20 shows the water particle velocity and acceleration magnitudes and directions throughout a progressive wave. Flow exists in all directions within the wave. As can be seen in Figure 1- 21 there is much greater variation in the flow field over the width of the nearshore structure at any point in time than there is for the structure in the offshore environment.

A

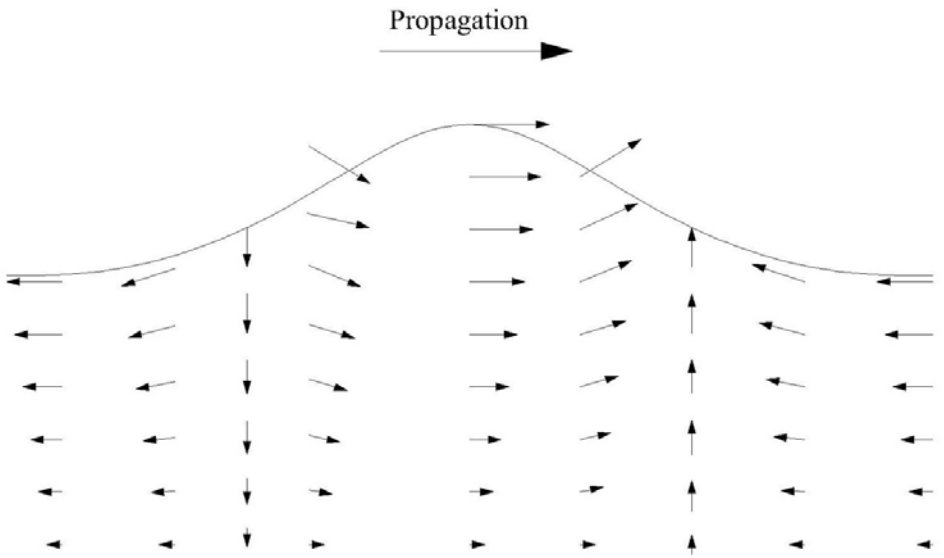

B

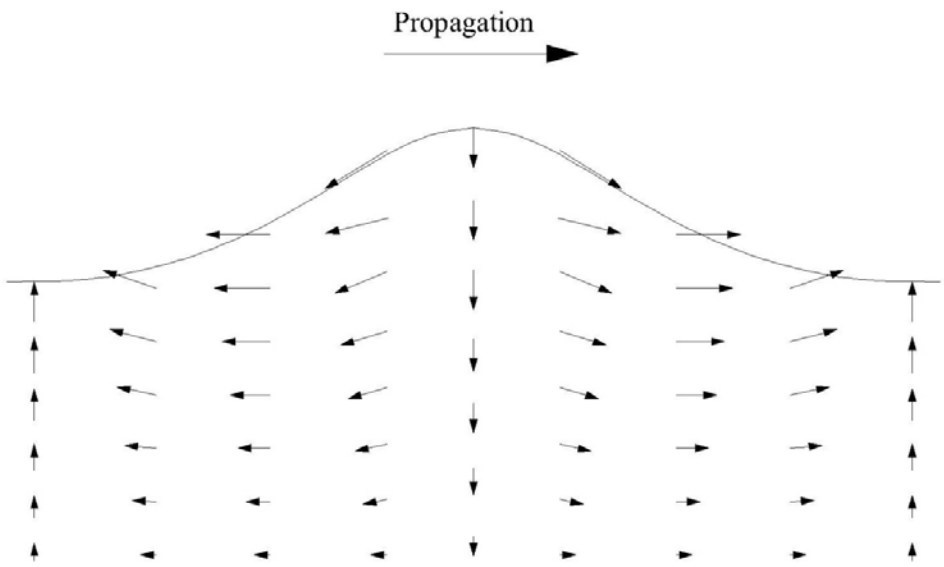

Figure 1- 20 Water particle kinematics in a progressive wave. A) velocity magnitudes and directions, B) acceleration magnitudes and directions.

A

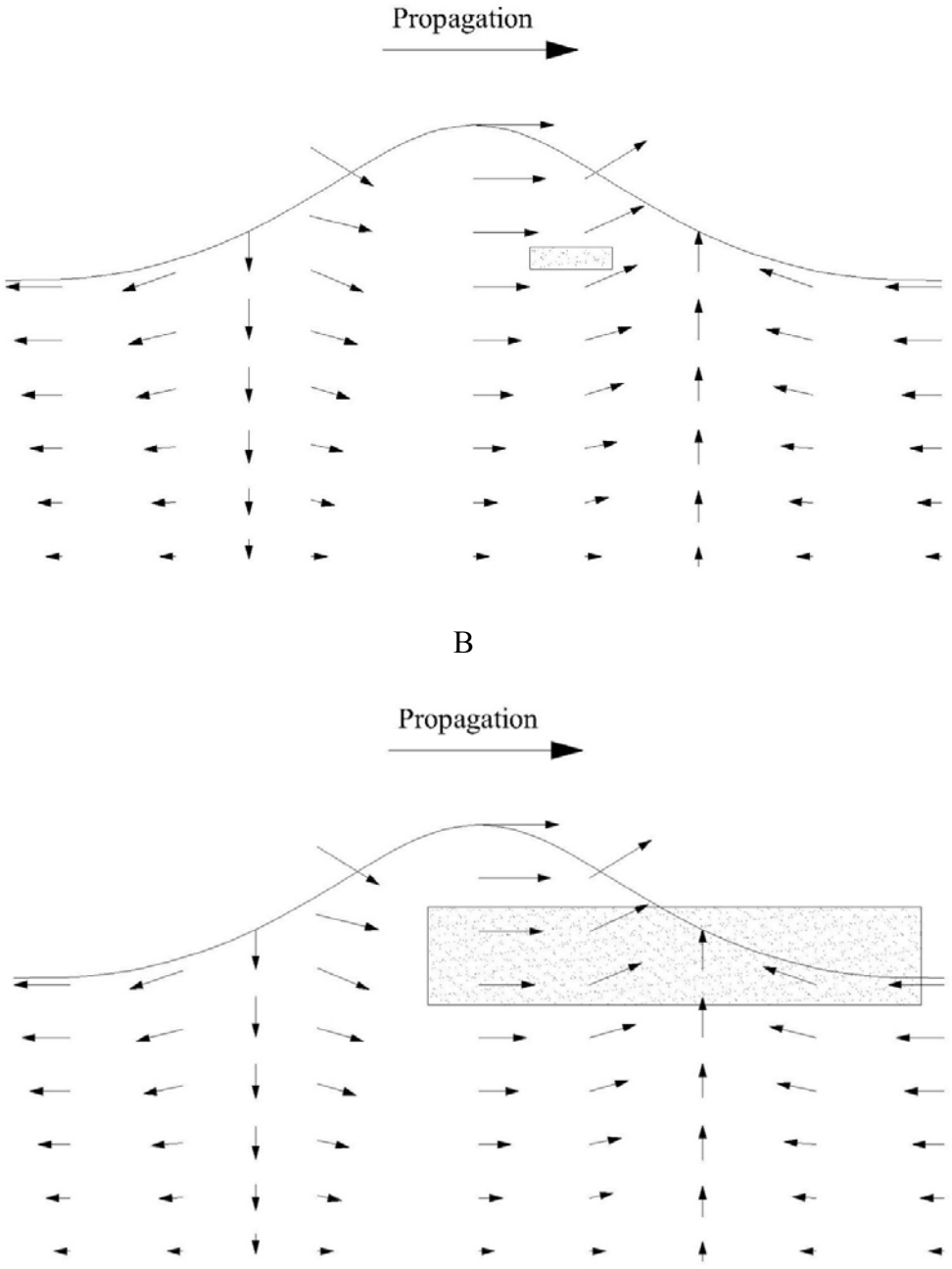

Figure 1- 21 Water particle velocities distribution over different size structures. A) structure width small compared to wave length, B) structure width comparable to wave length.

Another complexity resulting from a large structure width to wave length ratio is the effect of the structure on the wave. Alteration of the wave kinematics (velocities and accelerations) introduces errors in the theoretical model calculations which does not account for these effects.

Time dependent added mass

Because the structure is rarely (if ever) fully submerged by the wave, the added mass (or virtual mass) of the structure is in constant flux. The added mass is that mass of water beyond that displaced by the structure that is impacted by the structure. The time-varying nature of the added mass in the nearshore case adds an additional term to the time rate of change of the linear momentum. Because of this, accurate prediction of added mass quantities becomes essential.

There are, of course, other complicating aspects of the wave loading problem, but the ones outlined above are perhaps the more challenging from the standpoint of predictive model development.

Approach

A literature review on work related to wave forces on structures was conducted with emphasis on horizontal structures. The work of Morison, et al. (1950) and Kaplan et al. (1995) were most useful in the development of the theoretical model for wave forces on bridge superstructures in this study.

Following the literature review, a theoretical wave force model was developed which extended Kaplan's model to bridge superstructures located in coastal water environments. Physical model tests were performed in a wave tank to gain insight into the force mechanisms and to provide the information needed to compute empirical coefficients in the theoretical model.

The theoretical model was divided into two components 1) a component with the frequency of the wave (referred to as the quasi-static force and 2) a higher frequency component called the slamming force.

The wave tank tests started with a simple flat plate and progressed to model girder type bridge span with overhangs and rails. Adding components to the structure one at a time allowed the determination of the effect of that component on the forces. The progression of structures tested was as follows:

- A rectangular flat plate
- A rectangular slab of finite thickness

- A beam and slab bridge (no overhangs and no rails)
- A beam and slab bridge (with overhangs and no rails)
- A beam and slab bridge (with overhangs and with rails)

In this progression, two of the Florida coastal bridge types are covered (the slab and the beam and slab). While the segmental box girder span was not tested, it is basically a thick slab type bridge with slightly sloped sides and overhangs. The initial investigation of the flat plate was carried out by Marin (2009) and the basics of that study are summarized in Chapter 2.

In each set of tests, the structure elevation, water depth, and wave parameters were varied to cover a wide range of conditions. Three component load cells and pressure transducers were used to measure the forces and pressures. The range of the parameters covered by the tests is given in Table 4- 2 in Chapter 4.

The theoretical model was used to produce data needed in the development of parametric equations for computing horizontal and vertical wave forces and moments on bridge superstructures included in the AASHTO "Guide Specifications for Bridges Vulnerable to Coastal Storms."

CHAPTER 2 - LITERATURE REVIEW

Prior to the recent resurgence of interest in the topic, only two studies (Denson 1978, 1980) can be found that investigate the effects of vertical wave forces on bridge decks. In general, there are very few studies that consider vertical forcing on any structure that is of comparable width to the wave length.

While much work has been done on horizontal wave loading on structures, the work on vertical loading is limited. The majority of this work comes from aspects of wave loading on offshore platforms located in deep unprotected waters.

There has, however, been some work on wave loading on bridge deck-like structures as outlined below.

Previous Work on Wave Loading on Bridge Superstructures

The only studies found that dealt with wave forces on bridge superstructures are those by Denson (1978, 1980). Both papers were purely empirical physical model studies. The deficiencies of both papers are documented by Douglass el al. (2006), but in brief, Denson (1978, 1980) contains several significant flaws:

- The importance of wave period (only a single value was used in testing) and wavelength on the forcing was dismissed as insignificant due to the shallow-water environment.

- While the works of El Ghamry (1963, 1971), French (1970, 1979), and Wang (1970) were already published, Denson (1980) stated that no useful papers could be found as these papers referred to offshore structures.

- The differentiation (or even the existence) of the forcing mechanisms into a slowly-varying force and a short-duration slamming force was never made, despite the consensus in the rest of the literature. That the separation was never found in the raw data suggests severe problems in the instrumentation setup or the sampling frequency (indeed, the lone graph of raw data shows no higher frequency contributions).

- No model similitude or scaling is discussed. If scaling is carried out, then the test wave period of 3 sec would correspond to almost a 15 sec period in the prototype, a ridiculously unrealistic wave in bays or shallow water.

- For dimensional considerations, Denson (1980) states that the choice of a significant length parameter does not affect the results, only the shape of the plot, i.e. the width, length, and thickness of the structure are interchangeable quantities.

- There are large discrepancies between the measured forces of Denson (1978) and Denson (1980), the explanation of which is the inclusion of diaphragms in the later tested models.

These problems inherent to the study severely limit the usefulness and even question the validity of the presented results.

Denson (1978)

Denson (1978) experimentally examined forces on a slab and beam type bridge. The work was motivated by the damage to the Bay St. Louis Bridge in Mississippi caused by surge and wave action from Hurricane Camille. Denson (1978) states that no useful previous papers related to the topic could be found.

Physical model testing was carried out in a 44 ft long, 2 ft wide wave basin at Mississippi State University. A scale model (1:24) of the Bay St. Louis Bridge was subjected to monochromatic waves (all normal to the structure) with a range of wave heights, water depths, and clearance heights relative to SWL (some tests were done with a partially submerged structure). Only a single wave period (T = 3.0 s) was used. Strain gauges were used to record vertical and horizontal forces and moment.

No mention of filtering or description of the features of the physical model data is given. Maximums in the vertical and horizontal direction are referred to as lift force (F_L) and drag force (F_D), respectively. These measured forces were non-dimensionalized by γW^2 and maximum moments (M) were non-dimensionalized by γW^3 to produce forces per unit width. The non-dimensionalized forces and moments were then plotted against three parameters (Equation 2-1), where γ is the unit weight of water, Z_d is the water depth, Z_c is the clearance height of the bridge

relative to SWL, W is the width of the bridge parallel to wave propagation, and H is the wave height.

$$\frac{F_L}{\gamma W^2}, \frac{F_D}{\gamma W^2}, \frac{M}{\gamma W^3} = f\left(\frac{Z_d + Z_c}{W}, \frac{Z_d + Z_c}{Z_d}, \frac{H}{Z_d}\right) \quad (2\text{-}1)$$

The series of plots created were then offered as design curves. Denson (1978) concluded that the failures were mainly caused by the rolling moment and could have been avoided by using slightly larger anchoring systems.

Denson (1980)

Denson (1980) continued the experimental work of Denson (1978). Along with the beam and slab model (1:24) of the Bay St. Louis Bridge, a box-girder model (1:24) of an I-110 connector was also tested. The physical model tests were performed in a 40 ft. long, 16 ft. wide wave basin at Mississippi State University.

The models were struck with monochromatic waves with a range of wave heights, water depths, clearance heights relative to SWL (some tests were done with a partially submerged structure), and wave incidences. Only a single wave period (T = 3.0 sec.) was used as Denson (1980) refers to the wavelength and period as *insignificant* for shallow water waves. Vertical and horizontal forces and moments were measured using a single 6-axis strain gauge. 3D measurements were considered.

Maximum positive and negative forces in the vertical and horizontal direction are referred to as lift force (F_Z) and drag forces (F_X, F_Y), respectively. These measured forces were non-dimensionalized by γW^3 and maximum positive and negative moments (M) were non-dimensionalized by γW^4. The non-dimensionalized forces and moments were then plotted against three parameters (Equation 2-2), where γ is the unit weight of water, Z_d is the water depth, Z_c is the clearance height of the bridge relative to SWL, W is the width of the bridge parallel to wave propagation, H is the wave height, and θ is the angle of incidence of the wave.

$$\frac{F_{X,Y,Z}}{\gamma W^3}, \frac{M}{\gamma W^4} = f\left(\frac{Z_d + Z_c}{Z_d}, \frac{H}{Z_d}, \theta\right) \quad (2\text{-}2)$$

The series of plots created were then offered as design curves. The effect of angle of incidence was found to lessen the maximum forcing with increased angle (a wave propagating normal to the bridge is the most conservative case). Denson (1980) concludes that inexpensive anchorage systems will prevent failure.

U.S. Army Corp of Engineers (2006)

The Coastal Engineering Manual (CEM) by the U.S. Army Corps of Engineers (2006) breaks up the case of a horizontally oriented structure into two separate groups: submerged (or partially submerged) structures and emergent (sub aerial) structures. For a submerged structure, forces are calculated using a lift-based flow relationship (Equation 2-3) with the force (F_L) proportional to the square of the horizontal water velocity (u). An empirically determined lift coefficient (C_L) for each structure of interest and the projected horizontal area (A) is required.

$$F_L = C_L A\gamma\left(\frac{u^2}{2g}\right) \tag{2-3}$$

For an emergent structure, vertical forces (F_S) are calculated using a single slamming-type relationship (Equation 2-4) with the force proportional to the square of the vertical water velocity (w). Again, an experimentally determined coefficient (C_S) for each structure and the projected horizontal area of inundation (A) is required.

$$F_S = C_S A\gamma\left(\frac{w^2}{2g}\right) \tag{2-4}$$

Due to the limited work done on the topic, the Coastal Engineering Manual recommends the use of problem-specific numerical and physical modeling for the purposes of design.

Morison et al. (1950)

The Morison Equation was developed by Morison et al. (1950) for computing wave forces on a single vertical pile. Calculation of the forces using the Morison Equation requires an analytical model for the wave kinematics and empirically determined drag and inertia coefficients. Key to the validity of this equation is accurate wave field kinematics and accurate coefficients.

Versions of this equation have been used by the offshore industry for a number of years. Application is limited to cases where the elements and structures are slender when compared to the lengths of the waves encountered.

Previous Work on Offshore Platforms and Decks

The amount of work done on offshore platforms in the area of wave forcing on suspended elements is extensive, though the majority of this work is dedicated to cylindrical components. The works investigated here were limited to those dealing specifically with deck or platform like structures with a horizontal orientation. Limitations of work done in the genre include a deep water environment and wave/structure size ratios that are very small. Also, outside of the cylindrical elements, very little work was done on structures of finite thickness.

Kaplan (1992)

Kaplan (1992) further expanded the work done by Kaplan (1979) on wave forcing on suspended cylindrical elements and extended the basis of that work to suspended horizontal flat platform decks. For the flat decks, no experimental testing or comparisons were carried out.

The proposed theoretical model for vertical wave forces on horizontal decks was briefly described as the sum of the momentum and drag forces. The time derivative of the momentum contribution was taken and produced two separate components due to the intermittent submergence of the structure by the wave. This variation in inundation produces a variable added mass component which dictates the need for a theoretical added mass term (Equation 2-5) where L is the length of the structure (perpendicular to the propagation direction of the wave), $\bar{W}$ is the wetted width of the structure (parallel to the propagation direction of the wave), and ρ is the fluid density.

$$\text{Added Mass} = \rho \frac{\pi}{8} L \bar{W}^2 \tag{2-5}$$

The momentum was combined with a standard representation of the drag force (where C_D is the drag coefficient), giving the expression for the total vertical forcing (Equation 2-6). It is noted that the time derivative of the added mass expression is part of the equation.

$$\text{Total Vertical Forcing} = \rho\frac{\pi}{8}L\bar{W}^2\frac{\partial v}{\partial t} + \rho\frac{\pi}{4}L\frac{\partial \bar{W}}{\partial t}v + \frac{1}{2}C_D\rho L\bar{W}v|v| \tag{2-6}$$

Several remarks are made by Kaplan (1992). The terms involving the time derivative of the wetted width was only applied until the value first reached zero, at which point its use is discontinued regardless of later values. Since the model being treated was that of a plate of negligible thickness, neither buoyancy nor the mass of the plate itself is included. Also, the wave is considered long compared to the dimensions of the plate so no variability of the kinematics inside the wave is considered. The model represented is that of an infinitely long plate.

Kaplan et al. (1995)

Kaplan et al. (1995) expanded on the methods described by Kaplan (1992) for predicting the wave forcing on suspended cylindrical elements and suspended horizontal platform decks of negligible thickness. The expanded theoretical model is presented and compared with physical model test data to assess prediction capability.

From Kaplan (1992) the theoretical model was extended to situations of plated decks with finite aspect ratios. The total vertical forcing (F_V) was described as the combined sum of the change in momentum and drag effects (Equation 2-7), where ρ is the water density, L is the length of the structure perpendicular to the direction of wave propagation, $\bar{W}$ is the wetted width of the structure parallel to the direction of wave propagation, v is the vertical water particle velocity, dv/dt is the vertical water particle acceleration, C is the wave celerity, C_D is the drag coefficient, and A is the projected area in the vertical direction.

$$F_V = \rho\frac{\pi}{8}\frac{L\bar{W}^2}{\sqrt{1+\left(\frac{\bar{W}}{L}\right)^2}}\frac{\partial v}{\partial t} + \rho\frac{\pi}{4}\bar{W}LC\frac{1+\frac{1}{2}\left(\frac{\bar{W}}{L}\right)^2}{\left[1+\left(\frac{\bar{W}}{L}\right)^2\right]^{3/2}}v + \frac{1}{2}C_D\rho Av^2 \tag{2-7}$$

For the change in momentum, a modification to theoretical prediction of the added mass was needed for use with structures of finite measurements. For a thin plate, an expression derived by Payne (1981) was used (Equation 2-8) with variables as previously defined.

$$\text{Added Mass} = \rho \frac{\pi}{8} \frac{L\overline{W}^2}{\sqrt{1+\left(\frac{\overline{W}}{L}\right)^2}} \tag{2-8}$$

Equations are similarly defined for the total horizontal forcing (Equation 2-9) with an associated horizontal added mass (Equation 2-10), where c is the wetted vertical height of the structure, $\dot{c}$ is the time rate of change of the vertical wetted height, u is the horizontal water particle velocity, and $\dot{u}$ is the horizontal water particle acceleration.

$$F_H = \frac{2}{\pi}\rho c^2 L\dot{u} + \frac{4}{\pi}\rho c L \dot{c} u + \frac{1}{2} C_D \rho c L u^2 \tag{2-9}$$

$$\text{Added Mass} = \rho \frac{2}{\pi} c^2 L \tag{2-10}$$

In evaluating these equations, linear theory was used as applicable use was determined to be in very deep water with non depth limited waves. The theoretical model was compared with experimental data obtained from studies of offshore platform models (Murray et al. 1995). Agreement between measured and predicted forces was good in all cases except where additional structures in the wave field in front of the test platform caused significant diffraction.

Suchithra and Koola (1995)

Suchithra and Koola (1995) examined the forces acting on a horizontal slab for regular and freak waves. Physical model tests were done at the Ocean Engineering Centre at the Indian Institute of Technology, Madras, India in a 10 m long, 0.3 m wide wave tank.

The model slab was 0.25 m long, 0.25 m wide, 0.08m thick and made of Perspex. A series of tests were also run with girder-like stiffeners beneath the slab running in the longitudinal, lateral, and both longitudinal and lateral directions. Measurements were taken with a single load cell sampled at 1000 Hz. Tests were done for a range of wave periods and clearance heights relative to SWL (no tests were done with submerged or partially submerged slabs). In the data and the discussion of the data no mention is made of the division of the forcing into a slowly-varying force and a short duration force.

The predictive relationship developed for the maximum forcing (F_s) is given in Equation 2-11 where ρ is the fluid density, A is the area of contact, V is the vertical water particle velocity, and C_s is an empirical coefficient. This equation is referred to as a slamming equation.

$$F_s = \frac{1}{2} C_s \rho A V^2 \tag{2-11}$$

A formula for the coefficient, C_s, is given in Equation 2-12 where Z_c is the clearance height relative to SWL, λ_0 is the deep water wave length, and C_{ns} is a modified coefficient of singular value based on the clearance height. No method for obtaining C_{ns} is given.

$$C_s = C_{ns} \frac{\lambda_0}{Z_c} \tag{2-12}$$

Suchithra and Koola (1995) state that the wave period and the clearance height are the only variables that have an effect on the forcing magnitude. For tests done with the direction stiffeners, it was noted that the slamming force was noticeably reduced due to the presence of trapped air and it is suggested that adding air pocketing structures would reduce the forcing on horizontal slabs.

Bea et al. (1999)

Bea et al. (1999) concentrated on offshore platform decks that were suspended beneath the structure, specifically dealing with failed decks in the field. Data was compared from laboratory tests for wave forces on offshore platforms (Finnigan and Petrauskas 1997; Dean et al. 1985; Faltinsen et al. 1977; Jue 1993; Kjeldsen and Myrhaug 1979; Kjeldsen and Hasle 1985; Kjeldsen et al. 1986; Weggel 1997) with the guidelines of the American Petroleum Institute. The current methods were found excessively conservative and more extensive work and modifications to the guidelines were recommended.

An analytical model was presented as the sum of forcing components (Equation 2-13) similar to those derived from the Morison equation by Kaplan et al. (1995). While vertical components are discussed, the decks in question were porous or grated, so the concentration of the work was aimed at the horizontal component of the forcing. Fifth (5^{th}) order Stokes wave theory was used to compute the wave kinematics.

$$F = F_{Buoyancy} + F_{Slamming} + F_{Drag} + F_{Lift} + F_{Inertia} \quad (2\text{-}13)$$

Each component of the total forcing was then developed. The drag term (Equation 2-14) was identical to that given by Kaplan et al. (1995). The inertia term (Equation 2-15), though, contained neither a time dependent mass term nor the added mass itself in the calculation, instead basing the calculation on the volume of the structure (~~V~~), the water particle acceleration ($\dot{u}$), and a mass coefficient (C_M). A lift term was also included (Equation 2-16) where C_L is a lift coefficient and A is the projected area.

$$F_{Drag} = \frac{1}{2}\rho C_D A u^2 \quad (2\text{-}14)$$

$$F_{Inertia} = \frac{1}{2}\rho C_M \text{~~V~~}\dot{u} \quad (2\text{-}15)$$

$$F_{Lift} = \frac{1}{2}\rho C_L A u^2 \quad (2\text{-}16)$$

A slamming force equation with the force proportional to the square of the water velocity was also developed (Equation 2-17) using an empirical slamming coefficient (C_S).

$$F_{Slamming} = \frac{1}{2}\rho C_S A u^2 \quad (2\text{-}17)$$

While the equation itself was simple, the importance of the dynamic characteristics of the structure and the wave were also included by using a multiplication factor to give an 'effective' slamming force. This required knowledge of the structure's primary modes of vibration as well as the frequency of the slamming force among other variables. No method was provided for estimating these variables for the purposes of design.

The analytical models were evaluated numerically and compared with results from field data (Stear and Bea 1997; Imm et al. 1994; Cardone and Cox 1992; Vannan et al. 1994) for existing structures that had been subjected to wave loads. The horizontal force predictions were found to be extremely conservative. Further comparisons were made in Bea et al. (2001), though no changes to the analytical model were described.

Baarholm and Faltinsen (2004)

Baarholm and Faltinsen (2004) performed a numerical and experimental study on the vertical wave force on an offshore platform. Physical model tests were carried out at the Department of Marine Hydrodynamics, NTNU, Trondheim, Norway in a 13.5 m long, 0.6 m wide wave tank. The model was a box-shaped deck that spanned the full width of the tank with two vertical plates attached to the front and back of the deck to prevent any overtopping. Regular waves were used in the experiments.

In the measured data, a difference in the impact process was found between a slowly-varying force and a short duration force of significant magnitude. The short duration force was ignored in the study. Interestingly, measured negative magnitudes were large than the positive magnitudes.

The theoretical model devised was the 2D Laplace equation with dynamic (Bernoulli) and kinematic free surface boundary conditions. No bottom boundary condition was used as the water depth was assumed to be deep enough relative to the wave length to ignore. An additional boundary condition of a non-permeable structure was used.

The boundary value problem is solved numerically three separate ways, a Wagner-based method (Wagner 1932) that solves the perturbation velocity potential and two variations of a boundary-element method that uses Green's second identity (Faltinsen 1977) that solves the total velocity potential. The method described by Kaplan et al. (1995) is recommended for the propagation of the wave away from the structure when using the Wagner-based method.

The boundary-element methods showed excellent agreement to the experimental data for the single plot showed. A nearly identical study was done by Lai and Lee (1989).

Previous Work on Open Coast Jetties

Open coast jetties (not to be confused with jetties used in coastal shore management) are used for berthing and the loading and offloading of tankers and other sizable craft. These structures consist of deck or dock-like platforms suspended over supportive piles and occasionally beam or girder-like elements. Previous works on these structures have the same limitations as those on offshore platforms.

Overbeek and Klabbers (2001)

Overbeek and Klabbers (2001) were involved in the analysis and design of two jetty-type structures in the Caribbean. For a given design wave climate, they examined the existing literature and used simple methods for vertical force predictions. The two jetties summarily experienced significant wave action due to Hurricanes Iris, 1995, and Lenny, 1999. For Iris, design conditions were not reached. For Lenny, design conditions were believed to be exceeded.

100 years of statistical data was used to determine the design event for each structure. The prediction of the vertical forcing for the given conditions was divided into a slowly-varying pressure and an impact pressure. For the slowly-varying case, a simplistic hydrostatic pressure expression (Equation 2-18) similar to Wang (1970) and French (1970) was used, where P_{ve} was the maximum pressure, ρ was the fluid density, g was gravity, H_{cr} was the elevation of the wave crest above SWL, and d_c was the clearance of the deck above SWL.

$$P_{ve} = \rho g\left(H_{cr} - d_c\right) \tag{2-18}$$

For the impact pressure, another simplistic expression (Equation 2-19) was used, where P_{ve} was the maximum pressure, ρ was the fluid density, g was gravity, H_{max} was the maximum wave height, and c was an empirical coefficient. This equation was taken from Goda (2000).

$$P_{ve} = c\rho g H_{max} \tag{2-19}$$

Both jetties sustained significant damage including missing spans, excessive concrete spalling and tension cracks. Pressure vents and blowout panels were thought to have reduced the loading experienced even though failure occurred. The authors concluded that further work on the topic with practical guidelines was needed.

Tirindelli et al. (2002)

Tirindelli et al. (2002) investigated the current design methods for wave forcing on shipping jetties and performed experimental testing with which to compare the predictive capabilities of those methods. The three methods centered upon were those of Kaplan et al. (1995), Shih and Anastasiou (1992), and Bea et al. (1999).

Physical model tests (1:25) were conducted at a wave tank at HR Wallingford in the United Kingdom. Random waves were used following a JONSWAP spectra with vertical and horizontal measurements taken via four load cells attached to standalone elements within the model. Two separate water depths (0.60 m, 0.75 m) and four separate clearance heights from still water level (0.01 m, 0.06 m, 0.11 m, 0.16 m) were used (no submerged or partially submerged tests were done). Three separate model setups of a flat deck, a deck with beams, and a deck with beams and vertical side panels were also used. The vertical side panels were thought to prevent any effects or 3D flow effects (no setup extended the full width of the tank).

Analysis of the data and comparisons to it were done for the slowly-varying force only. The data exhibited considerable scatter, though it was concluded that both the vertical and horizontal maximum forces (positive and negative) varied linearly with the wave height. There was no consideration of the importance of period or wavelength. Comparisons with the data were made with the models of Kaplan et al. (1995) and Shih and Anastasiou (1992). Both models significantly under predicted versus the experimental data.

It should be noted that the authors of the paper erroneously applied the equations of Kaplan et al. (1995) by dropping the leading inertia term of the model, which was mistaken for a slamming term. Also of note are the input parameters for the given comparisons. The significant wave height (H_s) was used as input for the models while the models were being compared against the average of the 4 highest magnitude forces in 1000 waves ($F_{1/250}$). It would be expected then that the predictive capabilities of a model for $F_{1/250}$ using $H_{1/3}$ (which is H_s) would be poor.

McConnell et al. (2003)

McConnell et al. (2003) builds on the work presented by Tirindelli et al. (2002), breaking down and analyzing the experimental data collected to produce a system of predictive relationships.

Physical model tests (1:25) were conducted at a wave tank at HR Wallingford in the United Kingdom. Random waves were used following a JONSWAP spectra with vertical and horizontal measurements taken via four load cells attached to standalone elements within the model. Two separate water depths (0.60 m, 0.75 m) and four separate clearance heights from still water level (0.01 m, 0.06 m, 0.11 m, 0.16 m) were used (no submerged or partially submerged tests were

done). Three separate model setups of a flat deck, a deck with beams, and a deck with beams and vertical side panels were also used. The vertical side panels were thought to prevent any effects or 3D flow effects (no setup extended the full width of the tank).

In the analysis of the data, the paper concentrates on slowly-varying data (referred to as the *quasi-static* force) while the short-duration slamming force data is analyzed by Cuomo (2003). The significant forces derived were taken as the average of the 4 largest magnitude loads in 1000 waves ($F_{1/250}$). The horizontal and vertical forces were then non-dimensionalized by a *basic wave force* (Equation 2-20, Equation 2-21a, and Equation 2-21b) derived from hydrostatic principles in the vein of Wang (1970) and French (1970). In the basic wave force equations, η_{max} is the maximum wave crest elevation, b_w is the element width, b_l is the element length, b_h is the element depth, c_l is clearance above SWL, p_1 is the hydrostatic pressure at the top of the element, and p_2 is the hydrostatic pressure at the bottom of the element.

$$F_v^* = b_w b_l p_2 \tag{2-20}$$

$$F_h^* = b_w \left(\eta_{max} - c_l\right)\frac{p_2}{2} \qquad \text{for } \eta_{max} \le c_l + b_h \tag{2-21a}$$

$$F_h^* = b_w b_h \frac{p_1 + p_2}{2} \qquad \text{for } \eta_{max} > c_l + b_h \tag{2-21b}$$

Once the forces were non-dimensionalized, they were plotted against a single non-dimensional parameter, $(\eta_{max} - c_l)/H_s$, and best fit regression lines were fitted to each data set (positive vertical quasi-static force, negative vertical quasi-static force, positive horizontal quasi-static force, negative horizontal quasi-static force). From these fits, a general empirical relationship was developed (Equation 2-22), though it was noted that the data exhibited a significant degree of scatter. Tables for empirical coefficients, a and b are given in McConnell et al. (2003) for the setups tested.

$$\frac{F_{qs}}{F^*} = \frac{a}{\left[\dfrac{\left(\eta_{max} - c_l\right)}{H_s}\right]^b} \tag{2-22}$$

Several case studies were then worked with the developed equations. In the case studies where failures occurred, the quasi-static forces obtained from Equation 2-22 did not always predict those failures, a fact explained away as the contribution of the slamming force, stating that slamming forces may be up to 4 times greater than quasi-static vertical forces, the application and determination of which is not provided.

This study does not include the effects of the wave period or the wave length on the forcing. Also, all predictive forces are based on the experimental extrapolation of the forcing experienced by two instrumented elements of the model structure rather than the structure itself. By assuming the loading on the structure is uniform over the entire structure, application is limited to scenarios where the structure is much smaller than the wave.

Cuomo et al. (2003)

Cuomo et al. (2003) builds on the work of Tirindelli et al. (2002) by re-examining the short-duration vertical slamming force data. Wavelet analysis was described and used to filter out possible dynamic effects in the instrumentation.

With oscillations filtered out, the maximum vertical slamming forces (F_{max}) were non-dimensionalized by the positive vertical quasi-static force (F_{qs+}) of the corresponding test and plotted against the rise time (t_r) of the slamming force non-dimensionalized by the wave period (T). Envelope fits were done producing Equation 2-23, an empirical relationship for the slamming force. Coefficients, A and B, for the testing setups done are given by Cuomo et al. (2003).

$$\frac{F_{max}}{F_{qs+}} = A\left(\frac{t_r}{T}\right)^B \tag{2-23}$$

No method of obtaining the rise time of the slamming force was provided. Any oscillations in the time series data were attributed to the instrumentation rather than the possibility of resonant effects in the similarity of forcing frequencies and structure frequencies. Possible amplification of forcing magnitudes due to these similarities is not discussed.

Tirindelli et al. (2003)

Tirindelli et al. (2003) essentially reproduces the content of McConnell et al. (2003), with the exception of the means of non-dimensionalizing the significant forces.

The positive quasi-static force is non-dimensionalized by a buoyancy variant, $\rho g H_s A$ (where A is the projected area of interest). The positive data is still plotted against the relative clearance term, $(\eta_{max}-c_l)/H_s$. The negative quasi-static force is non-dimensionalized by what appears to be a shear drag term, $\rho C_o^2 A$. The negative data is plotted against the wave steepness, H_s/L_o (where L_o is the deep water wave length).

Brief discussions of the slamming force and the horizontal forcing also occur, with the importance of the wave period on forcing finally recognized. No equations are given.

Cuomo et al. (2007)

Cuomo et al. (2007) further expands on the work of McConnell et al. (2003), Tirindelli et al. (2003), and Cuomo et al. (2003). A brief description of the problem of offshore loading on jetties is given, followed by a description of the current predictive methods scattered throughout the literature. Particular attention is given to the methods described in Kaplan (1992) and Kaplan et al. (1995).

Working from the same experimental dataset of Tirindelli et al. (2002), the data was filtered using wavelet analysis (as described in Cuomo et al. 2003) to account for dynamic effects in the instrumentation. The forcing consisted of a short-duration slam force and slowly-varying quasi-static force. From this filtered data set, the values of the maximum positive and negative "quasi-static" force and the maximum slam force were signified. Each was calculated as the average of the 4 highest loadings experienced in 1000 waves ($F_{1/250}$). The wave field was composed of a JONSWAP spectrum.

The slowly varying forces were then plotted against $(\eta_{max}-Z_c)/Z_d$, a newly introduced parameter. Foregoing the power curve fits and the non-dimensionalizing basic wave force used in McConnell et al. (2003), the vertical and horizontal slowly-varying forces are now non-dimensionalized by $\rho g H_s A$ (a buoyancy based parameter) and linear fits are used for the

predictive relationships (Equation 2-24). No relationships for coefficients ‘a’ and ‘b’ in Equation 2-x were provided, though a table of values was given for the model setup.

$$\frac{F_{qs\text{-}1/250}}{\rho g H_s A} = a\left(\frac{\eta_{max} - Z_c}{Z_d}\right) + b \tag{2-24}$$

For the short-duration impact force, a straight multiplying factor relationship was developed based on the corresponding positive slowly-varying force (Equation 2-25). No relationship for coefficient ‘a’ was given, though a table of values for the model setup was given.

$$F_{slam\ 1/250} = aF_{qs+\ 1/250} \tag{2-25}$$

Comparisons between Equation 2-25 and select existing methods were calculated for the slowly-varying forces of the experimental data. Equation 2-25 showed better fit to the data than the other methods tested.

Da Costa and Scott (1988)

Da Costa and Scott (1988) examined the failure of the Jones Island East Dock in Milwaukee, Wisconsin, which failed under wave action from a moderate storm on Lake Michigan. The dock was a cantilevered concrete structure extending out from a vertical wall over the lake.

A hindcast was done to determine the wave characteristics and sea state. From this data it was found that the methods developed by El Ghamry (1971) and French (1979) failed to predict the failure of the dock for the given meteorological conditions. In analyzing the failure, it was determined that the short-duration slamming force was responsible for the failure as the dock was designed to withstand the slowly-varying wave forces. At the time, the conclusion was that no existing method was sufficient to predict slamming-type forces.

The backing vertical wall was thought to have produced standing wave effects and also contributed to the failure.

Sulisz et al. (2005)

Sulisz et al. (2005) conducted laboratory experiments and used theoretical methods to study the vibration of deck-like structures under the influence of progressive waves, building off the work

done with standing waves by Wilde et al. (1998). Physical model experiments were performed in 64 m long, 0.6 m wide wave tank at the Institute of Hydroengineering in Gdansk, Poland. The model was rectangular box composed of Plexiglas and stiffened internally by ribs. The support system was combination of strings and springs, while measurements were taken using accelerometers and wave gauges.

The structure was tested for free vibrations in air and submerged. Large variations were found in the vertical direction while the horizontal showed little variation between air and water. Forced vibrations were then measured from running waves past the structure. In the decomposition of the pressure transducer signals, significant forcing was found in the frequency of the wave period and in the structural frequency associated with the submerged structure.

Four distinct vibrating stages were found during the wave inundation cycle, none of which fall into the range of wave frequency. In the first stage, wave slamming induces very high frequency vibration in the structure as well as producing residual waves in the tank (some with acoustic frequencies). In the second stage, the structure vibrates at the free vibration frequency of the structure submerged in water. In the third stage, as water is shed from the structure, high frequency vibrations are sometimes produced again in the structure. In the fourth stage, the structure vibrates at the free vibration frequency of the structure in air.

Previous Work on Flat Plates and Docks

In the realm of nearshore structures, some work on dock structures has been done. In terms of experimental testing, the representative model used is almost always a flat plate. As a simple structure, a flat plate provides an excellent basis from which to build a work and test initial theories and their viability. Expansion from the thin plate model to fully realized bridge superstructure models, though, requires considerable work.

El Ghamry (1963)

El Ghamry (1963) studied vertical wave forces on docks and conducted physical model experiments in a 105 ft long, 1 ft wide wave tank at the University of California, Berkeley. A simple setup was used with the docks represented by pile supported rectangular horizontal decks.

A more complex model setup was also used with beamlike structures added to the underside of the deck to create airtight cavities.

In the tests, monochromatic waves were used and quantities of wave height, wave period, and the clearance of the deck above the waterline were varied (No tests were done with a submerged or partially submerged deck). Tests were done with both flat and sloping beds. Testing showed a slowly-varying force-time curve that changed greatly with the aforementioned wave characteristics, especially the wave period. Also shown in the data was an extremely high magnitude, short duration slamming force.

The short duration slamming forces were attributed to compression of trapped air between the structure and the wave. Data showed that the slamming forces in cases with air entrapment were an order of magnitude (in some cases two orders of magnitude) larger than those without air entrapment. This large discrepancy in the forces is suspected to be a dynamical error induced in either the model or the instrumentation (considering these ratios appear in no other experimental works). No equations or predictive methods were presented.

Wang (1970)

Wang (1970) studied vertical wave forces on horizontal plates and conducted physical model experiments in a wave basin at the Naval Civil Engineering Laboratory in Port Hueneme, California. In the tests, random waves generated from a central plunger were used with the model situated at four different locations spaced in an increasing radial line from the plunger. The waves used were meant to simulate explosion-generated waves. Wave heights ranged from 0.16 ft to 0.50 ft with the clearance height varied from 0 ft to 0.125 ft above SWL (no tests were done for submerged or partially submerged plates). Pressure transducers were used to measure pressures at various locations in the plate.

Testing showed a slowly-varying force along with a short-duration impact force. Wang (1970) produced Equation 2-26 for the slowly-varying force on the underside of the plate, where P is the maximum pressure, γ is the unit weight of water, η_{max} is the maximum wave crest elevation, Z_c is the clearance of the plate relative to SWL, and c is an empirical coefficient between 1 and 2.

$$P = c\gamma\left(\eta_{max} - Z_c\right) \tag{2-26}$$

The equation essentially stated that the forcing is proportional to the difference in hydrostatic pressure between the plate and the wave crest. For the short-duration impact force, Wang (1970) produced Equations 2-27 by taking the instantaneous change in momentum at the incipient moment of interaction between the wave and the plate for progressive waves. The mass used was that derived by Von Karman (1929) for landing seaplane floats.

$$\frac{P_i}{\gamma} = \frac{\pi}{2} H \tanh\left(\frac{2\pi h}{\lambda}\right)\sqrt{1 - \frac{4Z_c^2}{H^2}} \tag{2-27}$$

In Equation 2-27, H is the wave height, h is the water depth, λ is the wave length, Z_c is the clearance height relative to SWL, and γ is the unit weight of water. Wang (1970) recognizes the highly dynamic and complex nature of the impact force and recommends that a more precise and elegant method is needed. No comparisons are made.

French (1970)

French (1970) studied vertical wave forces on a flat horizontal plate. Physical model tests were conducted in 1.3 ft wide, 98 ft long wave tank at the California Institute of Technology. The model setup included a plate that spanned the full width of the tank. Monochromatic waves were used and tests were done with the properties of wave height, water depth, and clearance height from still water level varied. Wave period was not varied. Pressure transducers were used to measure pressures at various locations in the plate.

The data showed measurements similar to those of Wang (1970) with both a slowly-varying pressure and a short-duration, high magnitude slamming pressure. For the slowly-varying pressure, French (1970) concluded the maximum to be related to the hydrostatic difference between the wave crest and the plate clearance height from still water level, similar to the results of Wang (1970).

French (1979)

French (1979) studied vertical wave forces on a horizontal plate using a theoretical and experimental method. Physical model tests were carried out in a 30 m long, 0.4 m wide wave

tank. The model was an aluminum plate 13 mm thick, 1.5 m long, and 0.4 m wide (the plate spanned the full width of the tank), supported from above. To avoid any overtopping effects, a flat vertical plate was added to the upstream end of the plate.

Solitary waves were run past the plate for a range of wave heights, wave periods, water depths, and clearance height of the structure relative to SWL (no tests were done with a submerged or partially submerged plate). Pressures were measured with two pressure transducers mounted flush to the bottom of the plate. In the measured data there appeared two separate frequencies of forces, a slowly-varying extended force, and a short-duration peak pressure.

The predictive equations presented by French (1979) were based on Bernoulli flow principles and the conservation of mass and momentum. The peak pressure (P_{peak}) was equated to the stagnation pressure in steady flow (Equation 2-28) with the wave celerity (C) taking the place of the velocity component in the Bernoulli equation and the clearance height (Z_c) used as the elevation.

$$\frac{P_{peak}}{\rho} = \frac{1}{2}C^2 - gZ_c \tag{2-28}$$

The slowly varying force was divided into two individual components, the positive uplift pressure (P_{u+}) and the negative uplift pressure (P_{u-}). French (1979) used conservation of momentum, with the wave celerity as the characteristic velocity to produce Equation 2-29, where C is the wave celerity, Z_d is the water depth, Zc is the plate clearance relative to SWL, γ is the unit weight of water, g is gravity, W is the width of the plate, and x is the relative location of the wave front along the plate (measured from the leading edge of the plate).

$$\frac{P_u}{\gamma Z_d} = \frac{C^2}{gZ_d}\frac{\frac{Z_c}{Z_d}}{\left(1+\frac{Z_c}{Z_d}\right)^2} - \frac{Z_c}{Z_d}\frac{2+\frac{Z_c}{Z_d}}{2+2\frac{Z_c}{Z_d}} + \frac{(W-x)}{Z_d}\frac{\frac{Z_c}{Z_d}}{1+\frac{Z_c}{Z_d}}\frac{1}{g}\frac{dC}{dt} \tag{2-29}$$

The wave celerity was thought to be highly variable and follow conservation of mass once inundation occurred. Therefore, the wave celerity was a function of the clearance height (Z_c) and water depth (Z_d) and two separate celerities were used, C_p for positive pressures (Equation 2-

30a) and C_n for negative pressures (Equation 2-30b). In the equations, H is the wave height and η is the water surface elevation of the wave if the structure were not present.

$$\frac{C_p}{\sqrt{gZ_d}} = \frac{\eta}{Z_d}\left(\frac{1+\frac{Z_c}{Z_d}}{\frac{Z_c}{Z_d}}\right)\left\{1+\frac{H}{Z_d}-\frac{1}{2}\frac{H}{Z_d}\left(1+\frac{Z_c}{Z_d}\right)^2+\frac{\eta}{Z_d}\left[\frac{3}{4}\left(1+\frac{Z_c}{Z_d}\right)^2-\frac{7}{4}\right]\right\} \quad \text{(2-30a)}$$

$$\frac{C_n}{gZ_d} = \frac{Z_c}{Z_d}\left(1+\frac{Z_c}{Z_d}\right)\frac{2+\frac{Z_c}{Z_d}}{\left(1+\frac{Z_c}{Z_d}\right)\left(1+2\frac{Z_c}{Z_d}\right)} \quad \text{(2-30b)}$$

When compared to the experimental data, the equations produced excessively conservative predictions of the pressures.

Isaacson and Bhat (1996)

Isaacson and Bhat (1996) conducted a theoretical/experimental study of vertical forces on a rigid, suspended plate of negligible thickness. Physical model tests were done in 20 m long, 0.62 m wide wave tank at the Hydraulics Laboratory at the University of British Columbia.

The rectangular plate model did not extend the full width of the tank and was supported from above. Wave height, wave period, and clearance height relative to still water level were varied among the tests. Water depth was constant. Two load cells, one near the leading edge of the plate and one near the middle of the plate, were used to record the resulting forces. In total, 69 tests were performed (No tests were done for a submerged or partially submerged plate). Low pass filters were used to filter out the slamming force components from the load cell signals, so only the slowly-varying force was analyzed.

The theoretical expression developed was mathematically similar to that developed by Kaplan et al. (1995). The vertical force was assumed to be the sum of the time-varying components (time-rate of change of momentum, drag, and buoyancy). Included were the effects of added mass in the calculations. The added mass equation was for a non-specific structure shape with a single empirical coefficient. The equations were evaluated numerically. Due to the uncertainties

associated with the change in added mass as the latter portion of the wave strikes the structure no attempt was made to predict forces beyond the first half of the wave.

Selected results were presented in table form along with a single plot of predicted versus measured vertical force.

Current Work on Bridge Superstructures

The recent bridge failures of 2004 and 2005 have renewed interest in the topic. The following studies are currently ongoing. A design method for dealing with wave forces on bridge superstructures based on work by Sheppard and Marin (2009) was ratified into AASHTO Code in May of 2008.

Schumacher et al. (2008)

Schumacher et al. (2008) conducted large scale (1:5) physical model experiments in a 104 m long, 3.66 m wide wave tank at the O.H. Hinsdale Wave Research Laboratory at Oregon State University. The model was an actual reinforced concrete slab with scaled AASHTO Type III girders including diaphragms.

Tests were done with the structure braced as a rigid structure and also as a flexible structure in the horizontal direction with springs. Forces in the vertical and horizontal direction were measured with a series of load cells. Twelve (12) pressure transducers were located through the model deck and girders. Tests were done for a variety of ranges of water depth, wave heights, wave periods, and clearance height relative to SWL (some tests were done with partially submerged structures).

It is believed the large scale tests generate data with a high degree of validity. It was noted that peak horizontal and vertical forces do not occur simultaneously.

Douglas et al. (2006)

Douglas et al. (2006) studied wave forces on bridge superstructure decks using the failure of the US 90 Bridge over Biloxi Bay, Mississippi as a case study. Physical model tests were conducted at the Haynes Coastal Engineering Laboratory at Texas A&M University. A scale model (1:15) of the LA1 bridge in Louisiana was used. Lead weights were used to hold the model decks down

and the decks did not extend the full width of the tank. A single six component load cell was used to measure forcing and two wave periods (1.3s and 1.8s) were used with a variety of wave heights.

Presented was a theoretical method similar to that of French (1970), Wang (1970), and McConnell et al. (2004). The forcing was divided into a slowly varying component and slamming component. For the slowly varying component the force was a function of hydrostatic head and an empirical coefficient. For the slamming force, the relation developed by McConnell et al. (2004) was used.

Neither method takes into account the effects of wave period or the inherent kinematics of the wave.

Marin (2009)

Marin (2009) completed a theoretical and experimental study of wave loading on flat plates. The forcing was divided into two main components- the high frequency slamming force and the slowly varying quasi-steady force (frequency equivalent to the wave period). For the quasi-steady force, a theoretical model was developed based on a Morison-type equation system first described in Kaplan et al. (1995). The model was expanded to situations where the wave length and the plate length were of comparable size (similar to nearshore bridges) and adjusted to account for partially and fully submerged structures. From these tests an empirical relationship for the slamming force was developed.

The theoretical model was broken into dynamic and static components. The static component consisted of the buoyancy force given in Equation 2-31, where $\forall_S$ is the submerged volume of the structure at a given time. The dynamic components consisted of the inertia and drag forces. The drag force is given in Equation 2-32, where C_D is a drag coefficient, A is a projected surface area, and w is the fluid velocity. Due to the variation in structure inundation caused by the similar size ratio of the wave and the structure, the inertia term contains a time dependent mass variable, requiring the inclusion of a change in effective mass component in the inertia equation. The inertia equation is given in Equation 2-33, where C_M is a mass coefficient, m_e is the effective

mass (sum of the structure and added mass), w is the fluid velocity and $\partial w/\partial t$ is the fluid acceleration.

$$F_{Buoyancy} = \rho g \forall_S \tag{2-31}$$

$$F_{Drag} = \frac{1}{2} C_D \rho A w |w| \tag{2-32}$$

$$F_{Inertia} = C_M m_e \frac{\partial w}{\partial t} + C_M w \frac{\partial m_e}{\partial t} \tag{2-33}$$

To accurately evaluate the inertia component of the forces, a method for determining the effective mass (m_e) and the time rate of change of the effective mass ($\partial m_e/\partial t$) was needed. Determination of the effects of the time rate of change in added mass was also needed. A method described by Payne (1981) was modified to fit the requirements (Equations 2-34 and 2-35), where L is the structure length, $\bar{W}$ is the wetted width of the structure, and D is the thickness of the structure.

$$m_e = \rho \forall_S + \frac{\frac{1}{4}\rho\pi L^2 \bar{W}^2}{\sqrt{L^2 + \bar{W}^2}} \tag{2-34}$$

$$\frac{\partial m_e}{\partial t} = \rho L \left(\bar{D} \frac{\partial \bar{W}}{\partial t} + \bar{W} \frac{\partial \bar{D}}{\partial t} \right) + \frac{\frac{1}{4}\rho\pi L^3 \frac{\partial \bar{W}}{\partial t}}{\sqrt{L^2 + \bar{W}^2}} \left(1 - \frac{\bar{W}^2}{L^2 + \bar{W}^2} \right) \tag{2-35}$$

A numerical program was written to evaluate the theoretical model. Based on the input of known structure and wave variables, a wave and plate were generated on a grid with maximum element resolution of 1in. The grid extended from the sea bed to above the maximum wave crest vertically and a plate length upstream and downstream of the structure horizontally. The generated waves (a stream function model was used) were nonlinear and the kinematics was calculated for each grid element. The wave was then run past the structure and the theoretical equations were solved in every element for each time step. To verify the model and calibrate the coefficients for the model, experimental tests were done.

292 physical model tests were conducted in a 6 ft wide, 120 ft long wave tank at the Coastal Engineering Laboratory at the University of Florida. The scaled plate model (1:8) was based on the deck element of the failed I-10 Bridge over Escambia Bay, Florida. Tests were run for a continuous plate setup (plate extending the full width of the tank) and a finite plate setup (single plate centered in the tank). Tests were run for a wide range of periods, wave heights, water depths, and clearance heights (subaerial, submerged, and partially submerged). Forces were measured using four multi-axis load cells located at each corner of the instrumented structure. Water surface elevations upstream and downstream of the structure were measured using three capacitance-type wave gauges. All instrument sampling frequencies were 480 Hz and monochromatic waves were used.

Filters were created based on power spectral density calculations and implemented to remove ambient noise and separate the slamming and quasi-steady forces. Coefficients were then varied in the numerical program and used to fit force-time curves to the measured data. Equations for the determined coefficients were determined as functions of important problem parameters, namely the wave steepness (H/λ), the relative clearance height (Z_C/η), and the relative width (W/λ). Forces were given as Force per unit length.

To check the validity of the coefficients and the model, the numerical program was run against independent experimental data from Isaacson and Bhat (1996) and showed excellent agreement.

An empirical relation was found for the slamming force based on similar problem parameters to the coefficient equations. Two separate equations were developed for the slamming for the cases of continuous plate (no lateral free overtopping) and finite plate. No method for the determination of slamming duration was determined and the validity of the equations was not checked against independent data.

CHAPTER 3 - THEORETICAL MODEL FOR QUASI-STATIC FORCES

Wave forces on thin, flat, horizontal plates were investigated by Marin (2009). The wave loading problem becomes more complex for horizontal structures with finite thickness. Consider the structure shown in Figure 3- 1.

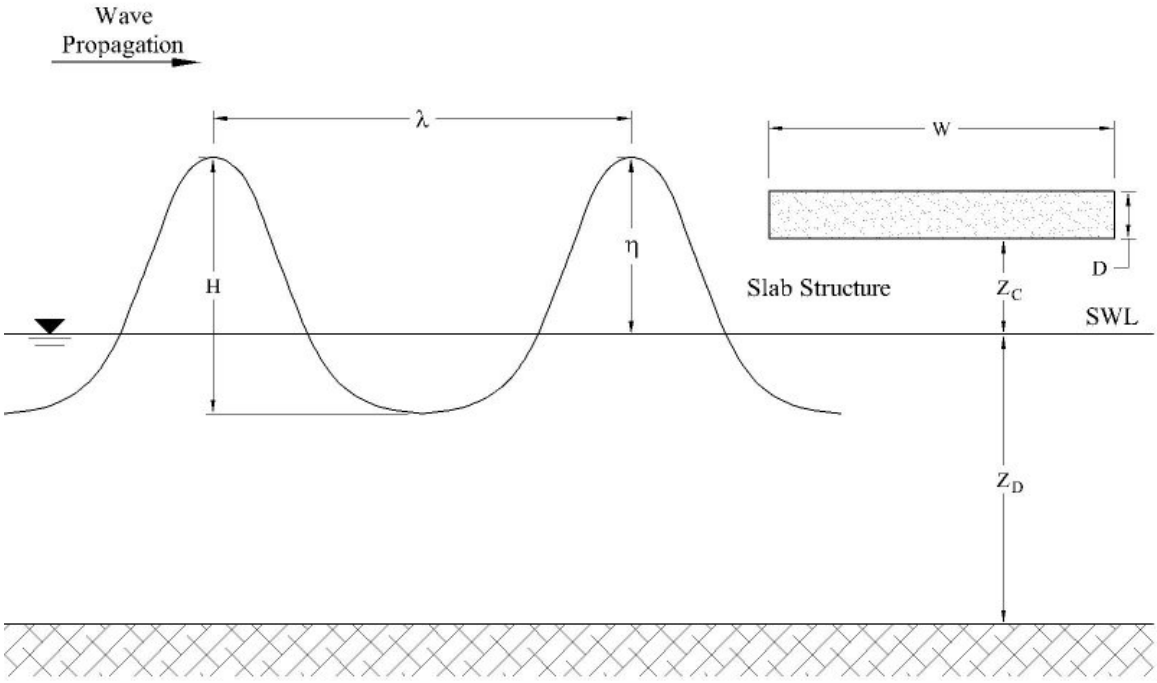

WAVE VARIABLES		STRUCTURE VARIABLES		FLUID VARIABLES	
H	- Wave Height	W	- Structure Width	Z_D	- Water Depth
T	- Wave Period	L	- Structure Length (into page)	ρ	- Water Density
λ	- Wave Length	D	- Structure Thickness	μ	- Water Viscosity
η	- Water Surface Elevation	Z_C	- Structure Clearance	g	- Gravity
k	- Wave Number	α	- Angle of Incidence		

Figure 3- 1 Definition sketch for wave loading on horizontal structures with finite thickness.

The total vertical force, F_Z, and horizontal force, F_X, on the slab as the wave propagates past the structure can be expressed as functions of the wave, fluid, and structural parameters,

$$F_{Z,X} = f\left(W,L,D,Z_C,Z_D,H,T,\lambda,C,\eta_{max},k,\rho,g,\alpha,\mu\right) \quad (3\text{-}1)$$

The structural variables are the slab width (W), the slab length (L), the slab thickness (D), and slab clearance (Z_C). Generally, the width is aligned in the direction of wave propagation while

the length is aligned normal to it (with the flow of traffic on the bridge). The fluid variables are the water depth (Z_D), the water density (ρ), and the dynamic viscosity (μ). The wave variables are the wave period (T), the wave height (H), the wavelength (λ), the maximum wave crest elevation (η_{max}), the wave celerity (C), the wave number (k), and the angle of incidence to the structure (α). The last important variable is gravity (g).

The contribution of these variables to the total forcing varies depending on the forcing being considered and the assumptions made about the fluid structure interaction. The variables that govern the vertical forcing will not all play as significant a role in the horizontal forcing and vice versa. In some cases, assumptions will eliminate certain variables all together. Some variables are functions of other variables and can be removed due to this redundancy. Some variables will have very little effect on the outcome and can be ignored altogether.

Model Assumptions

The flow and fluid-structure interaction processes associated with wave impact on structures of comparable sizes are complex. For this reason certain simplifying assumptions must be made for the theoretical model development:

- The structure is rigid and horizontal (no slope to the structure).
- The waves are monochromatic, non-breaking and two-dimensional.
- The waves approach the structure normal to the leading edge of the structure.
- The effects of the structure on the waves can be accounted for through experimentally determined drag and inertia coefficients.
- The total forcing can be treated on a 'per unit length' basis for a given wave and structure.
- The total forcing can be assessed as the sum of individual and independent forcing components.

The purpose and effect of some of these assumptions are briefly discussed below.

Rigid structure

The structures in this study are considered to be rigid. This assumption is adequate for the loading aspect of the problem. However it may not be appropriate when analyzing the response of these structures to storm surge and wave loading.

Monochromatic waves

The use of monochromatic waves produced conservative forces compared to random waves of the same height and period. In the case of the slamming force, random waves may possibly produce forces greater than monochromatic waves with equivalent heights and periods due to their distorted shapes. Waves approaching normal to the leading edge of the structure are thought to produce the most conservative forces and moments, however this was not tested.

While the problem is treated two-dimensionally and the forces and moments computed on a per unit structure length basis, it should be noted that the effect of finite structure length on the calculation of added mass must be taken into consideration as the variation of the added mass quantity is not linear with structure length (length normal to direction of wave propagation). However, the structure length was found to only affect the 2D legitimacy for extremely narrow spans (i.e. span width > 10 times span length), a situation never found in coastal highway bridges.

Model Development

The Buoyancy Force

The buoyancy force (F_B), which is simply the net hydrostatic force, is the most straightforward of the force components and acts only in the vertical direction. Any submerged portion of the structure will experience a buoyancy force equivalent to the weight of the volume of water displaced ($\forall_S$) by that part of the structure.

$$F_B = \rho g \forall_S \tag{3-2}$$

The submerged volume is a function of the wetted dimensions of the structure and therefore a function of time. Since the waves are assumed to approach normal to the span length the wetted

length is a constant value. The final expression for the buoyancy with $\overline{A}_S$ as the wetted cross sectional area and L the length of the span is

$$F_B = \rho g L \overline{A}_S \,. \tag{3-3}$$

Note that for structures of substantial thickness, the shape and slope of the wave can affect the buoyancy magnitude if only part of the structure is submerged (Figure 3- 2).

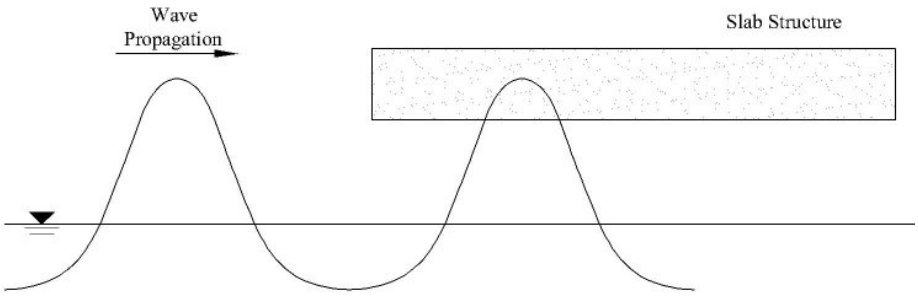

Figure 3- 2 Sketch showing partially inundated structure by wave.

Drag and Inertia Forces

The forces exerted on a completely submerged body in an accelerating fluid are due to drag and inertia. These are both lower frequency (frequency in the range of the wave period) forces derived from introducing the structure into the kinematic wave field.

The sum of the drag and inertia forces as the total forcing was first introduced in the Morison equation (Morison et al. 1950). Dealing with the forces on piles and elements that were small in comparison to the wave length, the Morison equation does not account for changes in added mass.

For bridge superstructures inertia forces appear to be larger than drag in the vertical direction while the opposite is true in the horizontal direction.

Drag force

In general the drag force (F_D) is composed of shear (skin friction) and normal components with the normal (pressure drag) component resulting from flow separation around the body. Most analytical treatments of drag lump the two components together with an expression that is

proportional to the projected area of the structure, the mass density of the fluid and the square of the approach velocity. The experimentally determined constant of proportionality is the drag coefficient which is a function of the structure shape, Reynolds Number (based on the structure width and approach velocity), surface roughness, etc.

Expressions for the horizontal and vertical drag forces are given in Equations 3-4a and 3-4b, where C_{DX} and, C_{DZ} are the horizontal and vertical drag coefficients, A_X is the projected area in the vertical plane, A_Z is the projected area in the horizontal plane, u and w are the horizontal and vertical approach velocities, and ρ is the fluid mass density.

$$F_{DX} = \frac{1}{2} C_{DX} \rho A_X u |u| \tag{3-4a}$$

$$F_{DZ} = \frac{1}{2} C_{DZ} \rho A_Z w |w| \tag{3-4b}$$

Partially submerged structure drag force scenarios

In analyzing the horizontal and vertical drag forces of a partially submerged span several different scenarios have to be considered. These are shown in Figure 3- 3 - Figure 3- 5.

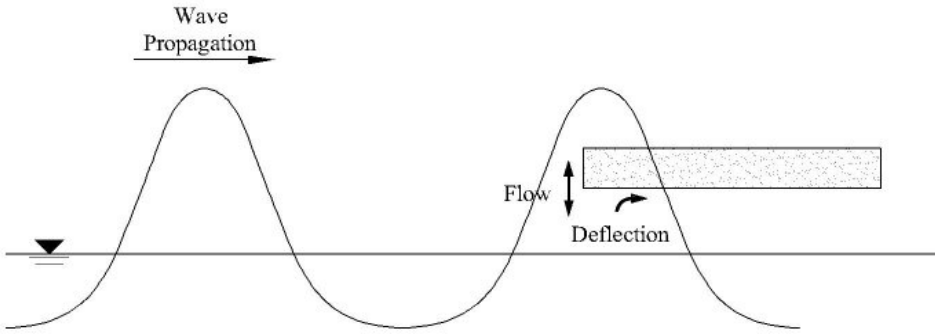

Figure 3- 3 Sketch of structure with leading edge inundated by wave.

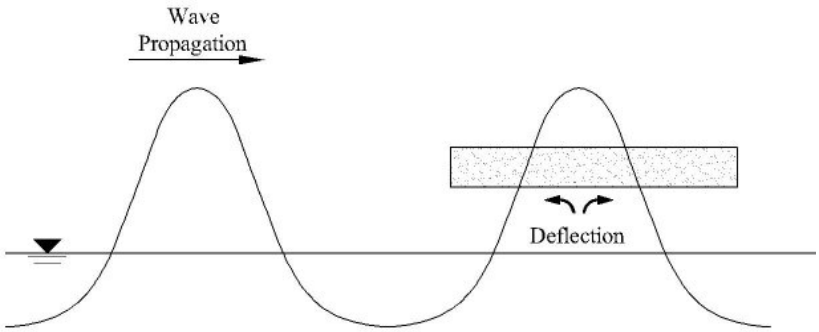

Figure 3- 4 Sketch of structure with its midsection inundated by the wave.

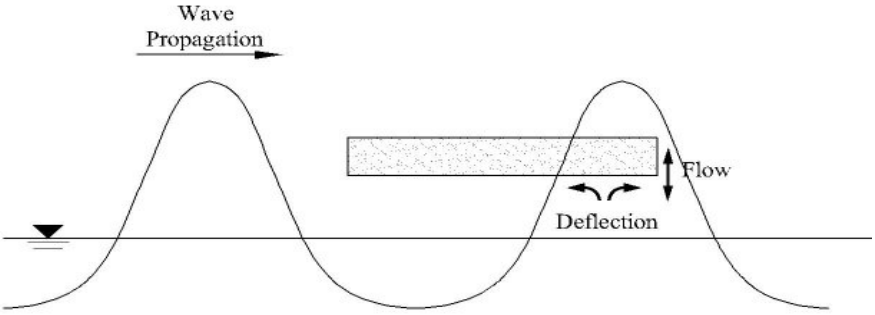

Figure 3- 5 Sketch of structure with its trailing edge inundated by the wave.

As the wave progresses past the structure the drag coefficient will vary significantly due to the changes in approach velocities and structure geometries. Some physical model drag tests were conducted at the Federal Highways Turner Fairbank Laboratory in McLean, VA to determine potential drag coefficients for beam and slab bridge decks. Starting with the FHWA values the final coefficients used in model developed in this study were adjusted to produce the best fit to the data.

Inertia force

The inertia force is force that results from the acceleration-induced pressure gradient field in the vicinity of the structure. The force component is proportional to the time rate of change of the linear momentum of the flow. For structures that are fully submerged or very small in comparison to the wave length, the equation is

$$F_{Inertia} = C_M \frac{\partial}{\partial t}[mU] = C_M m \frac{\partial}{\partial t}[U] \quad (3\text{-}5)$$

Complexities arise when there is intermittent submergence of the structure. This intermittent submergence creates time dependent mass terms. Kaplan et al. (1995) included the time dependent mass component, but used averaged water velocities and accelerations over the width of the structure. This assumption is valid for offshore structures where the design wave lengths are large compared to the width of the structures. However, for comparable structure widths and wave lengths average velocities and accelerations are not appropriate. For these situations the inertia force becomes,

$$F_{Inertia} = C_M \left[m \frac{\partial U}{\partial t} + U \frac{\partial m}{\partial t} \right]. \quad (3\text{-}6)$$

Added mass

The mass of water impacted by the presence of the structure is that displaced by the structure plus the surrounding water in the vicinity of the structure. The impacted surrounding water is referred to as the added mass and denoted by m_a. The displaced mass is denoted by m_s. The total impaced mass, referred to as the effective mass, m_e, is thus

$$m_e = m_s + m_a . \quad (3\text{-}7)$$

Note that both mass components are time dependent for situations where the structure is only partially submerged by the wave.

Inertial and time dependent mass equations

Substituting Equation 3-7 into Equation 3-6 results in Equations 3-8a and 3-8b for the horizontal and vertical directions respectively.

$$F_{X-Inertia} = \left(C_I m_e \frac{du}{dt} + C_M u \frac{dm_e}{dt} \right) \quad (3\text{-}8a)$$

$$F_{Z-Inertia} = \left(C_I m_e \frac{dw}{dt} + C_M w \frac{dm_e}{dt} \right) \quad (3\text{-}8b)$$

The first terms in Equations 3-8a and 3-8b is denoted by F_I and the second terms by F_M. The values of the coefficients, C_I and C_M must be determined empirically.

$$F_{IX} = C_{IX} m_e \frac{du}{dt} \tag{3-9a}$$

$$F_{IZ} = C_{IZ} m_e \frac{dw}{dt} \tag{3-9b}$$

$$F_{MX} = C_{MX} u \frac{dm_e}{dt} \tag{3-10a}$$

$$F_{MZ} = C_{MZ} w \frac{dm_e}{dt} \tag{3-10b}$$

The structural displaced mass is relatively easy to calculate since it is only the water mass displaced by the structure, ~~V~~$_S$. Likewise computation of the buoyancy force is straight forward, the magnitude being the weight of the water displaced by the structure. The displaced mass is

$$m_s = \rho \bar{A}_S L \,, \tag{3-11}$$

where $\bar{A}_s$ is the wetted cross-sectional area of the structure.

Deriving the added mass is a more involved process. For many simple shapes, theoretical equations for added mass have been developed from potential flow theory and can be found in texts such as Saprkaya 1981. These equations are often presented as two dimensional shapes oriented a certain way in the flow. Using coefficients based on the shape's geometric ratios, the added mass is then calculated per unit length orthogonal to the direction of the flow (Figure 3-6). However, because these relationships were developed from shapes that were infinitely long (which allows the subsequent use of a per unit length application at the cost of specific orientations), two separate problems arise.

The first problem is that the quantities predicted by the equations change with orientation of the object regardless of whether the orientation has an effect. Turning the object in the flow does not alter how the flow reacts to the presence of the object (Figure 3- 6B), since it has the exact same

dimensions and same projected area normal to the flow. Using this approach different values would be calculated for the two orientations shown in Figure 3- 6.

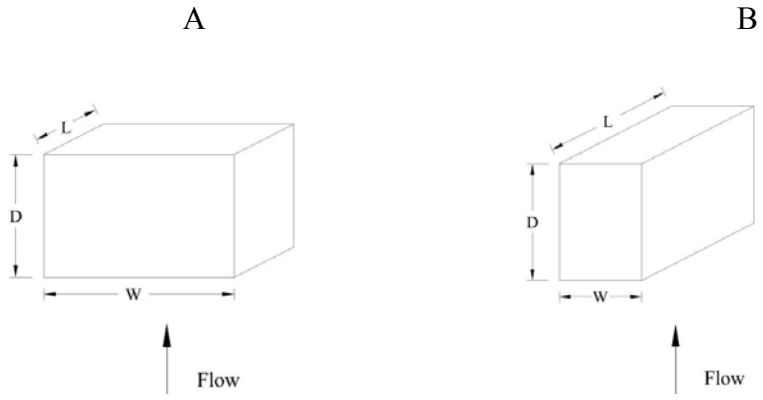

Figure 3- 6 Two orientations of the same body.

The second problem is that the per unit length designation makes the equation linear in one direction. While this would suggest that added mass has an additive property, experimental tests show this not to be true (Yu 1945). Using published methods the two objects in Figure 3- 7 would have different values of added mass. Experiments performed by Payne (1981) showed this to be incorrect.

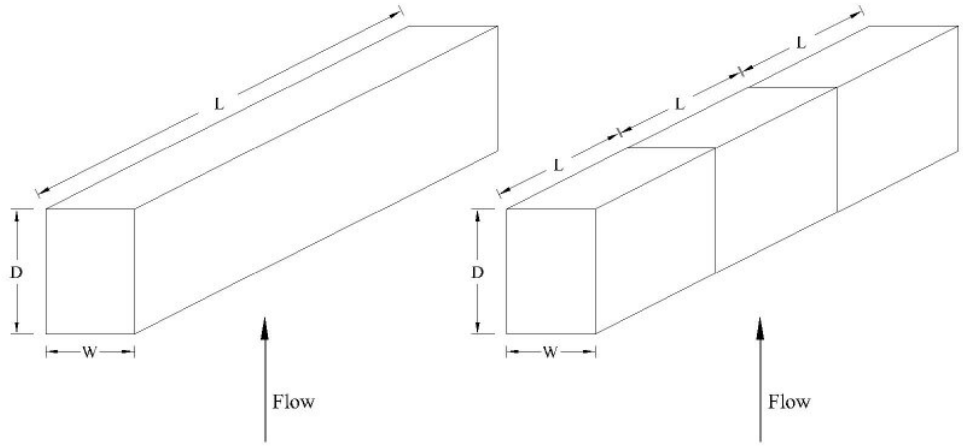

Figure 3- 7 Two equivalent bodies yielding different computed added mass.

Payne (1981) recognized the discrepancy and developed a modifier to be used in conjunction with those equations that eliminated the inconsistencies. This expression, given in Equation 3-12,

eliminated the discrepancy and produced the same result regardless of the orientation of the objects face.

$$\text{Payne's Multiplier} = \frac{L}{\sqrt{L^2 + W^2}} \tag{3-12}$$

Before applying Payne's factor, an expression for the added mass of a slab with finite thickness had to be developed. An expression for the added mass for the rectangle shown in Figure 3- 8 is given in Equation 3-13, where A is the dimension of the face perpendicular to the flow, B is the dimension of the face parallel to the flow, and α is the thickness to ratio coefficient.

$$m_a = \alpha\pi\rho\left(\frac{A}{2}\right)^2 \tag{3-13}$$

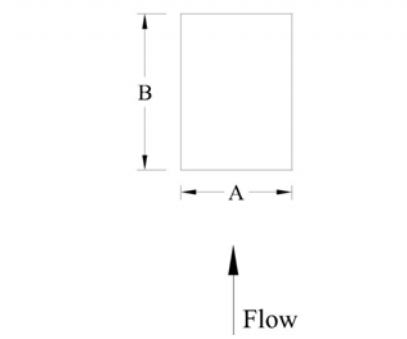

Figure 3- 8 Definition sketch for added mass computation.

Based on this information an added mass expression for a slab structure with finite thickness was developed. The flow is in the vertical direction. The dimension A is replaced by the span width, W and the dimension B is replaced by the span thickness, D. The length of the span, L, is added to remove the per unit length notation.

$$m_a = \alpha\pi\rho\,\tfrac{1}{4}W^2L \tag{3-14}$$

Applying Payne's multiplier produces an equation without orientation issues.

$$m_a = \alpha\rho\pi\,\tfrac{1}{4}\frac{W^2L^2}{\sqrt{L^2 + W^2}} \tag{3-15}$$

The next step is to replace the coefficient α with a relationship that covers the range of geometric ratios of interest for the slab span problem. Empirically determined coefficients were given in Sarpkaya 1981. These coefficients were plotted against the ratios of the corresponding widths and thicknesses and curve fitting produced a simple expression for α as a function of the thickness to width structure ratio, D/W.

$$\alpha = 1 + \tfrac{1}{2}\left(\frac{D}{W}\right)^{\frac{2}{5}} \tag{3-16}$$

Substituting α from Equation 3-16 into Equation 3-15 yields the added mass expression for a horizontal rectangular slab with flow in the vertical direction.

$$m_a = \rho\pi\tfrac{1}{4}\frac{W^2L^2}{\sqrt{L^2+W^2}} + \rho\pi\tfrac{1}{8}\frac{W^{8/5}D^{2/5}L^2}{\sqrt{L^2+W^2}} \tag{3-17}$$

Once again the intermittent submergence must be taken into account. Both the width and the thickness of the structure are time dependent parameters and must be replaced by their wetted counterparts $\bar{W}$ and $\bar{D}$, respectively. The wetted length is still constant due to the assumed wave approach angle being normal to the roadway. The time dependent expression for the added mass becomes:

$$m_a = \rho\pi\tfrac{1}{4}\frac{\bar{W}^2L^2}{\sqrt{L^2+\bar{W}^2}} + \rho\pi\tfrac{1}{8}\frac{\bar{W}^{8/5}\bar{D}^{2/5}L^2}{\sqrt{L^2+\bar{W}^2}} \tag{3-18}$$

Adding the structure displaced mass gives the complete expression for the time dependent effective mass of the structure (Equations 3-19a and 3-19b). For the case of horizontal flow, the dimensions A and B are simply rotated 90 degrees. As the length is the common parameter in both orientations, it does not need to be altered while the wetted widths and thicknesses are simply interchanged (Equation 3-19b).

$$m_{ez} = \rho\bar{A}_S L + \rho\pi\tfrac{1}{4}\frac{\bar{W}^2L^2}{\sqrt{L^2+\bar{W}^2}} + \rho\pi\tfrac{1}{8}\frac{\bar{W}^{8/5}\bar{D}^{2/5}L^2}{\sqrt{L^2+\bar{W}^2}} \tag{3-19a}$$

$$m_{ex} = \rho \bar{A}_S L + \rho\pi \tfrac{1}{4} \frac{\bar{D}^2 L^2}{\sqrt{L^2 + \bar{D}^2}} + \rho\pi \tfrac{1}{8} \frac{\bar{D}^{8/5} \bar{W}^{2/5} L^2}{\sqrt{L^2 + \bar{D}^2}} \tag{3-19b}$$

The time derivatives of these expressions are needed for mass rate of change force calculations,

$$\frac{\partial m_{ez}}{\partial t} = \rho \frac{\partial \bar{A}_S}{\partial t} L + \begin{Bmatrix} \rho\pi \dfrac{\bar{W} L^2}{\sqrt{\bar{W}^2 + L^2}} \left[\dfrac{1}{2} \dfrac{\partial \dot{W}}{\partial t} + \dfrac{1}{5} \left(\dfrac{\bar{D}}{\bar{W}} \right)^{2/5} \dfrac{\partial \dot{W}}{\partial t} + \dfrac{1}{20} \left(\dfrac{\bar{W}}{\bar{D}} \right)^{3/5} \dfrac{\partial \dot{D}}{\partial t} \right] \\ -\rho\pi \dfrac{\bar{W}^3 L^2}{\sqrt[3/2]{\bar{W}^2 + L^2}} \left[\dfrac{1}{4} \dfrac{\partial \dot{W}}{\partial t} + \dfrac{1}{8} \left(\dfrac{\bar{D}}{\bar{W}} \right)^{3/5} \dfrac{\partial \dot{W}}{\partial t} \right] \end{Bmatrix} \tag{3-20a}$$

,

$$\frac{\partial m_{ex}}{\partial t} = \rho \frac{\partial \bar{A}_S}{\partial t} L + \begin{Bmatrix} \rho\pi \dfrac{\bar{D} L^2}{\sqrt{\bar{D}^2 + L^2}} \left[\dfrac{1}{2} \dfrac{\partial \dot{D}}{\partial t} + \dfrac{1}{5} \left(\dfrac{\bar{W}}{\bar{D}} \right)^{2/5} \dfrac{\partial \dot{D}}{\partial t} + \dfrac{1}{20} \left(\dfrac{\bar{D}}{\bar{W}} \right)^{3/5} \dfrac{\partial \dot{W}}{\partial t} \right] \\ -\rho\pi \dfrac{\bar{D}^3 L^2}{\sqrt[3/2]{\bar{D}^2 + L^2}} \left[\dfrac{1}{4} \dfrac{\partial \dot{D}}{\partial t} + \dfrac{1}{8} \left(\dfrac{\bar{W}}{\bar{D}} \right)^{3/5} \dfrac{\partial \dot{D}}{\partial t} \right] \end{Bmatrix} \tag{3-20b}$$

.

By inserting the effective mass equations (Equation 3-19) and the effective mass rate equations (Equation 3-20) into the inertia force equations (Equation 3-9 and Equation 3-10) the forces can now be calculated.

Evaluating the effective mass and mass rate equations can be difficult due to the rather complex nature of the time dependence of the effective mass and its interaction over the full inundation cycle of the structure. For example as the wave initially strikes the structure, the effective mass is changing with time (Figure 3- 9A). The effective mass is also time dependent as the wave exits the structure (Figure 3- 9B). However, if the trailing edge of the wave reaches the structure before the leading edge exits then there is a period of time when the effective mass is mathematically constant (Figure 3- 10A). For a wave that is wider than the structure at the structure elevation, a similar period of time occurs when the effective mass is mathematically constant as the structure is fully submerged as shown in Figure 3- 10B.

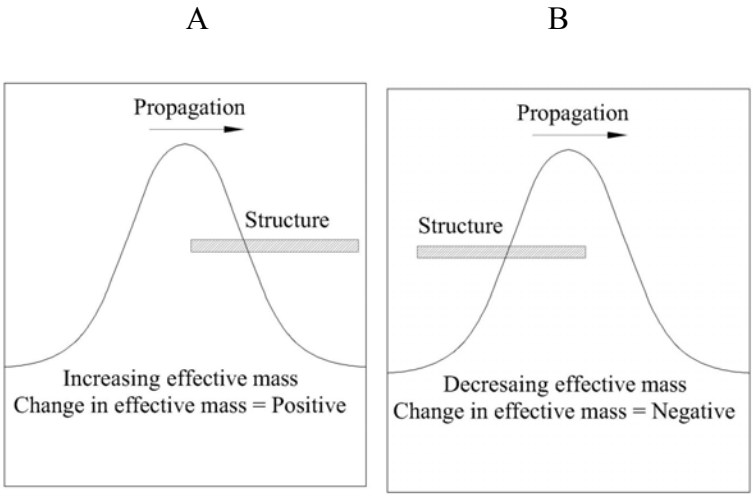

Figure 3- 9 Diagrams showing conditions for time varying added mass.

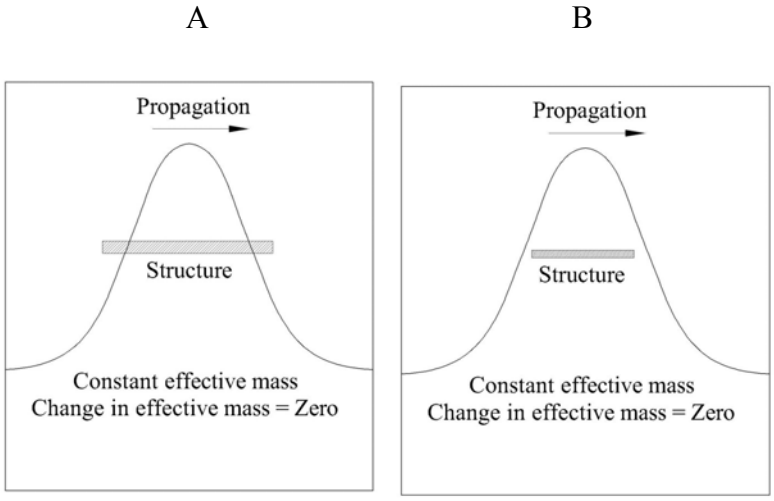

Figure 3- 10 Diagrams showing conditions of no change in added mass.

The resulting quasi-static wave force equations for bridge superstructures are as follows:

$$F_x = F_{Dx} + F_{x\text{-Inertia}} \tag{3-21a}$$

$$F_z = F_{Dz} + F_{z\text{-Inertia}} + F_B \tag{3-21b}$$

CHAPTER 4 - PHYSICAL MODEL TESTS

All tests were conducted in the air/sea wave tank located at the Coastal Engineering Laboratory at the University of Florida. The wave tank is 6 ft wide by 6 ft deep by 120 ft long. The wave maker has the capability of both paddle and piston modes of operation but was used solely in piston mode. Wave absorbers are located behind the paddle and at the downstream end of the tank in order to minimize wave reflection. A series of glass panels run the length of one side of the tank for viewing. The ranges of wave heights and periods as a function of water depth achievable in the tank are shown in Figure 4- 1.

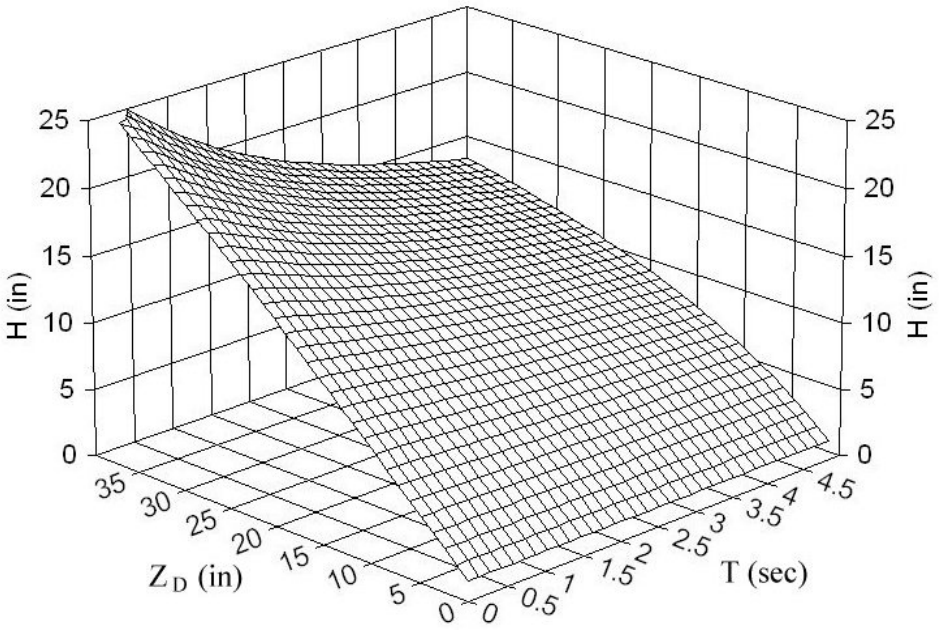

Figure 4- 1 Limiting wave heights as functions of wave period and water depth for the air-sea wave tank.

The tests were laid out in increasing levels of model complexity with differing arrays of instruments to capture the various force components. The increasing levels of complexity allowed for the contributions of normal bridge additions (i.e. overhangs, rails, girder spacing, etc.) to be determined. In all, 1100 individual tests were completed where the ranges of testing conditions used were chosen to represent the practical limits encountered in the nearshore environment.

Model and Model Support Design

Wave force data from previous physical model studies exhibit considerable scatter, a fact that is attributed to the highly dynamic nature of the forces being measured. Care was taken to design a robust system that would avoid these dynamic effects. Therefore, in constructing the model and its support systems, two important factors were considered in the design, frequency effects and scale effects.

Frequency effects

It was important to make the support structure as rigid as practical to have its primary mode of vibration for removed from the wave loading frequencies. The force measuring transducers were three component load cells so any motion of the support directly impacted the force measurements.

Consider the spring, mass, dashpot system shown in Figure 4- 2. The response of this simple, one degree of freedom system is described by the differential equation in Equation 4-1, where z is the displacement, m is the object mass, c is the damping coefficient, k is the spring constant, and F(t) is the time dependent forcing.

$$F(t) = m\frac{d^2z}{dt^2} + cm\frac{dz}{dt} + kz \qquad (4\text{-}1)$$

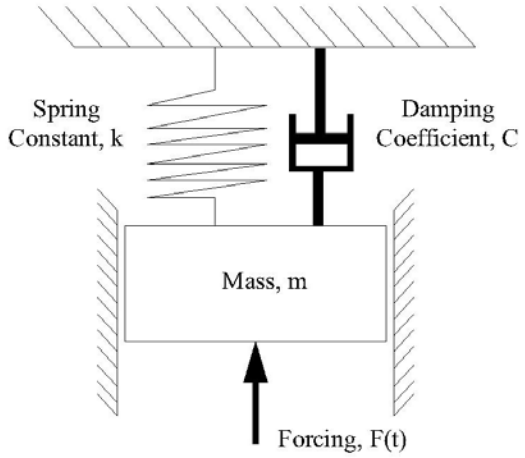

Figure 4- 2 Spring-mass-dashpot system

There are three important frequencies to this single degree of freedom system. They are the forcing frequency (ω), the system's natural frequency (ω_n), and the system's damped frequency (ω_d). How these frequencies relate to each other determines the response of the system under a given forcing situation. Expressions for the natural frequency and damped natural frequency are given in Equations 4.2 and 4.3 respectively.

$$\omega_n = \sqrt{\frac{k}{m}} \tag{4-2}$$

$$\omega_d = \omega_n \sqrt{1 - \left(\frac{c}{2m\omega_n} \right)^2} \tag{4-3}$$

Critical damping occurs when $c = 2m\omega_n$ (see Figure 4- 3).

Depending on how close the forcing frequency is to the structure dampened frequency and the level of damping, the magnitude of the displacement can be amplified or attenuated. The structure response as a function of damping magnitude and ratio of forcing to natural frequency is shown in Figure 4- 3. Note that as the forcing frequency approaches the natural frequency the response is significantly amplified. As the mass of the structure becomes large (as in the case of a bridge), the frequency of its fundamental mode of vibration becomes very low and thus far removed from the slamming frequencies.

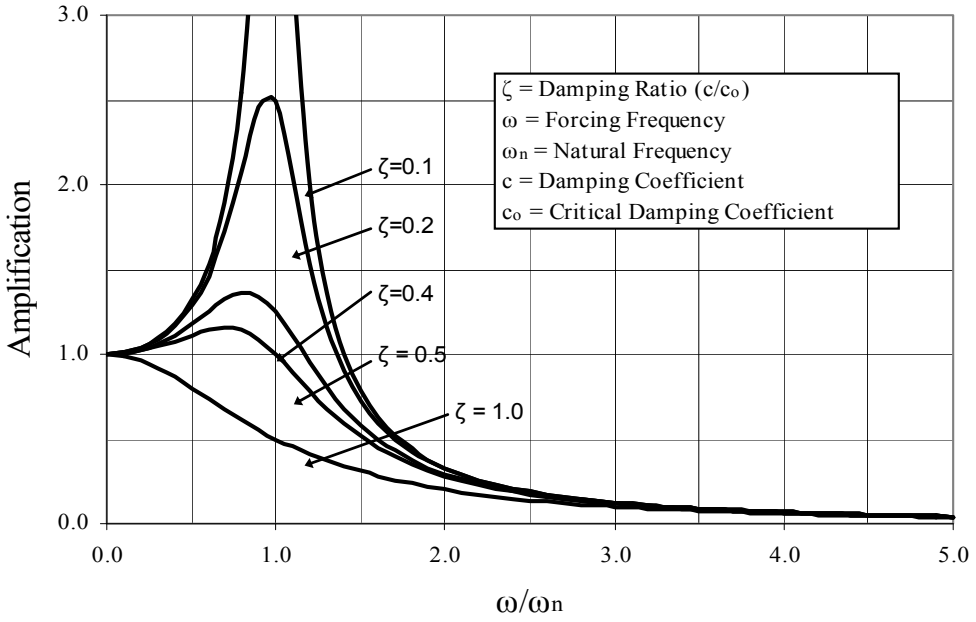

Figure 4- 3 Amplitude amplification as a function of driving frequency and damping.

From Figure 4- 3, it can be seen that the consequences regarding the effects of slamming is related directly to the structure itself. The structure's natural frequency will determine whether or not its response to slamming forces is significant. The response of a structure with a low fundamental mode of vibration may have minimal response to a high frequency excitation. However, if there is significant air entrapment, reducing the slamming force frequency the structure could respond. The presence of entrapped air will, in general reduce the magnitude of the slamming force but increase its duration and therefore lower its frequency.

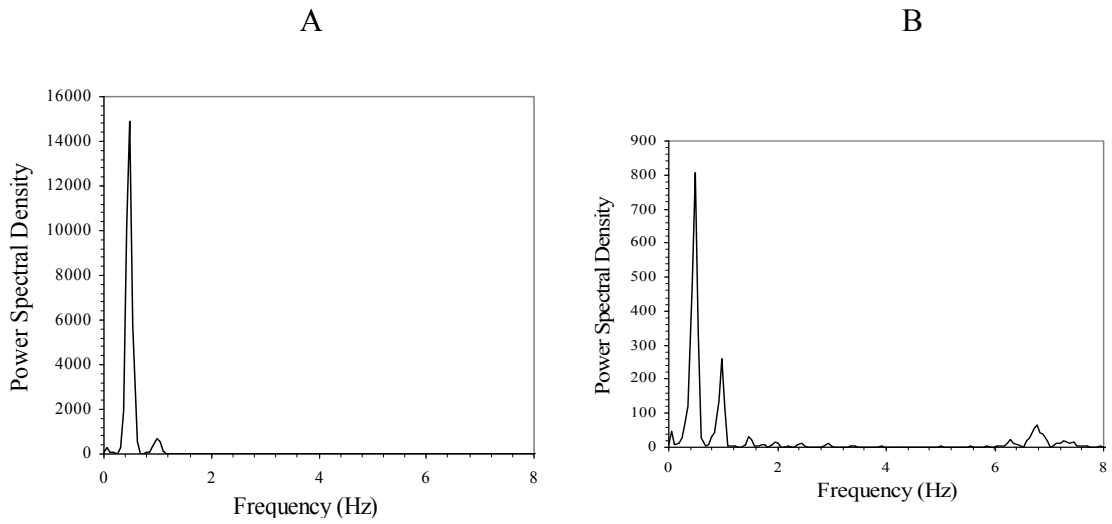

Figure 4- 4 Vertical load power spectra for A) submerged span and B) subaerial span (wave period = 2.0 s).

Examples of vertical force power spectral density plots for submerged A) and subaerial B) slab spans subjected to waves with a period of 2.0 s (frequency = 0.5 Hz) are shown in Figure 4- 4. In order to resolve the measured data signals, the sampling on all instrumentation needed to be at least twice the highest expected forcing frequency of interest, in this case the slamming frequency. The sampling frequency used was 480 Hz, capable of resolving frequencies up to 240 Hz.

Scale effects

In all physical modeling, geometric, kinematic, and dynamic similarity is important. The geometric scaling is handled by maintaining a single length scale between the prototypes and the models. For the models used in the study, the geometric scaling ratio was approximately 1:8.

The kinematic and dynamic scaling was handled by maintaining a single velocity scale ratio between the prototypes and the models. The similarity criteria chosen was Froude scaling since the inertia dominated the viscous forces. From the Froude number similarity between prototype and model, the velocity scaling ratio is the square root of the length scale. A relatively large model tends to minimize the scale effects.

Physical Models

The models used in the tests conducted as part of this study represent a segment of a continuous span running the width of the span. All tests were conducted with models with zero vertical incline and with wave propagation normal to the span length.

To reduce the effects of the wave tank walls, the models were divided into three independent equal, 2 ft sections as shown in Figure 4- 5. When placed side by side they formed a continuous span running the full width of the tank. The three structures were separated by very small gaps to isolate the instrumented center section from the two side panels.

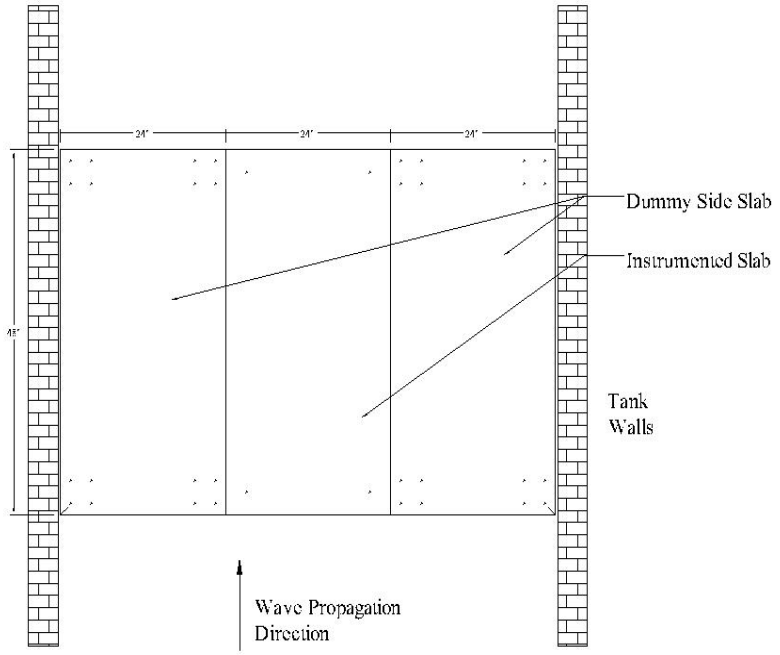

Figure 4- 5 Plan view of instrumented section and two rigid side panels.

Model Support Structure

In order to avoid effects induced by the presence of additional blockage in the flow field and to increase the ease of changing span elevations, the models were supported from above by a fixed carriage system (Figure 4- 6 and Figure 4- 7). The carriage consisted of a rigid steel frame locked onto the steel channel running the length of the concrete walls of the wave tank. From the main

steel frame, an H frame composed of steel channels was suspended by four 1¼ in steel travel screws used to set the elevation of the model decks. From the H frame, 30 in long 1in diameter steel pipes were used to connect the models.

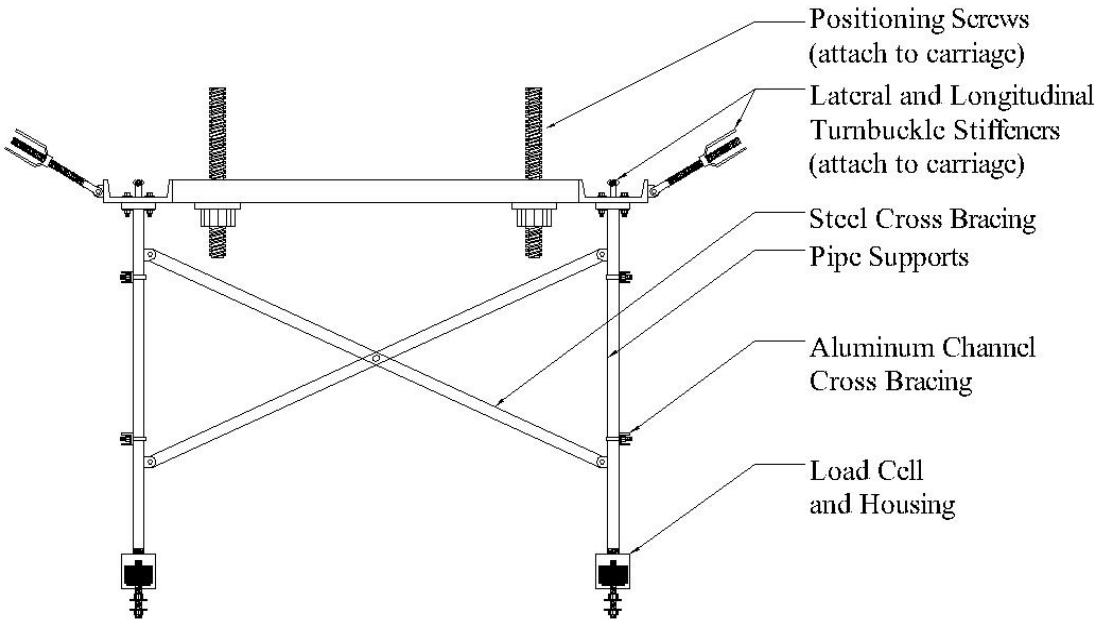

Figure 4- 6 Side view of model support structure and load cells.

For the two (uninstrumented) side panels flanges were welded to the pipe ends and attached to the models by four ½ in bolts for each flange. The center instrumented model panel was connected to the support via three-axis load cells as shown.

Cross bracing was used to stiffen the support structure. Eight ½ in turnbuckles were added as an additional longitudinal connection between the H frame and the solid steel carriage.

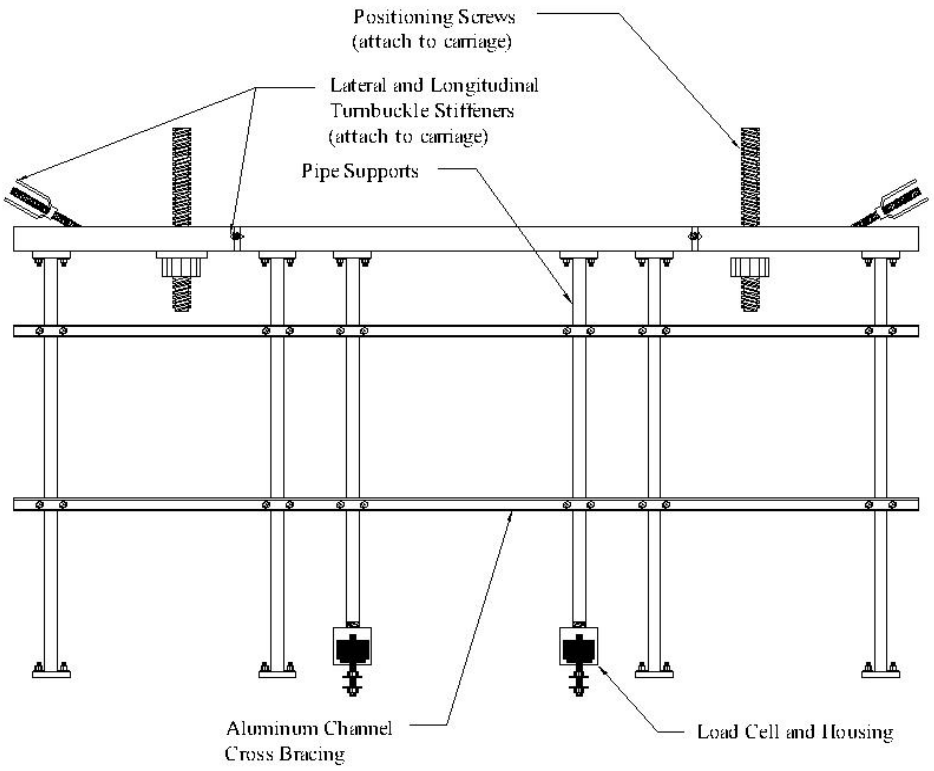

Figure 4- 7 Front view of model support structure and load cells.

Figure 4- 8 Support structure for the models.

Instrumentation

Four multi-directional (three axis) load cells were placed in aluminum housings and attached near the four corners of the center model panel. The load cells measured forces in the X (longitudinally down the tank), Y (laterally across the tank), and Z (vertical) directions. The electronics for the load cells were housed above the structure carriage in a grounded electrical box. The wire leads and cables from the load cells were routed through the support pipes. In the X and Y directions, the load cell working range was ±50 lbs per cell. In the Z direction, the load cell working range was ±200 lbs per cell. The frequency response of the load cells was 1000 Hz. All sampling was done at 480Hz.

For the tests conducted specifically for slamming, a series of pressure transducers were mounted along the width of the models (in the direction of wave propagation). This allowed measurement of localized pressures for determining load distributions. The transducers were mounted in such a way that the ports of each sensor were flush with the bottom side of each model. The working range of the pressure transducers was 0 – 5 psig. Depending on the model setup used, strings of six or ten transducers ran the width of the model. The frequency response of the pressure transducers was 1000 Hz.

Three capacitor-type wave gauges developed by engineers at the University of Florida were used to monitor the water surface elevation and wave heights. Wave gauges were located 32ft and 8ft upstream of the leading edge of the model, while the third gauge was located 8ft downstream from the trailing edge of the model. The frequency response of the wave gauges was 1000 Hz.

All measurements were controlled and recorded using LabView©. The model sections were located near the center of the tank, 68 ft from the wave maker. A diagram of the model and one of the wave gauges is shown in Figure 4- 9.

Model Setups

Two different model configurations were tested, one for total loading and one primarily for slamming loads. A number of tests were conducted with each configuration.

The dimensions of all the physical model setups involving beam and slab models are based on a 1:8 scale of the spans on the failed I-10 Escambia Bay Bridges during Hurricane Ivan. The slab models were not scaled to any particular bridge. The various tested models are described below in the order that they were studied.

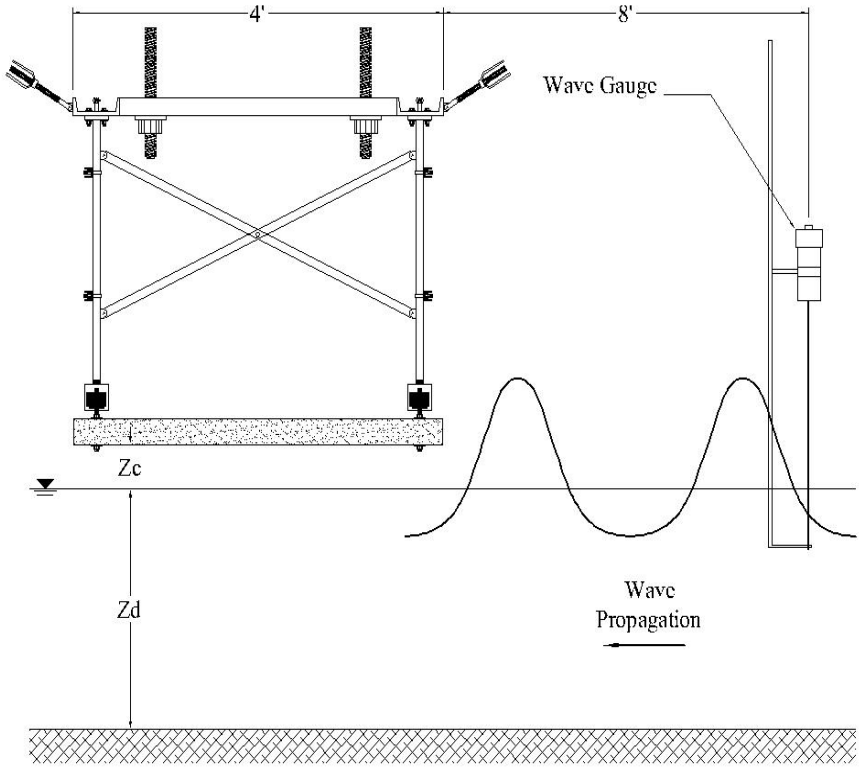

Figure 4- 9 Side view of model, model support and upstream wave gauge.

While thin, flat plate tests were also tested, their results are not directly applicable to bridge superstructures and thus not analyzed in this document. The data from those tests are, however, included in APPENDIX A for completeness. Slamming force tests with a flat plate instrumented with pressure transducers were, however, part of this study.

Model Spans Tested

The tests described below were primarily for investigating quasi-static forces.

Slab structure of finite thickness.

The slab structure of finite thickness was constructed of 1in thick sheets of polypropylene formed into a rectangular shell with internal girders also made of polypropylene for stiffening. All joints were sealed with silicone for water tightness. Each individual section of the three structures modeled measured 48 in wide by 24 in long by 7 in thick. When installed edge to edge, a continuous rectangular slab of 48 in wide by 72 in long by 7 in thick was created (Figure 4- 10).

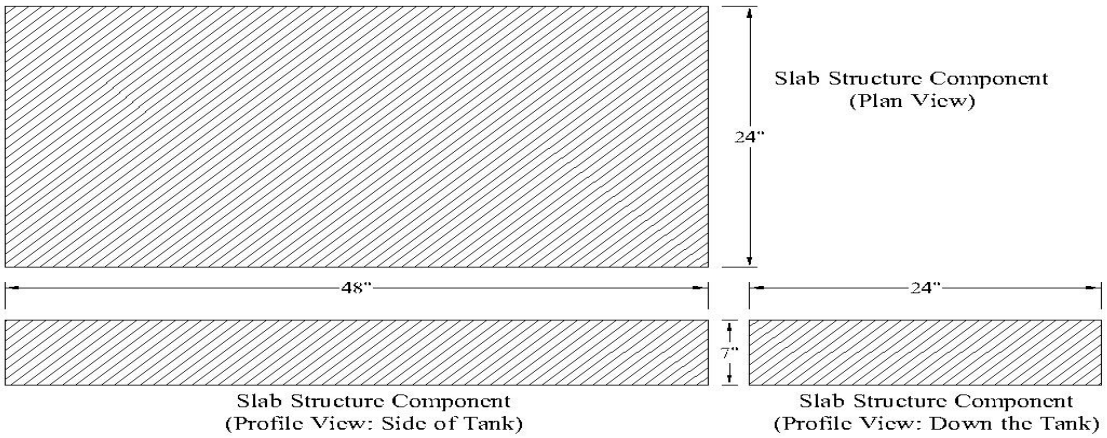

Figure 4- 10 A single panel of the model slab structure.

Beam and slab structure

The beam and slab structure was constructed of a 1 in thick polypropylene deck with a series of seven fiberglass girders (spaced 8 in on center) running along the underside of the deck. Polycarbonate glass sheets were used as diaphragms to enclose the girders on each side of the deck. Polycarbonate was chosen because its mass density is near that of water. The clear polycarbonate allowed the chambers between the beams to be viewed during the passage of the waves. All joints between the girders, diaphragms, and the deck were sealed with silicone for water tightness.

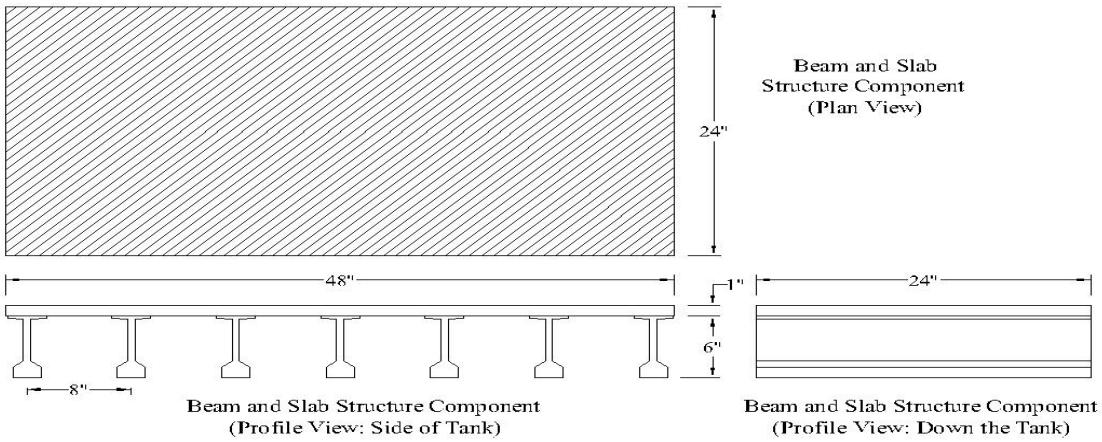

Figure 4- 11 Model beam and slab structure.

Beam and slab structure with overhangs

The beam and slab structure with overhangs was the same model as the beam and slab structure. One inch thick, 4 in long overhangs were added to both the upstream and downstream edges of each model section (Figure 4- 12).

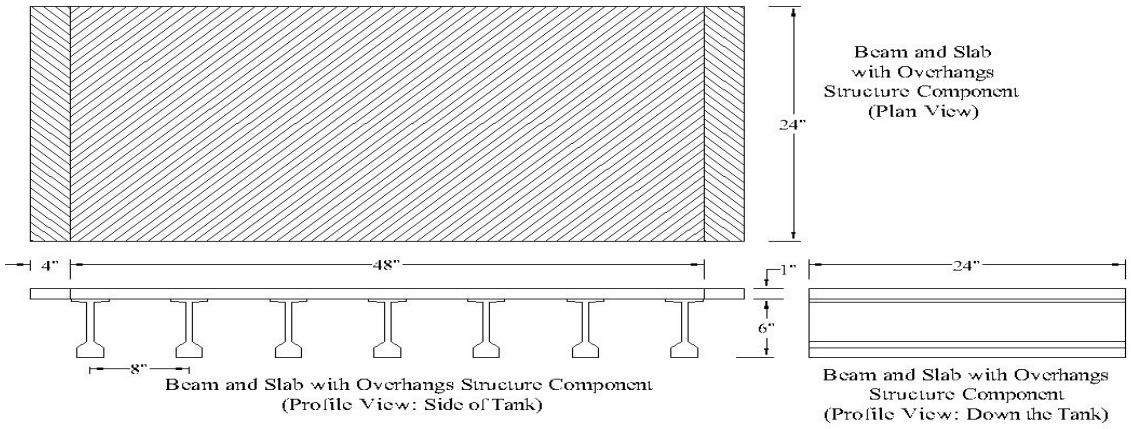

Figure 4- 12 Model beam and slab structure with overhangs.

Beam and slab structure with overhangs and rails

The beam and slab structure with overhangs and rails was the same model as the beam and slab structure with overhangs. One inch thick, 3 in tall rails were added to both the upstream and downstream overhangs of each model section (Figure 4- 13).

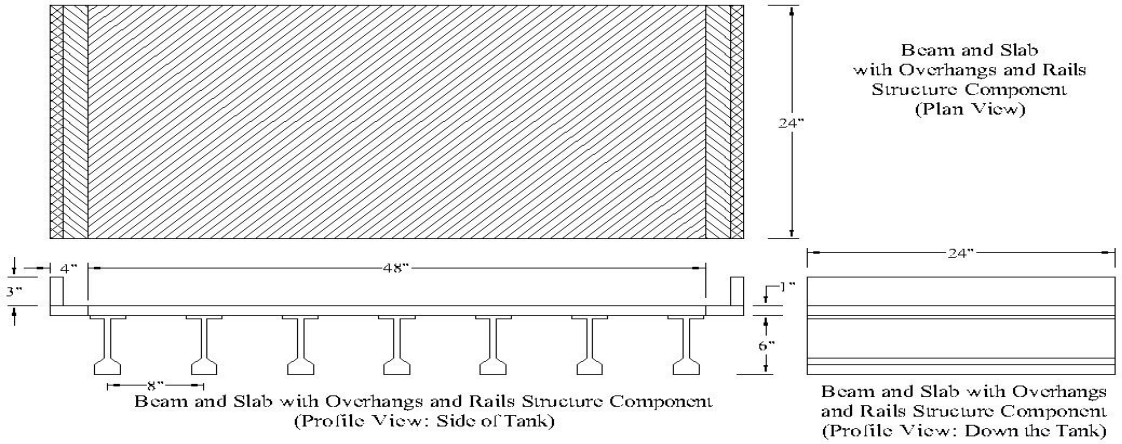

Figure 4- 13 Model beam and slab structure with overhangs and solid rails.

Beam and slab structure with overhangs and rails and larger beam spacing

The beam and slab structure with overhangs and rails was put through a separate set of tests with larger girder spacing. Four girders were used instead of seven to examine the effects of girder spacing on air entrapment and forcing (Figure 4- 14).

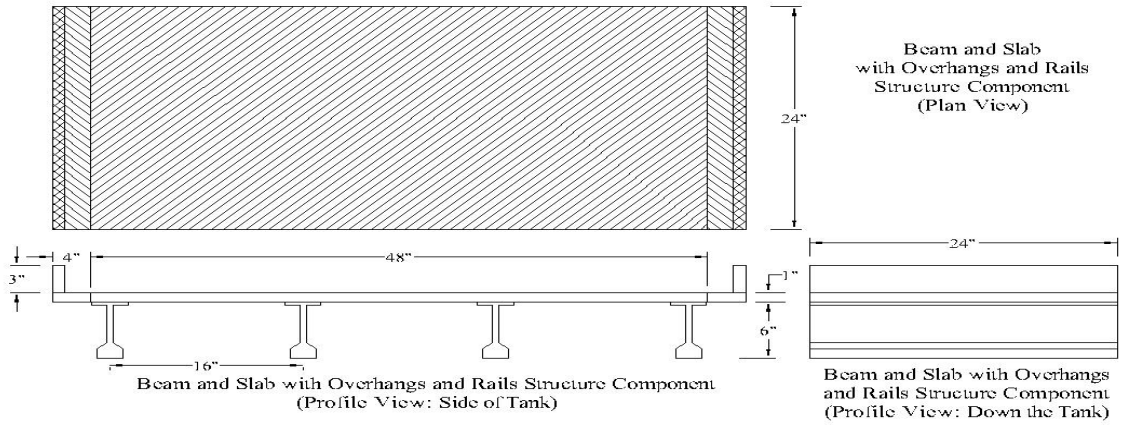

Figure 4- 14 Model beam and slab structure with overhangs and solid rails (with different beam spacing).

Slamming Force Tests

The models described below were instrumented with pressure transducers as well as load cells for the purpose of measuring both the total wave loading and the localized pressures over the width of the structure. While the quasi-static component of the force was also recorded in all data and is beneficial for comparative purposes, it was not the primary objective of these tests.

Flat plate

A flat plate structure of negligible thickness was constructed from a 1in thick polypropylene sheet. In addition to the load cell at the corners, ten pressure transducers were mounted along the centerline of the plate. The transducers were variably spaced with a higher concentration of sensors towards the upstream end of the model. Each individual section of the three structures modeled measured 48 in wide by 24 in long by 1 in thick. When installed edge to edge, a continuous rectangular slab of 48 in wide by 72 in long by 1 in thick was created. Layout and specific spacing of the pressure transducers is shown in Figure 4- 15.

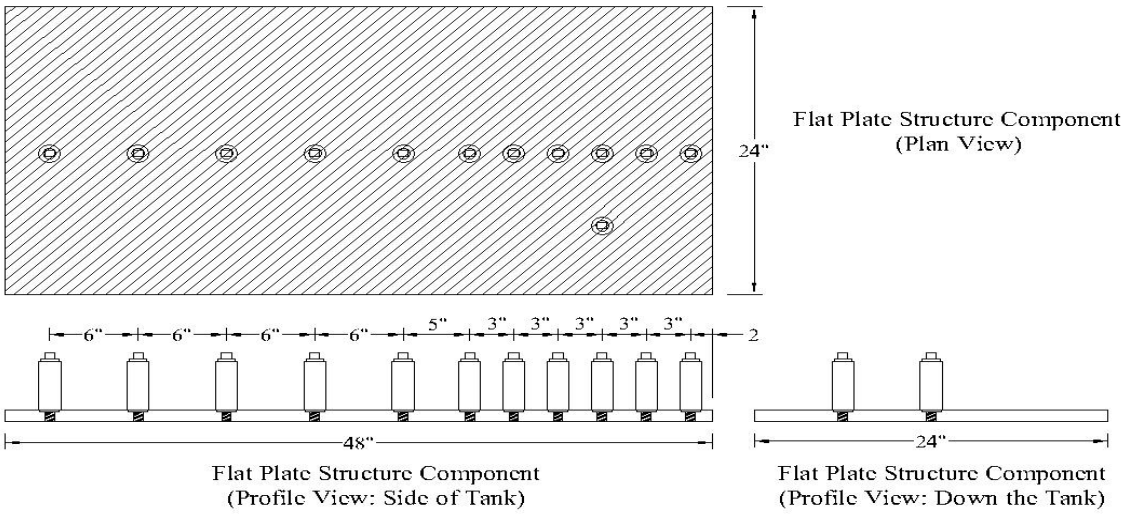

Figure 4- 15 Flat plate model instrumented for slamming forces.

Beam and slab structure with overhangs and rails

The beam and slab structure with overhangs and rails was the same model used in the tests concentrated on quasi-static forces. However, for these tests, six pressure transducers (spaced 8 in on center) were added to monitor the air pressure within each cavity created by the girders. Otherwise, the model dimensions and construction remained the same as the beam and slab with overhangs and rails model (Figure 4- 16).

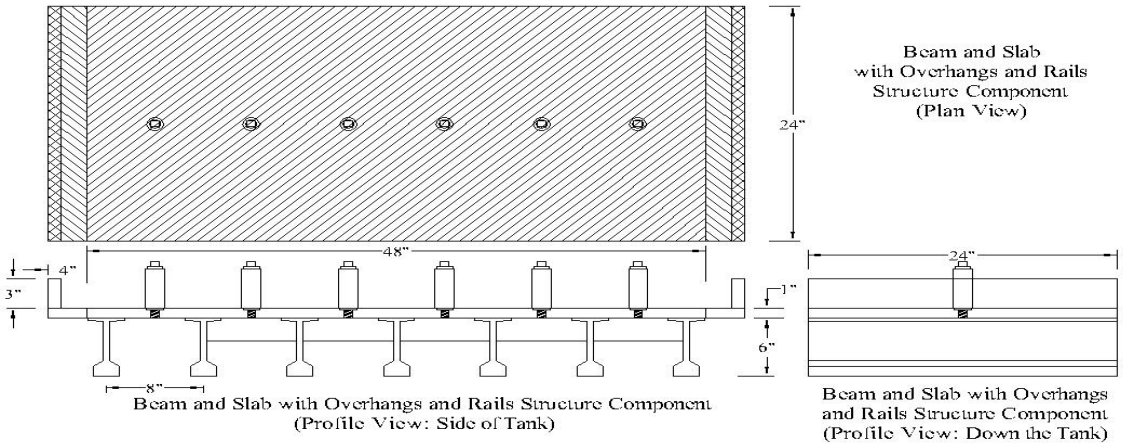

Figure 4- 16 Side view of model beam and slab structure with overhangs and solid rails instrumented for slamming forces.

Physical Model Tests

Over 1200 tests were performed on the assorted model setups and configurations. The breakdown of tests and the setups are given in Table 4- 1. Wave heights, wave periods, clearance heights, and water depths were varied over the tests. The range of parameters covered and their prototype equivalents are shown in

Table 4- 2. For each test, a train of monochromatic waves of approximately the same height and period were run past the structure and measurements taken. Photographs of tests with a flat plate structure and a girder span structure are shown in Figure 4- 17 and Figure 4- 18, respectively.

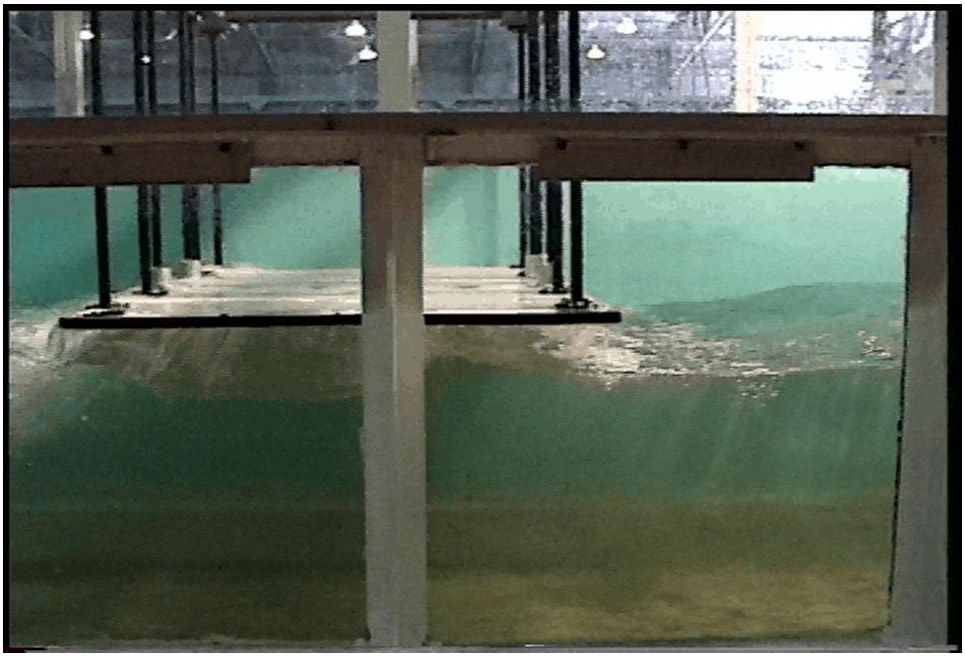

Figure 4- 17 Wave loading test with a thin, flat horizontal plate structure.

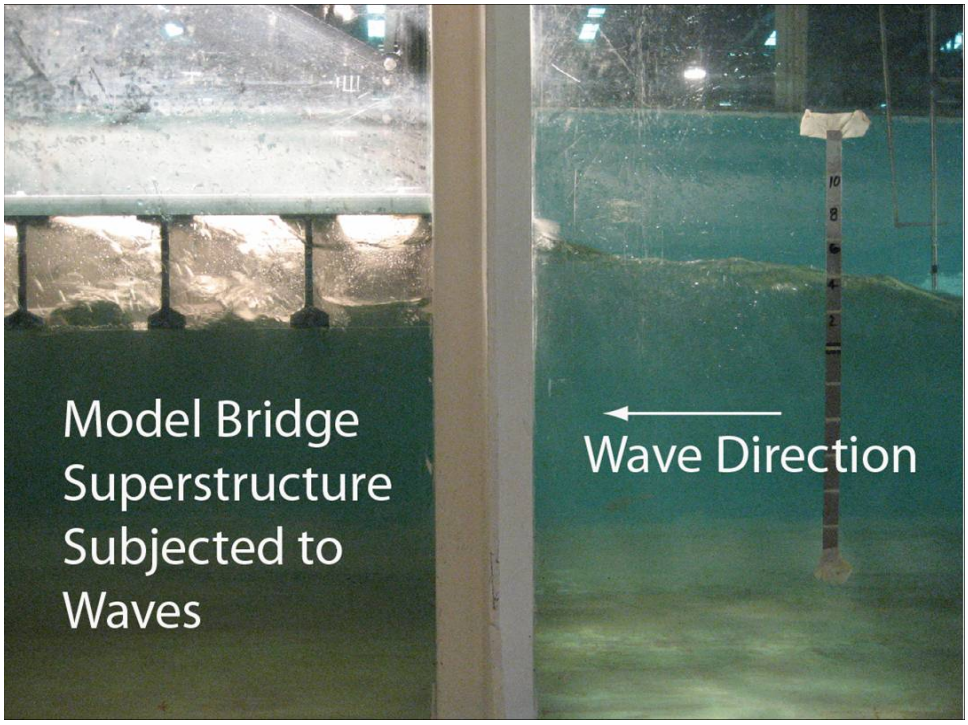

Figure 4- 18 Wave loading test with girder span structure.

Table 4- 1 Number and objective of tests performed

Test setup	Objective	Number of tests
Slab	Quasi-static	150
Beam and slab	Quasi-static	150
Beam and slab with overhangs	Quasi-static	150
Beam and slab with overhangs and rails	Quasi-static	150
Beam and slab with overhangs and rails (alternate)	Quasi-static	150
Flat Plate	Slamming	180
Beam and slab with overhangs and rails	Slamming	150
Beam and slab	Repeatability	80
Flat Plate	Repeatability	80

Table 4- 2 Range of water, wave and structure elevation values covered by the tests

Parameter	Range minimum	Range maximum
Water depth (ft)	1.50	3.00
Wave period (s)	1.00	3.50
Wave height (ft)	0.00	1.16
Clearance height (ft)	-8.00	4.00

Data Processing and Preliminary Results

Data from the experiments were reduced and analyzed as described below.

Spectral analysis

For all tests, power spectra were computed for the vertical and horizontal components of each of the load cells as well as for the combined signals of the two upstream (and two downstream) load cells. The same was done for all pressure transducers used. In all cases, the frequency with the highest power content was that of the wave frequency. Refer back to the example power spectrums for sub aerial and submerged cases for a slab test shown in Figure 4- 1.

In the submerged cases, there is very little energy present in the harmonic multiples of the wave frequency and no energy at all in the range of slamming. For a structure initially submerged or partially submerged, the natural frequency of the structure is lowered by the presence of the added mass of the water. There is also more damping of the structural response for this situation. In this case, there is less structural response at the higher frequencies. In the subaerial case the higher frequency slamming force excites the higher harmonics due to reduced damping.

In the power spectra of the upstream and downstream load cell pairs (Figure 4- 19), similar frequency content divisions were found as in the total forcing. However, from the upstream to the downstream pair a significant decrease in slamming frequency content is noticed. The presence of detectable action in the higher frequency range of the upstream load cell pairs does not always correspond to action in the downstream load cell pair. This difference suggests that slamming is limited to the upstream end of the structure for wave/structure size ratios of interest.

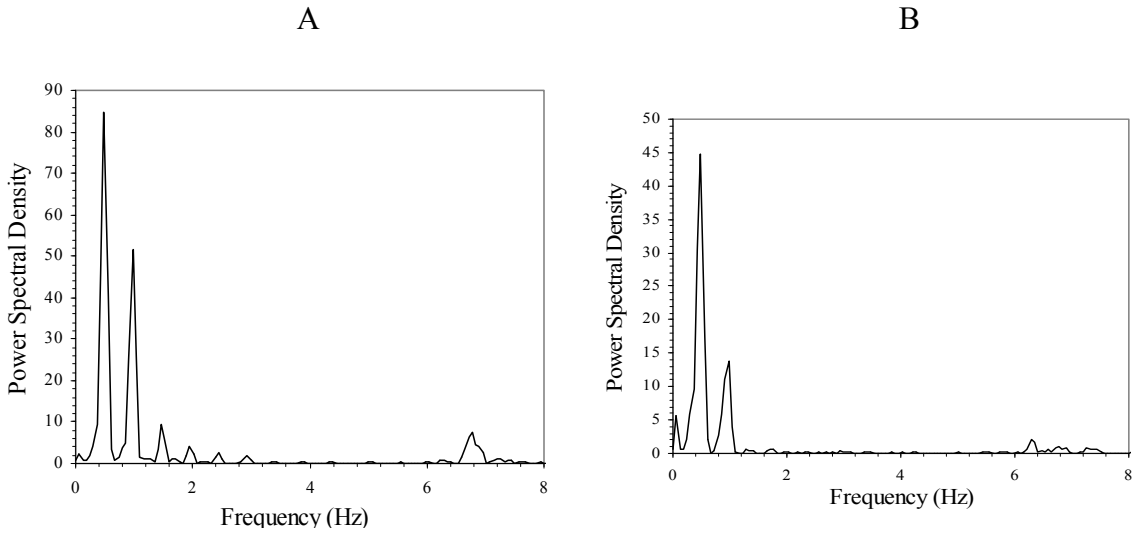

Figure 4- 19 Vertical force power spectral density for A) upstream and B) downstream load cells. Note the difference in vertical scales for A and B.

Signal filtering

A low-pass 8th order Butterworth filter was used to filter out the higher frequency components of the force. To determine attenuation effects of the filter on the lower frequency forcing, maximums and minimums were compared for test cases where higher frequency components were not present. Attenuation of the quasi-static force due to the filter proved to be negligible. The slamming force signal was then determined by subtracting the filtered quasi-static force from the original forcing. Example unfiltered and filtered vertical forces on subaerial spans are shown in Figure 4- 20 and Figure 4- 21. An example vertical slamming force time series is shown in Figure 4- 22.

A

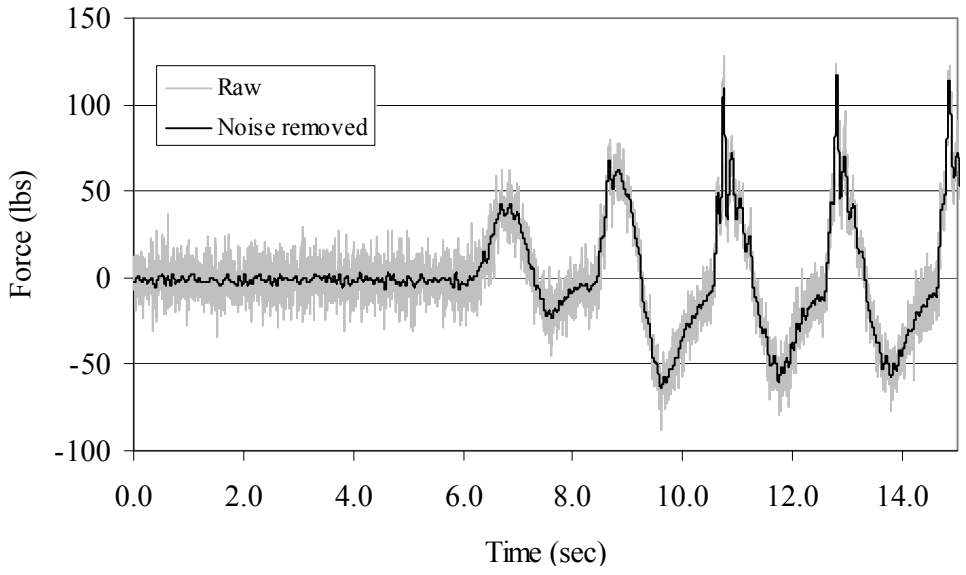

B

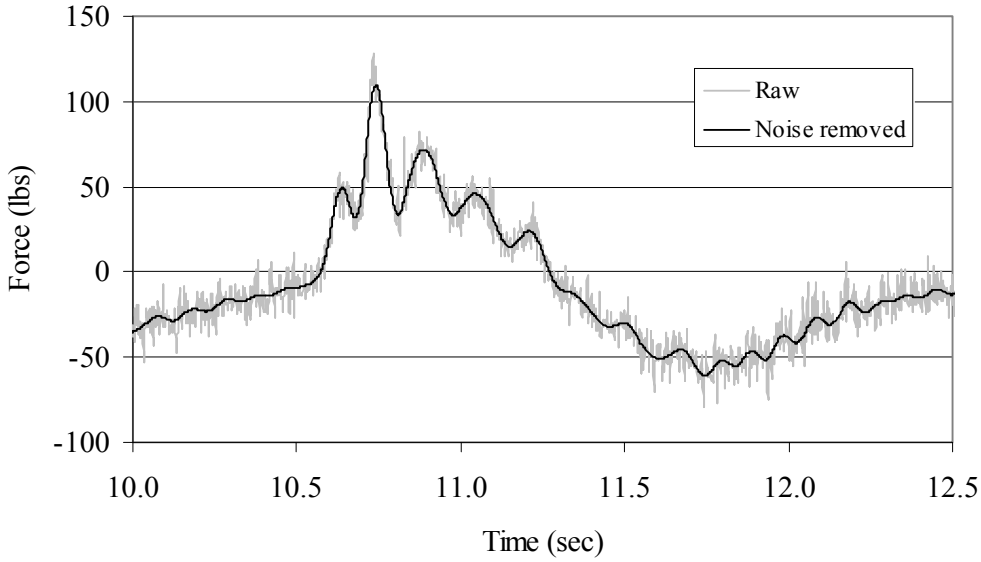

Figure 4- 20 Example of filtered and unfiltered vertical force for a subaerial slab. Forces for several waves in A). Force for a single wave in B).

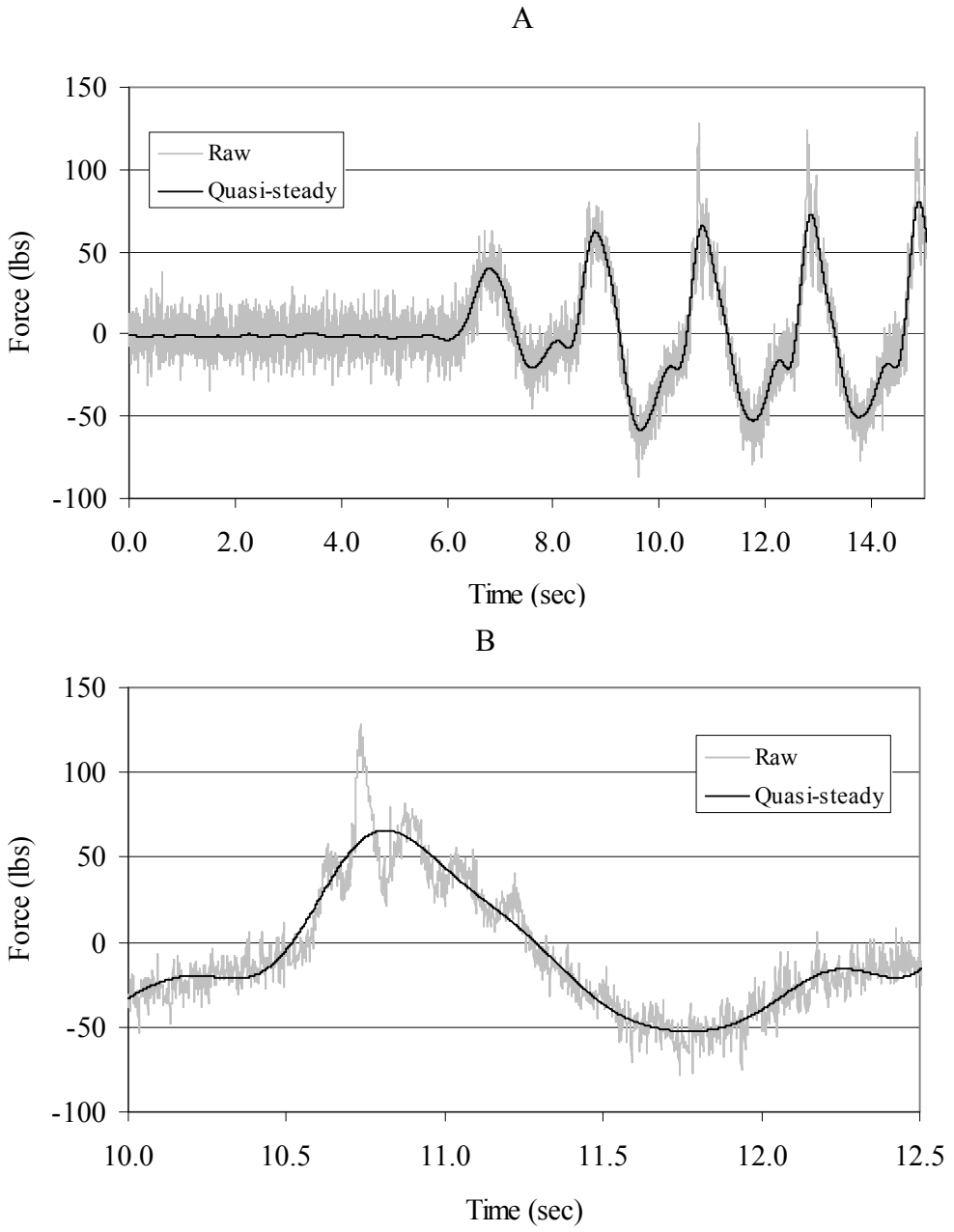

Figure 4- 21 Example of filtered and unfiltered vertical force for a subaerial slab. Forces for several waves in A). Force for a single wave in B).

A

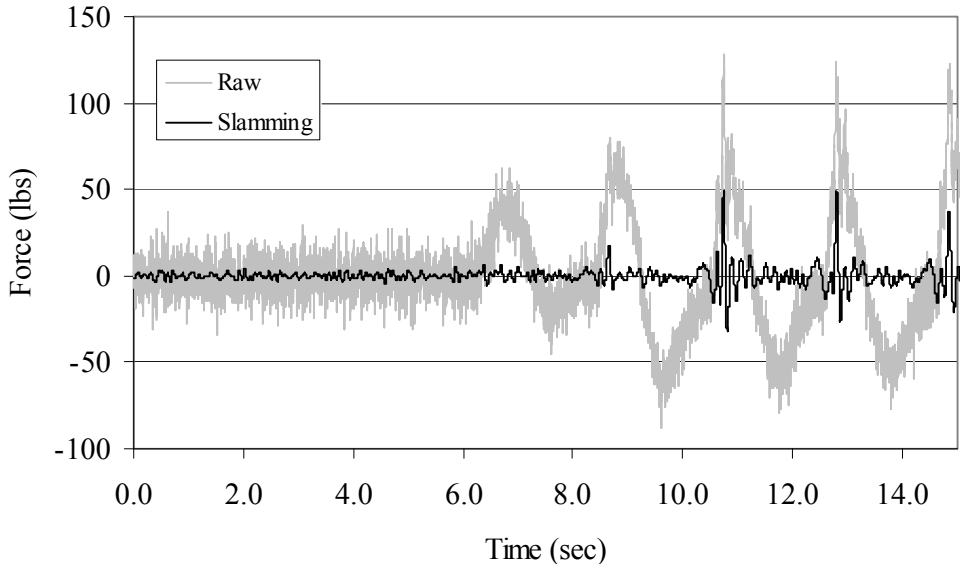

B

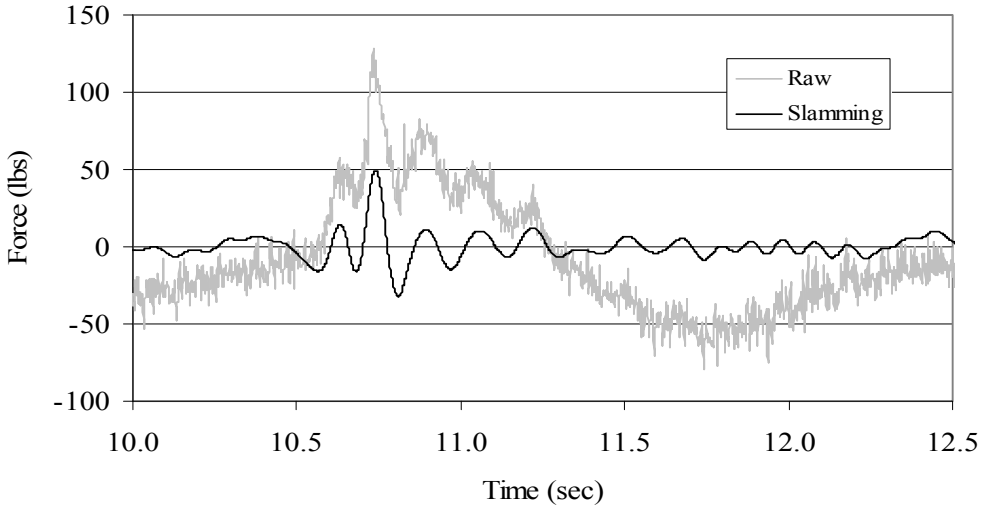

Figure 4- 22 Raw signal and slamming force examples for a subaerial slab structure. Forces for several waves in A). Force for a single wave in B).

Significant parameters extracted from the data

Once time series of the quasi-static, slamming force, and water surface elevation were known, a number of important parameters could be obtained.

For tests designed for quasi-static forces (slab tests, beam and slab tests, etc.), maximum and minimum values of the quasi-static forces (horizontal and vertical) were extracted and the maximum and minimum values of the moments about the lower downstream edge of structure calculated. In cases where slamming was present, the slamming force magnitude and duration were also extracted. Associated forces in the horizontal and vertical directions are noted and recorded.

For tests designed for slamming forces (flat plate tests, beam and slab tests), maximum values of the quasi-static and slamming forces (vertical only) were extracted and the maximum value of the moment about the downstream edge of structure calculated. The duration of the slamming force was also extracted. Associated forces in the vertical direction at the time of maximum vertical slamming force were noted and recorded.

From the water surface elevation data, wave heights and maximum wave crest elevations were obtained. This information is presented in APPENDICES A, B, and C.

Effects of girder spacing on quasi-static and slamming forces

For a subaerial beam and slab span, the spacing of the individual girders can have a significant effect on the loading experienced by the structure. This is due to the dependence of the quantity of entrapped air on the girder spacing. This volume of entrapped air is important to both the slamming and quasi-static forces.

For the quasi-static force, the presence of entrapped air increases the effective volume of the structure, which in turn increases both the buoyancy and the inertia forces. The amount of entrapped air depends on the girder spacing, span clearance height, and wave heights and lengths. The steeper the wave the greater the quantity of air removed by the progressing wave. The amount of entrapped air also depends on the spacing of the girders with the amount decreasing with increased spacing

Figure 4- 23 shows the effect of girder spacing on the vertical quasi-static force. The two spans in the figure are the same with the exception of their girder spacing. The wave height and period are the same within the accuracy of the wave maker for the two cases. For the seven girder (six chambers) case the centerline spacing was 8 in. For the four girder (three chambers) case the centerline spacing was 16 in. The wider spaced three chamber span traps less air and consequently experiences a smaller quasi-static vertical force.

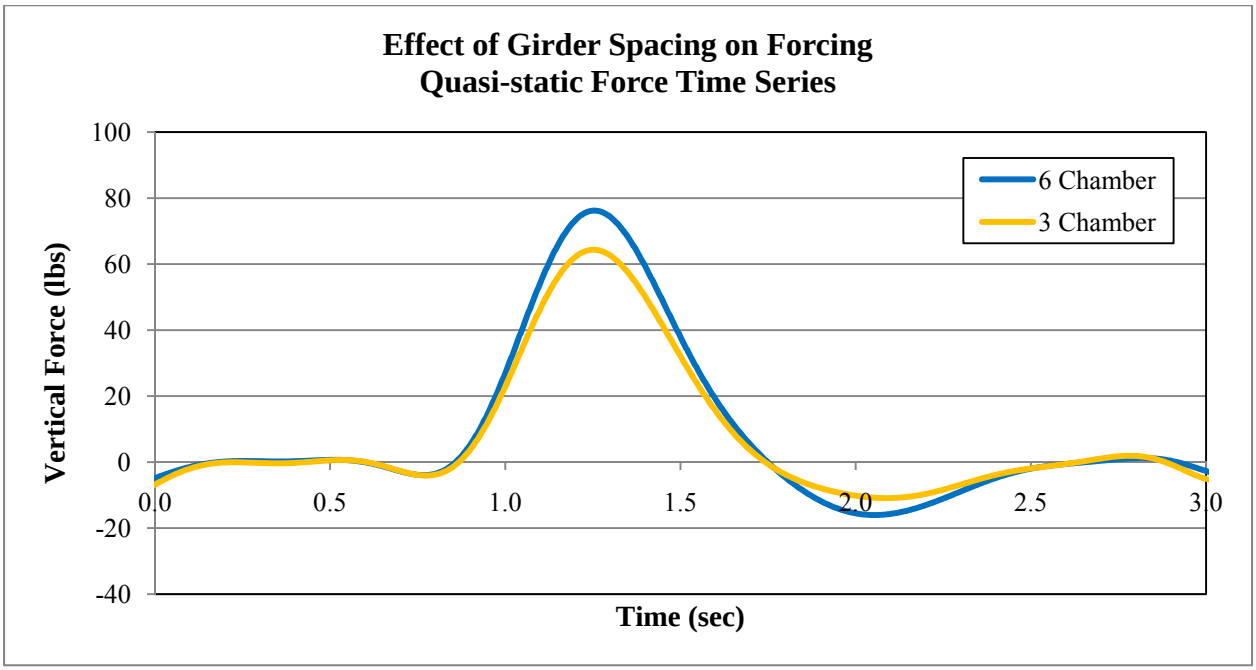

Figure 4- 23 Effect of girder spacing on the vertical quasi-static wave force.

For the slamming force, the presence of air produces a twofold effect. The first is that the entrapped air creates a lower contact surface, which otherwise may not be reached by the wave. Once the chamber is sealed by the water surface the entrapped air acts as an extension of the structure surface that conforms to the shape of the water surface. The air also acts as a spring as it is compressed. The net effect is that the magnitude of the slamming is reduced and the duration is lengthened.

The number of slamming pulses is directly related to the number of entrapped air chambers as can be seen in Figure 4- 24. The two spans in this figure are those described above (one with girders with 8 in. centerline spacing and one with 16 in. centerline spacing). Within the accuracy

of the wave maker the waves are the same for the two cases. Provided there is sufficient energy in the wave, the tendency is for the number of slamming pulses to equal the number of air entrapment chambers. Note that in the case of the seven chambers there are only six pulses due to energy dissipation as the wave progresses past the structure.

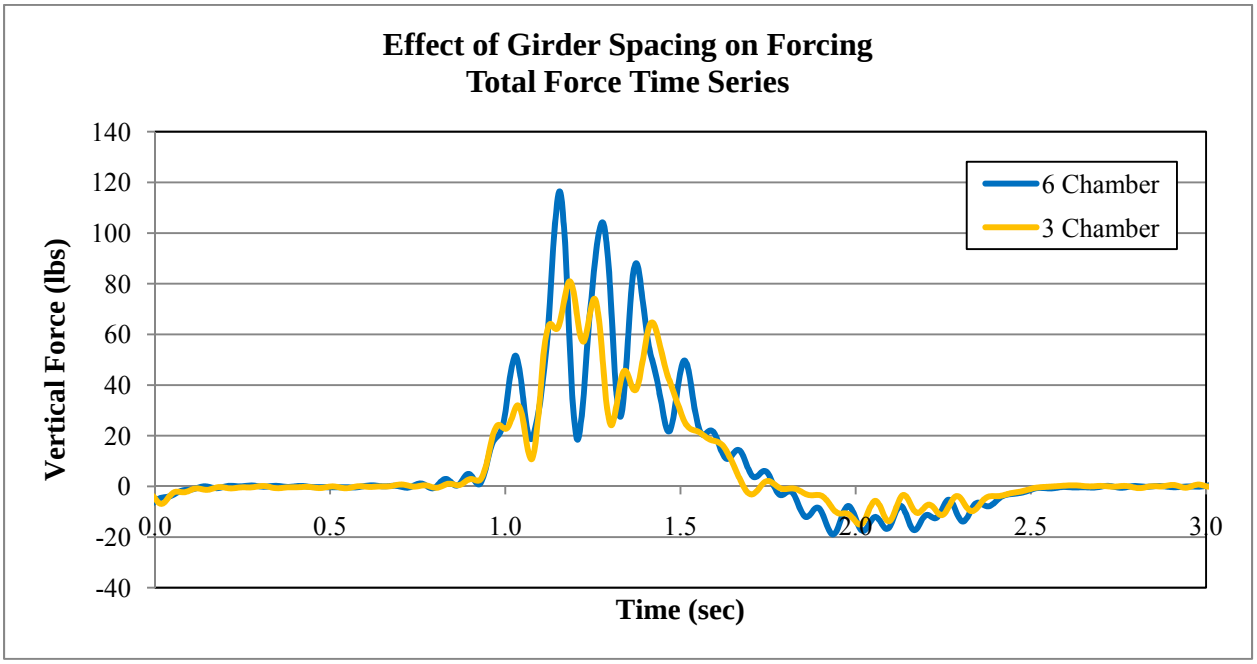

Figure 4- 24 Effect of girder spacing on the vertical wave slamming force.

CHAPTER 5 – SLAMMING FORCES

Slamming forces occur when the air-water interface comes in contact with the structure. The greater the surface area and the more parallel the water and structure surfaces the greater the magnitude of the slamming force. As with any rapidly changing, transient phenomenon the processes are complex and difficult to quantify. The shape of the water surface just prior to impact is random thus the area of impact in a real sea is random. Even in a controlled laboratory situation with monochromatic waves being generated in a wave tank there are slight differences from one wave to the next. If a model bridge superstructure is placed in the wave tank the approaching waves become even more distorted due to wave reflections from the structure. Therefore even in a laboratory situation it is not possible to produce an impact of a perfect monochromatic wave with a structure. In spite of these limitations much can be learned about wave slamming on horizontal, bridge span structures from monochromatic wave tank tests.

Wave slamming force tests were performed on three different structures and a range of wave heights and periods, structure positions relative to the still water level, and water depths as part of this study. For the flat plate tests pressure transducers were mounted as shown in Figure 4- 15. Figure 1- 17 is a schematic diagram showing the vertical component of the wave force during the passage of a single monochromatic wave. Typically there is a single, short duration, high magnitude slamming force located in time near the quasi-static maximum as shown schematically in Figure 1- 17. The structure, water depth and wave parameters for the flat plate tests are presented in Table C- 1. The measured forces and pressures for these tests are given in Table C- 2. A parametric slamming force equation for flat plates was developed in terms of the wave parameters and the plate width (in the direct of wave propagation) and plate position relative to the still water level,

$$ln\left(\frac{F_S}{\rho g H W\left(\eta - Z_C\right)/\lambda}\right) = -15.0 + 17.9\,exp\left(-\frac{H}{\lambda}\right) - 1.27\left(-\frac{Z_C}{\eta}\right), \qquad (5\text{-}1)$$

for $-1.0 < Z_C/\eta < 1.0$,

where
FS = slamming force,
r= mass density of water,
g = gravitational acceleration constant,
H = wave height,
W = width of span,
h=wave crest height above SWL,
Z_C = distance from SWL to bottom of span, and
l=wave length.

The slamming forces on the girder span structures were extracted from the load cell data and these data are presented in Table B- 2. Entrapped air between the girders can have a major impact on the slamming force. In general, the magnitude is attenuated and the duration is lengthened. Multiple shamming forces can occur, one for each cavity (between the girders). This is shown schematically in Figure 1- 19. In this case there are nine girders and eight cavities. This shift in frequency of the slamming from that for the flat plate (slab type span) could have a significant impact on the structure's dynamic response.

CHAPTER 6 – SUMMARY AND CONCLUSIONS

A theoretical model for wave loading on horizontal structures was developed in this study. It is an extension and modification of the models developed by Morison, et al. (1950) and Kaplan (1992, 1995) to include bridge superstructure shapes and the meteorological and oceanographic (met/ocean) conditions found in the locations of coastal bridges. The waves in water bodies with limited fetches such as bays, harbors and coastal waterways are shorter in length than those in the open ocean. Wave forces on bridge superstructures are more complex for these conditions where the span widths are similar in magnitude to the wave lengths. This results in large variations in the vertical force over the width of the span at any point in time. By necessity, the predictive equations contain empirical coefficients that must be determined experimentally.

To provide the information needed to compute the coefficients wave tanks tests were performed with model structures. Experiments were performed with three different structure types, flat plates, slab spans, and beam (girder) spans. The girder spans were tested with and without overhangs, with and without parapets and with two different girder spacings. The tests included a range of water depths, span locations relative to the still water level, and wave heights and periods (lengths). Three direction load cells on each corner of the instrumented panel were used to measure the horizontal, transverse and vertical forces. Pressure transducers were used to measure the pressure on the bottom of the spans. The pressure measurements were used primarily for measurement of the high frequency slamming forces.

Using the empirical coefficients determined from the laboratory data the predictive equations were used to predict the wave loads on the spans on the I-10 Escambia Bay bridges during Hurricane Ivan. Since it was not possible to know the quantity of air entrapped between the girders during the storm, two limiting cases were investigated, zero and maximum entrapment. Assuming the actual air entrapment was somewhere between the two limiting cases the equations did a good job of predicting both the cases where the wave loads exceeded and did not exceed the resistance (dead weight plus tie-downs). The water elevation and wave conditions at the bridge were provided by a detailed hindcast of Hurricane Ivan conducted by OEA, Inc. as part of the bridge hydraulic report for the replacement bridges.

The wave force is in general composed of a low frequency component sometimes referred to as the quasi-static force and a high frequency component called the slamming force. Both components were measured and analyzed in this study. The low frequency component has the frequency of the dominant wave which is typically in the range of 0.1Hz to 0.5 Hz. The slamming force frequency is much higher and its magnitude can be equal to or larger than the low frequency, quasi-static component. Both the frequency and the duration of the slamming force depend on structure type and elevation relative to the still water level as well as the wave properties. The frequency is lower and the duration longer for beam type spans with air entrapment. Analytically the two forces (quasi-static and slamming) are treated separately with the total force being the superposition of the two. The slamming force can occur before, at, or after the peak of the low frequency force. A somewhat conservative but realistic assumption is that the two peaks of the vertical forces occur at the same time. The theoretical model and the experiments were for waves approaching the spans at right angles. The lengths of the wave crests were assumed to be at least as long as the bridge spans; therefore, the wave forces are uniform over the length of the span. Waves approaching at angles other than 90 degrees need to be investigated. However, it is believed that angles other than 90 degrees will produce lesser entrapped air and smaller total forces.

In conclusion, this study has advanced the understanding and the ability to predict forces on bridge superstructures due to elevated water levels and waves. Slab and beam type bridge spans were investigated experimentally and the results used to test the theoretical model and to provide information needed to compute drag and inertia coefficients for the theoretical model. Work was initiated on vertical slamming on horizontal structures in this study, but this is a complex subject and more work is definitely needed.

REFERENCES

Baarholm, R., and Faltinsen, O. M. (2004). "Wave impact underneath horizontal decks." J. Marine Science and Tech., 9, 1-13.

Bea, R. G., Xu, T., Stear, J., and Ramos, R. (1999). "Wave forces on decks of offshore platforms." J. Waterway, Port, Coastal, Ocean Eng., 125(3), 136-144.

Bea, R. G., Iversen, R., and Xu, T. (2001). "Wave-in-deck forces on offshore platforms." J. Offshore Mech. Arctic Eng., 123, 10-21.

Cardone, V. J., and Cox, A. T. (1992). "Hindcast study of Hurricane Andrew, offshore Gulf of Mexico." Joint Industry Project Rep., Ocean-weather Inc., Cos Cob, Conn.

Chen, G., Witt III, E. C., Hoffman, D., Luna, and R., Sevi, A. (2005). "Analysis of the interstate 10 twin bridge's collapse during Hurricane Katrina." Science and the Storms: the USGS Response to the Hurricanes of 2005, USGS Circular 1306, USGS.

Cuomo, G., Allsop, W., and McConnell, K. (2003). "Dynamic wave loads on coastal structures: analysis of impulsive and pulsating wave loads." Proc., Coastal Structures 2003, COPRI, Portland, Or.

Cuomo, G., Tirindelli, M., and Allsop, W. (2007). "Wave-in-deck loads on exposed jetties." Coastal Eng., 54, 657-679.

Da Costa, S. L., and Scott, J. L. (1988). "Wave impact force on the Jones Island east dock, Milwaukee, Wisconsin." Proc., Oceans 88, 31, 1231-1238.

Dean, R. G., Torum, A., and Kjeldsen, S. P. (1985). "Wave forces on a pile in the surface zone from the wave crest to wave trough." Proc., Int. Symp. on Separated Flow Around Marine Structures, Norwegian Institute of Technology, Trondheim, Norway.

Denson, K. H. (1978). "Wave forces on causeway-type coastal bridges." Misc. Rep., Water Resources Research Institute, Mississippi State University, Starkville, Miss.

Denson, K. H. (1980). "Wave forces on causeway-type coastal bridges: Effects of angle of wave incidence and cross-section shape." Technical Rep. No. MSHD-RD-80-070, Water Resources Research Institute, Mississippi State University, Starkville, Miss.

Douglas, S. L., Chen, Q., and Olsen, J. M. (2006). "Wave forces on bridge decks." Draft Report, CTEREC, University of South Alabama, Mobile, Ala.

El Ghamry, O. A. (1963). "Wave forces on a dock." Research Technical Report HEL-9-1, Hydraulic Engineering Laboratory, Berkeley, Cal.

Faltinsen, O., Kjarland, O., Nottveit, A., and Vinje, T. (1977). "Water impact loads and dynamic response of horizontal circular cylinders in offshore structures." Proc., Offshore Technology Conf., SPE, Richardson, Tex.

Finnigan, T. D., and Petrauskas, C. (1997). "Wave-in-deck forces." Proc., 6th Int. Offshore and Polar Engineering Conf., ISOPE, Golden, Colo.

French, J. A. (1970). "Wave uplift pressures on horizontal platforms." Proc., Civil Eng. in the Oceans Conf., ASCE.

French, J. A. (1979). "Wave uplift pressures on horizontal platforms." Proc. Civil Eng. in the Oceans, ASCE, San Francisco, CA.

Goda, Y. (2000). "Random seas and design of maritime structures." Advanced Series on Ocean Engineering, 15, World Scientific.

Imm, G. R., O'Connor, J. M., and Stahl, B. (1994). "South Timbalier 161A: A successful application platform requalification technology." Proc., Offshore Technology Conf., SPE, Richardson, Tex.

Isaacson, M., and Bhat, S. (1996). "Wave forces on a horizontal plate." Int. J. Offshore Polar Eng., 6(1), 19-26.

Jue, M. C. (1993). "Extreme surface wave force on the supporting legs of offshore platforms." MS Thesis, Department of Naval Architecture and Offshore Engineering, University of California, Berkeley, Ca.

Kaplan, P. (1992). "Wave impact forces on offshore structures: Re-examination and new interpretations." Proc., Offshore Tech. Conf., SPE, Richardson, Tex.

Kaplan, P., Murray, J. J., and Yu, W. C. (1995). "Theoretical analysis of wave impact forces on platform deck structures." Proc., 14th Int. Conf. Offshore Mech. and Arctic Eng., ASME, New York.

Kjeldsen, S. P., and Myrhaug, D. (1979). "Breaking waves in deep water and resulting wave forces." Proc., Offshore Technology Conf., SPE, Richardson, Tex.

Kjeldsen, S. P., and Hasle, E. K. (1985). "Ekofisk jacket – Model experiments." Rep. No. NHL 85-0295, Norwegian Hydrodynamics Laboratory, Trondheim, Norway.

Kjeldsen, S. P., Torum, A., and Dean, R. G. (1986). "Wave forces on vertical piles caused by 2 and 3-dimensional breaking waves." Proc., Coastal Engineering Conf., ASCE, New York.

Marin, J. (2009). "Wave Loading on a Horizontal Plate", Master of Science Thesis, Civil and Coastal Engineering Department, University of Florida, Gainesville, Florida.

McConnell, K. J., Allsop, N. W. H., Cuomo, G., and Cruickshank, I. C. (2003). "New guidance for wave forces on jetties in exposed locations." Proc., 6th Int. Conf. on Coastal and Port Engineering in Developing Countries, COPEDEC, Columbo, Sri Lanka.

Morison, J. R., O'Brien, M. P., Johnson, J. W., and Schaaf, S. A. (1950). "The force exerted by surface waves on piles." Petrol. Trans., 189, 149-154.

Murray, J. J., Kaplan, P., and Yu, W. C. (1995). "Experimental and analytical studies of wave impact forces on Ekofisk platform structures." Proc., Offshore Tech. Conf., SPE, Richardson, Tex..

Overbeek, J., and Klabbers, I. M. (2001). "Design of jetty deck for extreme vertical wave loads."

Payne, P. R. (1981). "The virtual mass of a rectangular flat plate of finite aspect ratio." Ocean Eng., 8(5), 541-545.

Schumacher, T., Higgins, C., Bradner, C., Cox, D., and Yim, S. (2008). "Large-scale wave flume experiments on highway bridge superstructures exposed to hurricane wave forces." Proc., 6th National Seismic Conf. on Bridges and Highways, Charleston, SC.

Sarpkaya, T., and Isaacson, M. (1981). "Mechanics of wave forces on offshore structures." Van Nostrand Reinhold Co., New York.

Sheppard, D. Max and Miller, Willaim (2006). "Live-Bed Local Pier Scour Experiments", J. of Hydraulic Engineering, Vol. 132, No. 7, p. 635-642.

Stear, J., and Bea, R. G. (1997). "Ultimate limit state capacity analysis of two Gulf of Mexico platforms." Proc., Offshore Technology Conf., SPE, Richardson, Tex.

Suchithra, N., and Koola, P. M. (1995). "A study of wave impact on horizontal slabs." Ocean Eng., 22(7), 687-697.

Sulisz, W., Wilde, P., and Wisniewski, M. (2005). "Wave impact on elastically supported horizontal deck." Jo. Fluids and Structures, 21, 305-319.

Tirindelli, M., Cuomo, G., Allsop, N. W. H., and McConnell, K. J. (2002). "Exposed jetties: Inconsistencies and gaps in design methods for wave-induced forces." Proc., 28th Int. Conf. on Coastal Engineering, ASCE, Cardiff, UK.

Tirindelli, M., Cuomo, G., Allsop, N. W. H., and Lamberti, A. (2003). "Wave-in-deck forces on jetties and related structures." Proc., 13th Int. Offshore and Polar Eng. Conf., ISOPE, Honolulu, Haw.

U.S. Army Corp of Engineers (2006). "Coastal Engineering Manual." Manual No. EM 1110-2-1100, U.S. Army Corp of Engineers, Coastal and Hydraulics Laboratory, Vicksburg, Miss.

Vannan, M. T., Thompson, H. M., Griffin, J. J., and Gelpi, S. L. (1994). "An automated procedure for platform strength assessment." Proc., Offshore Technology Conf., SPE, Richardson, Tex.

Von Karman, T. (1929). "The impact of seaplane floats during landing." Report NACA-TN-321, Washington.

Wang, H. (1970). "Water wave pressure on horizontal plate." J. of the Hydraulics Division, 96(HY10), 1997-2017.

Weggel, J. R. (1997). "Breaking-wave loads on vertical walls suspended above mean sea level." J. Waterway, Port, Coastal, Ocean Eng., 123(3), 143-148.

Wilde, P., Szmidt, K., and Sobieraiski, E. (1998). "Phenomena in standing wave impact on a horizontal plate." Proc. 26th Coastal Eng. Conf., ASCE.

Yu, Y., (1945). "Virtual masses of rectangular plates and parallelpipeds in water." J. Applied Physics, 16, 724-729.

APPENDIX A – QUASI-STATIC FORCES ON FLAT PLATES

The following tables are a list of all physical model tests performed and the significant variables and values associated with each test. The tables are divided into variables and forces as well as tests done with and without side panels (i.e. continuous and finite width structures). The tests can be differentiated by the individual case prefix and reference number, ‘FPWS’ for tests done with side panels, and ‘FPNS’ for tests done without side panels.

Table A-1 contains the relevant fluid and structure parameters for all tests. Table A-2 contains the measured significant forces and moments for all tests. All dimensions are in feet, all forces are in pounds, and all times are in seconds.

Table A- 1 Structure and fluid parameters for all physical model tests.

Test case	Plate Width	Plate length	Plate Thick.	Plate Clear.	Water Depth	Wave Height	Wave Period	Wave Length	Wetted Width
FPWS001	4.00	6.00	0.08	0.00	1.58	0.32	3.00	20.65	4.00
FPWS002	4.00	6.00	0.08	0.00	1.58	0.63	3.00	20.65	4.00
FPWS003	4.00	6.00	0.08	0.00	1.58	0.54	2.50	16.92	4.00
FPWS004	4.00	6.00	0.08	0.00	1.58	0.83	2.50	16.92	4.00
FPWS005	4.00	6.00	0.08	0.00	1.58	0.58	2.00	13.12	3.51
FPWS006	4.00	6.00	0.08	0.00	1.58	0.75	2.00	13.12	3.73
FPWS007	4.00	6.00	0.08	0.00	1.58	0.61	1.50	9.17	3.66
FPWS008	4.00	6.00	0.08	0.00	1.58	0.67	1.50	9.17	2.41
FPWS009	4.00	6.00	0.08	0.00	1.58	0.58	1.00	4.94	3.26
FPWS010	4.00	6.00	0.08	0.00	1.58	0.52	1.00	4.94	2.47
FPWS011	4.00	6.00	0.08	0.08	1.58	0.45	3.00	20.65	4.00
FPWS012	4.00	6.00	0.08	0.08	1.58	0.68	3.00	20.65	4.00
FPWS013	4.00	6.00	0.08	0.08	1.58	0.48	2.50	16.92	4.00
FPWS014	4.00	6.00	0.08	0.08	1.58	0.75	2.50	16.92	4.00
FPWS015	4.00	6.00	0.08	0.08	1.58	0.42	2.00	13.12	4.00
FPWS016	4.00	6.00	0.08	0.08	1.58	0.58	2.00	13.12	4.00
FPWS017	4.00	6.00	0.08	0.08	1.58	0.63	1.50	9.17	4.00
FPWS018	4.00	6.00	0.08	0.08	1.58	0.67	1.50	9.17	4.00
FPWS019	4.00	6.00	0.08	0.08	1.58	0.58	1.00	4.94	1.66
FPWS020	4.00	6.00	0.08	0.08	1.58	0.50	1.00	4.94	1.98
FPWS021	4.00	6.00	0.08	0.17	1.58	0.38	3.00	20.65	3.17
FPWS022	4.00	6.00	0.08	0.17	1.58	0.64	3.00	20.65	4.00
FPWS023	4.00	6.00	0.08	0.17	1.58	0.48	2.50	16.92	4.00
FPWS024	4.00	6.00	0.08	0.17	1.58	0.71	2.50	16.92	4.00
FPWS025	4.00	6.00	0.08	0.17	1.58	0.46	2.00	13.12	3.25
FPWS026	4.00	6.00	0.08	0.17	1.58	0.60	2.00	13.12	4.00
FPWS027	4.00	6.00	0.08	0.17	1.58	0.50	1.50	9.17	2.54
FPWS028	4.00	6.00	0.08	0.17	1.58	0.65	1.50	9.17	3.25
FPWS029	4.00	6.00	0.08	0.17	1.58	0.50	1.00	4.94	1.51
FPWS030	4.00	6.00	0.08	0.17	1.58	0.44	1.00	4.94	1.19
FPWS031	4.00	6.00	0.08	0.25	1.58	0.40	3.00	20.65	0.00
FPWS032	4.00	6.00	0.08	0.25	1.58	0.58	3.00	20.65	3.53
FPWS033	4.00	6.00	0.08	0.25	1.58	0.46	2.50	16.92	0.00
FPWS034	4.00	6.00	0.08	0.25	1.58	0.75	2.50	16.92	4.00
FPWS035	4.00	6.00	0.08	0.25	1.58	0.48	2.00	13.12	0.00

Table A-1. Continued.

Test case	Plate Width	Plate length	Plate Thick.	Plate Clear.	Water Depth	Wave Height	Wave Period	Wave Length	Wetted Width
FPWS036	4.00	6.00	0.08	0.25	1.58	0.58	2.00	13.12	2.21
FPWS037	4.00	6.00	0.08	0.25	1.58	0.58	1.50	9.17	1.54
FPWS038	4.00	6.00	0.08	0.25	1.58	0.69	1.50	9.17	2.36
FPWS039	4.00	6.00	0.08	0.25	1.58	0.51	1.00	4.94	0.00
FPWS040	4.00	6.00	0.08	0.25	1.58	0.48	1.00	4.94	0.00
FPWS041	4.00	6.00	0.08	0.08	1.79	0.41	3.00	21.86	4.00
FPWS042	4.00	6.00	0.08	0.08	1.79	0.78	3.00	21.86	4.00
FPWS043	4.00	6.00	0.08	0.08	1.79	0.49	2.50	17.87	4.00
FPWS044	4.00	6.00	0.08	0.08	1.79	0.83	2.50	17.87	4.00
FPWS045	4.00	6.00	0.08	0.08	1.79	0.58	2.00	13.80	4.00
FPWS046	4.00	6.00	0.08	0.08	1.79	0.75	2.00	13.80	4.00
FPWS047	4.00	6.00	0.08	0.08	1.79	0.69	1.50	9.54	4.00
FPWS048	4.00	6.00	0.08	0.08	1.79	0.58	1.00	5.01	1.81
FPWS049	4.00	6.00	0.08	0.00	1.79	0.49	3.00	21.86	4.00
FPWS050	4.00	6.00	0.08	0.00	1.79	0.78	3.00	21.86	4.00
FPWS051	4.00	6.00	0.08	0.00	1.79	0.51	2.50	17.87	4.00
FPWS052	4.00	6.00	0.08	0.00	1.79	0.75	2.50	17.87	4.00
FPWS053	4.00	6.00	0.08	0.00	1.79	0.70	2.00	13.80	4.00
FPWS054	4.00	6.00	0.08	0.00	1.79	0.79	2.00	13.80	4.00
FPWS055	4.00	6.00	0.08	0.00	1.79	0.72	1.50	9.54	4.00
FPWS056	4.00	6.00	0.08	0.00	1.79	0.54	1.00	5.01	2.50
FPWS057	4.00	6.00	0.08	0.17	1.79	0.36	3.00	21.86	2.62
FPWS058	4.00	6.00	0.08	0.17	1.79	0.72	3.00	21.86	4.00
FPWS059	4.00	6.00	0.08	0.17	1.79	0.51	2.50	17.87	4.00
FPWS060	4.00	6.00	0.08	0.17	1.79	0.75	2.50	17.87	4.00
FPWS061	4.00	6.00	0.08	0.17	1.79	0.50	2.00	13.80	3.83
FPWS062	4.00	6.00	0.08	0.17	1.79	0.67	2.00	13.80	4.00
FPWS063	4.00	6.00	0.08	0.17	1.79	0.63	1.50	9.54	3.20
FPWS064	4.00	6.00	0.08	0.17	1.79	0.52	1.00	5.01	1.40
FPWS065	4.00	6.00	0.08	0.25	1.79	0.36	3.00	21.86	0.00
FPWS066	4.00	6.00	0.08	0.25	1.79	0.67	3.00	21.86	4.00
FPWS067	4.00	6.00	0.08	0.25	1.79	0.44	2.50	17.87	0.00
FPWS068	4.00	6.00	0.08	0.25	1.79	0.67	2.50	17.87	4.00
FPWS069	4.00	6.00	0.08	0.25	1.79	0.50	2.00	13.80	0.00
FPWS070	4.00	6.00	0.08	0.25	1.79	0.75	2.00	13.80	3.81

Table A-1. Continued.

Test case	Plate Width	Plate length	Plate Thick.	Plate Clear.	Water Depth	Wave Height	Wave Period	Wave Length	Wetted Width
FPWS071	4.00	6.00	0.08	0.25	1.79	0.64	1.50	9.54	2.01
FPWS072	4.00	6.00	0.08	0.25	1.79	0.54	1.00	5.01	0.60
FPWS073	4.00	6.00	0.08	0.00	2.06	0.51	3.00	23.30	4.00
FPWS074	4.00	6.00	0.08	0.00	2.06	0.86	3.00	23.30	4.00
FPWS075	4.00	6.00	0.08	0.00	2.06	0.58	2.50	19.00	4.00
FPWS076	4.00	6.00	0.08	0.00	2.06	0.76	2.50	19.00	4.00
FPWS077	4.00	6.00	0.08	0.00	2.06	0.67	2.00	14.58	4.00
FPWS078	4.00	6.00	0.08	0.00	2.06	0.81	2.00	14.58	4.00
FPWS079	4.00	6.00	0.08	0.00	2.06	0.72	1.50	9.95	4.00
FPWS080	4.00	6.00	0.08	0.00	2.06	0.50	1.00	5.06	2.53
FPWS081	4.00	6.00	0.08	0.08	2.06	0.50	3.00	23.30	4.00
FPWS082	4.00	6.00	0.08	0.08	2.06	0.85	3.00	23.30	4.00
FPWS083	4.00	6.00	0.08	0.08	2.06	0.69	2.50	19.00	4.00
FPWS084	4.00	6.00	0.08	0.08	2.06	0.75	2.50	19.00	4.00
FPWS085	4.00	6.00	0.08	0.08	2.06	0.67	2.00	14.58	4.00
FPWS086	4.00	6.00	0.08	0.08	2.06	0.83	2.00	14.58	4.00
FPWS087	4.00	6.00	0.08	0.08	2.06	0.78	1.50	9.95	2.97
FPWS088	4.00	6.00	0.08	0.08	2.06	0.54	1.00	5.06	1.71
FPWS089	4.00	6.00	0.08	0.17	2.06	0.44	3.00	23.30	4.00
FPWS090	4.00	6.00	0.08	0.17	2.06	0.83	3.00	23.30	4.00
FPWS091	4.00	6.00	0.08	0.17	2.06	0.51	2.50	19.00	4.00
FPWS092	4.00	6.00	0.08	0.17	2.06	0.99	2.50	19.00	4.00
FPWS093	4.00	6.00	0.08	0.17	2.06	0.63	2.00	14.58	4.00
FPWS094	4.00	6.00	0.08	0.17	2.06	0.79	2.00	14.58	4.00
FPWS095	4.00	6.00	0.08	0.17	2.06	0.69	1.50	9.95	3.48
FPWS096	4.00	6.00	0.08	0.17	2.06	0.52	1.00	5.06	1.35
FPWS097	4.00	6.00	0.08	0.25	2.06	0.40	3.00	23.30	0.00
FPWS098	4.00	6.00	0.08	0.25	2.06	0.75	3.00	23.30	4.00
FPWS099	4.00	6.00	0.08	0.25	2.06	0.54	2.50	19.00	1.88
FPWS100	4.00	6.00	0.08	0.25	2.06	0.86	2.50	19.00	4.00
FPWS101	4.00	6.00	0.08	0.25	2.06	0.58	2.00	14.58	2.40
FPWS102	4.00	6.00	0.08	0.25	2.06	0.75	2.00	14.58	4.00
FPWS103	4.00	6.00	0.08	0.25	2.06	0.75	1.50	9.95	2.81
FPWS104	4.00	6.00	0.08	0.25	2.06	0.54	1.00	5.06	0.61
FPWS105	4.00	6.00	0.08	0.08	2.25	0.52	3.00	24.23	4.00

Table A-1. Continued.

Test case	Plate Width	Plate length	Plate Thick.	Plate Clear.	Water Depth	Wave Height	Wave Period	Wave Length	Wetted Width
FPWS106	4.00	6.00	0.08	0.08	2.25	0.88	3.00	24.23	4.00
FPWS107	4.00	6.00	0.08	0.08	2.25	0.56	2.50	19.71	4.00
FPWS108	4.00	6.00	0.08	0.08	2.25	0.95	2.50	19.71	4.00
FPWS109	4.00	6.00	0.08	0.08	2.25	0.58	2.00	15.06	4.00
FPWS110	4.00	6.00	0.08	0.08	2.25	0.83	2.00	15.06	4.00
FPWS111	4.00	6.00	0.08	0.08	2.25	0.79	1.50	10.18	4.00
FPWS112	4.00	6.00	0.08	0.08	2.25	0.54	1.00	5.09	2.03
FPWS113	4.00	6.00	0.08	0.00	2.33	0.56	3.00	24.62	4.00
FPWS114	4.00	6.00	0.08	0.00	2.33	0.88	3.00	24.62	4.00
FPWS115	4.00	6.00	0.08	0.00	2.33	0.65	2.50	20.01	4.00
FPWS116	4.00	6.00	0.08	0.00	2.33	0.98	2.50	20.01	4.00
FPWS117	4.00	6.00	0.08	0.00	2.33	0.79	2.00	15.26	4.00
FPWS118	4.00	6.00	0.08	0.00	2.33	0.83	2.00	15.26	4.00
FPWS119	4.00	6.00	0.08	0.00	2.33	0.82	1.50	10.27	4.00
FPWS120	4.00	6.00	0.08	0.00	2.33	0.67	1.00	5.09	3.19
FPWS121	4.00	6.00	0.08	0.08	2.33	0.58	3.00	24.62	4.00
FPWS122	4.00	6.00	0.08	0.08	2.33	0.96	3.00	24.62	4.00
FPWS123	4.00	6.00	0.08	0.08	2.33	0.59	2.50	20.01	4.00
FPWS124	4.00	6.00	0.08	0.08	2.33	0.79	2.50	20.01	4.00
FPWS125	4.00	6.00	0.08	0.08	2.33	0.67	2.00	15.26	4.00
FPWS126	4.00	6.00	0.08	0.08	2.33	0.83	2.00	15.26	4.00
FPWS127	4.00	6.00	0.08	0.08	2.33	0.83	1.50	10.27	4.00
FPWS128	4.00	6.00	0.08	0.08	2.33	0.63	1.00	5.09	2.69
FPWS129	4.00	6.00	0.08	0.17	2.33	0.46	3.00	24.62	4.00
FPWS130	4.00	6.00	0.08	0.17	2.33	0.86	3.00	24.62	4.00
FPWS131	4.00	6.00	0.08	0.17	2.33	0.60	2.50	20.01	4.00
FPWS132	4.00	6.00	0.08	0.17	2.33	0.97	2.50	20.01	4.00
FPWS133	4.00	6.00	0.08	0.17	2.33	0.71	2.00	15.26	4.00
FPWS134	4.00	6.00	0.08	0.17	2.33	0.79	2.00	15.26	4.00
FPWS135	4.00	6.00	0.08	0.17	2.33	0.74	1.50	10.27	3.74
FPWS136	4.00	6.00	0.08	0.17	2.33	0.58	1.00	5.09	1.77
FPWS137	4.00	6.00	0.08	-0.42	2.33	0.58	3.00	24.62	4.00
FPWS138	4.00	6.00	0.08	-0.42	2.33	0.90	3.00	24.62	4.00
FPWS139	4.00	6.00	0.08	-0.42	2.33	0.65	2.50	20.01	4.00
FPWS140	4.00	6.00	0.08	-0.42	2.33	0.85	2.50	20.01	4.00

Table A-1. Continued.

Test case	Plate Width	Plate length	Plate Thick.	Plate Clear.	Water Depth	Wave Height	Wave Period	Wave Length	Wetted Width
FPWS141	4.00	6.00	0.08	-0.42	2.33	0.71	2.00	15.26	4.00
FPWS142	4.00	6.00	0.08	-0.42	2.33	0.79	2.00	15.26	4.00
FPWS143	4.00	6.00	0.08	-0.42	2.33	0.92	1.50	10.27	4.00
FPWS144	4.00	6.00	0.08	-0.42	2.33	0.50	1.00	5.09	4.00
FPWS145	4.00	6.00	0.08	-0.17	2.08	0.52	3.00	23.40	4.00
FPWS146	4.00	6.00	0.08	-0.17	2.08	0.88	3.00	23.40	4.00
FPWS147	4.00	6.00	0.08	-0.17	2.08	0.58	2.50	19.07	4.00
FPWS148	4.00	6.00	0.08	-0.17	2.08	0.77	2.50	19.07	4.00
FPWS149	4.00	6.00	0.08	-0.17	2.08	0.67	2.00	14.63	4.00
FPWS150	4.00	6.00	0.08	-0.17	2.08	0.83	2.00	14.63	4.00
FPWS151	4.00	6.00	0.08	-0.17	2.08	0.85	1.50	9.97	4.00
FPWS152	4.00	6.00	0.08	-0.17	2.08	0.58	1.00	5.07	3.54
FPWS153	4.00	6.00	0.08	-0.08	2.00	0.46	3.00	22.98	4.00
FPWS154	4.00	6.00	0.08	-0.08	2.00	0.79	3.00	22.98	4.00
FPWS155	4.00	6.00	0.08	-0.08	2.00	0.56	2.50	18.74	4.00
FPWS156	4.00	6.00	0.08	-0.08	2.00	0.79	2.50	18.74	4.00
FPWS157	4.00	6.00	0.08	-0.08	2.00	0.63	2.00	14.40	4.00
FPWS158	4.00	6.00	0.08	-0.08	2.00	0.75	2.00	14.40	4.00
FPWS159	4.00	6.00	0.08	-0.08	2.00	0.80	1.50	9.86	4.00
FPWS160	4.00	6.00	0.08	-0.08	2.00	0.59	1.00	5.05	3.60
FPWS161	4.00	6.00	0.08	-0.29	2.00	0.51	3.00	22.98	4.00
FPWS162	4.00	6.00	0.08	-0.29	2.00	0.79	3.00	22.98	4.00
FPWS163	4.00	6.00	0.08	-0.29	2.00	0.54	2.50	18.74	4.00
FPWS164	4.00	6.00	0.08	-0.29	2.00	0.78	2.50	18.74	4.00
FPWS165	4.00	6.00	0.08	-0.29	2.00	0.58	2.00	14.40	4.00
FPWS166	4.00	6.00	0.08	-0.29	2.00	0.83	2.00	14.40	4.00
FPWS167	4.00	6.00	0.08	-0.29	2.00	0.83	1.50	9.86	4.00
FPWS168	4.00	6.00	0.08	-0.29	2.00	0.58	1.00	5.05	4.00
FPWS169	4.00	6.00	0.08	-0.17	1.92	0.45	3.00	22.54	4.00
FPWS170	4.00	6.00	0.08	-0.17	1.92	0.77	3.00	22.54	4.00
FPWS171	4.00	6.00	0.08	-0.17	1.92	0.50	2.50	18.41	4.00
FPWS172	4.00	6.00	0.08	-0.17	1.92	0.77	2.50	18.41	4.00
FPWS173	4.00	6.00	0.08	-0.17	1.92	0.50	2.00	14.17	4.00
FPWS174	4.00	6.00	0.08	-0.17	1.92	0.71	2.00	14.17	4.00
FPWS175	4.00	6.00	0.08	-0.17	1.92	0.79	1.50	9.74	4.00

Table A-1. Continued.

Test case	Plate Width	Plate length	Plate Thick.	Plate Clear.	Water Depth	Wave Height	Wave Period	Wave Length	Wetted Width
FPWS176	4.00	6.00	0.08	-0.17	1.92	0.58	1.00	5.04	3.53
FPWS185	4.00	6.00	0.08	-0.17	1.75	0.39	3.00	21.62	4.00
FPWS186	4.00	6.00	0.08	-0.17	1.75	0.75	3.00	21.62	4.00
FPWS187	4.00	6.00	0.08	-0.17	1.75	0.50	2.50	17.69	4.00
FPWS188	4.00	6.00	0.08	-0.17	1.75	0.75	2.50	17.69	4.00
FPWS189	4.00	6.00	0.08	-0.17	1.75	0.50	2.00	13.67	4.00
FPWS190	4.00	6.00	0.08	-0.17	1.75	0.67	2.00	13.67	4.00
FPWS191	4.00	6.00	0.08	-0.17	1.75	0.69	1.50	9.47	4.00
FPWS192	4.00	6.00	0.08	-0.17	1.75	0.59	1.00	5.00	4.00
FPNS001	4.00	2.00	0.08	-0.04	2.33	0.68	3.56	29.69	4.00
FPNS002	4.00	2.00	0.08	-0.04	2.33	0.90	3.02	24.80	4.00
FPNS003	4.00	2.00	0.08	-0.04	2.33	0.87	2.46	19.63	4.00
FPNS004	4.00	2.00	0.08	-0.04	2.33	0.96	1.99	15.16	4.00
FPNS005	4.00	2.00	0.08	-0.04	2.33	0.92	1.54	10.68	2.09
FPNS006	4.00	2.00	0.08	-0.04	2.33	0.56	1.01	5.19	2.77
FPNS007	4.00	2.00	0.08	-0.35	2.67	0.57	3.42	30.21	4.00
FPNS008	4.00	2.00	0.08	-0.35	2.67	0.59	3.00	26.11	4.00
FPNS009	4.00	2.00	0.08	-0.35	2.67	0.66	2.49	21.04	4.00
FPNS010	4.00	2.00	0.08	-0.35	2.67	0.82	2.00	16.00	4.00
FPNS011	4.00	2.00	0.08	-0.35	2.67	0.87	1.55	11.15	4.00
FPNS012	4.00	2.00	0.08	-0.35	2.67	0.55	1.01	5.21	4.00
FPNS013	4.00	2.00	0.08	-0.35	2.67	0.50	3.55	31.47	4.00
FPNS014	4.00	2.00	0.08	-0.35	2.67	0.61	2.99	26.01	4.00
FPNS015	4.00	2.00	0.08	-0.35	2.67	0.63	2.47	20.84	4.00
FPNS016	4.00	2.00	0.08	-0.35	2.67	0.82	1.98	15.79	4.00
FPNS017	4.00	2.00	0.08	-0.35	2.67	0.84	1.53	10.93	4.00
FPNS018	4.00	2.00	0.08	-0.35	2.67	0.54	1.00	5.11	4.00
FPNS019	4.00	2.00	0.08	-0.25	2.58	0.46	3.52	30.73	4.00
FPNS020	4.00	2.00	0.08	-0.25	2.58	0.64	2.99	25.65	4.00
FPNS021	4.00	2.00	0.08	-0.25	2.58	0.73	2.55	21.36	4.00
FPNS022	4.00	2.00	0.08	-0.25	2.58	0.86	2.01	15.93	4.00
FPNS023	4.00	2.00	0.08	-0.25	2.58	0.92	1.53	10.85	4.00
FPNS024	4.00	2.00	0.08	-0.25	2.58	0.55	1.00	5.11	4.00
FPNS025	4.00	2.00	0.08	-0.25	2.58	0.46	3.53	30.83	4.00
FPNS026	4.00	2.00	0.08	-0.25	2.58	0.51	2.97	25.46	4.00

Table A-1. Continued.

Test case	Plate Width	Plate length	Plate Thick.	Plate Clear.	Water Depth	Wave Height	Wave Period	Wave Length	Wetted Width
FPNS027	4.00	2.00	0.08	-0.25	2.58	0.68	2.50	20.87	4.00
FPNS028	4.00	2.00	0.08	-0.25	2.58	0.83	1.99	15.72	4.00
FPNS029	4.00	2.00	0.08	-0.25	2.58	0.81	1.53	10.85	4.00
FPNS030	4.00	2.00	0.08	-0.25	2.58	0.56	1.01	5.21	4.00
FPNS031	4.00	2.00	0.08	-0.17	2.46	0.46	3.50	29.86	4.00
FPNS032	4.00	2.00	0.08	-0.17	2.46	0.54	2.97	24.91	4.00
FPNS033	4.00	2.00	0.08	-0.17	2.46	0.67	2.51	20.54	4.00
FPNS034	4.00	2.00	0.08	-0.17	2.46	0.90	2.00	15.55	4.00
FPNS035	4.00	2.00	0.08	-0.17	2.46	0.77	1.54	10.83	4.00
FPNS036	4.00	2.00	0.08	-0.17	2.46	0.59	3.40	28.93	4.00
FPNS037	4.00	2.00	0.08	-0.17	2.46	0.68	2.96	24.82	4.00
FPNS038	4.00	2.00	0.08	-0.17	2.46	0.93	2.46	20.06	4.00
FPNS039	4.00	2.00	0.08	-0.17	2.46	1.01	1.98	15.35	4.00
FPNS040	4.00	2.00	0.08	-0.17	2.46	0.85	1.53	10.72	2.89
FPNS041	4.00	2.00	0.08	-0.08	2.42	0.66	3.51	29.72	4.00
FPNS042	4.00	2.00	0.08	-0.08	2.42	0.79	2.98	24.82	4.00
FPNS043	4.00	2.00	0.08	-0.08	2.42	0.87	2.44	19.73	4.00
FPNS044	4.00	2.00	0.08	-0.08	2.42	0.95	2.00	15.46	4.00
FPNS045	4.00	2.00	0.08	-0.08	2.42	0.86	1.53	10.68	2.73
FPNS046	4.00	2.00	0.08	-0.08	2.42	0.48	3.46	29.26	4.00
FPNS047	4.00	2.00	0.08	-0.08	2.42	0.65	2.94	24.45	4.00
FPNS048	4.00	2.00	0.08	-0.08	2.42	0.79	2.46	19.92	4.00
FPNS049	4.00	2.00	0.08	-0.08	2.42	0.97	2.01	15.56	4.00
FPNS050	4.00	2.00	0.08	-0.08	2.42	0.85	1.52	10.57	2.64
FPNS051	4.00	2.00	0.08	0.00	2.29	0.52	3.55	29.36	4.00
FPNS052	4.00	2.00	0.08	0.00	2.29	0.68	2.95	23.97	4.00
FPNS053	4.00	2.00	0.08	0.00	2.29	0.64	2.48	19.68	4.00
FPNS054	4.00	2.00	0.08	0.00	2.29	0.89	1.98	14.97	4.00
FPNS055	4.00	2.00	0.08	0.00	2.29	0.85	1.53	10.53	4.00
FPNS056	4.00	2.00	0.08	0.00	2.29	0.61	3.56	29.45	4.00
FPNS057	4.00	2.00	0.08	0.00	2.29	0.67	3.05	24.88	4.00
FPNS058	4.00	2.00	0.08	0.00	2.29	0.74	2.45	19.40	4.00
FPNS059	4.00	2.00	0.08	0.00	2.29	0.84	2.00	15.16	4.00
FPNS060	4.00	2.00	0.08	0.00	2.29	0.91	1.57	10.94	4.00
FPNS061	4.00	2.00	0.08	0.06	2.25	0.61	3.45	28.23	4.00

Table A-1. Continued.

Test case	Plate Width	Plate length	Plate Thick.	Plate Clear.	Water Depth	Wave Height	Wave Period	Wave Length	Wetted Width
FPNS062	4.00	2.00	0.08	0.06	2.25	0.69	2.97	23.96	4.00
FPNS063	4.00	2.00	0.08	0.06	2.25	0.75	2.43	19.07	4.00
FPNS064	4.00	2.00	0.08	0.06	2.25	0.87	2.01	15.15	4.00
FPNS065	4.00	2.00	0.08	0.06	2.25	0.81	1.53	10.48	4.00
FPNS066	4.00	2.00	0.08	0.06	2.25	0.64	3.57	29.29	4.00
FPNS067	4.00	2.00	0.08	0.06	2.25	0.66	3.06	24.76	4.00
FPNS068	4.00	2.00	0.08	0.06	2.25	0.86	2.44	19.16	4.00
FPNS069	4.00	2.00	0.08	0.06	2.25	0.91	1.99	14.96	4.00
FPNS070	4.00	2.00	0.08	0.06	2.25	0.85	1.56	10.78	2.08
FPNS071	4.00	2.00	0.08	0.13	2.17	0.63	3.46	27.83	4.00
FPNS072	4.00	2.00	0.08	0.13	2.17	0.77	2.93	23.21	4.00
FPNS073	4.00	2.00	0.08	0.13	2.17	0.73	2.42	18.68	4.00
FPNS074	4.00	2.00	0.08	0.13	2.17	0.80	2.01	14.94	4.00
FPNS075	4.00	2.00	0.08	0.13	2.17	0.88	1.52	10.28	4.00
FPNS076	4.00	2.00	0.08	0.13	2.17	0.65	3.43	27.57	4.00
FPNS077	4.00	2.00	0.08	0.13	2.17	0.68	2.98	23.65	4.00
FPNS078	4.00	2.00	0.08	0.13	2.17	0.80	2.43	18.77	4.00
FPNS079	4.00	2.00	0.08	0.13	2.17	0.89	2.00	14.85	4.00
FPNS080	4.00	2.00	0.08	0.13	2.17	0.88	1.51	10.18	2.18
FPNS081	4.00	2.00	0.08	0.21	2.08	0.68	3.42	26.99	4.00
FPNS082	4.00	2.00	0.08	0.21	2.08	0.79	2.92	22.72	4.00
FPNS083	4.00	2.00	0.08	0.21	2.08	0.79	2.41	18.28	4.00
FPNS084	4.00	2.00	0.08	0.21	2.08	0.85	2.00	14.63	4.00
FPNS085	4.00	2.00	0.08	0.21	2.08	0.91	1.50	9.97	1.45
FPNS086	4.00	2.00	0.08	0.21	2.08	0.66	3.52	27.83	4.00
FPNS087	4.00	2.00	0.08	0.21	2.08	0.75	3.01	23.49	4.00
FPNS088	4.00	2.00	0.08	0.21	2.08	0.77	2.44	18.55	4.00
FPNS089	4.00	2.00	0.08	0.21	2.08	0.81	2.00	14.63	4.00
FPNS090	4.00	2.00	0.08	0.21	2.08	0.89	1.48	9.78	4.00
FPNS091	4.00	2.00	0.08	0.29	2.00	0.58	3.45	26.73	0.00
FPNS092	4.00	2.00	0.08	0.29	2.00	0.71	2.90	22.14	4.00
FPNS093	4.00	2.00	0.08	0.29	2.00	0.83	2.49	18.66	4.00
FPNS094	4.00	2.00	0.08	0.29	2.00	0.87	2.03	14.67	4.00
FPNS095	4.00	2.00	0.08	0.29	2.00	0.89	1.48	9.67	4.00
FPNS096	4.00	2.00	0.08	0.29	2.00	0.58	3.51	27.23	0.00

Table A-1. Continued.

Test case	Plate Width	Plate length	Plate Thick.	Plate Clear.	Water Depth	Wave Height	Wave Period	Wave Length	Wetted Width
FPNS097	4.00	2.00	0.08	0.29	2.00	0.73	3.02	23.15	4.00
FPNS098	4.00	2.00	0.08	0.29	2.00	0.82	2.43	18.15	4.00
FPNS099	4.00	2.00	0.08	0.29	2.00	0.79	2.07	15.02	4.00
FPNS100	4.00	2.00	0.08	0.29	2.00	0.82	1.52	10.05	1.73

Table A- 2 Significant force values for all physical model tests.

Test case	Vertical Max	Vertical Min	Quasi Max	Quasi Min	Slam Max	Moment max	Moment min
FPWS001	132.59	-17.13	86.29	-15.39	49.19	286.04	-13.17
FPWS002	191.57	-81.61	141.32	-41.03	71.20	448.86	-208.95
FPWS003	172.96	-14.16	122.52	-10.27	61.54	334.40	-45.35
FPWS004	190.74	-59.52	118.85	-42.18	79.97	395.96	-145.03
FPWS005	111.42	-71.76	64.87	-64.06	49.52	190.28	-182.98
FPWS006	169.11	-53.45	113.05	-29.40	57.40	322.02	-159.78
FPWS007	111.47	-88.19	77.77	-51.45	78.80	239.67	-206.89
FPWS008	92.18	-101.48	69.87	-64.04	34.99	245.86	-241.43
FPWS009	20.21	-4.98	19.68	-3.43	2.45	54.52	-10.49
FPWS010	53.76	-41.23	42.65	-35.05	22.52	161.38	-116.73
FPWS011	126.22	-49.42	63.47	-39.60	63.27	166.24	-118.54
FPWS012	237.20	-148.86	138.53	-94.99	110.82	479.22	-385.91
FPWS013	193.15	-32.76	115.84	-26.41	78.75	324.03	-86.56
FPWS014	194.54	-148.14	76.11	-122.17	123.48	493.57	-339.71
FPWS015	78.45	-45.67	56.24	-29.78	31.04	196.20	-112.72
FPWS016	140.35	-62.03	94.10	-39.65	54.13	348.81	-146.30
FPWS017	52.58	-71.51	40.23	-46.33	34.80	179.14	-171.72
FPWS018	67.32	-96.47	56.96	-72.72	45.29	167.14	-225.17
FPWS019	15.98	-21.47	9.80	-18.10	7.50	58.68	-68.14
FPWS020	3.58	-10.26	6.16	-9.05	2.54	15.24	-28.28
FPWS021	21.68	-19.44	9.57	-16.38	16.08	51.52	-42.46
FPWS022	85.28	-82.11	67.94	-56.23	37.82	243.85	-177.35
FPWS023	51.84	-31.28	31.54	-23.57	24.18	109.25	-72.64
FPWS024	69.67	-78.07	61.28	-47.62	40.17	185.35	-176.58
FPWS025	32.00	-27.69	14.67	-19.51	19.93	106.35	-60.64
FPWS026	53.22	-53.76	35.64	-34.08	28.02	163.21	-127.14
FPWS027	24.41	-35.40	10.62	-21.39	28.27	79.68	-99.05
FPWS028	44.53	-47.43	32.68	-36.70	19.34	114.18	-118.11
FPWS029	8.66	-12.50	2.70	-11.04	7.76	35.25	-41.93
FPWS030	7.84	-13.69	2.93	-13.22	5.02	33.86	-48.88
FPWS031	0.00	0.00	0.00	0.00	0.00	0.00	0.00
FPWS032	42.12	-70.70	30.13	-45.92	22.36	141.35	-149.22
FPWS033	0.00	0.00	0.00	0.00	0.00	0.00	0.00
FPWS034	42.56	-52.20	27.52	-32.15	18.29	150.15	-108.64
FPWS035	0.00	0.00	0.00	0.00	0.00	0.00	0.00

Table A-2. Continued.

Test case	Vertical Max	Vertical Min	Quasi Max	Quasi Min	Slam Max	Moment max	Moment min
FPWS036	24.95	-33.98	13.78	-26.78	12.65	88.20	-79.95
FPWS037	17.98	-17.02	3.82	-14.44	15.29	66.68	-51.07
FPWS038	15.74	-31.99	7.92	-23.09	15.20	67.62	-85.88
FPWS039	0.00	0.00	0.00	0.00	0.00	0.00	0.00
FPWS040	0.00	0.00	0.00	0.00	0.00	0.00	0.00
FPWS041	95.87	-30.74	54.80	-18.74	47.47	167.53	-70.30
FPWS042	163.48	-90.68	118.48	-60.15	61.58	369.88	-194.90
FPWS043	106.38	-35.25	65.10	-27.82	44.34	209.30	-94.08
FPWS044	134.57	-77.85	102.84	-48.47	55.80	307.70	-168.53
FPWS045	95.98	-57.94	73.54	-28.59	40.89	228.46	-130.14
FPWS046	182.92	-75.08	105.51	-50.41	78.48	430.56	-178.63
FPWS047	71.02	-100.09	46.75	-64.46	40.71	163.39	-228.40
FPWS048	18.25	-33.50	10.77	-26.55	12.57	70.90	-104.13
FPWS049	126.03	-28.43	76.20	-27.43	55.39	234.53	-60.52
FPWS050	265.58	-87.25	165.32	-52.76	100.26	541.44	-184.02
FPWS051	127.88	-35.45	92.42	-31.31	45.47	240.44	-82.64
FPWS052	217.66	-68.31	118.00	-51.72	115.42	391.41	-177.32
FPWS053	138.92	-96.35	65.91	-64.07	94.24	203.46	-215.91
FPWS054	115.36	-113.80	76.41	-77.17	67.65	210.93	-254.70
FPWS055	117.79	-95.34	61.63	-63.51	80.05	173.64	-217.29
FPWS056	75.38	-51.60	33.10	-38.30	42.94	160.44	-134.79
FPWS057	20.23	-29.43	14.55	-14.00	13.03	54.23	-54.15
FPWS058	113.72	-88.03	78.47	-54.47	52.65	198.38	-186.04
FPWS059	43.04	-38.92	28.95	-24.14	28.28	118.67	-76.28
FPWS060	90.85	-83.26	74.30	-49.65	46.13	213.51	-180.84
FPWS061	39.91	-24.68	22.93	-19.67	19.43	127.12	-55.42
FPWS062	77.61	-93.04	54.55	-44.67	54.30	211.45	-197.01
FPWS063	59.50	-60.94	29.08	-39.43	47.03	123.77	-173.64
FPWS064	7.91	-10.49	3.31	-9.64	5.07	32.63	-35.34
FPWS065	0.00	0.00	0.00	0.00	0.00	0.00	0.00
FPWS066	47.22	-77.60	45.40	-42.78	36.73	138.75	-154.12
FPWS067	0.00	0.00	0.00	0.00	0.00	0.00	0.00
FPWS068	65.36	-62.83	41.80	-37.61	40.58	161.07	-125.39
FPWS069	0.00	0.00	0.00	0.00	0.00	0.00	0.00
FPWS070	52.85	-66.02	34.67	-41.46	28.52	168.63	-137.22

Table A-2. Continued.

Test case	Vertical Max	Vertical Min	Quasi Max	Quasi Min	Slam Max	Moment max	Moment min
FPWS071	28.47	-27.92	12.35	-17.92	26.26	103.88	-76.76
FPWS072	1.60	-4.71	0.79	-3.96	2.94	3.91	-10.05
FPWS073	123.87	-33.59	74.70	-31.05	54.22	252.08	-57.91
FPWS074	193.96	-82.28	137.88	-59.53	63.78	370.46	-171.80
FPWS075	119.51	-38.76	95.04	-36.23	36.21	272.70	-95.14
FPWS076	235.30	-88.57	137.51	-63.13	102.42	428.92	-177.32
FPWS077	184.14	-53.85	111.87	-40.82	74.81	307.30	-130.89
FPWS078	179.95	-77.15	119.51	-61.87	68.66	340.02	-179.45
FPWS079	123.66	-104.70	69.22	-69.81	88.89	184.96	-253.43
FPWS080	8.30	-12.91	8.35	-12.76	2.43	16.28	-32.23
FPWS081	68.50	-37.20	58.07	-28.32	25.95	161.68	-85.97
FPWS082	160.62	-85.49	118.89	-48.08	75.16	351.16	-225.15
FPWS083	171.63	-56.91	96.77	-39.88	77.53	306.46	-135.09
FPWS084	174.93	-80.47	111.85	-50.48	80.79	435.43	-185.60
FPWS085	118.23	-40.65	78.56	-31.68	52.42	258.02	-112.11
FPWS086	213.09	-78.65	126.77	-60.58	99.66	485.26	-186.60
FPWS087	73.67	-100.06	50.02	-69.94	29.25	186.69	-230.21
FPWS088	14.67	-18.64	9.59	-16.37	10.97	59.61	-57.87
FPWS089	46.02	-31.26	34.36	-22.57	23.48	105.41	-64.96
FPWS090	148.03	-109.04	102.33	-75.37	56.19	325.91	-234.67
FPWS091	48.51	-37.43	37.16	-21.15	28.85	111.12	-80.09
FPWS092	100.98	-72.50	78.80	-44.51	35.68	228.29	-162.23
FPWS093	77.47	-80.59	58.10	-34.25	56.63	172.69	-163.70
FPWS094	192.04	-88.14	95.85	-58.88	106.13	347.89	-210.32
FPWS095	57.45	-73.09	35.60	-52.66	32.85	137.70	-181.75
FPWS096	12.62	-17.32	5.86	-16.98	6.76	53.77	-56.39
FPWS097	0.00	0.00	0.00	0.00	0.00	0.00	0.00
FPWS098	79.91	-74.65	64.31	-45.38	43.39	181.98	-170.36
FPWS099	9.36	-16.34	4.44	-14.40	5.47	29.34	-35.72
FPWS100	72.84	-59.27	61.22	-38.88	36.90	148.04	-137.69
FPWS101	24.96	-28.11	14.47	-21.95	18.84	79.75	-66.04
FPWS102	85.74	-103.28	54.86	-57.78	57.27	213.17	-215.20
FPWS103	29.20	-52.82	20.31	-38.59	23.11	106.46	-131.67
FPWS104	3.11	-10.37	0.95	-8.06	3.82	14.63	-35.54
FPWS105	98.64	-27.32	61.31	-21.70	37.33	175.37	-56.36

Table A-2. Continued.

Test case	Vertical Max	Vertical Min	Quasi Max	Quasi Min	Slam Max	Moment max	Moment min
FPWS106	192.26	-65.04	136.45	-54.37	69.32	361.75	-144.03
FPWS107	120.33	-43.48	74.28	-35.42	49.35	216.09	-112.58
FPWS108	235.30	-108.62	136.77	-56.54	111.66	597.68	-246.18
FPWS109	120.99	-78.77	89.10	-53.09	47.23	293.81	-187.36
FPWS110	211.64	-97.72	128.47	-60.02	107.59	525.75	-217.67
FPWS111	67.64	-111.60	57.47	-83.12	33.71	174.27	-243.60
FPWS112	13.66	-24.44	10.36	-20.15	4.44	58.12	-75.39
FPWS113	105.80	-46.44	73.31	-43.32	32.58	218.83	-78.46
FPWS114	224.44	-72.04	138.09	-62.29	110.28	410.39	-153.99
FPWS115	161.33	-58.30	101.98	-50.19	64.58	300.46	-133.71
FPWS116	217.86	-75.13	174.19	-55.25	54.99	441.90	-157.69
FPWS117	177.61	-82.61	112.56	-50.01	72.02	371.78	-179.29
FPWS118	226.16	-102.10	145.56	-62.40	91.65	503.75	-214.02
FPWS119	164.61	-126.72	80.67	-101.54	121.66	229.72	-339.24
FPWS120	48.81	-50.15	31.54	-41.74	19.18	140.23	-125.08
FPWS121	83.00	-32.44	61.63	-22.99	34.13	163.64	-76.28
FPWS122	169.70	-69.83	137.63	-51.34	49.35	338.27	-158.33
FPWS123	142.82	-42.88	82.52	-37.35	61.64	242.33	-105.69
FPWS124	177.31	-91.03	115.16	-53.47	71.25	375.61	-203.29
FPWS125	147.31	-63.49	96.60	-44.38	70.36	398.44	-149.88
FPWS126	228.76	-85.56	123.65	-63.29	123.30	613.14	-191.70
FPWS127	61.38	-107.73	58.57	-84.27	34.73	200.16	-238.33
FPWS128	9.00	-7.27	4.50	-8.63	4.68	35.22	-26.10
FPWS129	55.16	-26.62	34.56	-13.63	26.82	91.31	-58.09
FPWS130	160.88	-77.75	113.91	-48.25	66.29	350.89	-178.74
FPWS131	100.82	-39.57	62.75	-24.34	51.95	222.18	-104.28
FPWS132	113.61	-85.36	97.09	-51.37	69.51	371.25	-186.46
FPWS133	114.09	-73.02	79.78	-48.12	53.02	280.80	-164.07
FPWS134	165.69	-90.50	99.64	-66.98	72.90	437.01	-221.99
FPWS135	57.72	-102.99	41.80	-72.60	30.82	196.70	-238.65
FPWS136	0.98	-4.79	0.71	-3.01	2.41	1.87	-10.92
FPWS137	127.55	-8.57	127.97	-8.36	46.31	200.43	-47.58
FPWS138	187.73	-65.20	188.12	-64.44	57.33	340.47	-154.87
FPWS139	156.33	-32.16	155.46	-29.94	49.85	262.36	-80.88
FPWS140	193.06	-48.96	191.76	-48.56	50.26	340.53	-127.88

Table A-2. Continued.

Test case	Vertical Max	Vertical Min	Quasi Max	Quasi Min	Slam Max	Moment max	Moment min
FPWS141	147.85	-82.10	145.57	-76.10	56.46	258.51	-183.24
FPWS142	185.93	-62.10	182.99	-63.97	52.65	315.22	-158.24
FPWS143	132.00	-89.37	130.54	-84.61	58.88	303.68	-223.61
FPWS144	85.08	-23.58	82.95	-23.44	47.53	175.11	-117.11
FPWS145	103.35	-41.78	103.11	-39.91	45.59	161.94	-98.16
FPWS146	175.61	-64.34	160.95	-59.84	85.24	343.95	-144.15
FPWS147	115.44	-52.21	115.64	-49.03	47.99	211.21	-112.99
FPWS148	176.95	-86.40	150.23	-81.60	92.66	359.03	-168.14
FPWS149	118.01	-71.81	102.47	-62.49	64.92	215.40	-180.86
FPWS150	171.13	-80.57	136.60	-77.71	81.81	343.73	-196.89
FPWS151	152.33	-100.90	119.10	-75.46	89.29	338.65	-241.79
FPWS152	63.04	-27.19	58.37	-21.75	51.56	104.72	-121.93
FPWS153	105.09	-28.40	91.60	-28.45	58.64	172.69	-73.19
FPWS154	179.92	-57.20	139.04	-53.27	82.63	344.29	-117.84
FPWS155	150.69	-33.00	115.14	-29.84	77.58	267.99	-96.96
FPWS156	208.99	-60.11	144.12	-48.81	106.30	382.74	-160.76
FPWS157	149.81	-45.22	119.99	-28.28	77.65	275.75	-140.76
FPWS158	300.98	-58.49	158.16	-36.20	184.69	517.04	-161.13
FPWS159	121.64	-74.79	99.98	-49.47	79.20	247.64	-205.59
FPWS160	53.53	13.72	52.86	13.07	44.15	80.24	-20.93
FPWS161	122.32	-14.23	122.92	-14.11	48.77	193.53	-49.78
FPWS162	170.02	-37.83	169.35	-38.26	51.47	294.37	-110.77
FPWS163	133.93	-34.83	134.57	-31.43	47.35	210.72	-86.98
FPWS164	173.11	-53.20	172.80	-51.42	50.81	296.51	-100.07
FPWS165	122.32	-14.23	122.92	-14.11	48.77	193.53	-49.78
FPWS166	170.02	-37.83	169.35	-38.26	51.47	294.37	-110.77
FPWS167	116.26	-79.68	115.31	-69.68	69.42	260.52	-186.88
FPWS168	44.65	34.86	44.48	36.27	43.93	49.59	28.03
FPWS169	105.72	-31.40	105.00	-30.19	45.06	166.60	-81.31
FPWS170	159.11	-63.95	158.09	-58.84	48.75	293.36	-131.77
FPWS171	107.79	-48.24	106.49	-42.11	48.83	177.58	-124.15
FPWS172	150.27	-67.13	149.65	-65.10	51.38	273.55	-143.77
FPWS173	109.90	-69.39	102.25	-58.05	58.94	207.76	-171.67
FPWS174	134.76	-66.57	123.28	-60.42	60.51	250.20	-167.25
FPWS175	137.03	-93.34	109.30	-68.27	89.64	306.08	-221.45

Table A-2. Continued.

Test case	Vertical Max	Vertical Min	Quasi Max	Quasi Min	Slam Max	Moment max	Moment min
FPWS176	72.95	1.11	70.02	-2.43	47.95	120.53	-69.26
FPWS185	96.89	-22.68	97.02	-19.32	47.67	150.98	-68.38
FPWS186	164.77	-49.09	163.09	-45.61	47.95	291.54	-108.05
FPWS187	112.22	-33.20	110.86	-32.20	46.00	183.91	-88.35
FPWS188	152.29	-62.10	151.17	-59.52	53.28	280.61	-147.97
FPWS189	97.35	-47.70	95.32	-46.78	54.78	176.11	-136.72
FPWS190	109.72	-67.14	110.06	-60.19	57.86	221.35	-173.83
FPWS191	91.01	-120.52	83.00	-100.24	69.47	216.38	-281.18
FPWS192	84.64	-23.95	77.16	-20.65	54.27	160.63	-106.32
FPNS001	81.65	-99.79	77.06	-92.51	13.25	182.21	-216.64
FPNS002	84.98	-118.90	75.99	-103.55	26.02	207.08	-249.36
FPNS003	84.60	-82.67	85.81	-77.39	19.16	198.05	-165.13
FPNS004	122.31	-91.00	81.87	-78.88	41.28	285.13	-201.26
FPNS005	78.97	-138.40	54.22	-97.27	55.91	219.76	-300.88
FPNS006	21.74	-12.53	19.61	-14.61	3.91	65.40	-52.06
FPNS007	47.86	-40.14	45.64	-38.71	4.42	100.85	-81.67
FPNS008	71.73	-51.62	68.70	-49.40	4.65	156.03	-101.31
FPNS009	95.24	-77.39	94.71	-71.75	6.00	196.50	-156.17
FPNS010	111.36	-99.33	111.51	-91.85	7.94	258.14	-202.41
FPNS011	107.59	-117.43	102.96	-103.81	15.95	287.90	-244.52
FPNS012	8.76	-14.32	8.77	-13.44	2.83	14.14	-40.57
FPNS013	39.64	-41.15	38.04	-39.92	4.22	85.26	-87.83
FPNS014	83.40	-55.67	81.30	-54.38	4.86	182.08	-113.27
FPNS015	101.75	-75.28	101.12	-73.87	6.39	224.53	-143.85
FPNS016	109.19	-97.21	108.36	-88.14	8.16	252.04	-206.44
FPNS017	109.04	-106.58	104.09	-98.82	9.15	287.88	-227.00
FPNS018	23.32	-10.83	21.24	-9.64	3.73	49.14	-16.53
FPNS019	54.53	-44.95	51.93	-42.75	4.13	114.00	-90.62
FPNS020	74.87	-66.18	72.85	-64.90	4.22	176.77	-129.81
FPNS021	101.97	-80.81	100.38	-75.00	5.37	226.34	-174.75
FPNS022	93.58	-115.80	88.51	-108.72	5.29	210.02	-257.12
FPNS023	88.90	-130.67	83.49	-124.32	11.89	233.05	-292.94
FPNS024	14.11	-12.08	11.47	-10.65	3.42	40.43	-24.00
FPNS025	49.85	-47.68	48.31	-45.84	4.03	110.86	-92.67
FPNS026	68.32	-63.45	66.40	-56.92	6.65	160.26	-122.84

Table A-2. Continued.

Test case	Vertical Max	Vertical Min	Quasi Max	Quasi Min	Slam Max	Moment max	Moment min
FPNS027	101.68	-76.03	101.11	-72.22	7.25	232.72	-166.08
FPNS028	87.25	-119.69	86.71	-108.86	4.89	208.00	-263.65
FPNS029	65.74	-91.99	64.16	-82.52	11.23	188.07	-185.93
FPNS030	3.62	-30.02	3.17	-29.83	4.22	36.89	-89.67
FPNS031	63.90	-52.82	60.86	-49.63	4.40	131.61	-102.85
FPNS032	61.03	-67.79	59.08	-64.09	5.08	146.61	-150.09
FPNS033	88.18	-111.27	86.49	-104.21	4.79	201.87	-233.10
FPNS034	78.72	-137.24	67.49	-128.55	20.12	195.66	-282.20
FPNS035	78.94	-128.86	59.20	-120.68	20.44	171.26	-287.92
FPNS036	74.99	-76.62	72.95	-71.73	6.31	164.48	-164.17
FPNS037	75.41	-78.76	73.56	-73.84	17.19	190.10	-170.35
FPNS038	116.52	-118.13	104.47	-109.39	26.73	275.39	-253.49
FPNS039	165.86	-138.88	81.06	-129.35	88.66	374.61	-294.01
FPNS040	58.87	-88.59	57.15	-86.28	7.94	156.47	-196.28
FPNS041	74.04	-112.80	71.90	-107.68	10.92	172.85	-244.95
FPNS042	77.32	-112.68	64.45	-106.07	24.57	182.99	-254.32
FPNS043	87.06	-136.28	79.58	-120.72	20.06	230.29	-279.69
FPNS044	123.43	-143.59	64.13	-118.72	64.48	328.81	-291.18
FPNS045	84.98	-132.46	39.68	-117.18	71.35	224.84	-280.39
FPNS046	53.24	-102.22	47.23	-95.75	18.73	123.29	-218.78
FPNS047	71.29	-103.75	62.36	-98.58	22.66	165.75	-226.24
FPNS048	99.86	-140.61	78.32	-122.08	30.61	234.08	-296.70
FPNS049	109.42	-133.02	68.50	-120.00	42.87	258.64	-288.40
FPNS050	36.10	-88.55	32.41	-85.78	4.30	100.76	-209.39
FPNS051	88.67	-71.84	75.30	-64.80	13.55	206.72	-147.89
FPNS052	101.11	-70.66	85.36	-65.14	23.64	228.17	-140.44
FPNS053	83.07	-83.65	70.07	-78.31	22.94	210.11	-177.28
FPNS054	132.40	-80.63	98.92	-70.67	33.67	340.92	-177.75
FPNS055	145.73	-80.81	74.63	-66.97	76.75	248.20	-181.16
FPNS056	98.76	-76.49	87.81	-68.89	11.00	222.77	-161.61
FPNS057	87.34	-74.38	78.10	-67.65	19.50	201.53	-152.64
FPNS058	89.22	-85.62	79.28	-78.72	17.51	215.94	-183.64
FPNS059	93.13	-61.52	67.48	-57.15	29.25	248.68	-138.34
FPNS060	107.49	-93.22	69.34	-72.68	57.41	231.43	-199.40
FPNS061	79.86	-61.38	73.22	-54.93	26.11	179.12	-123.96

Table A-2. Continued.

Test case	Vertical Max	Vertical Min	Quasi Max	Quasi Min	Slam Max	Moment max	Moment min
FPNS062	85.40	-63.54	78.41	-59.10	27.38	255.72	-132.30
FPNS063	84.25	-89.21	68.05	-80.97	35.21	195.26	-184.79
FPNS064	139.13	-61.90	73.18	-49.71	69.87	364.15	-131.43
FPNS065	127.98	-73.08	67.68	-61.02	61.62	242.30	-173.99
FPNS066	83.99	-63.11	77.41	-59.58	24.05	210.82	-125.30
FPNS067	85.67	-60.90	72.62	-56.38	18.32	187.73	-133.84
FPNS068	92.42	-88.01	77.19	-81.81	18.30	217.05	-177.89
FPNS069	109.62	-63.51	65.96	-58.25	48.88	313.19	-132.25
FPNS070	140.39	-78.05	71.48	-64.36	71.88	260.13	-159.65
FPNS071	68.31	-53.93	56.64	-49.48	25.35	196.13	-114.44
FPNS072	86.48	-55.56	65.76	-52.01	28.19	243.98	-122.11
FPNS073	94.81	-76.05	60.69	-65.34	48.92	254.19	-148.59
FPNS074	87.93	-36.70	47.43	-29.13	40.66	247.06	-118.33
FPNS075	61.01	-62.23	52.43	-51.22	25.10	207.54	-165.19
FPNS076	55.68	-58.26	51.84	-56.95	9.02	141.50	-123.93
FPNS077	105.40	-55.71	70.73	-46.53	40.06	288.83	-128.06
FPNS078	109.35	-81.16	76.92	-66.44	42.91	299.31	-166.21
FPNS079	197.31	-69.58	75.52	-50.39	122.33	506.77	-177.40
FPNS080	59.21	-34.90	56.68	-21.05	24.01	195.89	-89.81
FPNS081	56.20	-30.00	45.15	-26.31	12.33	115.22	-65.25
FPNS082	76.25	-37.38	58.07	-35.68	24.46	231.59	-95.14
FPNS083	44.90	-43.75	41.06	-40.13	20.30	136.00	-96.77
FPNS084	51.08	-32.26	37.74	-24.42	18.60	173.29	-84.99
FPNS085	48.87	-42.97	41.47	-36.71	18.34	157.33	-118.12
FPNS086	56.85	-30.84	47.14	-28.30	11.15	122.22	-79.74
FPNS087	69.76	-31.51	60.50	-31.72	28.17	224.12	-85.57
FPNS088	57.92	-49.48	45.96	-39.86	21.01	147.34	-107.57
FPNS089	53.35	-38.00	39.22	-29.63	17.54	176.19	-109.20
FPNS090	50.01	-55.33	42.75	-41.06	19.04	157.57	-135.48
FPNS091	14.64	-17.94	13.15	-15.79	5.34	48.11	-39.24
FPNS092	65.35	-24.32	31.24	-21.70	34.62	192.46	-74.12
FPNS093	62.14	-51.00	44.13	-36.18	31.52	185.84	-133.78
FPNS094	32.20	-28.03	23.76	-21.05	12.82	95.82	-71.43
FPNS095	8.19	-22.10	3.22	-18.07	5.02	31.78	-67.92
FPNS096	25.25	-20.96	20.36	-20.01	7.70	95.82	-53.27

Table A-2. Continued.

Test case	Vertical Max	Vertical Min	Quasi Max	Quasi Min	Slam Max	Moment max	Moment min
FPNS097	14.86	-20.42	10.97	-18.71	8.84	62.29	-43.42
FPNS098	45.11	-38.18	30.41	-31.57	16.90	125.96	-79.63
FPNS099	26.93	-22.82	17.90	-17.10	13.54	93.35	-56.50
FPNS100	32.49	-35.71	19.13	-27.33	18.63	111.60	-100.47

APPENDIX B – QUASI-STATIC FORCES ON SLAB AND BEAM AND SLAB SPANS

The following tables are a list of all physical model tests performed and the significant variables and values associated with each test. The tables are divided into variables and forces. The tests can be differentiated by the individual case prefix and reference number. Four different setups were used in this section with ‘SLAB’ signifying tests done with the slab model, ‘BSXX’ signifying tests done with the beam and slab model with no overhangs or rails, ‘BSOX’ signifying tests done with the beam and slab model with overhangs but no rails, and ‘BSOR’ signifying tests done with the beam and slab model with overhangs and rails.

Table B-1 contains the relevant fluid and structure parameters for all tests. Table B-2 contains the measured significant forces and moments for all tests. All dimensions are in feet, all forces are in pounds, and all times are in seconds.

Column header abbreviations for Table B-1 are structure width, structure length, structure thickness, structure clearance height, water depth, wave height, wave period, wave length, and number of girders. Column header abbreviations for Table B-2 are total vertical maximum, total vertical minimum, quasi-static maximum, quasi-static minimum, associated horizontal to the quasi-static maximum, slamming maximum, horizontal maximum, horizontal minimum, and associated vertical to the horizontal maximum.

Table B- 1 Structure and fluid parameters for all physical model tests.

Test case	Struct. Width	Struct. Length	Struct. Thick.	Struct. Clear.	Water Depth	Wave Height	Wave Period	Wave Length	Girders
SLAB001	4.00	6.00	0.58	0.17	1.42	0.92	3.50	22.93	0
SLAB002	4.00	6.00	0.58	0.17	1.42	0.58	3.50	22.93	0
SLAB003	4.00	6.00	0.58	0.17	1.42	0.73	3.00	19.59	0
SLAB004	4.00	6.00	0.58	0.17	1.42	0.63	3.00	19.59	0
SLAB005	4.00	6.00	0.58	0.17	1.42	0.86	2.50	16.10	0
SLAB006	4.00	6.00	0.58	0.17	1.42	0.81	2.50	16.10	0
SLAB007	4.00	6.00	0.58	0.17	1.42	0.69	2.00	12.53	0
SLAB008	4.00	6.00	0.58	0.17	1.42	0.63	2.00	12.53	0
SLAB009	4.00	6.00	0.58	0.17	1.42	0.84	1.50	8.82	0
SLAB010	4.00	6.00	0.58	0.17	1.42	0.72	1.50	8.82	0
SLAB011	4.00	6.00	0.58	0.00	1.58	0.74	3.50	24.24	0
SLAB012	4.00	6.00	0.58	0.00	1.58	0.59	3.50	24.24	0
SLAB013	4.00	6.00	0.58	0.00	1.58	0.68	3.00	20.64	0
SLAB014	4.00	6.00	0.58	0.00	1.58	0.46	3.00	20.64	0
SLAB015	4.00	6.00	0.58	0.00	1.58	1.11	2.50	16.92	0
SLAB016	4.00	6.00	0.58	0.00	1.58	0.79	2.50	16.92	0
SLAB017	4.00	6.00	0.58	0.00	1.58	0.69	2.00	13.12	0
SLAB018	4.00	6.00	0.58	0.00	1.58	0.58	2.00	13.12	0
SLAB019	4.00	6.00	0.58	0.00	1.58	0.80	1.50	9.17	0
SLAB020	4.00	6.00	0.58	0.00	1.58	0.73	1.50	9.17	0
SLAB021	4.00	6.00	0.58	-0.29	1.88	1.22	3.50	26.31	0
SLAB022	4.00	6.00	0.58	-0.29	1.88	0.65	3.50	26.31	0
SLAB023	4.00	6.00	0.58	-0.29	1.88	0.59	3.00	22.31	0
SLAB024	4.00	6.00	0.58	-0.29	1.88	0.45	3.00	22.31	0
SLAB025	4.00	6.00	0.58	-0.29	1.88	1.03	2.50	18.23	0
SLAB026	4.00	6.00	0.58	-0.29	1.88	0.67	2.50	18.23	0
SLAB027	4.00	6.00	0.58	-0.29	1.88	0.78	2.00	14.05	0
SLAB028	4.00	6.00	0.58	-0.29	1.88	0.56	2.00	14.05	0
SLAB029	4.00	6.00	0.58	-0.29	1.88	0.85	1.50	9.67	0
SLAB030	4.00	6.00	0.58	-0.29	1.88	0.69	1.50	9.67	0
SLAB031	4.00	6.00	0.58	-0.63	2.21	0.96	3.50	28.41	0
SLAB032	4.00	6.00	0.58	-0.63	2.21	0.67	3.50	28.41	0
SLAB033	4.00	6.00	0.58	-0.63	2.21	0.70	3.00	24.02	0
SLAB034	4.00	6.00	0.58	-0.63	2.21	0.45	3.00	24.02	0
SLAB035	4.00	6.00	0.58	-0.63	2.21	1.02	2.50	19.55	0

Table B-1 Continued.

Test case	Struct. Width	Struct. Length	Struct. Thick.	Struct. Clear.	Water Depth	Wave Height	Wave Period	Wave Length	Girders
SLAB036	4.00	6.00	0.58	-0.63	2.21	0.82	2.50	19.55	0
SLAB037	4.00	6.00	0.58	-0.63	2.21	0.82	2.00	14.96	0
SLAB038	4.00	6.00	0.58	-0.63	2.21	0.71	2.00	14.96	0
SLAB039	4.00	6.00	0.58	-0.63	2.21	0.90	1.50	10.13	0
SLAB040	4.00	6.00	0.58	-0.63	2.21	0.85	1.50	10.13	0
SLAB041	4.00	6.00	0.58	0.17	1.75	0.95	3.50	25.45	0
SLAB042	4.00	6.00	0.58	0.17	1.75	0.54	3.50	25.45	0
SLAB043	4.00	6.00	0.58	0.17	1.75	0.77	3.00	21.62	0
SLAB044	4.00	6.00	0.58	0.17	1.75	0.47	3.00	21.62	0
SLAB045	4.00	6.00	0.58	0.17	1.75	0.95	2.50	17.69	0
SLAB046	4.00	6.00	0.58	0.17	1.75	0.63	2.50	17.69	0
SLAB047	4.00	6.00	0.58	0.17	1.75	0.77	2.00	13.67	0
SLAB048	4.00	6.00	0.58	0.17	1.75	0.70	2.00	13.67	0
SLAB049	4.00	6.00	0.58	0.17	1.75	0.86	1.50	9.47	0
SLAB050	4.00	6.00	0.58	0.17	1.75	0.75	1.50	9.47	0
SLAB051	4.00	6.00	0.58	0.00	1.92	1.02	3.50	26.59	0
SLAB052	4.00	6.00	0.58	0.00	1.92	0.50	3.50	26.59	0
SLAB053	4.00	6.00	0.58	0.00	1.92	0.60	3.00	22.54	0
SLAB054	4.00	6.00	0.58	0.00	1.92	0.39	3.00	22.54	0
SLAB055	4.00	6.00	0.58	0.00	1.92	0.86	2.50	18.40	0
SLAB056	4.00	6.00	0.58	0.00	1.92	0.66	2.50	18.40	0
SLAB057	4.00	6.00	0.58	0.00	1.92	0.63	2.00	14.17	0
SLAB058	4.00	6.00	0.58	0.00	1.92	0.46	2.00	14.17	0
SLAB059	4.00	6.00	0.58	0.00	1.92	0.77	1.50	9.74	0
SLAB060	4.00	6.00	0.58	0.00	1.92	0.64	1.50	9.74	0
SLAB061	4.00	6.00	0.58	-0.29	2.21	0.79	3.50	28.41	0
SLAB062	4.00	6.00	0.58	-0.29	2.21	0.46	3.50	28.41	0
SLAB063	4.00	6.00	0.58	-0.29	2.21	0.73	3.00	24.02	0
SLAB064	4.00	6.00	0.58	-0.29	2.21	0.44	3.00	24.02	0
SLAB065	4.00	6.00	0.58	-0.29	2.21	0.92	2.50	19.55	0
SLAB066	4.00	6.00	0.58	-0.29	2.21	0.66	2.50	19.55	0
SLAB067	4.00	6.00	0.58	-0.29	2.21	0.95	2.00	14.96	0
SLAB068	4.00	6.00	0.58	-0.29	2.21	0.65	2.00	14.96	0
SLAB069	4.00	6.00	0.58	-0.29	2.21	0.83	1.50	10.13	0
SLAB070	4.00	6.00	0.58	-0.29	2.21	0.65	1.50	10.13	0

Table B-1 Continued.

Test case	Struct. Width	Struct. Length	Struct. Thick.	Struct. Clear.	Water Depth	Wave Height	Wave Period	Wave Length	Girders
SLAB071	4.00	6.00	0.58	-0.63	2.54	1.33	3.50	30.31	0
SLAB072	4.00	6.00	0.58	-0.63	2.54	0.72	3.50	30.31	0
SLAB073	4.00	6.00	0.58	-0.63	2.54	0.92	3.00	25.57	0
SLAB074	4.00	6.00	0.58	-0.63	2.54	0.62	3.00	25.57	0
SLAB075	4.00	6.00	0.58	-0.63	2.54	0.96	2.50	20.73	0
SLAB076	4.00	6.00	0.58	-0.63	2.54	0.63	2.50	20.73	0
SLAB077	4.00	6.00	0.58	-0.63	2.54	1.15	2.00	15.74	0
SLAB078	4.00	6.00	0.58	-0.63	2.54	0.78	2.00	15.74	0
SLAB079	4.00	6.00	0.58	-0.63	2.54	1.13	1.50	10.48	0
SLAB080	4.00	6.00	0.58	-0.63	2.54	0.62	1.50	10.48	0
SLAB081	4.00	6.00	0.58	-0.17	2.08	0.60	3.50	27.65	0
SLAB082	4.00	6.00	0.58	-0.17	2.08	0.38	3.50	27.65	0
SLAB083	4.00	6.00	0.58	-0.17	2.08	0.73	3.00	23.40	0
SLAB084	4.00	6.00	0.58	-0.17	2.08	0.48	3.00	23.40	0
SLAB085	4.00	6.00	0.58	-0.17	2.08	0.80	2.50	19.08	0
SLAB086	4.00	6.00	0.58	-0.17	2.08	0.62	2.50	19.08	0
SLAB087	4.00	6.00	0.58	-0.17	2.08	1.00	2.00	14.63	0
SLAB088	4.00	6.00	0.58	-0.17	2.08	0.65	2.00	14.63	0
SLAB089	4.00	6.00	0.58	-0.17	2.08	0.86	1.50	9.97	0
SLAB090	4.00	6.00	0.58	-0.17	2.08	0.59	1.50	9.97	0
SLAB091	4.00	6.00	0.58	0.00	2.25	0.91	3.50	28.66	0
SLAB092	4.00	6.00	0.58	0.00	2.25	0.57	3.50	28.66	0
SLAB093	4.00	6.00	0.58	0.00	2.25	0.68	3.00	24.23	0
SLAB094	4.00	6.00	0.58	0.00	2.25	0.59	3.00	24.23	0
SLAB095	4.00	6.00	0.58	0.00	2.25	0.99	2.50	19.71	0
SLAB096	4.00	6.00	0.58	0.00	2.25	0.73	2.50	19.71	0
SLAB097	4.00	6.00	0.58	0.00	2.25	0.94	2.00	15.06	0
SLAB098	4.00	6.00	0.58	0.00	2.25	0.76	2.00	15.06	0
SLAB099	4.00	6.00	0.58	0.00	2.25	0.84	1.50	10.18	0
SLAB100	4.00	6.00	0.58	0.00	2.25	0.72	1.50	10.18	0
SLAB101	4.00	6.00	0.58	-0.29	2.54	0.98	3.50	30.31	0
SLAB102	4.00	6.00	0.58	-0.29	2.54	0.61	3.50	30.31	0
SLAB103	4.00	6.00	0.58	-0.29	2.54	0.88	3.00	25.57	0
SLAB104	4.00	6.00	0.58	-0.29	2.54	0.60	3.00	25.57	0
SLAB105	4.00	6.00	0.58	-0.29	2.54	0.92	2.50	20.73	0

Table B-1 Continued.

Test case	Struct. Width	Struct. Length	Struct. Thick.	Struct. Clear.	Water Depth	Wave Height	Wave Period	Wave Length	Girders
SLAB106	4.00	6.00	0.58	-0.29	2.54	0.63	2.50	20.73	0
SLAB107	4.00	6.00	0.58	-0.29	2.54	1.41	2.00	15.74	0
SLAB108	4.00	6.00	0.58	-0.29	2.54	1.10	2.00	15.74	0
SLAB109	4.00	6.00	0.58	-0.29	2.54	1.08	1.50	10.48	0
SLAB110	4.00	6.00	0.58	-0.29	2.54	0.95	1.50	10.48	0
SLAB111	4.00	6.00	0.58	-0.63	2.88	0.89	3.50	32.05	0
SLAB112	4.00	6.00	0.58	-0.63	2.88	0.52	3.50	32.05	0
SLAB113	4.00	6.00	0.58	-0.63	2.88	0.74	3.00	26.97	0
SLAB114	4.00	6.00	0.58	-0.63	2.88	0.61	3.00	26.97	0
SLAB115	4.00	6.00	0.58	-0.63	2.88	0.75	2.50	21.78	0
SLAB116	4.00	6.00	0.58	-0.63	2.88	0.57	2.50	21.78	0
SLAB117	4.00	6.00	0.58	-0.63	2.88	1.32	2.00	16.41	0
SLAB118	4.00	6.00	0.58	-0.63	2.88	1.21	2.00	16.41	0
SLAB119	4.00	6.00	0.58	-0.63	2.88	1.01	1.50	10.76	0
SLAB120	4.00	6.00	0.58	-0.63	2.88	0.97	1.50	10.76	0
SLAB121	4.00	6.00	0.58	-0.17	2.42	0.97	3.50	29.62	0
SLAB122	4.00	6.00	0.58	-0.17	2.42	0.58	3.50	29.62	0
SLAB123	4.00	6.00	0.58	-0.17	2.42	0.85	3.00	25.01	0
SLAB124	4.00	6.00	0.58	-0.17	2.42	0.60	3.00	25.01	0
SLAB125	4.00	6.00	0.58	-0.17	2.42	0.96	2.50	20.30	0
SLAB126	4.00	6.00	0.58	-0.17	2.42	0.76	2.50	20.30	0
SLAB127	4.00	6.00	0.58	-0.17	2.42	1.14	2.00	15.46	0
SLAB128	4.00	6.00	0.58	-0.17	2.42	0.80	2.00	15.46	0
SLAB129	4.00	6.00	0.58	-0.17	2.42	1.02	1.50	10.36	0
SLAB130	4.00	6.00	0.58	-0.17	2.42	0.78	1.50	10.36	0
SLAB131	4.00	6.00	0.58	0.00	2.58	0.97	3.50	30.54	0
SLAB132	4.00	6.00	0.58	0.00	2.58	0.55	3.50	30.54	0
SLAB133	4.00	6.00	0.58	0.00	2.58	0.79	3.00	25.75	0
SLAB134	4.00	6.00	0.58	0.00	2.58	0.52	3.00	25.75	0
SLAB135	4.00	6.00	0.58	0.00	2.58	0.83	2.50	20.87	0
SLAB136	4.00	6.00	0.58	0.00	2.58	0.74	2.50	20.87	0
SLAB137	4.00	6.00	0.58	0.00	2.58	1.15	2.00	15.83	0
SLAB138	4.00	6.00	0.58	0.00	2.58	1.26	2.00	15.83	0
SLAB139	4.00	6.00	0.58	0.00	2.58	0.99	1.50	10.52	0
SLAB140	4.00	6.00	0.58	0.00	2.58	0.85	1.50	10.52	0

Table B-1 Continued.

Test case	Struct. Width	Struct. Length	Struct. Thick.	Struct. Clear.	Water Depth	Wave Height	Wave Period	Wave Length	Girders
SLAB141	4.00	6.00	0.58	-0.29	2.88	1.00	3.50	32.05	0
SLAB142	4.00	6.00	0.58	-0.29	2.88	0.72	3.50	32.05	0
SLAB143	4.00	6.00	0.58	-0.29	2.88	1.04	3.00	26.97	0
SLAB144	4.00	6.00	0.58	-0.29	2.88	0.77	3.00	26.97	0
SLAB145	4.00	6.00	0.58	-0.29	2.88	0.92	2.50	21.78	0
SLAB146	4.00	6.00	0.58	-0.29	2.88	0.70	2.50	21.78	0
SLAB147	4.00	6.00	0.58	-0.29	2.88	1.45	2.00	16.41	0
SLAB148	4.00	6.00	0.58	-0.29	2.88	1.32	2.00	16.41	0
SLAB149	4.00	6.00	0.58	-0.29	2.88	1.14	1.50	10.76	0
SLAB150	4.00	6.00	0.58	-0.29	2.88	1.03	1.50	10.76	0
BSXX001	4.00	6.00	0.58	0.17	1.42	0.77	3.50	22.93	7
BSXX002	4.00	6.00	0.58	0.17	1.42	0.45	3.50	22.93	7
BSXX003	4.00	6.00	0.58	0.17	1.42	0.75	3.00	19.59	7
BSXX004	4.00	6.00	0.58	0.17	1.42	0.48	3.00	19.59	7
BSXX005	4.00	6.00	0.58	0.17	1.42	0.86	2.50	16.10	7
BSXX006	4.00	6.00	0.58	0.17	1.42	0.64	2.50	16.10	7
BSXX007	4.00	6.00	0.58	0.17	1.42	0.71	2.00	12.53	7
BSXX008	4.00	6.00	0.58	0.17	1.42	0.59	2.00	12.53	7
BSXX009	4.00	6.00	0.58	0.17	1.42	0.76	1.50	8.82	7
BSXX010	4.00	6.00	0.58	0.17	1.42	0.79	1.50	8.82	7
BSXX011	4.00	6.00	0.58	0.00	1.58	1.01	3.50	24.24	7
BSXX012	4.00	6.00	0.58	0.00	1.58	0.64	3.50	24.24	7
BSXX013	4.00	6.00	0.58	0.00	1.58	0.75	3.00	20.64	7
BSXX014	4.00	6.00	0.58	0.00	1.58	0.55	3.00	20.64	7
BSXX015	4.00	6.00	0.58	0.00	1.58	1.04	2.50	16.92	7
BSXX016	4.00	6.00	0.58	0.00	1.58	0.71	2.50	16.92	7
BSXX017	4.00	6.00	0.58	0.00	1.58	0.66	2.00	13.12	7
BSXX018	4.00	6.00	0.58	0.00	1.58	0.55	2.00	13.12	7
BSXX019	4.00	6.00	0.58	0.00	1.58	0.76	1.50	9.17	7
BSXX020	4.00	6.00	0.58	0.00	1.58	0.84	1.50	9.17	7
BSXX021	4.00	6.00	0.58	-0.29	1.88	0.79	3.50	26.31	7
BSXX022	4.00	6.00	0.58	-0.29	1.88	0.64	3.50	26.31	7
BSXX023	4.00	6.00	0.58	-0.29	1.88	0.54	3.00	22.31	7
BSXX024	4.00	6.00	0.58	-0.29	1.88	0.42	3.00	22.31	7
BSXX025	4.00	6.00	0.58	-0.29	1.88	0.92	2.50	18.23	7

Table B-1 Continued.

Test case	Struct. Width	Struct. Length	Struct. Thick.	Struct. Clear.	Water Depth	Wave Height	Wave Period	Wave Length	Girders
BSXX026	4.00	6.00	0.58	-0.29	1.88	0.87	2.50	18.23	7
BSXX027	4.00	6.00	0.58	-0.29	1.88	0.82	2.00	14.05	7
BSXX028	4.00	6.00	0.58	-0.29	1.88	0.56	2.00	14.05	7
BSXX029	4.00	6.00	0.58	-0.29	1.88	0.81	1.50	9.67	7
BSXX030	4.00	6.00	0.58	-0.29	1.88	0.77	1.50	9.67	7
BSXX031	4.00	6.00	0.58	-0.63	2.21	1.14	3.50	28.41	7
BSXX032	4.00	6.00	0.58	-0.63	2.21	0.65	3.50	28.41	7
BSXX033	4.00	6.00	0.58	-0.63	2.21	0.72	3.00	24.02	7
BSXX034	4.00	6.00	0.58	-0.63	2.21	0.53	3.00	24.02	7
BSXX035	4.00	6.00	0.58	-0.63	2.21	0.85	2.50	19.55	7
BSXX036	4.00	6.00	0.58	-0.63	2.21	0.69	2.50	19.55	7
BSXX037	4.00	6.00	0.58	-0.63	2.21	0.77	2.00	14.96	7
BSXX038	4.00	6.00	0.58	-0.63	2.21	0.77	2.00	14.96	7
BSXX039	4.00	6.00	0.58	-0.63	2.21	0.94	1.50	10.13	7
BSXX040	4.00	6.00	0.58	-0.63	2.21	0.90	1.50	10.13	7
BSXX041	4.00	6.00	0.58	0.17	1.75	0.65	3.50	25.45	7
BSXX042	4.00	6.00	0.58	0.17	1.75	0.72	3.50	25.45	7
BSXX043	4.00	6.00	0.58	0.17	1.75	0.61	3.00	21.62	7
BSXX044	4.00	6.00	0.58	0.17	1.75	0.58	3.00	21.62	7
BSXX045	4.00	6.00	0.58	0.17	1.75	0.85	2.50	17.69	7
BSXX046	4.00	6.00	0.58	0.17	1.75	0.68	2.50	17.69	7
BSXX047	4.00	6.00	0.58	0.17	1.75	0.78	2.00	13.67	7
BSXX048	4.00	6.00	0.58	0.17	1.75	0.81	2.00	13.67	7
BSXX049	4.00	6.00	0.58	0.17	1.75	0.79	1.50	9.47	7
BSXX050	4.00	6.00	0.58	0.17	1.75	0.81	1.50	9.47	7
BSXX051	4.00	6.00	0.58	0.00	1.92	0.86	3.50	26.59	7
BSXX052	4.00	6.00	0.58	0.00	1.92	0.58	3.50	26.59	7
BSXX053	4.00	6.00	0.58	0.00	1.92	0.71	3.00	22.54	7
BSXX054	4.00	6.00	0.58	0.00	1.92	0.53	3.00	22.54	7
BSXX055	4.00	6.00	0.58	0.00	1.92	0.83	2.50	18.40	7
BSXX056	4.00	6.00	0.58	0.00	1.92	0.71	2.50	18.40	7
BSXX057	4.00	6.00	0.58	0.00	1.92	0.84	2.00	14.17	7
BSXX058	4.00	6.00	0.58	0.00	1.92	0.91	2.00	14.17	7
BSXX059	4.00	6.00	0.58	0.00	1.92	0.80	1.50	9.74	7
BSXX060	4.00	6.00	0.58	0.00	1.92	0.69	1.50	9.74	7

Table B-1 Continued.

Test case	Struct. Width	Struct. Length	Struct. Thick.	Struct. Clear.	Water Depth	Wave Height	Wave Period	Wave Length	Girders
BSXX061	4.00	6.00	0.58	-0.29	2.21	0.80	3.50	28.41	7
BSXX062	4.00	6.00	0.58	-0.29	2.21	0.62	3.50	28.41	7
BSXX063	4.00	6.00	0.58	-0.29	2.21	0.64	3.00	24.02	7
BSXX064	4.00	6.00	0.58	-0.29	2.21	0.48	3.00	24.02	7
BSXX065	4.00	6.00	0.58	-0.29	2.21	0.88	2.50	19.55	7
BSXX066	4.00	6.00	0.58	-0.29	2.21	0.82	2.50	19.55	7
BSXX067	4.00	6.00	0.58	-0.29	2.21	1.12	2.00	14.96	7
BSXX068	4.00	6.00	0.58	-0.29	2.21	0.99	2.00	14.96	7
BSXX069	4.00	6.00	0.58	-0.29	2.21	0.91	1.50	10.13	7
BSXX070	4.00	6.00	0.58	-0.29	2.21	0.85	1.50	10.13	7
BSXX071	4.00	6.00	0.58	-0.63	2.54	1.06	3.50	30.31	7
BSXX072	4.00	6.00	0.58	-0.63	2.54	0.79	3.50	30.31	7
BSXX073	4.00	6.00	0.58	-0.63	2.54	0.94	3.00	25.57	7
BSXX074	4.00	6.00	0.58	-0.63	2.54	0.62	3.00	25.57	7
BSXX075	4.00	6.00	0.58	-0.63	2.54	0.80	2.50	20.73	7
BSXX076	4.00	6.00	0.58	-0.63	2.54	0.65	2.50	20.73	7
BSXX077	4.00	6.00	0.58	-0.63	2.54	1.42	2.00	15.74	7
BSXX078	4.00	6.00	0.58	-0.63	2.54	0.96	2.00	15.74	7
BSXX079	4.00	6.00	0.58	-0.63	2.54	1.03	1.50	10.48	7
BSXX080	4.00	6.00	0.58	-0.63	2.54	1.02	1.50	10.48	7
BSXX081	4.00	6.00	0.58	-0.17	2.08	0.83	3.50	27.65	7
BSXX082	4.00	6.00	0.58	-0.17	2.08	0.53	3.50	27.65	7
BSXX083	4.00	6.00	0.58	-0.17	2.08	0.92	3.00	23.40	7
BSXX084	4.00	6.00	0.58	-0.17	2.08	0.52	3.00	23.40	7
BSXX085	4.00	6.00	0.58	-0.17	2.08	0.86	2.50	19.08	7
BSXX086	4.00	6.00	0.58	-0.17	2.08	0.64	2.50	19.08	7
BSXX087	4.00	6.00	0.58	-0.17	2.08	0.89	2.00	14.63	7
BSXX088	4.00	6.00	0.58	-0.17	2.08	0.75	2.00	14.63	7
BSXX089	4.00	6.00	0.58	-0.17	2.08	0.91	1.50	9.97	7
BSXX090	4.00	6.00	0.58	-0.17	2.08	0.81	1.50	9.97	7
BSXX091	4.00	6.00	0.58	0.00	2.25	1.07	3.50	28.66	7
BSXX092	4.00	6.00	0.58	0.00	2.25	0.71	3.50	28.66	7
BSXX093	4.00	6.00	0.58	0.00	2.25	0.87	3.00	24.23	7
BSXX094	4.00	6.00	0.58	0.00	2.25	0.60	3.00	24.23	7
BSXX095	4.00	6.00	0.58	0.00	2.25	1.01	2.50	19.71	7

Table B-1 Continued.

Test case	Struct. Width	Struct. Length	Struct. Thick.	Struct. Clear.	Water Depth	Wave Height	Wave Period	Wave Length	Girders
BSXX096	4.00	6.00	0.58	0.00	2.25	0.86	2.50	19.71	7
BSXX097	4.00	6.00	0.58	0.00	2.25	1.04	2.00	15.06	7
BSXX098	4.00	6.00	0.58	0.00	2.25	0.90	2.00	15.06	7
BSXX099	4.00	6.00	0.58	0.00	2.25	1.01	1.50	10.18	7
BSXX100	4.00	6.00	0.58	0.00	2.25	0.96	1.50	10.18	7
BSXX101	4.00	6.00	0.58	-0.29	2.54	1.14	3.50	30.31	7
BSXX102	4.00	6.00	0.58	-0.29	2.54	0.69	3.50	30.31	7
BSXX103	4.00	6.00	0.58	-0.29	2.54	0.92	3.00	25.57	7
BSXX104	4.00	6.00	0.58	-0.29	2.54	0.60	3.00	25.57	7
BSXX105	4.00	6.00	0.58	-0.29	2.54	1.03	2.50	20.73	7
BSXX106	4.00	6.00	0.58	-0.29	2.54	0.72	2.50	20.73	7
BSXX107	4.00	6.00	0.58	-0.29	2.54	1.28	2.00	15.74	7
BSXX108	4.00	6.00	0.58	-0.29	2.54	1.02	2.00	15.74	7
BSXX109	4.00	6.00	0.58	-0.29	2.54	1.08	1.50	10.48	7
BSXX110	4.00	6.00	0.58	-0.29	2.54	1.07	1.50	10.48	7
BSXX111	4.00	6.00	0.58	-0.63	2.88	1.11	3.50	32.05	7
BSXX112	4.00	6.00	0.58	-0.63	2.88	0.75	3.50	32.05	7
BSXX113	4.00	6.00	0.58	-0.63	2.88	1.05	3.00	26.97	7
BSXX114	4.00	6.00	0.58	-0.63	2.88	0.78	3.00	26.97	7
BSXX115	4.00	6.00	0.58	-0.63	2.88	0.94	2.50	21.78	7
BSXX116	4.00	6.00	0.58	-0.63	2.88	0.61	2.50	21.78	7
BSXX117	4.00	6.00	0.58	-0.63	2.88	1.56	2.00	16.41	7
BSXX118	4.00	6.00	0.58	-0.63	2.88	1.35	2.00	16.41	7
BSXX119	4.00	6.00	0.58	-0.63	2.88	1.28	1.50	10.76	7
BSXX120	4.00	6.00	0.58	-0.63	2.88	1.09	1.50	10.76	7
BSXX121	4.00	6.00	0.58	-0.17	2.42	0.85	3.50	29.62	7
BSXX122	4.00	6.00	0.58	-0.17	2.42	0.57	3.50	29.62	7
BSXX123	4.00	6.00	0.58	-0.17	2.42	0.82	3.00	25.01	7
BSXX124	4.00	6.00	0.58	-0.17	2.42	0.63	3.00	25.01	7
BSXX125	4.00	6.00	0.58	-0.17	2.42	1.05	2.50	20.30	7
BSXX126	4.00	6.00	0.58	-0.17	2.42	0.72	2.50	20.30	7
BSXX127	4.00	6.00	0.58	-0.17	2.42	1.19	2.00	15.46	7
BSXX128	4.00	6.00	0.58	-0.17	2.42	0.98	2.00	15.46	7
BSXX129	4.00	6.00	0.58	-0.17	2.42	1.10	1.50	10.36	7
BSXX130	4.00	6.00	0.58	-0.17	2.42	1.05	1.50	10.36	7

Table B-1 Continued.

Test case	Struct. Width	Struct. Length	Struct. Thick.	Struct. Clear.	Water Depth	Wave Height	Wave Period	Wave Length	Girders
BSXX131	4.00	6.00	0.58	0.00	2.58	0.82	3.50	30.54	7
BSXX132	4.00	6.00	0.58	0.00	2.58	0.63	3.50	30.54	7
BSXX133	4.00	6.00	0.58	0.00	2.58	0.86	3.00	25.75	7
BSXX134	4.00	6.00	0.58	0.00	2.58	0.55	3.00	25.75	7
BSXX135	4.00	6.00	0.58	0.00	2.58	1.04	2.50	20.87	7
BSXX136	4.00	6.00	0.58	0.00	2.58	0.78	2.50	20.87	7
BSXX137	4.00	6.00	0.58	0.00	2.58	1.23	2.00	15.83	7
BSXX138	4.00	6.00	0.58	0.00	2.58	1.14	2.00	15.83	7
BSXX139	4.00	6.00	0.58	0.00	2.58	1.03	1.50	10.52	7
BSXX140	4.00	6.00	0.58	0.00	2.58	1.01	1.50	10.52	7
BSXX141	4.00	6.00	0.58	-0.29	2.88	1.20	3.50	32.05	7
BSXX142	4.00	6.00	0.58	-0.29	2.88	0.78	3.50	32.05	7
BSXX143	4.00	6.00	0.58	-0.29	2.88	1.04	3.00	26.97	7
BSXX144	4.00	6.00	0.58	-0.29	2.88	0.81	3.00	26.97	7
BSXX145	4.00	6.00	0.58	-0.29	2.88	0.97	2.50	21.78	7
BSXX146	4.00	6.00	0.58	-0.29	2.88	0.63	2.50	21.78	7
BSXX147	4.00	6.00	0.58	-0.29	2.88	1.64	2.00	16.41	7
BSXX148	4.00	6.00	0.58	-0.29	2.88	1.39	2.00	16.41	7
BSXX149	4.00	6.00	0.58	-0.29	2.88	1.20	1.50	10.76	7
BSXX150	4.00	6.00	0.58	-0.29	2.88	1.11	1.50	10.76	7
BSOX001	4.00	6.00	0.58	0.17	1.42	0.92	3.50	22.93	7
BSOX002	4.00	6.00	0.58	0.17	1.42	0.58	3.50	22.93	7
BSOX003	4.00	6.00	0.58	0.17	1.42	0.73	3.00	19.59	7
BSOX004	4.00	6.00	0.58	0.17	1.42	0.63	3.00	19.59	7
BSOX005	4.00	6.00	0.58	0.17	1.42	0.86	2.50	16.10	7
BSOX006	4.00	6.00	0.58	0.17	1.42	0.81	2.50	16.10	7
BSOX007	4.00	6.00	0.58	0.17	1.42	0.69	2.00	12.53	7
BSOX008	4.00	6.00	0.58	0.17	1.42	0.63	2.00	12.53	7
BSOX009	4.00	6.00	0.58	0.17	1.42	0.84	1.50	8.82	7
BSOX010	4.00	6.00	0.58	0.17	1.42	0.72	1.50	8.82	7
BSOX011	4.00	6.00	0.58	0.00	1.58	0.74	3.50	24.24	7
BSOX012	4.00	6.00	0.58	0.00	1.58	0.59	3.50	24.24	7
BSOX013	4.00	6.00	0.58	0.00	1.58	0.68	3.00	20.64	7
BSOX014	4.00	6.00	0.58	0.00	1.58	0.46	3.00	20.64	7
BSOX015	4.00	6.00	0.58	0.00	1.58	1.11	2.50	16.92	7

Table B-1 Continued.

Test case	Struct. Width	Struct. Length	Struct. Thick.	Struct. Clear.	Water Depth	Wave Height	Wave Period	Wave Length	Girders
BSOX016	4.00	6.00	0.58	0.00	1.58	0.79	2.50	16.92	7
BSOX017	4.00	6.00	0.58	0.00	1.58	0.69	2.00	13.12	7
BSOX018	4.00	6.00	0.58	0.00	1.58	0.58	2.00	13.12	7
BSOX019	4.00	6.00	0.58	0.00	1.58	0.80	1.50	9.17	7
BSOX020	4.00	6.00	0.58	0.00	1.58	0.73	1.50	9.17	7
BSOX021	4.00	6.00	0.58	-0.29	1.88	1.22	3.50	26.31	7
BSOX022	4.00	6.00	0.58	-0.29	1.88	0.65	3.50	26.31	7
BSOX023	4.00	6.00	0.58	-0.29	1.88	0.59	3.00	22.31	7
BSOX024	4.00	6.00	0.58	-0.29	1.88	0.45	3.00	22.31	7
BSOX025	4.00	6.00	0.58	-0.29	1.88	1.03	2.50	18.23	7
BSOX026	4.00	6.00	0.58	-0.29	1.88	0.67	2.50	18.23	7
BSOX027	4.00	6.00	0.58	-0.29	1.88	0.78	2.00	14.05	7
BSOX028	4.00	6.00	0.58	-0.29	1.88	0.56	2.00	14.05	7
BSOX029	4.00	6.00	0.58	-0.29	1.88	0.85	1.50	9.67	7
BSOX030	4.00	6.00	0.58	-0.29	1.88	0.69	1.50	9.67	7
BSOX031	4.00	6.00	0.58	-0.63	2.21	0.96	3.50	28.41	7
BSOX032	4.00	6.00	0.58	-0.63	2.21	0.67	3.50	28.41	7
BSOX033	4.00	6.00	0.58	-0.63	2.21	0.70	3.00	24.02	7
BSOX034	4.00	6.00	0.58	-0.63	2.21	0.45	3.00	24.02	7
BSOX035	4.00	6.00	0.58	-0.63	2.21	1.02	2.50	19.55	7
BSOX036	4.00	6.00	0.58	-0.63	2.21	0.82	2.50	19.55	7
BSOX037	4.00	6.00	0.58	-0.63	2.21	0.82	2.00	14.96	7
BSOX038	4.00	6.00	0.58	-0.63	2.21	0.71	2.00	14.96	7
BSOX039	4.00	6.00	0.58	-0.63	2.21	0.90	1.50	10.13	7
BSOX040	4.00	6.00	0.58	-0.63	2.21	0.85	1.50	10.13	7
BSOX041	4.00	6.00	0.58	0.17	1.75	0.95	3.50	25.45	7
BSOX042	4.00	6.00	0.58	0.17	1.75	0.54	3.50	25.45	7
BSOX043	4.00	6.00	0.58	0.17	1.75	0.77	3.00	21.62	7
BSOX044	4.00	6.00	0.58	0.17	1.75	0.47	3.00	21.62	7
BSOX045	4.00	6.00	0.58	0.17	1.75	0.95	2.50	17.69	7
BSOX046	4.00	6.00	0.58	0.17	1.75	0.63	2.50	17.69	7
BSOX047	4.00	6.00	0.58	0.17	1.75	0.77	2.00	13.67	7
BSOX048	4.00	6.00	0.58	0.17	1.75	0.70	2.00	13.67	7
BSOX049	4.00	6.00	0.58	0.17	1.75	0.86	1.50	9.47	7
BSOX050	4.00	6.00	0.58	0.17	1.75	0.75	1.50	9.47	7

Table B-1 Continued.

Test case	Struct. Width	Struct. Length	Struct. Thick.	Struct. Clear.	Water Depth	Wave Height	Wave Period	Wave Length	Girders
BSOX051	4.00	6.00	0.58	0.00	1.92	1.02	3.50	26.59	7
BSOX052	4.00	6.00	0.58	0.00	1.92	0.50	3.50	26.59	7
BSOX053	4.00	6.00	0.58	0.00	1.92	0.60	3.00	22.54	7
BSOX054	4.00	6.00	0.58	0.00	1.92	0.39	3.00	22.54	7
BSOX055	4.00	6.00	0.58	0.00	1.92	0.86	2.50	18.40	7
BSOX056	4.00	6.00	0.58	0.00	1.92	0.66	2.50	18.40	7
BSOX057	4.00	6.00	0.58	0.00	1.92	0.63	2.00	14.17	7
BSOX058	4.00	6.00	0.58	0.00	1.92	0.46	2.00	14.17	7
BSOX059	4.00	6.00	0.58	0.00	1.92	0.77	1.50	9.74	7
BSOX060	4.00	6.00	0.58	0.00	1.92	0.64	1.50	9.74	7
BSOX061	4.00	6.00	0.58	-0.29	2.21	0.79	3.50	28.41	7
BSOX062	4.00	6.00	0.58	-0.29	2.21	0.46	3.50	28.41	7
BSOX063	4.00	6.00	0.58	-0.29	2.21	0.73	3.00	24.02	7
BSOX064	4.00	6.00	0.58	-0.29	2.21	0.44	3.00	24.02	7
BSOX065	4.00	6.00	0.58	-0.29	2.21	0.92	2.50	19.55	7
BSOX066	4.00	6.00	0.58	-0.29	2.21	0.66	2.50	19.55	7
BSOX067	4.00	6.00	0.58	-0.29	2.21	0.95	2.00	14.96	7
BSOX068	4.00	6.00	0.58	-0.29	2.21	0.65	2.00	14.96	7
BSOX069	4.00	6.00	0.58	-0.29	2.21	0.83	1.50	10.13	7
BSOX070	4.00	6.00	0.58	-0.29	2.21	0.65	1.50	10.13	7
BSOX071	4.00	6.00	0.58	-0.63	2.54	1.33	3.50	30.31	7
BSOX072	4.00	6.00	0.58	-0.63	2.54	0.72	3.50	30.31	7
BSOX073	4.00	6.00	0.58	-0.63	2.54	0.92	3.00	25.57	7
BSOX074	4.00	6.00	0.58	-0.63	2.54	0.62	3.00	25.57	7
BSOX075	4.00	6.00	0.58	-0.63	2.54	0.96	2.50	20.73	7
BSOX076	4.00	6.00	0.58	-0.63	2.54	0.63	2.50	20.73	7
BSOX077	4.00	6.00	0.58	-0.63	2.54	1.15	2.00	15.74	7
BSOX078	4.00	6.00	0.58	-0.63	2.54	0.78	2.00	15.74	7
BSOX079	4.00	6.00	0.58	-0.63	2.54	1.13	1.50	10.48	7
BSOX080	4.00	6.00	0.58	-0.63	2.54	0.62	1.50	10.48	7
BSOX081	4.00	6.00	0.58	-0.17	2.08	0.60	3.50	27.65	7
BSOX082	4.00	6.00	0.58	-0.17	2.08	0.38	3.50	27.65	7
BSOX083	4.00	6.00	0.58	-0.17	2.08	0.73	3.00	23.40	7
BSOX084	4.00	6.00	0.58	-0.17	2.08	0.48	3.00	23.40	7
BSOX085	4.00	6.00	0.58	-0.17	2.08	0.80	2.50	19.08	7

Table B-1 Continued.

Test case	Struct. Width	Struct. Length	Struct. Thick.	Struct. Clear.	Water Depth	Wave Height	Wave Period	Wave Length	Girders
BSOX086	4.00	6.00	0.58	-0.17	2.08	0.62	2.50	19.08	7
BSOX087	4.00	6.00	0.58	-0.17	2.08	1.00	2.00	14.63	7
BSOX088	4.00	6.00	0.58	-0.17	2.08	0.65	2.00	14.63	7
BSOX089	4.00	6.00	0.58	-0.17	2.08	0.86	1.50	9.97	7
BSOX090	4.00	6.00	0.58	-0.17	2.08	0.59	1.50	9.97	7
BSOX091	4.00	6.00	0.58	0.00	2.25	0.91	3.50	28.66	7
BSOX092	4.00	6.00	0.58	0.00	2.25	0.57	3.50	28.66	7
BSOX093	4.00	6.00	0.58	0.00	2.25	0.68	3.00	24.23	7
BSOX094	4.00	6.00	0.58	0.00	2.25	0.59	3.00	24.23	7
BSOX095	4.00	6.00	0.58	0.00	2.25	0.99	2.50	19.71	7
BSOX096	4.00	6.00	0.58	0.00	2.25	0.73	2.50	19.71	7
BSOX097	4.00	6.00	0.58	0.00	2.25	0.94	2.00	15.06	7
BSOX098	4.00	6.00	0.58	0.00	2.25	0.76	2.00	15.06	7
BSOX099	4.00	6.00	0.58	0.00	2.25	0.84	1.50	10.18	7
BSOX100	4.00	6.00	0.58	0.00	2.25	0.72	1.50	10.18	7
BSOX101	4.00	6.00	0.58	-0.29	2.54	0.98	3.50	30.31	7
BSOX102	4.00	6.00	0.58	-0.29	2.54	0.61	3.50	30.31	7
BSOX103	4.00	6.00	0.58	-0.29	2.54	0.88	3.00	25.57	7
BSOX104	4.00	6.00	0.58	-0.29	2.54	0.60	3.00	25.57	7
BSOX105	4.00	6.00	0.58	-0.29	2.54	0.92	2.50	20.73	7
BSOX106	4.00	6.00	0.58	-0.29	2.54	0.63	2.50	20.73	7
BSOX107	4.00	6.00	0.58	-0.29	2.54	1.41	2.00	15.74	7
BSOX108	4.00	6.00	0.58	-0.29	2.54	1.10	2.00	15.74	7
BSOX109	4.00	6.00	0.58	-0.29	2.54	1.08	1.50	10.48	7
BSOX110	4.00	6.00	0.58	-0.29	2.54	0.95	1.50	10.48	7
BSOX111	4.00	6.00	0.58	-0.63	2.88	0.89	3.50	32.05	7
BSOX112	4.00	6.00	0.58	-0.63	2.88	0.52	3.50	32.05	7
BSOX113	4.00	6.00	0.58	-0.63	2.88	0.74	3.00	26.97	7
BSOX114	4.00	6.00	0.58	-0.63	2.88	0.61	3.00	26.97	7
BSOX115	4.00	6.00	0.58	-0.63	2.88	0.75	2.50	21.78	7
BSOX116	4.00	6.00	0.58	-0.63	2.88	0.57	2.50	21.78	7
BSOX117	4.00	6.00	0.58	-0.63	2.88	1.32	2.00	16.41	7
BSOX118	4.00	6.00	0.58	-0.63	2.88	1.21	2.00	16.41	7
BSOX119	4.00	6.00	0.58	-0.63	2.88	1.01	1.50	10.76	7
BSOX120	4.00	6.00	0.58	-0.63	2.88	0.97	1.50	10.76	7

Table B-1 Continued.

Test case	Struct. Width	Struct. Length	Struct. Thick.	Struct. Clear.	Water Depth	Wave Height	Wave Period	Wave Length	Girders
BSOX121	4.00	6.00	0.58	-0.17	2.42	0.97	3.50	29.62	7
BSOX122	4.00	6.00	0.58	-0.17	2.42	0.58	3.50	29.62	7
BSOX123	4.00	6.00	0.58	-0.17	2.42	0.85	3.00	25.01	7
BSOX124	4.00	6.00	0.58	-0.17	2.42	0.60	3.00	25.01	7
BSOX125	4.00	6.00	0.58	-0.17	2.42	0.96	2.50	20.30	7
BSOX126	4.00	6.00	0.58	-0.17	2.42	0.76	2.50	20.30	7
BSOX127	4.00	6.00	0.58	-0.17	2.42	1.14	2.00	15.46	7
BSOX128	4.00	6.00	0.58	-0.17	2.42	0.80	2.00	15.46	7
BSOX129	4.00	6.00	0.58	-0.17	2.42	1.02	1.50	10.36	7
BSOX130	4.00	6.00	0.58	-0.17	2.42	0.78	1.50	10.36	7
BSOX131	4.00	6.00	0.58	0.00	2.58	0.97	3.50	30.54	7
BSOX132	4.00	6.00	0.58	0.00	2.58	0.55	3.50	30.54	7
BSOX133	4.00	6.00	0.58	0.00	2.58	0.79	3.00	25.75	7
BSOX134	4.00	6.00	0.58	0.00	2.58	0.52	3.00	25.75	7
BSOX135	4.00	6.00	0.58	0.00	2.58	0.83	2.50	20.87	7
BSOX136	4.00	6.00	0.58	0.00	2.58	0.74	2.50	20.87	7
BSOX137	4.00	6.00	0.58	0.00	2.58	1.15	2.00	15.83	7
BSOX138	4.00	6.00	0.58	0.00	2.58	1.26	2.00	15.83	7
BSOX139	4.00	6.00	0.58	0.00	2.58	0.99	1.50	10.52	7
BSOX140	4.00	6.00	0.58	0.00	2.58	0.85	1.50	10.52	7
BSOX141	4.00	6.00	0.58	-0.29	2.88	1.00	3.50	32.05	7
BSOX142	4.00	6.00	0.58	-0.29	2.88	0.72	3.50	32.05	7
BSOX143	4.00	6.00	0.58	-0.29	2.88	1.04	3.00	26.97	7
BSOX144	4.00	6.00	0.58	-0.29	2.88	0.77	3.00	26.97	7
BSOX145	4.00	6.00	0.58	-0.29	2.88	0.92	2.50	21.78	7
BSOX146	4.00	6.00	0.58	-0.29	2.88	0.70	2.50	21.78	7
BSOX147	4.00	6.00	0.58	-0.29	2.88	1.45	2.00	16.41	7
BSOX148	4.00	6.00	0.58	-0.29	2.88	1.32	2.00	16.41	7
BSOX149	4.00	6.00	0.58	-0.29	2.88	1.14	1.50	10.76	7
BSOX150	4.00	6.00	0.58	-0.29	2.88	1.03	1.50	10.76	7
BSOR001	4.00	6.00	0.58	0.17	1.42	0.77	3.50	22.93	7
BSOR002	4.00	6.00	0.58	0.17	1.42	0.45	3.50	22.93	7
BSOR003	4.00	6.00	0.58	0.17	1.42	0.75	3.00	19.59	7
BSOR004	4.00	6.00	0.58	0.17	1.42	0.48	3.00	19.59	7
BSOR005	4.00	6.00	0.58	0.17	1.42	0.86	2.50	16.10	7

Table B-1 Continued.

Test case	Struct. Width	Struct. Length	Struct. Thick.	Struct. Clear.	Water Depth	Wave Height	Wave Period	Wave Length	Girders
BSOR006	4.00	6.00	0.58	0.17	1.42	0.64	2.50	16.10	7
BSOR007	4.00	6.00	0.58	0.17	1.42	0.71	2.00	12.53	7
BSOR008	4.00	6.00	0.58	0.17	1.42	0.59	2.00	12.53	7
BSOR009	4.00	6.00	0.58	0.17	1.42	0.76	1.50	8.82	7
BSOR010	4.00	6.00	0.58	0.17	1.42	0.79	1.50	8.82	7
BSOR011	4.00	6.00	0.58	0.00	1.58	1.01	3.50	24.24	7
BSOR012	4.00	6.00	0.58	0.00	1.58	0.64	3.50	24.24	7
BSOR013	4.00	6.00	0.58	0.00	1.58	0.75	3.00	20.64	7
BSOR014	4.00	6.00	0.58	0.00	1.58	0.55	3.00	20.64	7
BSOR015	4.00	6.00	0.58	0.00	1.58	1.04	2.50	16.92	7
BSOR016	4.00	6.00	0.58	0.00	1.58	0.71	2.50	16.92	7
BSOR017	4.00	6.00	0.58	0.00	1.58	0.66	2.00	13.12	7
BSOR018	4.00	6.00	0.58	0.00	1.58	0.55	2.00	13.12	7
BSOR019	4.00	6.00	0.58	0.00	1.58	0.76	1.50	9.17	7
BSOR020	4.00	6.00	0.58	0.00	1.58	0.84	1.50	9.17	7
BSOR021	4.00	6.00	0.58	-0.29	1.88	0.79	3.50	26.31	7
BSOR022	4.00	6.00	0.58	-0.29	1.88	0.64	3.50	26.31	7
BSOR023	4.00	6.00	0.58	-0.29	1.88	0.54	3.00	22.31	7
BSOR024	4.00	6.00	0.58	-0.29	1.88	0.42	3.00	22.31	7
BSOR025	4.00	6.00	0.58	-0.29	1.88	0.92	2.50	18.23	7
BSOR026	4.00	6.00	0.58	-0.29	1.88	0.87	2.50	18.23	7
BSOR027	4.00	6.00	0.58	-0.29	1.88	0.82	2.00	14.05	7
BSOR028	4.00	6.00	0.58	-0.29	1.88	0.56	2.00	14.05	7
BSOR029	4.00	6.00	0.58	-0.29	1.88	0.81	1.50	9.67	7
BSOR030	4.00	6.00	0.58	-0.29	1.88	0.77	1.50	9.67	7
BSOR031	4.00	6.00	0.58	-0.63	2.21	1.14	3.50	28.41	7
BSOR032	4.00	6.00	0.58	-0.63	2.21	0.65	3.50	28.41	7
BSOR033	4.00	6.00	0.58	-0.63	2.21	0.72	3.00	24.02	7
BSOR034	4.00	6.00	0.58	-0.63	2.21	0.53	3.00	24.02	7
BSOR035	4.00	6.00	0.58	-0.63	2.21	0.85	2.50	19.55	7
BSOR036	4.00	6.00	0.58	-0.63	2.21	0.69	2.50	19.55	7
BSOR037	4.00	6.00	0.58	-0.63	2.21	0.77	2.00	14.96	7
BSOR038	4.00	6.00	0.58	-0.63	2.21	0.77	2.00	14.96	7
BSOR039	4.00	6.00	0.58	-0.63	2.21	0.94	1.50	10.13	7
BSOR040	4.00	6.00	0.58	-0.63	2.21	0.90	1.50	10.13	7

Table B-1 Continued.

Test case	Struct. Width	Struct. Length	Struct. Thick.	Struct. Clear.	Water Depth	Wave Height	Wave Period	Wave Length	Girders
BSOR041	4.00	6.00	0.58	0.17	1.75	0.65	3.50	25.45	7
BSOR042	4.00	6.00	0.58	0.17	1.75	0.72	3.50	25.45	7
BSOR043	4.00	6.00	0.58	0.17	1.75	0.61	3.00	21.62	7
BSOR044	4.00	6.00	0.58	0.17	1.75	0.58	3.00	21.62	7
BSOR045	4.00	6.00	0.58	0.17	1.75	0.85	2.50	17.69	7
BSOR046	4.00	6.00	0.58	0.17	1.75	0.68	2.50	17.69	7
BSOR047	4.00	6.00	0.58	0.17	1.75	0.78	2.00	13.67	7
BSOR048	4.00	6.00	0.58	0.17	1.75	0.81	2.00	13.67	7
BSOR049	4.00	6.00	0.58	0.17	1.75	0.79	1.50	9.47	7
BSOR050	4.00	6.00	0.58	0.17	1.75	0.81	1.50	9.47	7
BSOR051	4.00	6.00	0.58	0.00	1.92	0.86	3.50	26.59	7
BSOR052	4.00	6.00	0.58	0.00	1.92	0.58	3.50	26.59	7
BSOR053	4.00	6.00	0.58	0.00	1.92	0.71	3.00	22.54	7
BSOR054	4.00	6.00	0.58	0.00	1.92	0.53	3.00	22.54	7
BSOR055	4.00	6.00	0.58	0.00	1.92	0.83	2.50	18.40	7
BSOR056	4.00	6.00	0.58	0.00	1.92	0.71	2.50	18.40	7
BSOR057	4.00	6.00	0.58	0.00	1.92	0.84	2.00	14.17	7
BSOR058	4.00	6.00	0.58	0.00	1.92	0.91	2.00	14.17	7
BSOR059	4.00	6.00	0.58	0.00	1.92	0.80	1.50	9.74	7
BSOR060	4.00	6.00	0.58	0.00	1.92	0.69	1.50	9.74	7
BSOR061	4.00	6.00	0.58	-0.29	2.21	0.80	3.50	28.41	7
BSOR062	4.00	6.00	0.58	-0.29	2.21	0.62	3.50	28.41	7
BSOR063	4.00	6.00	0.58	-0.29	2.21	0.64	3.00	24.02	7
BSOR064	4.00	6.00	0.58	-0.29	2.21	0.48	3.00	24.02	7
BSOR065	4.00	6.00	0.58	-0.29	2.21	0.88	2.50	19.55	7
BSOR066	4.00	6.00	0.58	-0.29	2.21	0.82	2.50	19.55	7
BSOR067	4.00	6.00	0.58	-0.29	2.21	1.12	2.00	14.96	7
BSOR068	4.00	6.00	0.58	-0.29	2.21	0.99	2.00	14.96	7
BSOR069	4.00	6.00	0.58	-0.29	2.21	0.91	1.50	10.13	7
BSOR070	4.00	6.00	0.58	-0.29	2.21	0.85	1.50	10.13	7
BSOR071	4.00	6.00	0.58	-0.63	2.54	1.06	3.50	30.31	7
BSOR072	4.00	6.00	0.58	-0.63	2.54	0.79	3.50	30.31	7
BSOR073	4.00	6.00	0.58	-0.63	2.54	0.94	3.00	25.57	7
BSOR074	4.00	6.00	0.58	-0.63	2.54	0.62	3.00	25.57	7
BSOR075	4.00	6.00	0.58	-0.63	2.54	0.80	2.50	20.73	7

Table B-1 Continued.

Test case	Struct. Width	Struct. Length	Struct. Thick.	Struct. Clear.	Water Depth	Wave Height	Wave Period	Wave Length	Girders
BSOR076	4.00	6.00	0.58	-0.63	2.54	0.65	2.50	20.73	7
BSOR077	4.00	6.00	0.58	-0.63	2.54	1.42	2.00	15.74	7
BSOR078	4.00	6.00	0.58	-0.63	2.54	0.96	2.00	15.74	7
BSOR079	4.00	6.00	0.58	-0.63	2.54	1.03	1.50	10.48	7
BSOR080	4.00	6.00	0.58	-0.63	2.54	1.02	1.50	10.48	7
BSOR081	4.00	6.00	0.58	-0.17	2.08	0.83	3.50	27.65	7
BSOR082	4.00	6.00	0.58	-0.17	2.08	0.53	3.50	27.65	7
BSOR083	4.00	6.00	0.58	-0.17	2.08	0.92	3.00	23.40	7
BSOR084	4.00	6.00	0.58	-0.17	2.08	0.52	3.00	23.40	7
BSOR085	4.00	6.00	0.58	-0.17	2.08	0.86	2.50	19.08	7
BSOR086	4.00	6.00	0.58	-0.17	2.08	0.64	2.50	19.08	7
BSOR087	4.00	6.00	0.58	-0.17	2.08	0.89	2.00	14.63	7
BSOR088	4.00	6.00	0.58	-0.17	2.08	0.75	2.00	14.63	7
BSOR089	4.00	6.00	0.58	-0.17	2.08	0.91	1.50	9.97	7
BSOR090	4.00	6.00	0.58	-0.17	2.08	0.81	1.50	9.97	7
BSOR091	4.00	6.00	0.58	0.00	2.25	1.07	3.50	28.66	7
BSOR092	4.00	6.00	0.58	0.00	2.25	0.71	3.50	28.66	7
BSOR093	4.00	6.00	0.58	0.00	2.25	0.87	3.00	24.23	7
BSOR094	4.00	6.00	0.58	0.00	2.25	0.60	3.00	24.23	7
BSOR095	4.00	6.00	0.58	0.00	2.25	1.01	2.50	19.71	7
BSOR096	4.00	6.00	0.58	0.00	2.25	0.86	2.50	19.71	7
BSOR097	4.00	6.00	0.58	0.00	2.25	1.04	2.00	15.06	7
BSOR098	4.00	6.00	0.58	0.00	2.25	0.90	2.00	15.06	7
BSOR099	4.00	6.00	0.58	0.00	2.25	1.01	1.50	10.18	7
BSOR100	4.00	6.00	0.58	0.00	2.25	0.96	1.50	10.18	7
BSOR101	4.00	6.00	0.58	-0.29	2.54	1.14	3.50	30.31	7
BSOR102	4.00	6.00	0.58	-0.29	2.54	0.69	3.50	30.31	7
BSOR103	4.00	6.00	0.58	-0.29	2.54	0.92	3.00	25.57	7
BSOR104	4.00	6.00	0.58	-0.29	2.54	0.60	3.00	25.57	7
BSOR105	4.00	6.00	0.58	-0.29	2.54	1.03	2.50	20.73	7
BSOR106	4.00	6.00	0.58	-0.29	2.54	0.72	2.50	20.73	7
BSOR107	4.00	6.00	0.58	-0.29	2.54	1.28	2.00	15.74	7
BSOR108	4.00	6.00	0.58	-0.29	2.54	1.02	2.00	15.74	7
BSOR109	4.00	6.00	0.58	-0.29	2.54	1.08	1.50	10.48	7
BSOR110	4.00	6.00	0.58	-0.29	2.54	1.07	1.50	10.48	7

Table B-1 Continued.

Test case	Struct. Width	Struct. Length	Struct. Thick.	Struct. Clear.	Water Depth	Wave Height	Wave Period	Wave Length	Girders
BSOR111	4.00	6.00	0.58	-0.63	2.88	1.11	3.50	32.05	7
BSOR112	4.00	6.00	0.58	-0.63	2.88	0.75	3.50	32.05	7
BSOR113	4.00	6.00	0.58	-0.63	2.88	1.05	3.00	26.97	7
BSOR114	4.00	6.00	0.58	-0.63	2.88	0.78	3.00	26.97	7
BSOR115	4.00	6.00	0.58	-0.63	2.88	0.94	2.50	21.78	7
BSOR116	4.00	6.00	0.58	-0.63	2.88	0.61	2.50	21.78	7
BSOR117	4.00	6.00	0.58	-0.63	2.88	1.56	2.00	16.41	7
BSOR118	4.00	6.00	0.58	-0.63	2.88	1.35	2.00	16.41	7
BSOR119	4.00	6.00	0.58	-0.63	2.88	1.28	1.50	10.76	7
BSOR120	4.00	6.00	0.58	-0.63	2.88	1.09	1.50	10.76	7
BSOR121	4.00	6.00	0.58	-0.17	2.42	0.85	3.50	29.62	7
BSOR122	4.00	6.00	0.58	-0.17	2.42	0.57	3.50	29.62	7
BSOR123	4.00	6.00	0.58	-0.17	2.42	0.82	3.00	25.01	7
BSOR124	4.00	6.00	0.58	-0.17	2.42	0.63	3.00	25.01	7
BSOR125	4.00	6.00	0.58	-0.17	2.42	1.05	2.50	20.30	7
BSOR126	4.00	6.00	0.58	-0.17	2.42	0.72	2.50	20.30	7
BSOR127	4.00	6.00	0.58	-0.17	2.42	1.19	2.00	15.46	7
BSOR128	4.00	6.00	0.58	-0.17	2.42	0.98	2.00	15.46	7
BSOR129	4.00	6.00	0.58	-0.17	2.42	1.10	1.50	10.36	7
BSOR130	4.00	6.00	0.58	-0.17	2.42	1.05	1.50	10.36	7
BSOR131	4.00	6.00	0.58	0.00	2.58	0.82	3.50	30.54	7
BSOR132	4.00	6.00	0.58	0.00	2.58	0.63	3.50	30.54	7
BSOR133	4.00	6.00	0.58	0.00	2.58	0.86	3.00	25.75	7
BSOR134	4.00	6.00	0.58	0.00	2.58	0.55	3.00	25.75	7
BSOR135	4.00	6.00	0.58	0.00	2.58	1.04	2.50	20.87	7
BSOR136	4.00	6.00	0.58	0.00	2.58	0.78	2.50	20.87	7
BSOR137	4.00	6.00	0.58	0.00	2.58	1.23	2.00	15.83	7
BSOR138	4.00	6.00	0.58	0.00	2.58	1.14	2.00	15.83	7
BSOR139	4.00	6.00	0.58	0.00	2.58	1.03	1.50	10.52	7
BSOR140	4.00	6.00	0.58	0.00	2.58	1.01	1.50	10.52	7
BSOR141	4.00	6.00	0.58	-0.29	2.88	1.20	3.50	32.05	7
BSOR142	4.00	6.00	0.58	-0.29	2.88	0.78	3.50	32.05	7
BSOR143	4.00	6.00	0.58	-0.29	2.88	1.04	3.00	26.97	7
BSOR144	4.00	6.00	0.58	-0.29	2.88	0.81	3.00	26.97	7
BSOR145	4.00	6.00	0.58	-0.29	2.88	0.97	2.50	21.78	7

Table B-1 Continued.

Test case	Struct. Width	Struct. Length	Struct. Thick.	Struct. Clear.	Water Depth	Wave Height	Wave Period	Wave Length	Girders
BSOR146	4.00	6.00	0.58	-0.29	2.88	0.63	2.50	21.78	7
BSOR147	4.00	6.00	0.58	-0.29	2.88	1.64	2.00	16.41	7
BSOR148	4.00	6.00	0.58	-0.29	2.88	1.39	2.00	16.41	7
BSOR149	4.00	6.00	0.58	-0.29	2.88	1.20	1.50	10.76	7
BSOR150	4.00	6.00	0.58	-0.29	2.88	1.11	1.50	10.76	7

Table B- 2 Significant force values for all physical model tests.

Test case	Vert. Max	Vert. Min	Quasi Max	Quasi Min	Horiz. Assoc.	Slam Max	Horiz. Max	Horiz. Min	Vert. Assoc.
SLAB001	6.36	-9.23	1.89	-4.95	0.00	5.36	0.29	-0.25	-0.01
SLAB002	89.03	-71.43	38.79	-38.44	3.01	51.89	4.19	-2.53	37.48
SLAB003	0.90	-0.37	0.67	-0.15	-0.04	0.44	0.12	-0.20	0.16
SLAB004	89.93	-56.77	35.29	-20.59	1.11	71.59	2.86	-2.28	-1.15
SLAB005	117.43	-89.31	50.76	-38.73	2.20	94.43	5.63	-4.11	10.15
SLAB006	120.32	-84.09	45.89	-38.49	7.12	80.20	7.26	-3.94	39.52
SLAB007	49.58	-60.21	16.68	-18.76	-0.32	55.15	1.59	-1.11	-2.43
SLAB008	75.19	-65.77	25.58	-22.20	0.98	62.31	2.77	-1.98	-8.18
SLAB009	30.59	-43.57	5.56	-13.89	-0.32	34.71	1.95	-1.40	-6.76
SLAB010	62.27	-74.67	21.07	-27.37	2.48	65.12	3.27	-2.10	20.50
SLAB011	112.02	-13.13	91.23	-12.12	2.27	23.81	2.65	-1.03	90.64
SLAB012	278.93	-30.52	156.82	-25.07	14.60	123.22	15.40	-5.79	155.07
SLAB013	77.52	-14.12	52.64	-10.51	0.64	32.10	1.38	-0.77	42.63
SLAB014	268.89	-92.24	118.86	-25.49	3.66	161.27	5.61	-2.53	97.13
SLAB015	174.19	-16.89	92.00	-14.27	1.42	93.33	2.86	-0.99	87.98
SLAB016	247.44	-43.01	136.88	-20.98	2.01	120.63	11.93	-2.74	127.88
SLAB017	187.22	-68.03	82.92	-18.78	1.83	111.87	5.05	-2.47	67.59
SLAB018	264.27	-69.93	127.51	-33.02	9.38	143.56	10.58	-3.40	102.01
SLAB019	163.26	-109.72	58.51	-42.43	3.38	138.32	5.19	-1.94	46.94
SLAB020	201.03	-93.90	78.13	-47.36	2.64	158.76	9.84	-2.82	63.43
SLAB021	97.34	-61.40	86.99	-62.87	3.59	14.39	4.46	-1.26	77.41
SLAB022	207.12	-109.54	180.16	-105.50	8.34	35.29	8.64	-2.19	166.29
SLAB023	77.68	-74.93	70.44	-76.84	2.87	19.46	3.45	-1.32	58.59
SLAB024	196.41	-115.00	169.17	-115.11	7.96	73.37	11.61	-2.22	114.16
SLAB025	112.87	-72.27	94.37	-74.94	4.95	31.92	7.02	-1.29	75.37
SLAB026	199.45	-113.92	165.85	-112.28	11.52	61.94	12.42	-2.79	156.05
SLAB027	126.02	-84.34	91.23	-87.05	4.91	51.75	8.01	-1.29	67.66
SLAB028	228.09	-113.37	166.81	-113.88	6.24	78.22	12.87	-1.98	139.64
SLAB029	254.94	-91.77	118.01	-108.17	11.04	156.54	14.48	-7.39	93.87
SLAB030	323.63	-103.00	144.67	-121.73	9.06	190.17	16.49	-4.24	122.88
SLAB031	97.95	-123.03	102.11	-121.49	4.23	13.81	4.31	-2.98	101.98
SLAB032	157.97	-243.14	169.26	-224.08	7.73	28.83	7.87	-4.83	161.16
SLAB033	100.39	-131.45	101.29	-137.31	4.24	43.33	6.64	-2.75	79.26
SLAB034	157.64	-214.51	168.21	-218.97	7.16	66.27	10.04	-4.09	109.58
SLAB035	87.08	-168.12	92.19	-174.72	4.81	49.50	6.30	-3.77	37.40

Table B-2 Continued.

Test case	Vert. Max	Vert. Min	Quasi Max	Quasi Min	Horiz. Assoc.	Slam Max	Horiz. Max	Horiz. Min	Vert. Assoc.
SLAB036	159.32	-256.25	163.96	-253.53	8.28	64.12	9.60	-3.82	90.48
SLAB037	112.06	-188.33	110.86	-198.52	6.75	74.36	9.08	-3.42	66.60
SLAB038	126.75	-275.23	122.79	-273.09	6.22	91.26	14.49	-5.12	58.46
SLAB039	162.23	-146.65	82.74	-156.04	8.80	149.24	13.00	-5.83	14.97
SLAB040	154.59	-282.78	96.29	-289.81	10.53	117.69	11.43	-4.66	18.90
SLAB041	34.95	-47.70	14.03	-18.61	0.12	28.25	1.67	-1.07	7.74
SLAB042	141.33	-78.47	97.03	-33.63	4.02	75.67	9.52	-3.67	90.95
SLAB043	7.77	-14.13	1.58	-5.78	-0.27	11.32	0.59	-0.47	-5.63
SLAB044	124.97	-77.11	67.17	-36.52	5.35	70.49	10.96	-8.56	65.86
SLAB045	53.35	-52.07	24.47	-20.02	0.70	48.07	1.94	-1.42	15.76
SLAB046	123.60	-85.46	61.31	-35.38	1.10	72.37	9.03	-7.93	15.23
SLAB047	64.33	-63.58	13.58	-19.43	0.13	60.06	2.23	-1.47	-9.73
SLAB048	138.08	-87.61	49.04	-39.08	4.62	105.33	12.04	-9.27	-2.68
SLAB049	40.34	-54.74	11.82	-17.11	-0.38	45.81	3.11	-2.54	3.81
SLAB050	87.03	-94.49	25.12	-32.54	0.62	75.07	4.08	-3.97	-11.74
SLAB051	93.01	-15.04	93.40	-13.16	1.01	27.11	1.48	-0.55	74.91
SLAB052	212.76	-24.14	177.10	-20.86	6.75	61.00	10.92	-1.67	167.17
SLAB053	150.11	-34.90	93.27	-31.39	1.91	73.22	7.44	-3.95	81.91
SLAB054	356.06	-44.58	176.92	-35.96	16.68	209.19	17.19	-6.41	147.05
SLAB055	155.15	-15.96	94.17	-13.88	4.37	61.65	5.24	-1.56	91.53
SLAB056	347.52	-32.50	175.07	-29.12	14.77	181.61	18.06	-7.62	171.18
SLAB057	238.48	-48.39	104.01	-31.34	5.14	135.89	10.35	-6.99	54.63
SLAB058	306.92	-42.63	170.49	-37.90	9.83	160.69	17.85	-14.34	126.43
SLAB059	177.94	-85.60	76.10	-48.09	3.27	104.66	12.70	-2.21	70.11
SLAB060	274.20	-127.38	96.86	-57.85	7.30	178.69	20.14	-9.75	76.84
SLAB061	111.37	-90.62	103.33	-93.11	3.87	14.01	5.12	-1.47	89.18
SLAB062	196.61	-111.42	194.63	-108.55	5.29	18.51	6.58	-2.62	92.79
SLAB063	129.52	-80.45	106.54	-82.81	6.17	37.86	8.66	-1.62	71.32
SLAB064	239.33	-128.49	196.36	-129.05	7.85	82.68	15.12	-2.74	133.89
SLAB065	132.14	-104.06	112.34	-104.50	4.84	38.54	8.14	-1.53	57.90
SLAB066	195.61	-109.96	158.61	-106.80	6.48	57.03	10.06	-1.94	141.62
SLAB067	205.02	-102.38	133.83	-99.06	7.54	87.45	11.70	-1.72	110.71
SLAB068	268.48	-119.65	179.22	-119.72	4.10	142.76	13.87	-1.86	121.94
SLAB069	272.77	-95.58	136.66	-117.94	11.82	157.09	17.19	-6.82	110.27
SLAB070	280.39	-118.84	158.04	-135.91	8.59	159.00	17.41	-6.05	126.42

Table B-2 Continued.

Test case	Vert. Max	Vert. Min	Quasi Max	Quasi Min	Horiz. Assoc.	Slam Max	Horiz. Max	Horiz. Min	Vert. Assoc.
SLAB071	110.19	-151.76	114.86	-159.72	4.39	16.30	4.53	-3.19	114.64
SLAB072	169.47	-271.91	178.14	-282.59	7.73	37.78	7.84	-5.43	177.80
SLAB073	101.01	-126.14	101.48	-126.93	4.75	20.79	6.64	-2.45	100.44
SLAB074	176.34	-217.57	183.54	-221.46	8.73	57.30	11.36	-4.39	133.08
SLAB075	103.88	-137.23	110.08	-141.93	4.70	40.00	7.21	-3.21	83.58
SLAB076	166.32	-256.25	167.62	-268.74	9.04	122.94	9.64	-4.33	100.91
SLAB077	91.96	-180.92	95.08	-183.32	5.21	61.32	8.48	-3.82	79.43
SLAB078	142.48	-292.15	130.98	-285.31	8.03	91.84	14.07	-5.08	97.93
SLAB079	193.86	-198.89	87.74	-208.58	11.53	148.77	11.79	-4.50	49.77
SLAB080	203.54	-263.36	122.74	-284.02	8.68	113.20	12.58	-4.79	36.14
SLAB081	83.75	-27.01	43.18	-14.48	0.13	43.09	2.32	-1.80	38.44
SLAB082	175.44	-21.52	116.59	-17.05	9.34	60.42	9.34	-2.98	115.15
SLAB083	68.12	-36.71	33.79	-22.95	1.63	47.67	2.57	-1.33	33.37
SLAB084	236.43	-62.90	152.91	-48.86	15.52	105.63	20.55	-15.71	76.87
SLAB085	84.79	-60.38	32.29	-18.61	1.85	60.99	4.37	-4.03	-4.71
SLAB086	160.00	-52.93	104.03	-36.39	4.87	73.28	13.11	-7.37	53.00
SLAB087	112.59	-103.32	66.57	-39.01	1.51	68.31	7.30	-5.64	42.87
SLAB088	169.92	-101.11	93.68	-50.27	4.64	109.67	17.60	-13.48	30.44
SLAB089	126.55	-133.63	32.38	-36.72	2.79	122.94	7.27	-4.05	3.08
SLAB090	141.69	-131.84	51.30	-48.18	5.92	125.89	9.81	-5.50	18.32
SLAB091	91.50	-11.86	89.69	-10.60	1.40	22.13	1.76	-0.91	88.99
SLAB092	244.19	-20.20	180.20	-17.24	8.78	72.54	12.21	-2.47	169.36
SLAB093	188.36	-28.66	96.14	-19.17	3.31	92.25	10.86	-4.00	86.34
SLAB094	362.14	-37.15	196.15	-29.85	15.12	178.98	16.14	-3.53	185.58
SLAB095	233.24	-43.38	108.21	-18.86	7.71	127.16	8.99	-3.63	104.91
SLAB096	305.83	-27.26	160.75	-27.13	13.06	146.65	15.97	-7.93	159.31
SLAB097	239.02	-49.16	113.20	-33.22	5.99	132.33	14.84	-9.17	89.21
SLAB098	351.81	-64.17	185.71	-40.48	12.00	175.10	22.78	-15.75	138.82
SLAB099	193.79	-107.95	73.12	-44.99	5.66	163.04	15.52	-6.83	68.90
SLAB100	278.17	-129.91	109.11	-57.34	11.21	184.56	18.63	-9.62	76.15
SLAB101	108.02	-104.97	107.09	-104.55	2.55	9.13	3.97	-1.56	76.70
SLAB102	268.11	-105.47	243.13	-98.90	5.05	43.77	7.12	-2.33	194.47
SLAB103	103.83	-75.34	93.28	-81.16	3.55	37.95	5.92	-1.52	64.51
SLAB104	238.22	-119.67	211.77	-117.70	11.30	63.92	13.27	-2.27	139.12
SLAB105	138.54	-89.42	114.56	-92.93	5.58	42.32	10.01	-1.67	78.11

Table B-2 Continued.

Test case	Vert. Max	Vert. Min	Quasi Max	Quasi Min	Horiz. Assoc.	Slam Max	Horiz. Max	Horiz. Min	Vert. Assoc.
SLAB106	245.02	-122.84	216.61	-114.46	6.15	63.92	11.99	-2.58	124.65
SLAB107	153.91	-99.94	123.43	-100.75	4.24	53.38	9.56	-1.37	92.49
SLAB108	267.70	-113.79	200.78	-122.51	4.98	99.70	14.74	-1.99	121.37
SLAB109	272.36	-95.57	124.85	-110.66	8.46	160.12	13.35	-3.23	104.81
SLAB110	404.65	-120.63	186.17	-136.89	16.89	237.33	22.46	-8.30	158.34
SLAB111	112.71	-148.42	116.28	-153.33	4.03	43.59	4.31	-2.96	111.67
SLAB112	185.50	-278.17	194.73	-285.52	7.47	34.85	7.63	-5.79	178.81
SLAB113	93.27	-124.22	97.64	-129.08	3.61	35.02	5.66	-3.09	82.78
SLAB114	164.89	-233.22	166.84	-237.30	8.06	55.78	11.33	-4.94	121.18
SLAB115	107.53	-150.62	102.57	-157.54	5.03	39.10	6.46	-3.23	85.45
SLAB116	157.85	-260.05	165.10	-261.03	7.42	61.94	11.26	-5.89	139.86
SLAB117	126.74	-242.63	112.51	-245.62	7.12	100.03	14.24	-4.59	54.11
SLAB118	190.47	-319.45	138.15	-318.29	10.11	89.27	14.59	-5.08	90.29
SLAB119	155.15	-168.00	75.88	-178.13	10.35	121.62	11.59	-4.72	56.32
SLAB120	217.87	-303.42	113.30	-317.88	9.47	143.79	11.39	-6.42	55.43
SLAB121	123.68	-20.72	61.92	-16.75	2.27	61.95	5.39	-6.12	34.99
SLAB122	156.44	-21.97	113.92	-21.35	4.84	42.85	9.55	-6.36	86.05
SLAB123	78.68	-54.77	46.16	-26.54	-2.51	59.32	9.21	-7.85	11.23
SLAB124	214.62	-55.21	142.33	-47.24	10.56	101.47	22.99	-22.22	89.18
SLAB125	108.46	-75.37	65.22	-25.10	3.74	54.74	14.99	-14.54	32.41
SLAB126	174.06	-84.81	97.90	-32.87	4.55	92.65	15.30	-13.82	86.18
SLAB127	146.35	-110.41	89.54	-49.02	9.46	75.47	18.99	-17.45	25.44
SLAB128	226.61	-112.81	115.44	-53.43	6.75	111.67	21.22	-17.43	19.43
SLAB129	146.58	-123.99	45.15	-49.56	2.46	120.04	11.20	-9.09	-14.58
SLAB130	166.82	-121.65	58.14	-50.23	2.93	133.93	24.99	-16.94	39.60
SLAB131	128.73	-36.48	105.17	-14.97	2.82	73.77	4.32	-2.51	96.48
SLAB132	232.05	-27.27	188.15	-22.86	7.00	76.31	16.60	-7.98	176.14
SLAB133	335.92	-27.14	144.24	-23.79	4.86	191.69	17.49	-11.82	92.52
SLAB134	354.55	-43.20	211.76	-36.67	14.79	176.56	25.32	-15.08	198.53
SLAB135	298.82	-45.00	123.29	-19.12	3.96	191.94	11.66	-7.72	91.69
SLAB136	347.50	-29.54	189.11	-27.70	13.81	167.61	20.38	-14.85	155.88
SLAB137	348.52	-54.24	165.27	-32.52	13.94	214.91	36.44	-29.15	116.59
SLAB138	380.72	-80.33	202.13	-42.06	16.37	187.65	37.17	-29.40	124.80
SLAB139	330.23	-142.30	112.77	-75.68	26.82	232.19	29.41	-17.70	95.15
SLAB140	293.63	-143.87	113.61	-67.28	7.02	196.04	24.80	-21.87	62.67

Table B-2 Continued.

Test case	Vert. Max	Vert. Min	Quasi Max	Quasi Min	Horiz. Assoc.	Slam Max	Horiz. Max	Horiz. Min	Vert. Assoc.
SLAB141	124.44	-108.81	120.89	-107.24	3.26	12.60	3.84	-1.89	79.57
SLAB142	209.24	-122.56	213.09	-117.04	5.74	56.86	7.37	-3.03	174.24
SLAB143	173.38	-101.26	144.93	-105.86	5.66	46.66	9.03	-2.60	93.28
SLAB144	267.10	-128.38	236.32	-126.98	10.25	64.79	11.21	-3.83	224.53
SLAB145	216.40	-120.77	175.76	-119.60	6.94	64.46	10.00	-2.39	91.96
SLAB146	330.97	-123.43	307.08	-112.32	4.02	88.28	15.53	-3.69	210.08
SLAB147	231.90	-108.27	169.05	-101.99	10.68	97.34	11.28	-2.72	111.33
SLAB148	266.94	-121.73	227.23	-120.70	8.91	81.38	16.27	-2.96	227.00
SLAB149	368.38	-116.13	164.04	-132.61	7.99	213.85	23.39	-5.14	139.51
SLAB150	394.33	-127.40	179.81	-147.15	24.18	240.93	24.31	-7.12	153.11
BSXX001	134.92	-41.48	70.82	-28.69	6.27	68.43	7.81	-5.16	52.94
BSXX002	61.48	-48.46	26.44	-18.96	0.85	41.84	2.50	-1.86	-1.08
BSXX003	89.51	-41.10	57.94	-21.99	2.39	56.17	4.51	-2.88	52.30
BSXX004	86.36	-69.87	25.92	-17.43	0.05	69.74	2.59	-1.67	-5.54
BSXX005	138.20	-67.07	66.81	-28.74	2.47	73.20	6.86	-3.85	44.72
BSXX006	71.77	-66.96	31.09	-21.07	0.97	58.52	1.75	-1.16	26.92
BSXX007	119.09	-72.80	44.83	-30.12	1.37	94.54	4.23	-2.35	9.31
BSXX008	48.98	-68.97	18.73	-20.93	-0.17	62.43	1.51	-0.70	12.17
BSXX009	99.50	-103.99	29.43	-33.37	1.54	103.36	3.24	-0.99	15.96
BSXX010	86.25	-110.98	33.00	-34.21	2.87	99.80	4.32	-0.70	30.22
BSXX011	159.69	-27.48	154.96	-22.24	4.43	44.78	7.31	-0.59	145.85
BSXX012	109.95	-23.35	108.34	-22.69	2.33	22.26	4.11	-0.28	104.14
BSXX013	237.74	-47.08	131.25	-27.99	2.88	117.73	6.48	-0.77	129.17
BSXX014	194.99	-35.16	112.81	-26.28	0.55	82.71	7.96	-2.35	110.68
BSXX015	199.44	-29.03	126.95	-25.57	10.99	73.17	12.56	-3.91	109.39
BSXX016	158.43	-16.14	106.70	-14.57	3.32	61.04	5.69	-0.46	106.69
BSXX017	245.97	-38.14	140.49	-27.34	6.08	105.79	9.49	-3.41	116.55
BSXX018	153.99	-33.11	95.21	-31.10	2.77	77.50	7.50	-3.10	77.12
BSXX019	214.95	-109.58	92.24	-52.19	4.78	156.77	9.55	-7.14	70.86
BSXX020	176.06	-104.03	70.77	-57.19	5.73	145.77	7.40	-6.58	34.73
BSXX021	129.01	-102.64	133.93	-100.61	6.00	19.71	6.01	-2.10	133.81
BSXX022	100.05	-88.19	105.14	-91.07	4.32	9.20	4.44	-1.59	103.30
BSXX023	126.55	-100.65	133.75	-105.63	6.76	9.58	6.92	-1.92	121.55
BSXX024	93.46	-82.65	97.92	-87.22	3.96	31.36	4.23	-1.65	95.88
BSXX025	125.82	-109.68	133.58	-109.65	6.08	18.58	6.36	-2.20	132.50

Table B-2 Continued.

Test case	Vert. Max	Vert. Min	Quasi Max	Quasi Min	Horiz. Assoc.	Slam Max	Horiz. Max	Horiz. Min	Vert. Assoc.
BSXX026	125.27	-98.56	131.38	-96.23	5.74	13.94	6.03	-1.71	126.12
BSXX027	123.60	-108.21	128.38	-114.52	5.98	69.10	6.52	-2.19	122.20
BSXX028	101.28	-96.50	104.32	-95.13	4.56	43.01	4.60	-1.82	104.17
BSXX029	113.19	-100.42	109.85	-114.34	5.63	40.75	7.00	-1.42	100.54
BSXX030	131.02	-105.68	102.51	-110.36	3.80	56.38	6.75	-1.73	78.77
BSXX031	113.66	-195.82	122.64	-196.29	5.92	26.39	6.64	-7.63	92.17
BSXX032	57.77	-121.53	60.98	-125.39	3.17	7.48	3.37	-4.86	60.71
BSXX033	101.49	-155.47	109.13	-159.52	5.30	26.89	8.89	-5.77	77.80
BSXX034	62.26	-115.82	66.00	-119.31	4.58	6.96	5.72	-4.10	62.52
BSXX035	91.19	-174.41	97.21	-174.71	6.24	24.44	6.79	-6.53	95.61
BSXX036	64.48	-118.10	68.84	-120.94	4.64	9.57	5.57	-5.07	56.17
BSXX037	75.88	-140.36	83.83	-145.21	7.01	11.96	7.82	-5.54	66.14
BSXX038	71.89	-137.08	73.34	-142.75	6.77	15.24	7.39	-5.60	73.30
BSXX039	84.16	-155.81	73.67	-161.32	7.33	41.94	9.73	-6.64	70.31
BSXX040	71.81	-159.46	63.39	-165.52	6.10	42.69	10.01	-5.46	10.94
BSXX041	94.83	-37.06	57.18	-28.74	1.91	71.81	8.08	-5.91	22.80
BSXX042	132.89	-66.22	76.84	-31.65	0.60	61.99	9.22	-4.80	66.87
BSXX043	121.57	-64.39	76.13	-24.19	-0.42	66.45	9.17	-7.75	45.35
BSXX044	100.00	-40.29	49.90	-30.01	2.12	53.25	5.29	-3.26	49.78
BSXX045	140.28	-30.15	83.29	-28.28	2.76	70.43	12.38	-8.08	45.99
BSXX046	123.77	-36.72	56.67	-25.00	5.12	80.58	7.58	-6.15	20.86
BSXX047	100.10	-60.39	64.75	-38.63	-2.14	47.96	7.86	-7.06	62.92
BSXX048	166.78	-79.09	81.67	-39.19	2.61	111.33	10.10	-7.73	25.03
BSXX049	129.69	-113.42	46.31	-45.23	8.08	103.87	8.94	-3.54	34.59
BSXX050	122.79	-106.53	40.89	-42.83	4.24	114.60	9.85	-6.58	39.83
BSXX051	167.44	-22.00	140.93	-20.80	4.83	46.55	6.19	-1.92	136.77
BSXX052	82.52	-17.20	84.16	-17.17	1.82	20.50	2.27	-0.56	66.90
BSXX053	253.15	-23.15	152.96	-20.27	1.85	108.31	9.72	-1.99	130.34
BSXX054	193.28	-33.66	102.66	-28.60	5.59	93.60	7.38	-1.49	80.39
BSXX055	244.98	-34.12	144.51	-27.83	10.67	102.49	13.06	-7.33	89.13
BSXX056	182.19	-21.42	121.45	-19.01	0.63	93.67	7.17	-2.61	78.57
BSXX057	271.43	-46.55	151.15	-33.48	11.03	134.08	14.54	-6.75	118.56
BSXX058	259.62	-38.70	158.63	-36.61	11.17	115.50	17.38	-7.44	123.38
BSXX059	213.21	-103.58	100.32	-61.77	11.42	116.12	14.32	-13.78	26.08
BSXX060	182.97	-117.07	84.13	-58.14	6.09	126.01	10.57	-11.07	-23.72

Table B-2 Continued.

Test case	Vert. Max	Vert. Min	Quasi Max	Quasi Min	Horiz. Assoc.	Slam Max	Horiz. Max	Horiz. Min	Vert. Assoc.
BSXX061	141.62	-127.70	149.92	-131.74	5.60	15.93	5.85	-2.90	134.34
BSXX062	100.51	-109.92	105.30	-113.58	4.05	7.67	4.24	-2.05	104.91
BSXX063	148.43	-112.38	150.42	-115.09	8.65	14.96	9.76	-2.90	150.34
BSXX064	115.34	-93.75	119.46	-98.72	5.16	6.54	5.86	-1.89	95.15
BSXX065	129.38	-110.99	137.32	-111.58	5.64	20.55	7.32	-2.16	137.21
BSXX066	113.64	-123.65	119.59	-119.05	5.52	17.15	5.88	-2.08	110.67
BSXX067	127.71	-108.81	133.25	-116.80	5.64	55.01	6.88	-2.12	131.49
BSXX068	123.85	-112.88	123.83	-117.35	5.67	31.28	6.96	-2.29	118.42
BSXX069	167.65	-116.24	125.06	-115.97	1.77	101.66	10.77	-2.61	123.05
BSXX070	132.61	-116.62	108.04	-117.80	1.76	138.29	9.37	-2.10	96.32
BSXX071	96.26	-192.71	102.54	-197.09	4.62	18.34	5.01	-7.55	84.25
BSXX072	77.57	-164.12	82.16	-168.23	3.63	22.65	4.15	-5.80	81.37
BSXX073	109.11	-150.47	118.66	-156.48	7.56	15.35	9.27	-7.26	113.03
BSXX074	84.41	-119.57	91.50	-123.39	5.83	10.05	6.18	-6.47	84.95
BSXX075	104.20	-165.16	107.65	-170.57	7.16	29.21	8.32	-7.09	71.08
BSXX076	60.22	-143.95	63.50	-146.50	5.12	9.90	5.28	-5.60	54.33
BSXX077	100.67	-160.93	108.48	-169.93	7.57	19.15	9.62	-6.99	92.83
BSXX078	74.13	-143.68	74.01	-148.57	6.07	17.06	6.98	-5.74	46.40
BSXX079	109.77	-169.50	79.41	-168.61	9.83	48.28	10.99	-7.23	11.72
BSXX080	106.09	-183.56	81.72	-182.53	11.62	48.59	12.78	-7.00	81.60
BSXX081	195.75	-34.74	133.72	-32.71	11.05	78.54	12.73	-4.68	116.79
BSXX082	70.43	-53.32	45.40	-28.09	-1.68	47.10	6.15	-4.81	10.68
BSXX083	176.96	-48.56	126.99	-45.89	-1.97	65.47	18.31	-7.91	116.02
BSXX084	72.41	-55.91	36.51	-26.54	-2.65	60.08	5.17	-3.29	0.16
BSXX085	158.70	-42.64	87.27	-31.21	4.15	84.56	15.73	-9.11	48.44
BSXX086	81.39	-49.16	52.22	-23.56	0.99	33.49	7.23	-6.20	21.36
BSXX087	173.22	-94.37	93.37	-47.49	6.79	82.74	18.03	-12.13	31.66
BSXX088	142.16	-101.27	61.76	-40.17	4.45	90.44	8.31	-6.94	44.27
BSXX089	133.49	-111.93	54.96	-48.88	8.30	102.56	14.86	-10.84	6.41
BSXX090	126.70	-105.43	44.00	-44.59	5.05	109.15	13.30	-7.84	27.40
BSXX091	141.61	-35.30	141.31	-29.82	4.79	43.28	5.66	-0.93	141.28
BSXX092	131.95	-23.21	108.42	-18.22	3.50	55.69	4.36	-1.95	96.70
BSXX093	307.08	-43.09	190.27	-37.54	13.08	118.90	28.54	-12.51	145.77
BSXX094	222.80	-30.35	116.05	-29.00	11.23	106.75	16.27	-6.50	104.00
BSXX095	264.39	-35.33	185.87	-30.94	4.27	114.17	20.34	-7.82	169.27

Table B-2 Continued.

Test case	Vert. Max	Vert. Min	Quasi Max	Quasi Min	Horiz. Assoc.	Slam Max	Horiz. Max	Horiz. Min	Vert. Assoc.
BSXX096	201.26	-23.84	140.56	-20.45	-4.46	81.59	20.63	-11.61	118.94
BSXX097	276.31	-86.00	174.55	-41.15	7.70	188.66	25.15	-14.04	138.28
BSXX098	266.12	-54.69	161.78	-42.35	6.60	121.64	19.97	-12.39	112.49
BSXX099	285.11	-125.14	123.57	-91.41	15.80	169.99	27.29	-22.48	8.37
BSXX100	242.84	-115.68	95.58	-68.51	5.30	154.38	17.77	-16.13	5.28
BSXX101	175.29	-120.69	183.47	-120.75	6.66	28.42	7.02	-3.18	171.81
BSXX102	103.20	-103.74	107.79	-102.90	3.23	13.42	3.56	-1.83	101.83
BSXX103	150.80	-123.21	161.51	-120.54	6.46	23.45	9.19	-2.70	155.43
BSXX104	106.55	-93.13	111.16	-97.33	4.31	6.01	5.76	-1.98	93.60
BSXX105	177.69	-115.82	169.13	-115.55	6.16	38.55	8.43	-2.47	169.13
BSXX106	108.15	-118.62	113.44	-115.25	4.99	19.38	5.74	-1.82	111.63
BSXX107	199.86	-124.50	166.11	-122.18	8.99	52.28	10.32	-2.35	157.83
BSXX108	115.77	-106.01	117.19	-110.05	5.63	25.22	7.21	-1.82	112.97
BSXX109	143.13	-125.98	135.11	-121.30	5.00	50.08	10.10	-2.11	94.09
BSXX110	145.11	-117.75	130.88	-115.14	4.42	67.82	11.09	-2.55	105.40
BSXX111	93.45	-201.42	98.49	-208.10	4.65	12.97	5.13	-6.41	85.64
BSXX112	69.03	-153.15	72.67	-158.23	3.79	9.19	3.86	-5.27	67.26
BSXX113	118.44	-160.08	128.92	-165.41	7.15	15.65	8.51	-8.54	102.07
BSXX114	82.36	-135.10	89.61	-139.91	5.40	12.11	6.01	-8.01	80.20
BSXX115	108.51	-184.00	118.89	-188.60	7.15	16.91	8.76	-7.17	117.30
BSXX116	67.11	-148.38	71.46	-151.44	4.88	36.07	5.65	-6.25	56.65
BSXX117	97.91	-184.60	107.68	-192.45	7.67	99.33	9.38	-7.72	92.77
BSXX118	93.13	-155.08	99.62	-161.44	7.67	57.17	8.86	-6.13	84.56
BSXX119	124.76	-200.37	82.62	-208.30	11.09	53.82	11.85	-7.53	82.45
BSXX120	69.96	-189.04	58.07	-192.60	8.21	33.69	10.96	-6.31	7.38
BSXX121	123.77	-21.11	93.86	-16.07	3.10	36.95	5.41	-1.87	78.98
BSXX122	73.78	-30.33	44.60	-18.38	1.62	43.08	1.62	-0.64	30.95
BSXX123	202.88	-93.87	144.04	-67.21	12.93	65.66	24.15	-12.46	85.19
BSXX124	145.12	-43.52	76.18	-34.16	6.62	81.61	6.70	-3.86	37.05
BSXX125	236.50	-47.20	110.34	-40.96	0.10	129.00	13.16	-6.37	98.45
BSXX126	111.44	-56.84	63.02	-30.36	2.81	54.29	8.81	-4.88	36.82
BSXX127	189.80	-82.06	153.22	-58.55	3.29	64.53	25.18	-14.94	68.02
BSXX128	179.99	-98.14	87.21	-44.56	-1.33	124.88	9.34	-5.86	58.55
BSXX129	170.61	-122.00	83.63	-75.50	7.78	107.08	16.04	-5.98	65.82
BSXX130	123.36	-116.44	40.07	-49.27	1.53	103.05	7.56	-2.73	35.57

Table B-2 Continued.

Test case	Vert. Max	Vert. Min	Quasi Max	Quasi Min	Horiz. Assoc.	Slam Max	Horiz. Max	Horiz. Min	Vert. Assoc.
BSXX131	156.94	-27.48	113.97	-24.19	1.49	63.28	6.82	-2.35	103.36
BSXX132	98.09	-23.44	87.02	-16.92	1.52	32.69	2.11	-1.15	51.97
BSXX133	252.65	-35.51	180.76	-30.54	3.87	118.93	20.90	-4.79	147.35
BSXX134	185.75	-27.90	111.05	-19.40	2.92	91.33	7.96	-1.14	107.32
BSXX135	323.82	-40.20	197.65	-33.63	8.38	162.04	18.21	-2.72	181.10
BSXX136	204.78	-30.05	144.32	-26.16	0.01	79.66	11.44	-2.33	124.15
BSXX137	263.28	-64.06	195.07	-43.73	8.21	133.14	24.92	-11.76	132.76
BSXX138	227.56	-41.23	155.15	-32.84	10.08	91.08	17.98	-5.52	116.58
BSXX139	232.95	-131.78	101.00	-98.38	7.32	156.40	16.89	-11.99	51.67
BSXX140	239.81	-113.45	101.66	-80.28	9.77	162.49	16.11	-9.27	49.62
BSXX141	157.31	-139.16	163.57	-128.47	4.93	30.32	5.73	-3.17	151.02
BSXX142	96.76	-108.32	101.26	-111.85	3.15	17.59	3.47	-2.06	97.37
BSXX143	151.40	-132.04	161.59	-129.04	7.52	61.08	8.27	-3.73	148.36
BSXX144	118.61	-103.97	125.71	-106.88	5.67	10.89	6.37	-2.02	110.58
BSXX145	193.91	-123.18	185.62	-122.81	8.59	37.36	8.66	-2.98	171.80
BSXX146	129.62	-114.88	137.14	-114.28	5.43	22.96	6.50	-2.26	135.92
BSXX147	241.72	-120.54	193.05	-116.77	9.05	141.25	12.81	-2.37	188.63
BSXX148	137.61	-114.09	127.32	-119.67	5.78	26.59	7.83	-2.41	127.28
BSXX149	133.33	-140.69	135.16	-135.91	2.92	46.70	12.29	-2.36	79.80
BSXX150	139.93	-131.57	115.09	-116.39	8.27	86.69	9.16	-2.45	94.81
BSOX001	35.53	-46.68	11.19	-16.90	-0.10	41.96	0.98	-0.61	10.90
BSOX002	87.13	-68.38	43.98	-40.46	5.95	45.62	6.18	-3.57	40.93
BSOX003	4.08	-0.74	4.47	-0.54	0.84	0.97	0.84	-0.13	4.47
BSOX004	52.09	-61.60	29.34	-22.32	-0.37	42.31	2.61	-1.82	-6.89
BSOX005	43.59	-38.98	10.82	-19.95	0.82	33.56	2.02	-1.27	8.39
BSOX006	94.08	-87.93	36.08	-34.69	1.52	72.79	4.69	-2.72	-2.82
BSOX007	7.06	-9.95	2.57	-5.86	0.22	5.42	0.33	-0.09	-4.54
BSOX008	53.97	-52.31	11.83	-16.00	0.98	45.69	1.86	-1.56	-5.31
BSOX009	35.51	-52.63	6.31	-13.04	0.87	39.28	1.52	-0.83	3.05
BSOX010	69.66	-77.92	15.66	-26.36	1.64	69.72	4.06	-1.62	10.03
BSOX011	107.40	-7.60	82.45	-6.06	1.63	29.16	1.64	-0.52	80.53
BSOX012	245.83	-30.70	163.33	-18.72	14.30	114.30	15.21	-3.56	130.64
BSOX013	81.52	-10.91	68.17	-7.69	0.72	37.33	1.38	-0.70	38.15
BSOX014	307.99	-52.60	139.58	-20.85	4.10	224.03	10.66	-3.04	115.45
BSOX015	177.28	-13.11	85.81	-8.02	1.60	91.54	2.47	-1.48	73.79

Table B-2 Continued.

Test case	Vert. Max	Vert. Min	Quasi Max	Quasi Min	Horiz. Assoc.	Slam Max	Horiz. Max	Horiz. Min	Vert. Assoc.
BSOX016	255.79	-22.69	144.89	-18.27	9.50	118.39	13.12	-4.95	144.29
BSOX017	166.11	-60.59	71.96	-21.65	1.10	104.75	3.06	-1.20	52.52
BSOX018	237.50	-92.43	125.30	-48.93	8.87	126.87	9.35	-2.47	112.28
BSOX019	165.28	-76.69	58.10	-45.13	5.01	112.61	5.01	-1.46	52.67
BSOX020	241.31	-108.40	89.48	-55.13	13.74	174.09	15.51	-3.95	74.32
BSOX021	103.13	-53.70	92.68	-54.82	4.50	13.15	5.52	-1.46	76.73
BSOX022	205.82	-112.45	170.90	-111.16	1.14	54.95	9.41	-1.74	136.18
BSOX023	94.48	-68.69	82.11	-70.97	4.48	15.42	4.89	-1.35	81.33
BSOX024	205.47	-128.16	153.74	-134.28	6.84	188.32	14.25	-2.04	113.34
BSOX025	105.72	-97.54	94.10	-100.93	5.09	21.00	6.45	-1.37	66.61
BSOX026	176.52	-124.23	147.68	-120.96	8.07	55.91	11.39	-1.79	80.88
BSOX027	106.92	-80.03	93.53	-82.64	5.62	40.43	7.91	-1.25	62.75
BSOX028	197.51	-119.26	152.66	-114.20	4.09	72.14	11.20	-1.53	114.89
BSOX029	161.74	-95.38	87.38	-105.50	11.50	88.05	12.36	-2.70	71.06
BSOX030	253.49	-106.63	143.52	-118.58	9.03	140.20	16.61	-5.58	101.33
BSOX031	68.44	-127.77	72.87	-130.12	2.56	11.62	2.93	-3.18	67.01
BSOX032	112.38	-210.91	121.09	-216.83	3.91	25.07	4.31	-5.29	115.78
BSOX033	69.06	-120.98	73.67	-126.27	2.40	73.73	4.58	-2.66	61.51
BSOX034	144.90	-163.50	150.49	-168.13	4.04	45.25	7.57	-5.33	150.43
BSOX035	83.51	-148.98	86.57	-145.39	3.71	25.27	4.05	-3.82	82.46
BSOX036	127.52	-202.09	130.01	-209.57	5.31	41.97	6.33	-5.14	121.93
BSOX037	79.89	-151.90	82.20	-149.38	4.21	35.98	5.36	-3.66	74.36
BSOX038	145.38	-165.69	120.47	-176.15	4.50	48.79	7.50	-4.65	93.31
BSOX039	155.11	-130.07	70.60	-142.99	10.88	123.14	10.88	-4.60	31.42
BSOX040	221.10	-185.93	101.62	-205.16	14.08	166.09	15.79	-5.45	62.62
BSOX041	27.18	-32.30	14.21	-16.65	0.09	24.34	1.32	-1.09	-2.44
BSOX042	164.90	-52.41	85.45	-34.09	10.62	81.61	12.42	-5.63	81.67
BSOX043	23.76	-23.27	4.09	-10.43	-0.29	23.69	0.76	-0.61	-10.14
BSOX044	181.01	-85.83	78.19	-42.62	4.86	103.17	13.46	-8.79	45.88
BSOX045	48.19	-36.60	19.28	-19.58	0.35	35.30	1.78	-0.77	17.52
BSOX046	141.37	-81.52	73.78	-40.71	4.18	92.74	10.29	-8.14	13.47
BSOX047	53.84	-56.25	15.71	-18.65	0.43	55.56	1.21	-1.16	2.76
BSOX048	121.06	-97.41	42.23	-37.98	1.28	103.97	7.56	-6.39	-2.47
BSOX049	72.01	-81.66	12.73	-25.57	-1.19	82.29	4.76	-2.44	-7.47
BSOX050	122.90	-107.85	29.57	-37.04	1.69	103.31	4.62	-2.02	-21.32

Table B-2 Continued.

Test case	Vert. Max	Vert. Min	Quasi Max	Quasi Min	Horiz. Assoc.	Slam Max	Horiz. Max	Horiz. Min	Vert. Assoc.
BSOX051	122.97	-10.05	87.89	-9.80	1.08	39.81	4.41	-1.25	84.60
BSOX052	329.96	-35.65	187.71	-30.96	15.56	144.15	19.32	-3.04	183.27
BSOX053	126.61	-37.88	68.54	-16.90	0.05	59.01	3.36	-1.19	65.16
BSOX054	242.46	-25.80	137.23	-20.55	7.04	116.28	8.68	-2.63	119.34
BSOX055	153.61	-52.75	95.46	-21.91	0.65	71.69	6.58	-4.31	65.73
BSOX056	238.45	-32.27	154.44	-26.68	7.11	84.94	16.76	-11.38	128.03
BSOX057	177.84	-66.96	96.12	-26.69	3.26	111.26	11.36	-6.88	79.02
BSOX058	323.21	-60.36	160.29	-40.79	8.34	169.97	15.25	-8.97	146.20
BSOX059	224.70	-129.11	88.49	-42.38	6.44	159.04	12.53	-7.10	77.57
BSOX060	259.98	-119.12	102.14	-57.57	10.33	170.45	17.21	-8.74	82.03
BSOX061	102.68	-82.57	98.16	-85.56	3.35	8.65	4.34	-1.24	85.87
BSOX062	192.49	-114.18	198.10	-109.90	4.34	26.23	7.30	-2.23	161.08
BSOX063	88.77	-88.59	82.09	-92.68	2.51	17.47	5.30	-1.60	56.79
BSOX064	205.98	-121.29	188.74	-120.24	6.04	64.95	13.52	-2.74	142.30
BSOX065	119.12	-103.84	104.62	-112.82	3.53	90.94	8.66	-1.28	-11.88
BSOX066	209.04	-113.12	176.50	-110.40	5.32	168.34	10.25	-1.95	29.87
BSOX067	159.81	-105.05	131.98	-107.49	4.97	57.80	9.37	-1.95	82.05
BSOX068	253.50	-112.28	182.10	-108.18	6.34	101.44	11.69	-2.02	143.45
BSOX069	293.58	-110.26	160.42	-118.12	7.59	155.75	18.27	-5.85	128.37
BSOX070	286.83	-106.16	154.46	-119.52	12.36	160.86	18.71	-5.55	115.99
BSOX071	79.21	-151.16	84.07	-157.24	3.16	32.30	3.56	-3.08	84.07
BSOX072	131.99	-260.43	139.66	-244.67	4.59	26.22	5.29	-6.66	125.54
BSOX073	91.20	-108.65	94.03	-112.90	5.07	39.11	7.27	-2.44	58.58
BSOX074	130.73	-185.82	142.15	-190.07	7.38	49.90	9.18	-5.63	134.92
BSOX075	96.85	-132.98	99.34	-136.19	4.16	29.59	5.94	-3.58	89.97
BSOX076	137.17	-195.38	134.27	-198.94	5.86	78.72	9.25	-5.46	111.91
BSOX077	88.12	-166.91	84.49	-168.92	5.52	57.48	7.21	-3.83	74.03
BSOX078	133.87	-191.76	113.53	-198.26	5.33	65.70	8.35	-4.98	24.66
BSOX079	139.97	-150.09	60.40	-160.69	9.44	120.75	10.07	-4.39	8.89
BSOX080	229.86	-189.42	118.20	-206.28	10.64	250.51	12.25	-5.86	-28.56
BSOX081	39.69	-65.73	23.13	-19.71	-0.37	40.91	2.14	-1.89	2.10
BSOX082	202.87	-45.06	116.74	-37.69	14.07	88.12	15.76	-6.77	72.29
BSOX083	62.29	-39.41	19.65	-16.28	-0.06	54.05	1.16	-0.90	19.10
BSOX084	111.11	-66.89	68.67	-28.15	-0.20	60.94	6.05	-4.66	40.85
BSOX085	90.07	-68.06	44.04	-25.39	-0.79	46.28	5.83	-4.94	-7.68

Table B-2 Continued.

Test case	Vert. Max	Vert. Min	Quasi Max	Quasi Min	Horiz. Assoc.	Slam Max	Horiz. Max	Horiz. Min	Vert. Assoc.
BSOX086	159.24	-80.02	93.53	-38.45	3.37	90.17	12.77	-10.09	10.02
BSOX087	101.87	-81.55	39.68	-33.48	-0.14	65.20	3.91	-3.66	-0.27
BSOX088	165.76	-109.50	80.33	-49.99	-1.29	87.10	13.77	-12.18	20.28
BSOX089	127.20	-127.76	38.61	-43.27	3.96	114.82	10.16	-5.18	32.72
BSOX090	162.04	-130.97	51.37	-44.46	15.15	122.59	18.41	-4.97	47.23
BSOX091	93.30	-13.49	92.99	-11.82	-0.65	21.04	2.28	-0.79	74.54
BSOX092	225.25	-32.02	183.24	-24.17	5.30	73.69	14.14	-1.86	176.48
BSOX093	248.82	-36.99	110.01	-25.73	4.46	139.05	10.59	-4.57	94.17
BSOX094	359.37	-45.46	183.71	-34.25	9.70	180.25	16.14	-9.43	152.41
BSOX095	185.23	-28.16	96.99	-15.24	1.60	107.46	8.67	-5.00	77.08
BSOX096	277.13	-36.37	165.48	-31.97	11.78	134.17	17.23	-9.95	139.20
BSOX097	237.08	-63.86	126.10	-30.41	6.32	142.98	11.24	-7.39	72.34
BSOX098	343.61	-69.63	186.05	-49.61	12.16	170.41	24.91	-18.67	132.58
BSOX099	200.77	-97.24	80.85	-48.20	4.44	156.37	13.85	-7.84	72.91
BSOX100	268.86	-167.31	113.32	-68.95	5.24	203.30	17.90	-11.36	90.44
BSOX101	111.58	-114.26	106.87	-113.91	3.00	23.62	4.05	-1.68	81.29
BSOX102	216.26	-121.51	220.46	-114.87	5.74	32.23	7.55	-2.51	97.24
BSOX103	133.32	-118.82	107.79	-123.90	5.09	43.53	10.55	-1.87	69.94
BSOX104	228.12	-133.81	189.30	-129.68	7.51	78.90	13.92	-3.31	133.77
BSOX105	120.20	-90.88	106.16	-93.65	4.67	30.06	7.91	-1.37	69.70
BSOX106	271.00	-121.92	216.83	-118.48	11.89	89.81	13.77	-2.33	176.14
BSOX107	150.45	-111.07	126.19	-110.44	4.52	60.26	9.97	-1.84	78.04
BSOX108	280.22	-123.42	200.32	-122.31	8.89	100.44	13.90	-2.01	138.78
BSOX109	220.79	-95.36	112.11	-109.60	12.44	123.39	15.45	-4.42	92.33
BSOX110	286.69	-131.59	156.28	-133.19	14.97	153.36	20.78	-8.13	118.30
BSOX111	70.02	-166.98	73.93	-171.45	3.04	21.68	3.17	-3.65	68.33
BSOX112	128.78	-267.57	135.65	-269.83	4.71	37.04	5.00	-6.19	104.12
BSOX113	77.87	-137.28	84.05	-137.41	4.03	21.71	4.52	-3.33	83.81
BSOX114	151.22	-193.19	150.64	-197.25	7.42	39.83	8.64	-6.44	131.63
BSOX115	91.27	-148.64	96.40	-150.90	4.07	15.28	5.19	-3.70	79.18
BSOX116	138.39	-219.40	142.25	-228.07	7.29	39.31	8.13	-6.02	113.82
BSOX117	91.83	-157.66	85.89	-163.39	5.04	54.03	6.61	-4.29	80.47
BSOX118	185.32	-200.80	139.38	-210.45	6.25	77.18	10.71	-5.44	74.71
BSOX119	143.10	-132.12	79.57	-148.73	8.70	104.81	9.31	-4.16	33.35
BSOX120	196.64	-217.03	99.44	-203.88	10.53	144.53	11.55	-5.89	60.17

Table B-2 Continued.

Test case	Vert. Max	Vert. Min	Quasi Max	Quasi Min	Horiz. Assoc.	Slam Max	Horiz. Max	Horiz. Min	Vert. Assoc.
BSOX121	60.28	-18.46	36.40	-12.92	0.08	36.73	2.17	-2.04	15.11
BSOX122	144.51	-20.48	114.91	-19.86	1.99	77.85	8.74	-6.33	70.44
BSOX123	104.74	-44.20	62.36	-25.62	5.88	48.28	12.14	-11.28	22.35
BSOX124	219.76	-62.57	165.94	-44.91	6.99	91.45	26.46	-21.64	104.92
BSOX125	151.60	-84.92	69.22	-36.35	7.30	82.59	18.47	-16.32	-21.46
BSOX126	249.92	-110.27	126.28	-35.26	5.79	129.29	19.27	-12.35	66.37
BSOX127	114.69	-75.28	62.51	-30.75	0.44	56.68	14.99	-12.73	56.19
BSOX128	249.27	-123.02	140.41	-59.83	5.56	142.08	25.43	-23.22	69.59
BSOX129	156.02	-140.13	38.74	-43.44	4.40	143.66	12.48	-6.42	31.77
BSOX130	190.69	-138.14	70.27	-64.60	9.39	148.02	21.42	-13.64	59.74
BSOX131	96.52	-13.52	98.29	-10.80	0.94	22.07	2.52	-1.59	73.29
BSOX132	217.10	-30.97	187.12	-25.64	-3.36	80.05	11.75	-4.34	165.98
BSOX133	224.29	-30.99	105.60	-21.89	6.87	123.28	10.74	-6.62	91.95
BSOX134	382.22	-56.18	225.60	-46.45	18.01	202.44	31.56	-16.55	215.83
BSOX135	255.87	-55.32	122.96	-21.23	3.08	136.72	7.69	-9.40	102.33
BSOX136	370.92	-32.90	206.91	-34.84	11.47	164.51	14.14	-11.03	190.74
BSOX137	247.25	-47.01	151.80	-34.04	0.44	124.80	12.43	-17.50	146.71
BSOX138	308.24	-106.59	199.37	-69.58	12.20	147.08	36.91	-28.92	125.24
BSOX139	248.67	-113.60	92.52	-50.32	4.73	184.61	19.18	-19.04	26.72
BSOX140	320.25	-185.97	101.96	-101.18	7.79	228.53	19.90	-15.37	56.90
BSOX141	121.05	-103.38	121.37	-107.84	2.66	10.71	3.61	-2.11	105.76
BSOX142	254.24	-131.32	264.63	-123.86	4.25	83.98	8.74	-3.69	211.65
BSOX143	156.00	-98.45	132.86	-100.65	5.00	46.49	11.00	-2.04	83.85
BSOX144	328.29	-121.01	240.89	-119.34	11.24	146.72	14.36	-3.01	171.70
BSOX145	187.29	-111.08	160.85	-108.33	4.58	45.38	9.57	-2.20	121.31
BSOX146	367.99	-125.59	273.19	-117.01	9.60	97.84	14.46	-3.56	187.94
BSOX147	202.82	-109.19	163.02	-104.50	5.38	60.81	9.92	-1.83	107.71
BSOX148	275.27	-115.39	219.69	-111.61	8.01	108.08	14.20	-3.50	134.30
BSOX149	299.36	-118.47	140.55	-127.36	17.76	175.89	25.11	-8.08	116.43
BSOX150	296.18	-114.75	189.44	-114.66	15.84	167.78	21.04	-4.59	131.15
BSOR001	6.36	-9.23	1.89	-4.95	0.00	5.36	0.29	-0.25	-0.01
BSOR002	89.03	-71.43	38.79	-38.44	3.01	51.89	4.19	-2.53	37.48
BSOR003	0.90	-0.37	0.67	-0.15	-0.04	0.44	0.12	-0.20	0.16
BSOR004	89.93	-56.77	35.29	-20.59	1.11	71.59	2.86	-2.28	-1.15
BSOR005	117.43	-89.31	50.76	-38.73	2.20	94.43	5.63	-4.11	10.15

Table B-2 Continued.

Test case	Vert. Max	Vert. Min	Quasi Max	Quasi Min	Horiz. Assoc.	Slam Max	Horiz. Max	Horiz. Min	Vert. Assoc.
BSOR006	120.32	-84.09	45.89	-38.49	7.12	80.20	7.26	-3.94	39.52
BSOR007	49.58	-60.21	16.68	-18.76	-0.32	55.15	1.59	-1.11	-2.43
BSOR008	75.19	-65.77	25.58	-22.20	0.98	62.31	2.77	-1.98	-8.18
BSOR009	30.59	-43.57	5.56	-13.89	-0.32	34.71	1.95	-1.40	-6.76
BSOR010	62.27	-74.67	21.07	-27.37	2.48	65.12	3.27	-2.10	20.50
BSOR011	112.02	-13.13	91.23	-12.12	2.27	23.81	2.65	-1.03	90.64
BSOR012	278.93	-30.52	156.82	-25.07	14.60	123.22	15.40	-5.79	155.07
BSOR013	77.52	-14.12	52.64	-10.51	0.64	32.10	1.38	-0.77	42.63
BSOR014	268.89	-92.24	118.86	-25.49	3.66	161.27	5.61	-2.53	97.13
BSOR015	174.19	-16.89	92.00	-14.27	1.42	93.33	2.86	-0.99	87.98
BSOR016	247.44	-43.01	136.88	-20.98	2.01	120.63	11.93	-2.74	127.88
BSOR017	187.22	-68.03	82.92	-18.78	1.83	111.87	5.05	-2.47	67.59
BSOR018	264.27	-69.93	127.51	-33.02	9.38	143.56	10.58	-3.40	102.01
BSOR019	163.26	-109.72	58.51	-42.43	3.38	138.32	5.19	-1.94	46.94
BSOR020	201.03	-93.90	78.13	-47.36	2.64	158.76	9.84	-2.82	63.43
BSOR021	97.34	-61.40	86.99	-62.87	3.59	14.39	4.46	-1.26	77.41
BSOR022	207.12	-109.54	180.16	-105.50	8.34	35.29	8.64	-2.19	166.29
BSOR023	77.68	-74.93	70.44	-76.84	2.87	19.46	3.45	-1.32	58.59
BSOR024	196.41	-115.00	169.17	-115.11	7.96	73.37	11.61	-2.22	114.16
BSOR025	112.87	-72.27	94.37	-74.94	4.95	31.92	7.02	-1.29	75.37
BSOR026	199.45	-113.92	165.85	-112.28	11.52	61.94	12.42	-2.79	156.05
BSOR027	126.02	-84.34	91.23	-87.05	4.91	51.75	8.01	-1.29	67.66
BSOR028	228.09	-113.37	166.81	-113.88	6.24	78.22	12.87	-1.98	139.64
BSOR029	254.94	-91.77	118.01	-108.17	11.04	156.54	14.48	-7.39	93.87
BSOR030	323.63	-103.00	144.67	-121.73	9.06	190.17	16.49	-4.24	122.88
BSOR031	97.95	-123.03	102.11	-121.49	4.23	13.81	4.31	-2.98	101.98
BSOR032	157.97	-243.14	169.26	-224.08	7.73	28.83	7.87	-4.83	161.16
BSOR033	100.39	-131.45	101.29	-137.31	4.24	43.33	6.64	-2.75	79.26
BSOR034	157.64	-214.51	168.21	-218.97	7.16	66.27	10.04	-4.09	109.58
BSOR035	87.08	-168.12	92.19	-174.72	4.81	49.50	6.30	-3.77	37.40
BSOR036	159.32	-256.25	163.96	-253.53	8.28	64.12	9.60	-3.82	90.48
BSOR037	112.06	-188.33	110.86	-198.52	6.75	74.36	9.08	-3.42	66.60
BSOR038	126.75	-275.23	122.79	-273.09	6.22	91.26	14.49	-5.12	58.46
BSOR039	162.23	-146.65	82.74	-156.04	8.80	149.24	13.00	-5.83	14.97
BSOR040	154.59	-282.78	96.29	-289.81	10.53	117.69	11.43	-4.66	18.90

Table B-2 Continued.

Test case	Vert. Max	Vert. Min	Quasi Max	Quasi Min	Horiz. Assoc.	Slam Max	Horiz. Max	Horiz. Min	Vert. Assoc.
BSOR041	34.95	-47.70	14.03	-18.61	0.12	28.25	1.67	-1.07	7.74
BSOR042	141.33	-78.47	97.03	-33.63	4.02	75.67	9.52	-3.67	90.95
BSOR043	7.77	-14.13	1.58	-5.78	-0.27	11.32	0.59	-0.47	-5.63
BSOR044	124.97	-77.11	67.17	-36.52	5.35	70.49	10.96	-8.56	65.86
BSOR045	53.35	-52.07	24.47	-20.02	0.70	48.07	1.94	-1.42	15.76
BSOR046	123.60	-85.46	61.31	-35.38	1.10	72.37	9.03	-7.93	15.23
BSOR047	64.33	-63.58	13.58	-19.43	0.13	60.06	2.23	-1.47	-9.73
BSOR048	138.08	-87.61	49.04	-39.08	4.62	105.33	12.04	-9.27	-2.68
BSOR049	40.34	-54.74	11.82	-17.11	-0.38	45.81	3.11	-2.54	3.81
BSOR050	87.03	-94.49	25.12	-32.54	0.62	75.07	4.08	-3.97	-11.74
BSOR051	93.01	-15.04	93.40	-13.16	1.01	27.11	1.48	-0.55	74.91
BSOR052	212.76	-24.14	177.10	-20.86	6.75	61.00	10.92	-1.67	167.17
BSOR053	150.11	-34.90	93.27	-31.39	1.91	73.22	7.44	-3.95	81.91
BSOR054	356.06	-44.58	176.92	-35.96	16.68	209.19	17.19	-6.41	147.05
BSOR055	155.15	-15.96	94.17	-13.88	4.37	61.65	5.24	-1.56	91.53
BSOR056	347.52	-32.50	175.07	-29.12	14.77	181.61	18.06	-7.62	171.18
BSOR057	238.48	-48.39	104.01	-31.34	5.14	135.89	10.35	-6.99	54.63
BSOR058	306.92	-42.63	170.49	-37.90	9.83	160.69	17.85	-14.34	126.43
BSOR059	177.94	-85.60	76.10	-48.09	3.27	104.66	12.70	-2.21	70.11
BSOR060	274.20	-127.38	96.86	-57.85	7.30	178.69	20.14	-9.75	76.84
BSOR061	111.37	-90.62	103.33	-93.11	3.87	14.01	5.12	-1.47	89.18
BSOR062	196.61	-111.42	194.63	-108.55	5.29	18.51	6.58	-2.62	92.79
BSOR063	129.52	-80.45	106.54	-82.81	6.17	37.86	8.66	-1.62	71.32
BSOR064	239.33	-128.49	196.36	-129.05	7.85	82.68	15.12	-2.74	133.89
BSOR065	132.14	-104.06	112.34	-104.50	4.84	38.54	8.14	-1.53	57.90
BSOR066	195.61	-109.96	158.61	-106.80	6.48	57.03	10.06	-1.94	141.62
BSOR067	205.02	-102.38	133.83	-99.06	7.54	87.45	11.70	-1.72	110.71
BSOR068	268.48	-119.65	179.22	-119.72	4.10	142.76	13.87	-1.86	121.94
BSOR069	272.77	-95.58	136.66	-117.94	11.82	157.09	17.19	-6.82	110.27
BSOR070	280.39	-118.84	158.04	-135.91	8.59	159.00	17.41	-6.05	126.42
BSOR071	110.19	-151.76	114.86	-159.72	4.39	16.30	4.53	-3.19	114.64
BSOR072	169.47	-271.91	178.14	-282.59	7.73	37.78	7.84	-5.43	177.80
BSOR073	101.01	-126.14	101.48	-126.93	4.75	20.79	6.64	-2.45	100.44
BSOR074	176.34	-217.57	183.54	-221.46	8.73	57.30	11.36	-4.39	133.08
BSOR075	103.88	-137.23	110.08	-141.93	4.70	40.00	7.21	-3.21	83.58

Table B-2 Continued.

Test case	Vert. Max	Vert. Min	Quasi Max	Quasi Min	Horiz. Assoc.	Slam Max	Horiz. Max	Horiz. Min	Vert. Assoc.
BSOR076	166.32	-256.25	167.62	-268.74	9.04	122.94	9.64	-4.33	100.91
BSOR077	91.96	-180.92	95.08	-183.32	5.21	61.32	8.48	-3.82	79.43
BSOR078	142.48	-292.15	130.98	-285.31	8.03	91.84	14.07	-5.08	97.93
BSOR079	193.86	-198.89	87.74	-208.58	11.53	148.77	11.79	-4.50	49.77
BSOR080	203.54	-263.36	122.74	-284.02	8.68	113.20	12.58	-4.79	36.14
BSOR081	83.75	-27.01	43.18	-14.48	0.13	43.09	2.32	-1.80	38.44
BSOR082	175.44	-21.52	116.59	-17.05	9.34	60.42	9.34	-2.98	115.15
BSOR083	68.12	-36.71	33.79	-22.95	1.63	47.67	2.57	-1.33	33.37
BSOR084	236.43	-62.90	152.91	-48.86	15.52	105.63	20.55	-15.71	76.87
BSOR085	84.79	-60.38	32.29	-18.61	1.85	60.99	4.37	-4.03	-4.71
BSOR086	160.00	-52.93	104.03	-36.39	4.87	73.28	13.11	-7.37	53.00
BSOR087	112.59	-103.32	66.57	-39.01	1.51	68.31	7.30	-5.64	42.87
BSOR088	169.92	-101.11	93.68	-50.27	4.64	109.67	17.60	-13.48	30.44
BSOR089	126.55	-133.63	32.38	-36.72	2.79	122.94	7.27	-4.05	3.08
BSOR090	141.69	-131.84	51.30	-48.18	5.92	125.89	9.81	-5.50	18.32
BSOR091	91.50	-11.86	89.69	-10.60	1.40	22.13	1.76	-0.91	88.99
BSOR092	244.19	-20.20	180.20	-17.24	8.78	72.54	12.21	-2.47	169.36
BSOR093	188.36	-28.66	96.14	-19.17	3.31	92.25	10.86	-4.00	86.34
BSOR094	362.14	-37.15	196.15	-29.85	15.12	178.98	16.14	-3.53	185.58
BSOR095	233.24	-43.38	108.21	-18.86	7.71	127.16	8.99	-3.63	104.91
BSOR096	305.83	-27.26	160.75	-27.13	13.06	146.65	15.97	-7.93	159.31
BSOR097	239.02	-49.16	113.20	-33.22	5.99	132.33	14.84	-9.17	89.21
BSOR098	351.81	-64.17	185.71	-40.48	12.00	175.10	22.78	-15.75	138.82
BSOR099	193.79	-107.95	73.12	-44.99	5.66	163.04	15.52	-6.83	68.90
BSOR100	278.17	-129.91	109.11	-57.34	11.21	184.56	18.63	-9.62	76.15
BSOR101	108.02	-104.97	107.09	-104.55	2.55	9.13	3.97	-1.56	76.70
BSOR102	268.11	-105.47	243.13	-98.90	5.05	43.77	7.12	-2.33	194.47
BSOR103	103.83	-75.34	93.28	-81.16	3.55	37.95	5.92	-1.52	64.51
BSOR104	238.22	-119.67	211.77	-117.70	11.30	63.92	13.27	-2.27	139.12
BSOR105	138.54	-89.42	114.56	-92.93	5.58	42.32	10.01	-1.67	78.11
BSOR106	245.02	-122.84	216.61	-114.46	6.15	63.92	11.99	-2.58	124.65
BSOR107	153.91	-99.94	123.43	-100.75	4.24	53.38	9.56	-1.37	92.49
BSOR108	267.70	-113.79	200.78	-122.51	4.98	99.70	14.74	-1.99	121.37
BSOR109	272.36	-95.57	124.85	-110.66	8.46	160.12	13.35	-3.23	104.81
BSOR110	404.65	-120.63	186.17	-136.89	16.89	237.33	22.46	-8.30	158.34

Table B-2 Continued.

Test case	Vert. Max	Vert. Min	Quasi Max	Quasi Min	Horiz. Assoc.	Slam Max	Horiz. Max	Horiz. Min	Vert. Assoc.
BSOR111	112.71	-148.42	116.28	-153.33	4.03	43.59	4.31	-2.96	111.67
BSOR112	185.50	-278.17	194.73	-285.52	7.47	34.85	7.63	-5.79	178.81
BSOR113	93.27	-124.22	97.64	-129.08	3.61	35.02	5.66	-3.09	82.78
BSOR114	164.89	-233.22	166.84	-237.30	8.06	55.78	11.33	-4.94	121.18
BSOR115	107.53	-150.62	102.57	-157.54	5.03	39.10	6.46	-3.23	85.45
BSOR116	157.85	-260.05	165.10	-261.03	7.42	61.94	11.26	-5.89	139.86
BSOR117	126.74	-242.63	112.51	-245.62	7.12	100.03	14.24	-4.59	54.11
BSOR118	190.47	-319.45	138.15	-318.29	10.11	89.27	14.59	-5.08	90.29
BSOR119	155.15	-168.00	75.88	-178.13	10.35	121.62	11.59	-4.72	56.32
BSOR120	217.87	-303.42	113.30	-317.88	9.47	143.79	11.39	-6.42	55.43
BSOR121	123.68	-20.72	61.92	-16.75	2.27	61.95	5.39	-6.12	34.99
BSOR122	156.44	-21.97	113.92	-21.35	4.84	42.85	9.55	-6.36	86.05
BSOR123	78.68	-54.77	46.16	-26.54	-2.51	59.32	9.21	-7.85	11.23
BSOR124	214.62	-55.21	142.33	-47.24	10.56	101.47	22.99	-22.22	89.18
BSOR125	108.46	-75.37	65.22	-25.10	3.74	54.74	14.99	-14.54	32.41
BSOR126	174.06	-84.81	97.90	-32.87	4.55	92.65	15.30	-13.82	86.18
BSOR127	146.35	-110.41	89.54	-49.02	9.46	75.47	18.99	-17.45	25.44
BSOR128	226.61	-112.81	115.44	-53.43	6.75	111.67	21.22	-17.43	19.43
BSOR129	146.58	-123.99	45.15	-49.56	2.46	120.04	11.20	-9.09	-14.58
BSOR130	166.82	-121.65	58.14	-50.23	2.93	133.93	24.99	-16.94	39.60
BSOR131	128.73	-36.48	105.17	-14.97	2.82	73.77	4.32	-2.51	96.48
BSOR132	232.05	-27.27	188.15	-22.86	7.00	76.31	16.60	-7.98	176.14
BSOR133	335.92	-27.14	144.24	-23.79	4.86	191.69	17.49	-11.82	92.52
BSOR134	354.55	-43.20	211.76	-36.67	14.79	176.56	25.32	-15.08	198.53
BSOR135	298.82	-45.00	123.29	-19.12	3.96	191.94	11.66	-7.72	91.69
BSOR136	347.50	-29.54	189.11	-27.70	13.81	167.61	20.38	-14.85	155.88
BSOR137	348.52	-54.24	165.27	-32.52	13.94	214.91	36.44	-29.15	116.59
BSOR138	380.72	-80.33	202.13	-42.06	16.37	187.65	37.17	-29.40	124.80
BSOR139	330.23	-142.30	112.77	-75.68	26.82	232.19	29.41	-17.70	95.15
BSOR140	293.63	-143.87	113.61	-67.28	7.02	196.04	24.80	-21.87	62.67
BSOR141	124.44	-108.81	120.89	-107.24	3.26	12.60	3.84	-1.89	79.57
BSOR142	209.24	-122.56	213.09	-117.04	5.74	56.86	7.37	-3.03	174.24
BSOR143	173.38	-101.26	144.93	-105.86	5.66	46.66	9.03	-2.60	93.28
BSOR144	267.10	-128.38	236.32	-126.98	10.25	64.79	11.21	-3.83	224.53
BSOR145	216.40	-120.77	175.76	-119.60	6.94	64.46	10.00	-2.39	91.96

Table B-2 Continued.

Test case	Vert. Max	Vert. Min	Quasi Max	Quasi Min	Horiz. Assoc.	Slam Max	Horiz. Max	Horiz. Min	Vert. Assoc.
BSOR146	330.97	-123.43	307.08	-112.32	4.02	88.28	15.53	-3.69	210.08
BSOR147	231.90	-108.27	169.05	-101.99	10.68	97.34	11.28	-2.72	111.33
BSOR148	266.94	-121.73	227.23	-120.70	8.91	81.38	16.27	-2.96	227.00
BSOR149	368.38	-116.13	164.04	-132.61	7.99	213.85	23.39	-5.14	139.51
BSOR150	394.33	-127.40	179.81	-147.15	24.18	240.93	24.31	-7.12	153.11

APPENDIX C – SLAMMING FORCE ON FLAT PLATES

The following tables are a list of all physical model tests performed and the significant variables and values associated with each test. The tables are divided into variables and forces. The tests can be differentiated by the individual case prefix and reference number. All flat plate slamming cases contain the prefix ‘SLAM’.

Table C-1 contains the relevant fluid and structure parameters for all tests. Table C-2 contains the measured significant forces and moments for all tests. All dimensions are in feet, all forces are in pounds, and all times are in seconds.

Column header abbreviations for Table C-1 are plate width, plate length, plate thickness, plate clearance height, water depth, wave height, wave period, and wave length. Column header abbreviations for Table C-2 are total vertical maximum, total vertical minimum, quasi-static maximum, quasi-static minimum, slamming maximum, and pressure maximum.

Table C- 1 Structure and fluid parameters for all physical model tests.

Test case	Struct. Width	Struct. Length	Struct. Thick.	Struct. Clear.	Water Depth	Wave Height	Wave Period	Wave Length
SLAM001	4.00	6.00	0.08	0.25	2.42	0.50	3.50	29.63
SLAM002	4.00	6.00	0.08	0.25	2.42	0.95	3.50	29.63
SLAM003	4.00	6.00	0.08	0.25	2.42	0.50	3.00	25.01
SLAM004	4.00	6.00	0.08	0.25	2.42	0.79	3.00	25.01
SLAM005	4.00	6.00	0.08	0.25	2.42	0.69	2.50	20.30
SLAM006	4.00	6.00	0.08	0.25	2.42	0.92	2.50	20.30
SLAM007	4.00	6.00	0.08	0.25	2.42	0.76	2.00	15.46
SLAM008	4.00	6.00	0.08	0.25	2.42	1.07	2.00	15.46
SLAM009	4.00	6.00	0.08	0.25	2.42	0.78	1.50	10.36
SLAM010	4.00	6.00	0.08	0.25	2.42	0.97	1.50	10.36
SLAM011	4.00	6.00	0.08	0.17	2.50	0.48	3.50	30.09
SLAM012	4.00	6.00	0.08	0.17	2.50	1.00	3.50	30.09
SLAM013	4.00	6.00	0.08	0.17	2.50	0.52	3.00	25.38
SLAM014	4.00	6.00	0.08	0.17	2.50	0.91	3.00	25.38
SLAM015	4.00	6.00	0.08	0.17	2.50	0.67	2.50	20.59
SLAM016	4.00	6.00	0.08	0.17	2.50	0.95	2.50	20.59
SLAM017	4.00	6.00	0.08	0.17	2.50	0.76	2.00	15.65
SLAM018	4.00	6.00	0.08	0.17	2.50	1.09	2.00	15.65
SLAM019	4.00	6.00	0.08	0.17	2.50	0.70	1.50	10.45
SLAM020	4.00	6.00	0.08	0.17	2.50	1.03	1.50	10.45
SLAM021	4.00	6.00	0.08	0.08	2.58	0.44	3.50	30.54
SLAM022	4.00	6.00	0.08	0.08	2.58	1.00	3.50	30.54
SLAM023	4.00	6.00	0.08	0.08	2.58	0.37	3.00	25.75
SLAM024	4.00	6.00	0.08	0.08	2.58	0.91	3.00	25.75
SLAM025	4.00	6.00	0.08	0.08	2.58	0.49	2.50	20.87
SLAM026	4.00	6.00	0.08	0.08	2.58	0.99	2.50	20.87
SLAM027	4.00	6.00	0.08	0.08	2.58	0.70	2.00	15.83
SLAM028	4.00	6.00	0.08	0.08	2.58	1.20	2.00	15.83
SLAM029	4.00	6.00	0.08	0.08	2.58	0.64	1.50	10.52
SLAM030	4.00	6.00	0.08	0.08	2.58	1.04	1.50	10.52
SLAM031	4.00	6.00	0.08	0.00	2.67	0.47	3.50	30.99
SLAM032	4.00	6.00	0.08	0.00	2.67	1.91	3.50	30.99
SLAM033	4.00	6.00	0.08	0.00	2.67	0.45	3.00	26.11
SLAM034	4.00	6.00	0.08	0.00	2.67	0.95	3.00	26.11
SLAM035	4.00	6.00	0.08	0.00	2.67	0.48	2.50	21.14

Table C-1 Continued.

Test case	Struct. Width	Struct. Length	Struct. Thick.	Struct. Clear.	Water Depth	Wave Height	Wave Period	Wave Length
SLAM036	4.00	6.00	0.08	0.00	2.67	0.90	2.50	21.14
SLAM037	4.00	6.00	0.08	0.00	2.67	0.77	2.00	16.00
SLAM038	4.00	6.00	0.08	0.00	2.67	1.36	2.00	16.00
SLAM039	4.00	6.00	0.08	0.00	2.67	0.66	1.50	10.59
SLAM040	4.00	6.00	0.08	0.00	2.67	1.01	1.50	10.59
SLAM041	4.00	6.00	0.08	-0.08	2.75	0.43	3.50	31.42
SLAM042	4.00	6.00	0.08	-0.08	2.75	1.06	3.50	31.42
SLAM043	4.00	6.00	0.08	-0.08	2.75	0.47	3.00	26.46
SLAM044	4.00	6.00	0.08	-0.08	2.75	1.00	3.00	26.46
SLAM045	4.00	6.00	0.08	-0.08	2.75	0.52	2.50	21.40
SLAM046	4.00	6.00	0.08	-0.08	2.75	0.90	2.50	21.40
SLAM047	4.00	6.00	0.08	-0.08	2.75	0.92	2.00	16.17
SLAM048	4.00	6.00	0.08	-0.08	2.75	1.40	2.00	16.17
SLAM049	4.00	6.00	0.08	-0.08	2.75	0.75	1.50	10.66
SLAM050	4.00	6.00	0.08	-0.08	2.75	1.09	1.50	10.66
SLAM051	4.00	6.00	0.08	-0.17	2.83	0.50	3.50	31.85
SLAM052	4.00	6.00	0.08	-0.17	2.83	1.10	3.50	31.85
SLAM053	4.00	6.00	0.08	-0.17	2.83	0.56	3.00	26.80
SLAM054	4.00	6.00	0.08	-0.17	2.83	0.99	3.00	26.80
SLAM055	4.00	6.00	0.08	-0.17	2.83	0.55	2.50	21.66
SLAM056	4.00	6.00	0.08	-0.17	2.83	0.90	2.50	21.66
SLAM057	4.00	6.00	0.08	-0.17	2.83	0.78	2.00	16.33
SLAM058	4.00	6.00	0.08	-0.17	2.83	1.44	2.00	16.33
SLAM059	4.00	6.00	0.08	-0.17	2.83	0.84	1.50	10.73
SLAM060	4.00	6.00	0.08	-0.17	2.83	1.15	1.50	10.73
SLAM061	4.00	6.00	0.08	0.25	2.08	0.43	3.50	27.69
SLAM062	4.00	6.00	0.08	0.25	2.08	0.85	3.50	27.69
SLAM063	4.00	6.00	0.08	0.25	2.08	0.41	3.00	23.41
SLAM064	4.00	6.00	0.08	0.25	2.08	0.75	3.00	23.41
SLAM065	4.00	6.00	0.08	0.25	2.08	0.56	2.50	19.08
SLAM066	4.00	6.00	0.08	0.25	2.08	1.62	2.50	19.08
SLAM067	4.00	6.00	0.08	0.25	2.08	0.63	2.00	14.63
SLAM068	4.00	6.00	0.08	0.25	2.08	0.88	2.00	14.63
SLAM069	4.00	6.00	0.08	0.25	2.08	0.66	1.50	9.97
SLAM070	4.00	6.00	0.08	0.25	2.08	0.80	1.50	9.97

Table C-1 Continued.

Test case	Struct. Width	Struct. Length	Struct. Thick.	Struct. Clear.	Water Depth	Wave Height	Wave Period	Wave Length
SLAM071	4.00	6.00	0.08	0.17	2.17	0.38	3.50	28.19
SLAM072	4.00	6.00	0.08	0.17	2.17	0.74	3.50	28.19
SLAM073	4.00	6.00	0.08	0.17	2.17	0.48	3.00	23.82
SLAM074	4.00	6.00	0.08	0.17	2.17	0.83	3.00	23.82
SLAM075	4.00	6.00	0.08	0.17	2.17	0.47	2.50	19.40
SLAM076	4.00	6.00	0.08	0.17	2.17	0.75	2.50	19.40
SLAM077	4.00	6.00	0.08	0.17	2.17	0.54	2.00	14.85
SLAM078	4.00	6.00	0.08	0.17	2.17	0.82	2.00	14.85
SLAM079	4.00	6.00	0.08	0.17	2.17	0.64	1.50	10.08
SLAM080	4.00	6.00	0.08	0.17	2.17	0.81	1.50	10.08
SLAM081	4.00	6.00	0.08	0.08	2.25	0.35	3.50	28.68
SLAM082	4.00	6.00	0.08	0.08	2.25	0.74	3.50	28.68
SLAM083	4.00	6.00	0.08	0.08	2.25	0.35	3.00	24.23
SLAM084	4.00	6.00	0.08	0.08	2.25	0.77	3.00	24.23
SLAM085	4.00	6.00	0.08	0.08	2.25	0.53	2.50	19.71
SLAM086	4.00	6.00	0.08	0.08	2.25	0.82	2.50	19.71
SLAM087	4.00	6.00	0.08	0.08	2.25	0.56	2.00	15.06
SLAM088	4.00	6.00	0.08	0.08	2.25	1.01	2.00	15.06
SLAM089	4.00	6.00	0.08	0.08	2.25	0.57	1.50	10.18
SLAM090	4.00	6.00	0.08	0.08	2.25	0.86	1.50	10.18
SLAM091	4.00	6.00	0.08	0.00	2.33	0.41	3.50	29.16
SLAM092	4.00	6.00	0.08	0.00	2.33	0.86	3.50	29.16
SLAM093	4.00	6.00	0.08	0.00	2.33	0.40	3.00	24.62
SLAM094	4.00	6.00	0.08	0.00	2.33	0.74	3.00	24.62
SLAM095	4.00	6.00	0.08	0.00	2.33	0.51	2.50	20.01
SLAM096	4.00	6.00	0.08	0.00	2.33	0.89	2.50	20.01
SLAM097	4.00	6.00	0.08	0.00	2.33	0.64	2.00	15.26
SLAM098	4.00	6.00	0.08	0.00	2.33	1.09	2.00	15.26
SLAM099	4.00	6.00	0.08	0.00	2.33	0.66	1.50	10.27
SLAM100	4.00	6.00	0.08	0.00	2.33	0.88	1.50	10.27
SLAM101	4.00	6.00	0.08	-0.08	2.42	0.42	3.50	29.63
SLAM102	4.00	6.00	0.08	-0.08	2.42	0.86	3.50	29.63
SLAM103	4.00	6.00	0.08	-0.08	2.42	0.36	3.00	25.01
SLAM104	4.00	6.00	0.08	-0.08	2.42	0.75	3.00	25.01
SLAM105	4.00	6.00	0.08	-0.08	2.42	0.52	2.50	20.30

Table C-1 Continued.

Test case	Struct. Width	Struct. Length	Struct. Thick.	Struct. Clear.	Water Depth	Wave Height	Wave Period	Wave Length
SLAM106	4.00	6.00	0.08	-0.08	2.42	0.82	2.50	20.30
SLAM107	4.00	6.00	0.08	-0.08	2.42	0.69	2.00	15.46
SLAM108	4.00	6.00	0.08	-0.08	2.42	1.17	2.00	15.46
SLAM109	4.00	6.00	0.08	-0.08	2.42	0.64	1.50	10.36
SLAM110	4.00	6.00	0.08	-0.08	2.42	0.91	1.50	10.36
SLAM111	4.00	6.00	0.08	-0.17	2.50	0.38	3.50	30.09
SLAM112	4.00	6.00	0.08	-0.17	2.50	0.78	3.50	30.09
SLAM113	4.00	6.00	0.08	-0.17	2.50	0.43	3.00	25.38
SLAM114	4.00	6.00	0.08	-0.17	2.50	0.90	3.00	25.38
SLAM115	4.00	6.00	0.08	-0.17	2.50	0.47	2.50	20.59
SLAM116	4.00	6.00	0.08	-0.17	2.50	0.88	2.50	20.59
SLAM117	4.00	6.00	0.08	-0.17	2.50	0.69	2.00	15.65
SLAM118	4.00	6.00	0.08	-0.17	2.50	1.21	2.00	15.65
SLAM119	4.00	6.00	0.08	-0.17	2.50	0.85	1.50	10.45
SLAM120	4.00	6.00	0.08	-0.17	2.50	1.04	1.50	10.45
SLAM121	4.00	6.00	0.08	0.25	1.75	0.39	3.50	25.56
SLAM122	4.00	6.00	0.08	0.25	1.75	0.66	3.50	25.56
SLAM123	4.00	6.00	0.08	0.25	1.75	0.51	3.00	21.63
SLAM124	4.00	6.00	0.08	0.25	1.75	0.75	3.00	21.63
SLAM125	4.00	6.00	0.08	0.25	1.75	0.53	2.50	17.69
SLAM126	4.00	6.00	0.08	0.25	1.75	0.79	2.50	17.69
SLAM127	4.00	6.00	0.08	0.25	1.75	0.50	2.00	13.67
SLAM128	4.00	6.00	0.08	0.25	1.75	0.73	2.00	13.67
SLAM129	4.00	6.00	0.08	0.25	1.75	0.61	1.50	9.47
SLAM130	4.00	6.00	0.08	0.25	1.75	0.76	1.50	9.47
SLAM131	4.00	6.00	0.08	0.17	1.83	0.29	3.50	26.11
SLAM132	4.00	6.00	0.08	0.17	1.83	0.69	3.50	26.11
SLAM133	4.00	6.00	0.08	0.17	1.83	0.42	3.00	22.09
SLAM134	4.00	6.00	0.08	0.17	1.83	0.69	3.00	22.09
SLAM135	4.00	6.00	0.08	0.17	1.83	0.44	2.50	18.05
SLAM136	4.00	6.00	0.08	0.17	1.83	0.81	2.50	18.05
SLAM137	4.00	6.00	0.08	0.17	1.83	0.53	2.00	13.92
SLAM138	4.00	6.00	0.08	0.17	1.83	0.82	2.00	13.92
SLAM139	4.00	6.00	0.08	0.17	1.83	0.75	1.50	9.61
SLAM140	4.00	6.00	0.08	0.17	1.83	0.58	1.50	9.61

Table C-1 Continued.

Test case	Struct. Width	Struct. Length	Struct. Thick.	Struct. Clear.	Water Depth	Wave Height	Wave Period	Wave Length
SLAM141	4.00	6.00	0.08	0.08	1.92	0.35	3.50	26.65
SLAM142	4.00	6.00	0.08	0.08	1.92	0.74	3.50	26.65
SLAM143	4.00	6.00	0.08	0.08	1.92	0.38	3.00	22.54
SLAM144	4.00	6.00	0.08	0.08	1.92	0.73	3.00	22.54
SLAM145	4.00	6.00	0.08	0.08	1.92	0.42	2.50	18.40
SLAM146	4.00	6.00	0.08	0.08	1.92	0.77	2.50	18.40
SLAM147	4.00	6.00	0.08	0.08	1.92	0.46	2.00	14.17
SLAM148	4.00	6.00	0.08	0.08	1.92	0.69	2.00	14.17
SLAM149	4.00	6.00	0.08	0.08	1.92	0.57	1.50	9.74
SLAM150	4.00	6.00	0.08	0.08	1.92	0.74	1.50	9.74
SLAM151	4.00	6.00	0.08	0.00	2.00	0.50	3.50	27.17
SLAM152	4.00	6.00	0.08	0.00	2.00	0.75	3.50	27.17
SLAM153	4.00	6.00	0.08	0.00	2.00	0.36	3.00	22.98
SLAM154	4.00	6.00	0.08	0.00	2.00	0.71	3.00	22.98
SLAM155	4.00	6.00	0.08	0.00	2.00	0.49	2.50	18.75
SLAM156	4.00	6.00	0.08	0.00	2.00	0.82	2.50	18.75
SLAM157	4.00	6.00	0.08	0.00	2.00	0.47	2.00	14.40
SLAM158	4.00	6.00	0.08	0.00	2.00	0.75	2.00	14.40
SLAM159	4.00	6.00	0.08	0.00	2.00	0.50	1.50	9.86
SLAM160	4.00	6.00	0.08	0.00	2.00	0.81	1.50	9.86
SLAM161	4.00	6.00	0.08	-0.08	2.08	0.42	3.50	27.69
SLAM162	4.00	6.00	0.08	-0.08	2.08	0.86	3.50	27.69
SLAM163	4.00	6.00	0.08	-0.08	2.08	0.31	3.00	23.41
SLAM164	4.00	6.00	0.08	-0.08	2.08	0.77	3.00	23.41
SLAM165	4.00	6.00	0.08	-0.08	2.08	0.42	2.50	19.08
SLAM166	4.00	6.00	0.08	-0.08	2.08	0.82	2.50	19.08
SLAM167	4.00	6.00	0.08	-0.08	2.08	0.49	2.00	14.63
SLAM168	4.00	6.00	0.08	-0.08	2.08	0.82	2.00	14.63
SLAM169	4.00	6.00	0.08	-0.08	2.08	0.59	1.50	9.97
SLAM170	4.00	6.00	0.08	-0.08	2.08	0.78	1.50	9.97
SLAM171	4.00	6.00	0.08	-0.17	2.17	0.40	3.50	28.19
SLAM172	4.00	6.00	0.08	-0.17	2.17	1.01	3.50	28.19
SLAM173	4.00	6.00	0.08	-0.17	2.17	0.37	3.00	23.82
SLAM174	4.00	6.00	0.08	-0.17	2.17	0.76	3.00	23.82
SLAM175	4.00	6.00	0.08	-0.17	2.17	0.48	2.50	19.40

Table C-1 Continued.

Test case	Struct. Width	Struct. Length	Struct. Thick.	Struct. Clear.	Water Depth	Wave Height	Wave Period	Wave Length
SLAM176	4.00	6.00	0.08	-0.17	2.17	0.91	2.50	19.40
SLAM177	4.00	6.00	0.08	-0.17	2.17	0.59	2.00	14.85
SLAM178	4.00	6.00	0.08	-0.17	2.17	1.10	2.00	14.85
SLAM179	4.00	6.00	0.08	-0.17	2.17	0.66	1.50	10.08
SLAM180	4.00	6.00	0.08	-0.17	2.17	0.84	1.50	10.08

Table C- 2 Significant force values for all physical model tests.

Test case	Vert. Max	Vert. Min	Quasi Max	Quasi Min	Slam Max	Pressure Max
SLAM001	4.41	-13.52	3.21	-9.71	2.40	0.03
SLAM002	157.09	-78.13	107.43	-46.24	58.40	0.22
SLAM003	22.75	-29.70	17.17	-20.16	13.21	0.13
SLAM004	152.04	-122.28	120.41	-89.89	83.18	0.44
SLAM005	54.75	-37.72	41.58	-35.72	29.38	0.16
SLAM006	135.74	-87.36	87.38	-55.55	73.47	0.31
SLAM007	100.99	-103.60	47.34	-41.43	74.65	0.16
SLAM008	188.66	-150.49	93.81	-80.07	127.29	0.31
SLAM009	39.59	-50.52	31.14	-46.71	19.58	0.20
SLAM010	55.23	-114.10	43.41	-73.53	63.02	0.29
SLAM011	56.30	-22.82	37.22	-20.68	22.14	0.10
SLAM012	216.19	-92.89	142.94	-64.22	82.90	0.18
SLAM013	104.44	-65.26	69.59	-40.03	50.08	0.19
SLAM014	238.97	-87.80	152.64	-73.73	98.16	0.55
SLAM015	88.94	-39.45	67.21	-27.98	37.68	0.20
SLAM016	203.12	-106.35	138.35	-59.12	112.39	0.59
SLAM017	115.25	-114.08	84.02	-50.92	79.37	0.17
SLAM018	327.88	-142.51	164.99	-97.14	189.95	0.26
SLAM019	65.86	-67.71	43.74	-55.62	27.85	0.19
SLAM020	86.80	-142.62	64.91	-91.63	58.45	0.26
SLAM021	92.46	-25.74	61.53	-20.26	33.67	0.11
SLAM022	188.06	-80.25	125.22	-67.81	65.47	0.21
SLAM023	89.98	-33.37	58.30	-19.53	38.34	0.13
SLAM024	276.40	-109.09	181.73	-56.38	95.36	0.48
SLAM025	106.11	-36.49	67.55	-23.62	45.14	0.18
SLAM026	296.94	-88.70	155.98	-60.78	150.17	0.50
SLAM027	139.49	-54.12	112.41	-42.53	43.84	0.20
SLAM028	331.70	-102.88	182.84	-86.08	199.09	0.37
SLAM029	78.00	-77.40	64.20	-60.44	47.08	0.17
SLAM030	121.61	-153.93	94.57	-107.23	81.10	0.37
SLAM031	102.65	-35.73	78.71	-32.33	25.53	0.04
SLAM032	155.19	-89.51	129.92	-76.11	33.74	0.11
SLAM033	124.56	-44.93	103.23	-38.52	38.92	0.15
SLAM034	313.28	-100.68	212.86	-67.58	123.43	0.35
SLAM035	167.06	-45.31	102.99	-39.92	71.69	0.10

Table C-2 Continued.

Test case	Vert. Max	Vert. Min	Quasi Max	Quasi Min	Slam Max	Pressure Max
SLAM036	247.96	-113.38	192.43	-75.51	77.13	0.25
SLAM037	218.99	-80.58	120.02	-49.55	106.83	0.21
SLAM038	270.23	-109.63	200.87	-82.79	83.94	0.30
SLAM039	133.57	-108.38	84.25	-56.88	75.69	0.16
SLAM040	153.39	-135.67	116.85	-111.97	93.83	0.29
SLAM041	54.69	-89.40	48.49	-91.70	27.27	0.03
SLAM042	114.36	-142.42	113.29	-139.04	45.30	0.15
SLAM043	85.88	-80.19	60.26	-81.97	32.71	0.05
SLAM044	285.02	-125.00	191.74	-123.68	101.06	0.30
SLAM045	104.65	-103.36	67.30	-102.07	38.76	0.05
SLAM046	230.17	-132.57	172.08	-127.47	109.42	0.25
SLAM047	88.51	-110.32	72.82	-107.61	55.98	0.10
SLAM048	400.02	-148.88	174.46	-126.67	226.17	0.28
SLAM049	95.99	-118.19	70.50	-97.82	63.45	0.15
SLAM050	125.40	-150.33	111.35	-141.49	89.69	0.19
SLAM051	63.09	-111.64	66.30	-112.21	10.72	0.01
SLAM052	113.46	-153.55	120.86	-147.93	42.14	0.06
SLAM053	82.19	-101.07	89.60	-103.48	12.10	0.02
SLAM054	218.70	-128.88	174.84	-129.28	59.87	0.14
SLAM055	88.00	-120.91	89.47	-122.21	44.31	0.05
SLAM056	206.27	-142.25	170.15	-138.27	76.29	0.10
SLAM057	88.00	-105.48	65.74	-104.66	41.17	0.05
SLAM058	241.47	-141.01	163.43	-138.71	80.32	0.12
SLAM059	61.46	-110.57	59.40	-105.80	20.42	0.08
SLAM060	151.62	-171.43	112.30	-142.29	83.32	0.17
SLAM061	9.64	-18.67	8.05	-17.33	6.69	0.12
SLAM062	149.89	-79.56	98.33	-73.98	64.49	0.17
SLAM063	1.59	-1.66	1.89	-1.43	1.24	0.00
SLAM064	100.68	-76.73	81.58	-57.00	56.45	0.27
SLAM065	33.34	-40.69	17.69	-20.11	22.27	0.09
SLAM066	96.46	-78.90	72.33	-53.75	58.98	0.22
SLAM067	58.26	-79.02	28.51	-31.20	52.92	0.09
SLAM068	99.21	-123.49	60.13	-57.96	79.48	0.19
SLAM069	28.55	-37.56	18.60	-28.88	28.15	0.48
SLAM070	53.19	-87.71	37.10	-56.64	44.29	0.18

Table C-2 Continued.

Test case	Vert. Max	Vert. Min	Quasi Max	Quasi Min	Slam Max	Pressure Max
SLAM071	39.66	-20.75	35.35	-18.71	19.06	0.49
SLAM072	165.20	-96.54	106.28	-54.46	76.81	0.13
SLAM073	69.03	-45.51	58.82	-24.00	31.29	0.19
SLAM074	138.40	-50.75	105.32	-36.98	54.15	0.19
SLAM075	60.25	-31.38	39.21	-23.24	27.62	0.14
SLAM076	147.59	-62.71	109.10	-49.78	81.02	0.32
SLAM077	80.51	-67.09	40.27	-29.80	54.88	0.51
SLAM078	241.11	-109.37	115.32	-76.13	153.37	0.19
SLAM079	55.20	-74.55	41.24	-42.97	34.20	0.23
SLAM080	103.43	-95.71	68.82	-74.54	42.41	0.21
SLAM081	70.94	-23.01	59.41	-21.31	21.30	0.16
SLAM082	162.81	-78.29	120.84	-62.12	51.74	0.07
SLAM083	75.48	-18.95	47.14	-15.97	30.58	0.11
SLAM084	209.40	-88.83	159.31	-47.42	71.52	0.29
SLAM085	135.59	-45.46	79.87	-27.28	62.86	0.19
SLAM086	222.66	-102.74	140.21	-56.24	89.27	0.31
SLAM087	127.29	-51.15	93.38	-32.57	49.36	0.21
SLAM088	269.01	-86.62	166.79	-75.79	130.49	0.29
SLAM089	83.49	-67.12	62.13	-54.78	58.18	0.17
SLAM090	113.94	-148.07	94.06	-95.51	84.50	0.22
SLAM091	100.35	-28.17	70.01	-27.73	34.52	0.07
SLAM092	142.11	-73.49	121.40	-64.19	31.56	0.12
SLAM093	135.99	-27.51	82.65	-22.09	53.44	0.11
SLAM094	231.92	-78.55	157.28	-48.42	84.17	0.26
SLAM095	125.76	-33.94	95.18	-30.22	41.97	0.10
SLAM096	216.61	-84.44	156.49	-65.03	105.35	0.45
SLAM097	154.28	-60.96	111.07	-43.61	57.65	0.17
SLAM098	235.98	-105.22	172.99	-81.11	88.15	0.25
SLAM099	128.84	-95.43	89.30	-57.11	63.45	0.23
SLAM100	151.23	-120.69	105.83	-87.39	77.84	0.21
SLAM101	69.22	-93.64	51.85	-94.95	37.27	0.04
SLAM102	104.37	-136.00	103.14	-132.42	36.78	0.06
SLAM103	92.00	-83.12	61.64	-83.26	40.03	0.06
SLAM104	241.15	-109.59	151.01	-111.07	90.22	0.30
SLAM105	86.41	-96.88	63.79	-96.88	34.33	0.05

Table C-2 Continued.

Test case	Vert. Max	Vert. Min	Quasi Max	Quasi Min	Slam Max	Pressure Max
SLAM106	230.42	-119.27	127.81	-115.91	110.48	0.19
SLAM107	73.87	-92.69	61.58	-93.91	50.45	0.07
SLAM108	320.68	-133.60	139.36	-120.87	192.62	0.29
SLAM109	88.57	-107.85	68.54	-90.20	45.32	0.09
SLAM110	139.17	-168.97	100.95	-131.01	67.57	0.15
SLAM111	53.06	-85.93	56.49	-88.97	6.73	0.01
SLAM112	104.13	-140.72	96.97	-139.17	43.37	0.05
SLAM113	72.65	-84.24	77.69	-85.32	9.84	0.01
SLAM114	217.32	-119.06	174.28	-119.88	69.41	0.13
SLAM115	76.43	-104.72	81.68	-104.38	24.42	0.02
SLAM116	208.55	-126.45	152.60	-129.21	69.98	0.09
SLAM117	73.23	-107.95	67.33	-106.31	29.47	0.04
SLAM118	157.08	-129.99	142.81	-137.08	72.49	0.20
SLAM119	93.51	-122.57	71.35	-108.55	34.21	0.08
SLAM120	162.17	-155.49	117.98	-130.89	68.80	0.12
SLAM121	1.64	-10.39	1.84	-9.21	2.89	0.03
SLAM122	43.69	-39.85	36.06	-37.93	13.36	0.19
SLAM123	0.96	-4.13	1.50	-3.18	2.27	0.01
SLAM124	62.60	-51.22	46.81	-30.17	32.33	0.25
SLAM125	15.04	-21.18	8.47	-17.52	8.44	0.46
SLAM126	92.43	-78.45	58.80	-58.37	49.28	0.24
SLAM127	6.92	-15.41	3.36	-15.13	6.02	0.08
SLAM128	55.85	-74.25	38.56	-42.38	37.28	0.17
SLAM129	25.58	-41.40	14.25	-24.34	24.95	0.47
SLAM130	33.76	-44.61	22.60	-40.49	27.08	0.18
SLAM131	14.93	-14.66	9.20	-15.21	6.73	0.14
SLAM132	121.45	-85.12	97.88	-58.43	57.37	0.23
SLAM133	21.80	-22.77	17.82	-15.83	11.77	0.10
SLAM134	103.27	-45.03	77.55	-26.78	40.94	0.13
SLAM135	30.55	-36.00	24.05	-20.42	17.38	0.11
SLAM136	101.14	-83.89	90.85	-56.92	51.45	0.24
SLAM137	70.69	-96.14	47.73	-35.92	56.88	0.11
SLAM138	134.22	-77.46	80.84	-53.17	74.92	0.18
SLAM139	65.24	-88.34	47.49	-65.08	35.10	0.21
SLAM140	43.33	-39.89	31.46	-34.86	19.08	0.16

Table C-2 Continued.

Test case	Vert. Max	Vert. Min	Quasi Max	Quasi Min	Slam Max	Pressure Max
SLAM141	63.12	-22.52	48.51	-17.43	22.31	0.12
SLAM142	142.45	-61.73	103.77	-51.51	43.19	0.16
SLAM143	78.49	-21.50	56.17	-16.05	27.84	0.10
SLAM144	172.64	-56.67	143.14	-39.86	66.70	0.21
SLAM145	99.36	-31.21	62.46	-21.14	37.46	0.09
SLAM146	210.21	-107.51	137.86	-54.15	72.88	0.32
SLAM147	132.88	-52.97	81.54	-33.27	68.49	0.20
SLAM148	259.12	-95.80	138.26	-70.40	122.72	0.23
SLAM149	79.36	-66.89	62.15	-55.25	58.04	0.13
SLAM150	83.31	-90.45	78.39	-75.71	66.25	0.18
SLAM151	63.09	-111.64	66.30	-112.21	10.72	0.01
SLAM152	129.37	-70.24	127.22	-60.21	20.03	0.05
SLAM153	117.89	-29.15	81.45	-29.49	50.27	0.18
SLAM154	237.53	-97.63	172.39	-52.68	87.14	0.28
SLAM155	135.02	-43.20	84.12	-38.13	57.29	0.13
SLAM156	203.39	-75.13	162.91	-64.01	58.46	0.15
SLAM157	143.78	-58.87	96.24	-39.28	56.62	0.15
SLAM158	212.04	-103.89	149.45	-90.31	87.09	0.25
SLAM159	100.98	-78.48	69.04	-44.35	51.86	0.14
SLAM160	132.89	-122.48	102.97	-79.45	82.83	0.16
SLAM161	62.45	-79.68	57.86	-82.56	14.17	0.02
SLAM162	125.73	-141.47	121.69	-124.81	41.44	0.06
SLAM163	80.25	-73.87	48.16	-75.00	36.85	0.05
SLAM164	299.58	-111.72	172.81	-113.35	131.84	0.29
SLAM165	60.26	-85.06	49.98	-90.98	35.11	0.05
SLAM166	181.97	-141.44	118.09	-122.56	74.55	0.10
SLAM167	82.32	-85.08	57.71	-81.70	32.83	0.06
SLAM168	326.50	-152.44	129.63	-110.08	273.26	0.33
SLAM169	102.40	-111.21	72.44	-86.63	58.24	0.16
SLAM170	118.64	-146.89	83.19	-110.56	58.62	0.13
SLAM171	60.57	-81.83	64.33	-84.65	9.62	0.01
SLAM172	142.21	-158.89	143.35	-151.24	40.69	0.06
SLAM173	54.80	-80.66	58.14	-84.84	24.80	0.03
SLAM174	176.48	-112.49	149.75	-114.73	37.88	0.07
SLAM175	68.68	-98.08	72.80	-100.85	30.37	0.05

Table C-2 Continued.

Test case	Vert. Max	Vert. Min	Quasi Max	Quasi Min	Slam Max	Pressure Max
SLAM176	151.87	-123.93	132.85	-123.94	40.52	0.05
SLAM177	87.97	-99.74	76.02	-96.27	66.96	0.08
SLAM178	146.12	-117.93	132.29	-122.59	34.24	0.11
SLAM179	120.23	-120.76	78.56	-110.31	49.61	0.10
SLAM180	144.76	-162.36	102.43	-127.38	75.48	0.15